VOLUME 26 (1961) No. 4

NUCLEAR PHYSICS

JOURNAL DEVOTED TO THE EXPERIMENTAL AND THEORETICAL STUDY OF THE FUNDAMENTAL CONSTITUENTS OF MATTER AND THEIR INTERACTIONS

EDITOR: L. ROSENFELD · COPENHAGEN

LAST NUMBER OF THIS VOLUME

J. HUMBLET and L. ROSENFELD, Theory of nuclear reactions. I. Resonant states and collision matrix 529

L. ROSENFELD, Theory of nuclear reactions. II. The foundation of the optical model 579

STAVROS FALLIEROS, Centre-of-mass invariance and the energy shift in the nuclear dipole state 594

G. J. F. LEGGE, A search for fine structure in the reactions $B^{10}(d, \alpha_0)Be^8$ and $B^{10}(d, \alpha_1)Be^{8*}$ 608

G. J. F. LEGGE, C^{12} level structure in the excitation region 20.5—26.5 MeV 616

F. A. BRISBOUT, C. CAULD, J. LEHANE, C. B. McCUSTER, J. MALOS, K. NISHIKAWA and L. G. VAN LOON, The production and properties of mesons at high energies 634

W. F. EDWARDS and C. J. GALLAGHER, Jr, The decay of Se^{75} 649

YASUSHI TAKAHASHI, The structure of the nucleon core by the Hartree approximation 658

W. F. EDWARDS, J. W. M. DUMOND and F. BOEHM, An intensity calibration of the two metre curved-crystal spectrometer 670

VLADIMÍR ŠACHL, Dispersion relations for photoproduction of π--mesons on deuterons 681

Book reviews 693

Instructions to contributors 723

Author index 712

Subject index 716

September 1961

NORTH-HOLLAND PUBLISHING COMPANY - AMSTERDAM

EDITORIAL BOARD

AUSTRALIA & NEW ZEALAND:	H. Messel (Sydney), M. L. Oliphant (Canberra)
AUSTRIA:	B. Karlik (Vienna), H. Thirring (Vienna)
BELGIUM:	M. de Hemptinne (Louvain), J. Verhaeghe (Ghent)
CANADA:	G. Volkoff (Vancouver)
DENMARK:	C. Møller (Copenhagen), S. Rozental (Copenhagen), G. E. Brown (Copenhagen)
FINLAND:	L. Simons (Helsinki)
FRANCE:	A. Berthelot (Saclay), S. Gorodetzky (Strasbourg)
GERMANY (DEM. REP.):	G. Hertz (Leipzig)
GERMANY (FED. REP.):	W. Gentner (Freiburg i. B.), J. H. D. Jensen (Heidelberg)
GREAT BRITAIN:	W. E. Burcham (Birmingham), T. H. R. Skyrme (Harwell)
HUNGARY:	L. Janossy (Budapest)
INDIA:	H. Bhabha (Bombay), R. Ramanna (Trombay)
IRISH REPUBLIC:	J. McConnell (Maynooth)
ISRAEL:	G. Racah (Jerusalem)
ITALY:	E. Amaldi (Rome)
JAPAN:	S. Kikuchi (Tokay), S. Tomonaga (Tokyo)
MEXICO:	M. Moshinsky (Mexico)
NETHERLANDS:	H. Brinkman (Groningen), S. R. de Groot (Leiden)
NORWAY:	E. Hylleraas (Oslo), A. Lundby (Oslo), H. Wergeland (Trondheim)
POLAND:	L. Infeld (Warsaw), J. Werle (Warsaw)
PORTUGAL:	J. M. Araújo (Porto), J. R. de Almeida Santos (Coimbra)
SOUTH AMERICA:	G. Beck (Rio de Janeiro), J. Leite Lopes (Rio de Janeiro)
SPAIN:	J. M. Otero (Madrid), C. Sanchez del Rio (Madrid)
SWEDEN:	O. Klein (Stockholm), K. Siegbahn (Uppsala), I. Waller (Uppsala)
SWITZERLAND:	P. Huber (Basel), P. Scherrer (Zürich)
U.A.R. & ARAB COUNTRIES:	F. El Bedewi (Cairo), M. G. Nooh (Cairo)
U.S.A.:	H. H. Barschall (Madison, Wisconsin), S. Devons (New York), V. F. Weisskopf (Cambridge, Mass.)
U.S.S.R.:	M. A. Markov (Moscow), I. S. Shapiro (Moscow), D. V. Skobeltzyn (Moscow)
YUGOSLAVIA:	I. Supek (Zagreb)

CONTRIBUTIONS may be sent to the Editor, Professor L. Rosenfeld, NORDITA, Blegdamsvej 17, Copenhagen Ø, either directly, or preferably through the intermediary of one of the members of the Editorial Board of the country or region in which the author is working. They may be written in English, French or German.

NUCLEAR PHYSICS is published in fortnightly issues. The subscription price per volume of 700 pages is fl 57.00; 114s; $ 15.00. Post-free.

SUBSCRIPTIONS should be sent to the publishers, NORTH-HOLLAND PUBLISHING COMPANY P.O. Box 103, Amsterdam or to any subscription-agent.

BOOKS FOR REVIEW should be sent to Professor Rosenfeld.

No part of this issue may be reproduced in any form, by print, photoprint, microfilm or any other means without permission from the publisher.

Printed in the Netherlands

NUCLEAR PHYSICS

EDITORIAL BOARD

AUSTRALIA & NEW ZEALAND:	H. Messel (Sydney), M. L. Oliphant (Canberra)
AUSTRIA:	B. Karlik (Vienna), H. Thirring (Vienna)
BELGIUM:	M. de Hemptinne (Louvain), J. Verhaeghe (Ghent)
CANADA:	G. Volkoff (Vancouver)
DENMARK:	C. Møller (Copenhagen), S. Rozental (Copenhagen), G. E. Brown (Copenhagen)
FINLAND:	L. Simons (Helsinki)
FRANCE:	A. Berthelot (Saclay), S. Gorodetzky (Strasbourg)
GERMANY (DEM. REP.):	G. Hertz (Leipzig)
GERMANY (FED. REP.):	W. Gentner (Freiburg i. B.), J. H. D. Jensen (Heidelberg)
GREAT BRITAIN:	W. E. Burcham (Birmingham), T. H. R. Skyrme (Harwell)
HUNGARY:	L. Janossy (Budapest)
INDIA:	H. Bhabha (Bombay), R. Ramanna (Trombay)
IRISH REPUBLIC:	J. McConnell (Maynooth)
ISRAEL:	G. Racah (Jerusalem)
ITALY:	E. Amaldi (Rome)
JAPAN:	S. Kikuchi (Tokai), S. Tomonaga (Tokyo)
MEXICO:	M. Moshinsky (Mexico)
NETHERLANDS:	H. Brinkman (Groningen), S. R. de Groot (Leiden)
NORWAY:	E. Hylleraas (Oslo), A. Lundby (Oslo), H. Wergeland (Trondheim)
POLAND:	L. Infeld (Warsaw), J. Werle (Warsaw)
PORTUGAL:	J. M. Araújo (Porto), J. R. de Almeida Santos (Coimbra)
SOUTH AMERICA:	G. Beck (Rio de Janeiro), J. Leite Lopes (Rio de Janeiro)
SPAIN:	J. M. Otero (Madrid), C. Sanchez del Rio (Madrid)
SWEDEN:	O. Klein (Stockholm), K. Siegbahn (Uppsala), I. Waller (Uppsala)
SWITZERLAND:	P. Huber (Basel), P. Scherrer (Zürich)
U.A.R. & ARAB COUNTRIES:	F. El Bedewi (Cairo), M. G. Nooh (Cairo)
U.S.A.:	H. H. Barschall (Madison, Wisconsin), S. Devons (New York), V. F. Weisskopf (Cambridge, Mass.)
U.S.S.R.:	M. A. Markov (Moscow), I. S Shapiro (Moscow), D. V. Skobeltzyn (Moscow)
YUGOSLAVIA:	I. Supek (Zagreb)

NUCLEAR PHYSICS

JOURNAL DEVOTED TO THE EXPERIMENTAL AND THEORETICAL STUDY OF THE FUNDAMENTAL CONSTITUENTS OF MATTER AND THEIR INTERACTIONS

EDITOR: L. ROSENFELD - COPENHAGEN

VOLUME XXVI

JULY 1961 — SEPTEMBER 1961

NORTH-HOLLAND PUBLISHING COMPANY - AMSTERDAM

PRINTED IN THE NETHERLANDS

2.A.2:
2.C

Nuclear Physics **26** (1961) 529—578; © *North-Holland Publishing Co., Amsterdam*
Not to be reproduced by photoprint or microfilm without written permission from the publisher

THEORY OF NUCLEAR REACTIONS
I. Resonant States and Collision Matrix

J. HUMBLET †
Institute for Theoretical Physics of the University, Copenhagen
and California Institute of Technology, Pasadena
and
L. ROSENFELD
NORDITA — *Nordisk Institut for Teoretisk Atomfysik, Copenhagen*

Received 15 May 1961

Abstract: A new formulation of the general theory of nuclear reactions is proposed, on the basis of a definition of the resonant states as decaying states corresponding to complex eigenvalues of the total energy of the compound system. A characterization of these states is derived from "natural" boundary conditions expressing the absence of incoming waves in all channels: such boundary conditions yield in a unified form the bound states, the proper resonant states and "virtual" states of a type familiar from the case of the ^1S state of the deuteron. The dispersion formulae for elements of the collision matrix determining the reaction cross-sections are established, as immediate consequences of their analytical behaviour as functions of the complex energy variable, by application of the Mittag-Leffler theorem on the representation of meromorphic functions. The presentation thus obtained, besides being simpler than the usual ones, has over the latter the advantage of eliminating every arbitrary element from the specification of the resonances and of the non-resonant background; these elements of the description are, in particular, independent of the choice of the channel radii, and appear altogether as intrinsic properties of the compound system.

Introduction

Since the first theories of nuclear reactions were proposed some twenty-five years ago, numerous papers have been written with the purpose of justifying the existence of formulae of the dispersion type for the cross sections, which have been found well suited to represent the experimental data. In view of the obvious insufficiency of perturbation treatments [1]), special methods had to be devised, involving in particular a definition of the resonance levels. In spite of the progress made in this direction by successive theories, none of these can be said to be satisfactory from the physical point of view, inasmuch as the definitions of the resonances they propose contain arbitrary elements.

The R-matrix theory developed by Wigner and his collaborators †† introduces the resonances in a very indirect and complicated way. It is particularly regrettable that a central role be assigned to such a quantity as the R-matrix, which has no direct physical meaning; when simplifying assumptions or

† On leave of absence from the University of Liège, Belgium.
†† For references, see the review article by Lane and Thomas [2]).

approximations are introduced, they must consequently concern the R-matrix itself, and may still leave the collision matrix in a very complicated form. One should also remember that in the R-matrix theory one has to introduce a number of quantities which are essentially dependent on the "channel radii". This is in fact the case with the R-matrix itself, whereas a physical quantity such as the collision matrix does not, of course, show such a dependence. The definition of the resonances which had been proposed earlier by Kapur and Peierls [3]) avoids most of the complications of the R-matrix formalism, but is nevertheless very artificial, since the positions of the resonance levels it introduces are explicitly dependent on the energy of the incoming particles.

It is our purpose, in several papers of which this is the first, to develop a theory of nuclear reactions free from such arbitrary features, and in which the resonances directly appear as intrinsic properties of the compound system. The possibility of setting up a "natural" definition of the resonance levels was indicated long ago by Siegert [4]) and used in an earlier paper [5]) to establish a rigorous dispersion formula for the special case of elastic scattering by a fixed potential field of finite range †. This dispersion formula was derived from a Mittag-Leffler type of expansion of the scattering amplitudes.

Recently, Peierls [7]) and Le Couteur [8]), using the same natural definition of the resonances, have made interesting contributions to the analysis of the structure of the dispersion formulae when several channels are involved. However, Peierls uses the less general Cauchy type of expansion, while Le Couteur is mainly concerned with the expansion of the collision matrix as an infinite product. On the other hand, a direct extension of the method developed in the case of elastic scattering [5]) to more general types of nuclear reactions proves possible without essential complications. An outline of the main physical ideas enabling such an extension under neglect of spins and Coulomb effects has been given by one of us in several courses of lectures during the last few years: the most recent of these [9]) forms the starting point for the more complete theory developed here ††.

Before treating the general case of nuclear reactions in the second part of this paper, we have found it convenient to devote a first part to a renewed discussion of the elastic scattering. In sections 1 and 2, the main results obtained earlier [5]) for the elastic scattering of neutral spinless particles are briefly summarized and some new results added; the accent here is put on the physical interpretation of the methods employed rather than on their mathematical justification, which is fully discussed in ref. [5]). Section 3 deals with the elastic

† For this case, one should also consult a review article by Newton [6]), where further references will be found. In a further paper (preprint), Newton extends some of his results to more general problems.

†† An abstract of the present paper has been submitted to the Kingston Conference on Nuclear Structure [10]).

scattering of charged spinless particles, which was not discussed in ref. [5]). *The first part must be regarded as an introduction to the notations and methods used in the general case of nuclear reactions.* Many of the properties of the wave function are more easily recognized in the case of elastic scattering, and later we shall only have to justify their extension to the general case.

In this paper, the theory of nuclear reactions will be limited to the analysis of the properties of the collision matrix and to its expansion. The corresponding properties and expansion of the cross sections will be discussed in another paper. However, in the case of elastic scattering the cross sections have also been written down in order to facilitate the physical interpretation of the parameters introduced in the expansion of the scattering matrix.

Part I: ELASTIC SCATTERING OF SPINLESS PARTICLES

1. Neutral Particles: Scattering Matrix and Resonant States

1.1. DEFINITION OF THE SCATTERING MATRIX

Let us consider the elastic scattering of neutral spinless particles by a target nucleus and assume that the interaction may be represented by a real potential V which is spherically symmetric in the barycentric system of reference.

If the method of partial waves is used, the solutions of the Schrödinger equation $H\Psi = E\Psi$, for a total energy E, take the form, in polar coordinates r, Ω ($\equiv \theta, \varphi$, the polar axis being the direction of the incoming particles),

$$\Psi = \sum_l \Psi_l = \frac{1}{\sqrt{4\pi}} \sum_{l=0}^{\infty} \sqrt{2l+1}\, i^l P_l(\cos\theta)\, \frac{u_l(r)}{r}. \tag{1.1}$$

The radial wave-function u_l is a solution of the equation

$$\left(\frac{\mathrm{d}^2}{\mathrm{d}r^2} + k^2 - \frac{l(l+1)}{r^2} - v(r)\right) u_l(r, k) = 0, \tag{1.2a}$$

satisfying the condition

$$u_l(0, k) = 0. \tag{1.2b}$$

In these equations we have introduced the notations

$$k^2 = 2ME/\hbar^2 \tag{1.3}$$

and

$$v(r) = 2MV(r)/\hbar^2, \tag{1.4}$$

where M is the reduced mass. It will be convenient to call k^2 an energy and $v(r)$ a potential. We assume that the potential $v(r)$ is everywhere finite, and that it vanishes identically at all distances larger than some finite distance a:

$$v(r) \equiv 0 \text{ for } r > a; \tag{1.5}$$

the limiting distance a is normally of the order of magnitude of a nuclear radius, although it can be taken much larger if necessary, as we shall see later. It appears that the restriction (1.5) on the potential — excluding an exponentially decreasing behaviour, for instance — is quite essential for the mathematical simplicity and generality of the following discussion. On the other hand, it clearly does not imply any serious physical limitation (cf. section 3).

For $r > a$, solutions of eq. (1.2a) are the well-known spherical Bessel and Hankel functions defined by

$$\mathcal{J}_l(x) = \sqrt{\tfrac{1}{2}\pi x}\, J_{l+\frac{1}{2}}(x), \qquad \mathcal{J}_{-l-1}(x) = \sqrt{\tfrac{1}{2}\pi x}\, J_{-l-\frac{1}{2}}(x), \tag{1.6}$$

$$\mathcal{H}_l^{(1)}(x) = \sqrt{\tfrac{1}{2}\pi x}\, H^{(1)}_{l+\frac{1}{2}}(x), \qquad \mathcal{H}_l^{(2)}(x) = \sqrt{\tfrac{1}{2}\pi x}\, H^{(2)}_{l+\frac{1}{2}}(x), \tag{1.7}$$

where $x \equiv kr$. They satisfy the relations

$$\mathcal{H}_l^{(1)} + \mathcal{H}_l^{(2)} = 2\mathcal{J}_l, \tag{1.8}$$

$$\mathcal{H}_l^{(1)} = \mathcal{J}_l - i(-1)^l \mathcal{J}_{-l-1}, \qquad \mathcal{H}_l^{(2)} = \mathcal{J}_l + i(-1)^l \mathcal{J}_{-l-1}. \tag{1.9}$$

It is useful to recall the asymptotic expressions

$$\mathcal{J}_l \sim \frac{2^l l!}{(2l+1)!}\, x^{l+1}, \qquad \mathcal{H}_l^{(1)} \sim -i\,\frac{(2l)!}{2^l l!}\, x^{-l} \quad \text{(for small } x\text{)}, \tag{1.10}$$

$$\mathcal{H}_l^{(1)} \sim i^{-(l+1)}\, e^{ix}, \qquad \mathcal{H}_l^{(2)} \sim i^{l+1}\, e^{-ix} \qquad \text{(for large } x\text{)}. \tag{1.11}$$

For $r > a$, we choose two linearly independent solutions of eq. (1.2a)

$$O_l(r, k) = i\mathcal{H}_l^{(1)}(kr), \qquad I_l(r, k) = -i\mathcal{H}_l^{(2)}(kr), \tag{1.12}$$

whose asymptotic behaviour for $kr \gg 1$ is

$$O_l \sim e^{i(kr - \frac{1}{2}l\pi)}, \qquad I_l \sim e^{-i(kr - \frac{1}{2}l\pi)}, \tag{1.13}$$

and which therefore respectively represent an outgoing and an incoming spherical wave. Consequently, for $r > a$, the solution of eq. (1.2a) may be written as a superposition of outgoing and incoming waves of appropriate amplitudes x_l, y_l in the form

$$u_l = x_l O_l + y_l I_l. \tag{1.14}$$

For reasons that will appear later, O_l and I_l have not been normalized to unit flux.

The exterior solution (1.14) must be joined smoothly to the interior solution u_l, which embodies the effect of the potential field. Using the notation

$$f'(r, k) = f'(r) \equiv \frac{d}{dr} f(r, k), \qquad f'(a, k) = f'(a) \equiv \left[\frac{d}{dr} f(r, k)\right]_{r=a},$$

we write down the conditions expressing the continuity of u_l and u'_l for $r = a$:

$$u_l(a, k) = x_l O_l(a, k) + y_l I_l(a, k), \tag{1.15a}$$

$$u'_l(a, k) = x_l O'_l(a, k) + y_l I'_l(a, k). \tag{1.15b}$$

From these we may now derive an expression for the amplitudes x_l, y_l in terms of the interior radial wave-function u_l and its derivative. It is convenient to make a systematic use of the notion of Wronskian of two functions f and g,

$$W(f, g; r, k) \equiv f(r, k)g'(r, k) - f'(r, k)g(r, k); \tag{1.16}$$

this Wronskian will also be written more briefly as $W(f, g)$ or $W(f, g; k)$ when no confusion is possible. It is well known that the Wronskian of $\mathscr{H}_l^{(1)}$ and $\mathscr{H}_l^{(2)}$ is independent of r:

$$W(\mathscr{H}_l^{(1)}, \mathscr{H}_l^{(2)}; r, k) = -2ik, \tag{1.17}$$

or, by eqs. (1.12),

$$W(O_l, I_l; r, k) = -2ik. \tag{1.18}$$

We thus get from eqs. (1.15)

$$x_l = -\frac{1}{2ik} W(u_l, I_l; a, k), \tag{1.19a}$$

$$y_l = \frac{1}{2ik} W(u_l, O_l; a, k). \tag{1.19b}$$

The ratios

$$U_l = -\frac{x_l}{y_l} = \frac{W(u_l, I_l; a, k)}{W(u_l, O_l; a, k)}, \tag{1.20}$$

for the different values of l, are the elements of the *scattering matrix* (which is diagonal in the very simple case considered here). The scattering cross sections obviously depend on these quantities U_l and the values

$$y_l^{(\mathrm{un})} = \frac{i}{k}\sqrt{\pi(2l+1)} \tag{1.21}$$

of the amplitudes corresponding to an incoming flux of one particle. In fact, taking account of eq. (1.21), the differential and integrated cross sections are readily expressed in terms of U_l in the form

$$\mathrm{d}\sigma(\Omega) = \frac{1}{4k^2}\left|\sum_l (2l+1)P_l(\cos\theta)(1-U_l)\right|^2 \mathrm{d}\Omega, \tag{1.22}$$

$$\sigma = \sum_l \sigma_l = \frac{\pi}{k^2}\sum_l (2l+1)|1-U_l|^2. \tag{1.23}$$

1.2. PROPERTIES OF THE SCATTERING MATRIX

Our task is now to study the behaviour of the scattering matrix element U_l as a function of k, especially with a view to relating it to the observed resonance features of the cross sections. In this investigation we shall clearly have to treat k as a complex variable. Let us first determine somewhat more precisely the properties of the radial wave-function $u_l(r, k)$ which enters into the definition (1.20) of U_l.

Since the physical quantities (1.22), (1.23) only depend on the radial function u_l through the matrix element U_l, we see that the normalization of u_l need not actually be related, as it would seem from eq. (1.19b), to the particular value (1.21) of y_l which occurs in the expression for the cross sections: this normalization may be fixed arbitrarily. For our case of a potential everywhere finite, a convenient choice, satisfying the requirement (1.2b), is that defined by the condition

$$\lim_{r\to 0} \frac{u_l(r, k)}{r^{l+1}} = \frac{2^l l!}{(2l+1)!}. \tag{1.24}$$

It is well known [5, 6]) that with this normalization u_l and u'_l are integral functions of k^2 for any positive and finite value of r. Further, the potential $v(r)$ being real, u_l and u'_l are also real functions of k^2, so that

$$u_l(r,-k) = u_l(r, k), \tag{1.25a}$$

$$u_l(r, k)^* = u_l(r, k^*) = u_l(r,-k^*); \tag{1.25b}$$

similar relations being also valid for u'_l.

From the properties

$$\mathscr{H}_l^{(1)}(-kr) = (-1)^{l+1}\mathscr{H}_l^{(2)}(kr), \tag{1.26a}$$

$$\mathscr{H}_l^{(1)}(kr)^* = \mathscr{H}_l^{(2)}(k^*r) \tag{1.26b}$$

and eqs. (1.12), one gets

$$O_l(-k) = (-1)^l I_l(k), \qquad O_l(k)^* = I_l(k^*) = (-1)^l O_l(-k^*). \tag{1.27}$$

The definition (1.20) of U_l then immediately leads to the relations

$$U_l(k)U_l(-k) = 1, \tag{1.28}$$

$$U_l(k)^* = U_l(-k^*), \tag{1.29}$$

whence

$$U_l(k^*)^*U_l(k) = 1. \tag{1.30}$$

For real k, eq. (1.30) expresses the unitarity of the scattering matrix:

$$U_l(k)^*U_l(k) = 1 \qquad \text{(for real } k\text{)}, \tag{1.31}$$

from which one derives for the partial cross section σ_l defined by eq. (1.23)

the equivalent, and somewhat simpler, expression

$$\sigma_l = \frac{2\pi}{k^2}(2l+1)\,\mathrm{Re}\,[1-U_l(k)]. \tag{1.32}$$

1.3. DEFINITION AND FORMAL PROPERTIES OF THE RESONANT STATES

The characteristic parameters determining the resonance levels, their positions and widths, must be mathematically defined by some additional boundary condition imposed on the quantity $u_l(a, k)$ on which the matrix element U_l depends. Considering that the resonances correspond to maxima of the cross sections, the expression (1.20) for U_l suggests as a suitable resonance condition the equation

$$W(u_l, O_l; a, k) = 0. \tag{1.33}$$

Regarded as an equation in k, it indeed defines, for each value of l, a set of (complex) roots k_{ln}, some of which we may expect to be associated with resonances. Eq. (1.33) is the "natural" boundary condition first introduced by Siegert [4]). Let us start by discussing its consequences from a purely mathematical point of view, and then show that it indeed provides an adequate representation of the physical situation.

The roots k_{ln} of eq. (1.33) may be described as complex eigenvalues of the radial wave equation (1.2), with corresponding eigenfunctions

$$u_{ln}(r) \equiv u_l(r, k_{ln}). \tag{1.34}$$

For each k_{ln} we have identically

$$W(u_l, O_l; a, k_{ln}) = 0. \tag{1.35}$$

The complex quantities k_{ln} will be written in the form

$$k_{ln} = \kappa_{ln} - i\gamma_{ln}, \tag{1.36}$$

where κ_{ln} and γ_{ln} are real and where the minus sign has been chosen because, as we shall see presently, γ_{ln} is never negative when $\kappa_{ln} \neq 0$. We shall often omit the index l in k_{ln}, κ_{ln} and γ_{ln}.

Let us now discuss the location of the eigenvalues k_n in the complex k-plane. On account of eqs. (1.25b), (1.27), one has, on taking the complex conjugate of eq. (1.35),

$$W(u_l, O_l; a, -k_{ln}^*) = 0; \tag{1.37}$$

this shows that if $k_{ln} = \kappa_{ln} - i\gamma_{ln}$ is a solution of the boundary condition (1.33), the same is true of

$$-k_{ln}^* = -\kappa_{ln} - i\gamma_{ln}. \tag{1.38}$$

Without any restriction, we may therefore always assume that

$$\kappa_{ln} \geqq 0. \tag{1.39}$$

Starting from the wave equation (1.2) and the boundary identity (1.35), together with their complex conjugates, we can easily prove that

$$|u_{ln}(a)|^2[L_l(k_n)-L_l(k_n)^*] = (k_n^{*2}-k_n^2)\int_0^a |u_{ln}(r)|^2 \mathrm{d}r, \tag{1.40}$$

where

$$L_l(k) = \frac{\mathscr{H}_l^{(1)\prime}(ka)}{\mathscr{H}_l^{(1)}(ka)}, \qquad L_l(k)^* = L_l(-k^*), \tag{1.41}$$

the last equation being a consequence of eqs. (1.26). Using the recurrence relations between the spherical Hankel functions, we can show [5]) that

$$|\mathscr{H}_l^{(1)}(k_n a)|^2[L_l(k_n)-L_l(k_n)^*] = i(k_n+k_n^*)|\mathscr{H}_0^{(1)}(k_n a)|^2+(k_n^2-k_n^{*2})\mathscr{N}_{ln}(a), \tag{1.42}$$

where the quantity $\mathscr{N}_{ln}(a)$ is zero for $l = 0$ and, for $l \neq 0$, is given by the essentially real and positive expression

$$\mathscr{N}_{ln}(a) = |ak_n^2|^{-1}\{(2l-1)|\mathscr{H}_{l-1}^{(1)}(k_n a)|^2 + (2l-5)|\mathscr{H}_{l-3}^{(1)}(k_n a)|^2 + \ldots + (2\pm 1)|\mathscr{H}_{\frac{1}{2}\pm\frac{1}{2}}^{(1)}(k_n a)|^2\}, \tag{1.43}$$

the $\pm$ sign corresponding to the parity of l.

For $k_n+k_n^* = 2\kappa_n \neq 0$, eqs. (1.40) and (1.42) yield

$$2\gamma_n = \frac{|u_{ln}(a)/O_l(a, k_n)|^2|\mathrm{e}^{ik_n a}|^2}{\int_0^a |u_{ln}(r)|^2\mathrm{d}r + \left|\frac{u_{ln}(a)}{O_l(a, k_n)}\right|^2 \mathscr{N}_{ln}(a)}, \tag{1.44}$$

showing that γ_n *is positive when* κ_n *is not zero.* Consequently, the eigenvalues $k_n = \kappa_n - i\gamma_n$ for which $\gamma_n < 0$ (upper k-plane) necessarily have $\kappa_n = 0$: they lie on the imaginary axis, and they clearly correspond to the real (bound) levels of the system, since their energy $-\gamma_{ln}^2$ is negative and their radial wave function has the asymptotic form $\exp(ik_n r) = \exp(-|\gamma_n| r)$. In the lower k-plane the eigenvalues are symmetrical with respect to the imaginary axis or lie on it. It was shown in ref. [5]) that there is no solution of the boundary condition (1.33) on the real axis, except possibly at $k = 0$, but we shall disregard this very special case in what follows. In ref. [5]) it was also proved that the number of solutions obeying the boundary condition (1.33) is infinite and that only a finite number of them can be of the type $k_n = -i\gamma_n$ (γ_n positive or negative).

Another important property of the eigenvalues k_{ln} is that they are *independent of the limiting distance a.* This must be understood in the following way:

1) if $v(r) \equiv 0$ for $r > a$, then, for $b > a$, the two boundary conditions

$$W(u_l, O_l; a, k) = 0 \tag{1.33}$$

and

$$W(u_l, O_l; b, k) = 0 \tag{1.45}$$

have exactly the same set of roots k_{ln};

2) if $|v(r)|$ is sufficiently small between a and b, the roots of (1.33) and (1.45) whose moduli are not too large are nearly equal; this may even be true for $b \to \infty$ under suitable conditions [5]).

The eigenvalues introduced in the R-matrix formalism [2]) and in the Kapur-Peierls theory [3]) have no such property. Here it is simply connected with the fact that the boundary condition (1.33) has the form of a Wronskian put equal to zero. From the equation (1.2a) and that satisfied by $O_l(r, k)$,

$$\left(\frac{\mathrm{d}^2}{\mathrm{d}r^2} + k^2 - \frac{l(l+1)}{r^2}\right) O_l(r, k) = 0, \tag{1.46}$$

we easily derive, by a well-known procedure, the relation

$$W(u_l, O_l; b, k) = W(u_l, O_l; a, k) - \int_a^b v(r) u_l(r, k) O_l(r, k)\,\mathrm{d}r, \tag{1.47}$$

which proves the announced property of the eigenvalues k_{ln}.

From eq. (1.47) and the similar one with I_l instead of O_l we see that the scattering matrix U_l, which is the ratio of the two Wronskians, is itself "independent of a".

1.4. EXPANSION OF THE SCATTERING MATRIX

We noticed earlier that the functions u_l and u'_l are integral functions of k^2; obviously, $k^l O_l$, $k^l I_l$ and their derivatives are likewise integral functions of k. Consequently U_l is a meromorphic function of k. We shall assume here that its poles k_n are all simple. We may then expand U_l by means of the following theorem, which is a straightforward consequence of the Mittag-Leffler theorem:

Let $f(k)$ be a meromorphic function of k whose poles k_n are all simple and such that

$$0 < |k_1| \leqq |k_2| \leqq \ldots, \tag{1.48}$$

and let ρ_n be the residue of $f(k)$ at $k = k_n$; if there exists an integer $M \geqq 0$ such that the series

$$\sum_n \frac{|\rho_n|}{|k_n|^{M+1}} \tag{1.49}$$

is convergent, we have

$$f(k) = \varepsilon(k) + \sum_{n=1}^{\infty} \left(\frac{k}{k_n}\right)^M \frac{\rho_n}{k - k_n}, \tag{1.50}$$

where $\varepsilon(k)$ is an integral function of k, while the series is absolutely and uniformly convergent for all values of k uniformly distant from the poles k_n.

In applying this theorem to the scattering matrix element U_l, the most delicate point is the proof of the convergence of the series (1.49) and the determination of the least value of M ensuring this convergence; in fact, this requires a study of the asymptotic distribution of the eigenvalues k_{ln} in the complex k-plane. For a fixed potential field of finite range, this investigation has been carried out in ref. [5]): it is found that one must take $M \geqq 1$.

To justify completely the application of the theorem (1.50) to the expansion of U_l, we still have to verify, according to the first inequality (1.48), that $k = 0$ is not a pole of U_l. Indeed, from the definition (1.20) of U_l, with eqs. (1.12) and the relation (1.8) between Bessel and Hankel functions, we have

$$U_l - 1 = -2 \frac{W(u_l, \mathscr{J}_l; a, k)}{W(u_l, \mathscr{H}_l^{(1)}; a, k)}; \tag{1.51}$$

eqs. (1.10) then yield, for small ka, the asymptotic expression

$$U_l - 1 \sim \frac{-2i}{2l+1} \left(\frac{2^l l!}{(2l)!} \right)^2 (ka)^{2l+1} \frac{au'_l(a, 0) - (l+1)u_l(a, 0)}{au'_l(a, 0) + lu_l(a, 0)}. \tag{1.52}$$

As we have excluded the exceptional case of a resonant level in $k = 0$, this formula shows that $k = 0$ is actually a zero of order $2l+1$ of $U_l - 1$.

The residue $\rho_l(k_{ln})$ of U_l is easily evaluated (its explicit expression may be found in ref. [5])); for $\rho_l(-k_{ln}^*)$ one has [5])

$$\rho_l(-k_{ln}^*) = -\rho_l(k_{ln})^*. \tag{1.53}$$

Ordering the eigenvalues k_{ln} (and $-k_{ln}^*$) according to increasing moduli, one may therefore write for $U_l - 1$ expansions of the general type †

$$U_l(k) - 1 = {}^M Q_l(k) + k^M \sum_{n=1}^{\infty} \left(\frac{{}^M R_{ln}}{k - k_{ln}} - (-1)^M \frac{{}^M R_{ln}^*}{k + k_{ln}^*} \right), \tag{1.54}$$

where ${}^M Q_l(k)$ is an integral function of k, while the coefficient ${}^M R_{ln}$ is defined by

$${}^M R_{ln} = \varepsilon_{ln} \rho_l(k_{ln}) / k_{ln}^M,$$
$$\varepsilon_{ln} = \begin{cases} 1 & \text{for} \quad \kappa_{ln} \neq 0, \\ \frac{1}{2} & \text{for} \quad \kappa_{ln} = 0. \end{cases} \tag{1.55}$$

Since the property of $U_l(k)$ expressed by eq. (1.29) is exhibited by the term involving the series in the expansion (1.54), it must also belong to the integral function ${}^M Q_l(k)$:

$${}^M Q_l(k)^* = {}^M Q_l(-k^*). \tag{1.56}$$

† In the comparison with ref. [5]) one should be attentive to some differences in the notations; the main expansions in ref. [5]) were written for the amplitude of the scattered wave $\frac{1}{2}(U_l - 1)$.

As none of the poles k_{ln}, $-k_{ln}^*$ lie on the real k-axis, the expansions (1.54) are valid for all real values of k, which are those of physical interest. For such real k, the properties (1.29), (1.56) imply that the real parts of U_l and ${}^MQ_l$, as well as that of the series term, are even functions of k, i.e. functions of the energy E. According to eq. (1.32), this is therefore also the case for the cross sections σ_l. Since, according to eq. (1.52), ${}^MQ_l(0) = 0$, we may also write for real k and E

$$-2 \operatorname{Re} {}^MQ_l(k) = k^2 \, {}^MC_l(E), \tag{1.57}$$

where ${}^MC_l(E)$ is a function of E which is finite for $E = 0$.

In particular, let us consider the case when the smallest value of M is adopted. Introducing the notations

$$\bar{Q} = {}^1Q_l, \qquad \bar{C}_l = {}^1C_l, \qquad \bar{R}_{ln} = {}^1R_{ln}, \tag{1.58}$$

we have the following expansion of the cross section:

$$\sigma_l = \pi(2l+1)\left[\bar{C}_l(E) - 4 \operatorname{Re} \sum_n \frac{\bar{R}_{ln}}{k^2 - k_{ln}^2}\right]. \tag{1.59}$$

The last term may be put into a more explicit form by means of the following notations:

$$\frac{\hbar^2}{2M} k_{ln}^2 \equiv \mathscr{E}_{ln} = E_{ln} - \tfrac{1}{2} i \Gamma_{ln}, \tag{1.60}$$

i.e.

$$E_{ln} = \frac{\hbar^2}{2M} (\kappa_{ln}^2 - \gamma_{ln}^2), \qquad \Gamma_{ln} = \frac{\hbar^2}{2M} 4 \kappa_{ln} \gamma_{ln} \tag{1.61}$$

and

$$-\frac{2\hbar^2}{M} \bar{R}_{ln} = -\varepsilon_{ln} \frac{2\hbar^2}{M k_{ln}} \rho_{ln} \equiv \bar{A}_{ln} + i \bar{B}_{ln}. \tag{1.62}$$

We then have

$$\sigma_l(E) = \pi(2l+1)\left[\bar{C}_l(E) + \sum_{n=1}^{\infty} \frac{\frac{1}{2}\Gamma_{ln} \bar{B}_{ln} + (E - E_{ln}) \bar{A}_{ln}}{(E - E_{ln})^2 + \frac{1}{4}\Gamma_{ln}^2}\right]. \tag{1.63}$$

Another form of expansion for the cross sections σ_l is of course given by the formula (1.23), which, together with eqs. (1.54), becomes

$$\sigma_l = \pi(2l+1)\left|\bar{Q}_l(k) + \sum_{n=1}^{\infty}\left(\frac{\bar{R}_{ln}}{k - k_{ln}} + \frac{\bar{R}_{ln}^*}{k + k_{ln}^*}\right)\right|^2, \tag{1.64}$$

where

$$\bar{Q}_l(k) = \frac{1}{k} {}^1Q_l(k) \tag{1.65}$$

is an integral function of k. Here again, eq. (1.29) may be used to show that

the last factor of eq. (1.64) is a function of k^2 or E, but this expansion is not well adapted to bring out the E-dependence explicitly.

It is also important to observe that none of the above expansions is appropriate to exhibit the behaviour of σ_l at small energies. According to eq. (1.52), the latter behaviour is obtained by taking $M = 2l+1$. Both parts of the expansion (1.54) then have, like U_l-1, a zero of order $2l+1$ at $k = 0$. With the notations

$$Q_l(k) = \frac{{}^{2l+1}Q_l(k)}{k^{2l+1}}, \qquad R_{ln} = {}^{2l+1}R_{ln} = \frac{\bar{R}_{ln}}{k_{ln}^{2l}}, \tag{1.66}$$

we obtain, instead of eq. (1.64),

$$\sigma_l = \pi(2l+1)k^{4l}\left|Q_l(k) + \sum_n \left(\frac{R_{ln}}{k-k_{ln}} + \frac{R_{ln}^*}{k+k_{ln}^*}\right)\right|^2. \tag{1.67}$$

It is also easy to derive an expansion of the type (1.63) showing the small-energy behaviour explicitly; it suffices to take $M = 4l+1$; then, although ${}^{4l+1}Q_l$ has only a zero of order $2l+1$ in $k = 0$, the real part of this quantity is, for real k, a function of E which vanishes like E^{2l+1} at $E = 0$. The two terms of the expansion of σ_l so obtained are then proportional to E^{2l}.

Finally, it is useful to observe here that the two special cases of the expansion (1.54) which have been used to derive eqs. (1.64) and (1.67) may be obtained directly by application of the theorem (1.50) with $M = 0$ to the quantities

$$\bar{S}_l = \frac{1}{k}(U_l-1) \qquad \text{and} \qquad S_l = \frac{1}{k^{2l+1}}(U_l-1), \tag{1.68}$$

respectively.

2. Neutral Particles: Physical Interpretation

2.1. PHYSICAL PROPERTIES OF THE RESONANT STATES

We shall now use the formulae just established for the cross sections to discuss the physical meaning of the complex eigenvalues k_{ln} introduced by the condition (1.33), and of the real quantities E_{ln} and Γ_{ln} derived from them by means of eqs. (1.60), (1.61). The very form of the donominators in the sum over n in the cross section (1.63) shows that E_{ln} and Γ_{ln} (if they are positive) must be associated with the position and width of a resonance level of the compound system formed by the incoming particle and the target nucleus. Although the concept of resonance has its full meaning only when nuclear reactions are treated as many-body processes, we shall nevertheless introduce it here because the main features of resonance are already present in the elastic scattering, as far as the mathematical aspect of the problem is concerned.

This will in fact lead us to a perfectly natural physical formulation of the mathematical problem involved in the theory of nuclear reactions. Moreover, the following considerations may describe an actual physical situation if it is assumed that the potential $v(r)$ is strongly repulsive for r just smaller than a.

According to eq. (1.19b), the boundary condition (1.33) corresponds to a physical situation in which there is no incoming wave. We know that this is the case for a bound state (since for such a state an incoming wave, proportional to $\exp(-ik_n r) = \exp(|\gamma_n| r)$, would increase exponentially with r), and it is quite natural to take this property of "no incoming wave" as characteristic also for the resonant states associated with a compound system of positive energy. This point of view is exactly that adopted by Gamow in his theory of α-decay. Of course, the resonant states defined in this way, in contrast to the actual bound states, will not be completely stationary; they must decay in time according to an exponential law.

2.1.1. *Resonant states*

Let us first consider the physical situation corresponding to a *proper resonant* state k_{ln}, i.e., one for which $\kappa_{ln} > \gamma_{ln} > 0$; both E_{ln} and Γ_{ln} are then positive. In this state, the asymptotic form of the wave function for large r, including the time factor, is proportional to $\exp(ik_{ln} r - i\mathscr{E}_{ln} t/\hbar)$, i.e.

$$\exp[i(\kappa_{ln} r - E_{ln} t/\hbar)] \exp\left(-\frac{\Gamma_{ln} t}{2\hbar}\right) \exp(\gamma_{ln} r), \tag{2.1}$$

where E_{ln} and Γ_{ln} are defined by eqs. (1.61). The first factor of the product (2.1) represents an outgoing wave of wave number κ_{ln} associated with a state of positive energy E_{ln}. The second factor shows that this state decays at the rate $\Gamma_{ln}/\hbar$, which is in conformity with the usual interpretation of the width of a resonance level. Since the velocity of the outgoing particle is

$$v_{ln} = \frac{\hbar \kappa_{ln}}{M}, \tag{2.2}$$

we see that the exponential increase with r of the last factor of the product (2.1) may be interpreted, in a familiar way, as due to the fact that, at a distance r, one finds those particles which left the decaying centre at a time $t - r/v_{ln}$ when the amplitude there was larger by the factor

$$\exp\left(\frac{\Gamma_{ln}}{2\hbar} \frac{r}{v_{ln}}\right) = \exp(\gamma_{ln} r).$$

We must now discuss the physical situation corresponding to the solution $-k_{ln}^* = -\kappa_{ln} - i\gamma_{ln}$ of the boundary condition (1.33). By changing, in the

product (2.1), κ_{ln} into $-\kappa_{ln}$, and consequently Γ_{ln} into $-\Gamma_{ln}$, we obtain

$$\exp\left[-i(\kappa_{ln}r+E_{ln}t/\hbar)\right]\exp\left(\frac{\Gamma_{ln}t}{2\hbar}\right)\exp\left(\gamma_{ln}r\right), \tag{2.3}$$

where E_{ln} and Γ_{ln} are still positive. We now have an incoming wave whose amplitude increases with time. This result means that the eigenfunction corresponding to $-k_{ln}^*$ is simply related to that corresponding to k_{ln} by time reversal.

Indeed, a purely decaying state is characterized just as well by putting equal to zero the amplitude of the incoming part of the wave function Ψ, or the amplitude of the outgoing part of the time-reverse $\Phi \equiv K\Psi$. Now, if the Hamiltonian operator is invariant for time-reversal, and the energy E complex, the function Φ is a solution of the equation $H\Phi = E^*\Phi$. The resonant state is therefore defined by the condition

$$W(u_l, I_l; a, k_{ln}^*) = 0 \tag{2.4}$$

as well as by

$$W(u_l, O_l; a, k_{ln}) = 0.$$

We see from eqs. (1.25), (1.27) that these two conditions are identical. The former will give a purely ingoing $\Phi_l = K\Psi_l$ wave and the latter a purely outgoing Ψ_l wave.

Consequently, we must consider k_{ln} and $-k_{ln}^*$ associated not with two different resonant states, but with a single one only. This conclusion explains why in eq. (1.63) we could associate k_{ln} with $-k_{ln}^*$ in a single resonance term.

2.1.2. *Bound states and virtual states*

Let us now discuss the levels k_{ln} for which $E_{ln} \leqq 0$, i.e., $|\gamma_{ln}| \geqq \kappa_{ln} \geqq 0$. It may be that there is no level of this type associated with a given potential $v(r)$, but examples of the actual occurrence of such eigenvalues are known. Anyway, their number is always finite because, for large $|k_{ln}|$, i.e. large n, we have [5]) $\kappa_{ln} = \mathrm{O}(n)$ and $\gamma_{ln} = \mathrm{O}(\log n)$.

Firstly, we may have eigenvalues corresponding to *bound states*. Then $-\gamma_{ln} = \mathrm{Im}\, k_{ln} > 0$, $\kappa_{ln} = 0$ and therefore

$$E_{ln} = -\gamma_{ln}^2, \qquad \Gamma_{ln} = 0.$$

For $l = 0$, for instance, the corresponding term in the cross section (1.63) is

$$\frac{\pi \bar{A}_{0n}}{E-E_{0n}} = \frac{\pi \bar{A}_{0n}}{E+|E_{0n}|}; \tag{2.5}$$

it takes its maximum value for $E = 0$. It is well known that the ^{3}S bound state of the deuteron gives a contribution of this type to the proton-neutron scattering cross section at low energies.

Secondly, we may have negative E_{ln} with positive γ_{ln}, if $\frac{3}{2}\pi \leqq \arg k_n \leqq \frac{7}{4}\pi$, so that $0 \leqq \kappa_n \leqq \gamma_n$ and hence

$$E_{ln} \leqq 0, \qquad \Gamma_{ln} \geqq 0;$$

$\arg(-k_n^*)$ is then in the interval $(\frac{5}{4}\pi, \frac{3}{2}\pi)$. An example of such a level is also provided by the proton-neutron system, whose ^{1}S state is of the type $k_n = -i\gamma_n (\gamma_n > 0)$; its contribution to the cross section is again an expression of the form (2.5).

More examples of levels which are not bound although $E_{ln} < 0$, and additional information about their physical meaning, will be found in the recent papers by Nussenzveig [11]) and by Beck and Nussenzveig [12]). To distinguish them from the proper resonant states, such levels may be called *virtual*; the corresponding terms in eq. (1.63) have to be added to those associated with the true resonances in order to give a complete expression for the cross section. Of course we could also suppose these terms to be removed from the resonant part and added to the non-resonant part $\bar{C}_l$. However, we shall not do so, at least when exact formulae are concerned, because this would destroy the analytic definition of this separation into resonant and non-resonant part. Moreover, there is experimental evidence [13]) in favour of negative energy "resonances" of the type corresponding to virtual states with $\Gamma_{ln} > 0$; they give rise to a very pronounced increase of the cross section when the energy E goes to zero.

2.1.3. *Potential scattering*

According to its mathematical definition as integral function, the non-resonant term $\bar{Q}_l$ is a smoothly varying function of k. We may consider it as corresponding to the well-known *potential scattering* term present in other theories, although it is not here related to the scattering by a hard sphere of radius a. On the contrary, *it has the same independence of a as the positions of the levels k_n themselves*. This is not the case when, instead of expanding according to the Mittag-Leffler theorem, one applies the Cauchy theorem [14]) to expand the product $U_0 e^{2ika}$, or more generally $U_l O_l(a, k)/I_l(a, k)$. For this reason, we have abandoned the use of such expansions, which were considered in refs. [7, 15]).

Because one may choose different values for the exponent M, the separation between potential scattering and resonance scattering is not unique; each choice of M corresponds to a different separation of the two contributions. In practice, this ambiguity (which is obviously inherent in the whole conception of the resonance process and quite general) might be used to facilitate the fitting of the theoretical cross section to the experimental data: it gives more freedom than the usual definition of the potential scattering to adjust the "background"

against which the resonances are determined. If one is concerned with the behaviour of the cross section at small energies, there is, as we have seen, a definite choice of M which makes this behaviour explicit.

2.1.4. *Case of no potential*

In concluding this discussion, we want to point out that a very strong argument in favour of the definition of the resonant states adopted here is that *it gives no resonant states when there is no potential.* This is a consequence of the fact that the corresponding function u_l is simply $\mathcal{J}_l(kr)/k^{l+1}$, for which

$$W(u_l, O_l; a, k) = -\frac{1}{k^l}.$$

In other formalisms [2, 3]) the boundary conditions adopted define resonant states also for $v(r) \equiv 0$, which is of course less satisfactory.

2.2 THE BREIT-WIGNER APPROXIMATION

It is easy to prove [5]) that if a resonant state k_n is such that

$$\gamma_n \ll |\kappa_n - \kappa_{n\pm1}| \tag{2.6a}$$

and if $2\kappa_n$ is of the order of $\kappa_{n+1}+\kappa_{n-1}$, it may be considered "narrow", i.e.

$$\gamma_n \ll \kappa_n, \tag{2.6b}$$

$$\Gamma_n \ll E_{n+1} - E_{n-1}. \tag{2.6c}$$

As in ref. [5]) it can be shown that for such a narrow level one has approximately

$$\bar{A}_{ln} = 0, \qquad \bar{B}_{ln} = \frac{2\Gamma_{ln}}{|k_{ln}|^2}, \tag{2.7}$$

so that in this approximation the contribution of this level to the resonance part of the cross section (1.63) is

$$\frac{4\pi(2l+1)}{|k_{ln}|^2} \frac{\frac{1}{4}\Gamma_{ln}^2}{(E-E_{ln})^2 + \frac{1}{4}\Gamma_{ln}^2}. \tag{2.8}$$

For $E \approx E_{ln}$, this term will be the principal one in the cross section; it is then approximately equal to the Breit-Wigner cross section.

The same conclusion may be reached in quite a different way, which has the advantage of showing explicitly that the asymmetric term in $\bar{A}_{ln}\,(E-E_{ln})$ in the cross section (1.63) mainly corresponds to the interference between the potential scattering and the resonance scattering terms appearing in the cross section (1.64). This we shall now see by proving that $\bar{A}_{ln}$ vanishes when the potential scattering is neglected.

Let us assume that in a finite range of energy the scattering matrix (1.54), for $M = 1$, may be written in the form

$$U_l = 1+k\bar{Q}_l(k)+k\left(\frac{\bar{R}_{ln}}{k-k_{ln}}+\frac{\bar{R}^*_{ln}}{k+k^*_{ln}}\right), \tag{2.9}$$

where the contributions of the resonant states $n' \neq n$ have been neglected or incorporated in the potential scattering. From the property (1.28) it is evident that the scattering matrix U_l is zero for $k = -k_n$:

$$1-k_n\bar{Q}_l(-k_n)+\tfrac{1}{2}\bar{R}_{ln}+\frac{k_n\bar{R}^*_{ln}}{k_n-k^*_n} = 0. \tag{2.10}$$

One has also $U_l = 0$ for $k = k_n^*$, but because of eq. (1.29) this leads to the same relation. Eq. (2.10) may be used to obtain $\bar{A}_{ln}$ and $\bar{B}_{ln}$, defined by eq. (1.62), in the form

$$\bar{A}_{ln} = \frac{2\Gamma_n}{\kappa_n^2}\,\mathrm{Im}\,[1-k_n\bar{Q}_l(-k_n)], \tag{2.11a}$$

$$\bar{B}_{ln} = \frac{2\Gamma_n}{\kappa_n^2}\,\mathrm{Re}\,[1-k_n\bar{Q}_l(-k_n)]-\frac{2M}{\hbar^2}\left(\frac{\Gamma_n}{\kappa_n^2}\right)^2\mathrm{Im}\,[1-k_n\bar{Q}_l(-k_n)]. \tag{2.11b}$$

When the contribution $k_n\bar{Q}_l(-k_n)$ from the potential scattering is neglected, the corresponding values of $\bar{A}_{ln}$ and $\bar{B}_{ln}$ simply become those given by eqs. (2.7).

The preceding results also show that if the potential scattering $\bar{Q}_l(k)$ is known (or neglected), the behaviour of the cross section near a resonance is entirely determined by two parameters only, e.g. the position E_{ln} of the maximum and the width Γ_{ln}. Similar approximations could be investigated for a multilevel form of U_l, but the computation of the coefficients $\bar{A}_{ln}$, $\bar{B}_{ln}$. in terms of the E_{ln}, Γ_{ln} becomes very tedious.

2.3. ANOTHER EXPANSION OF THE SCATTERING MATRIX

Let us return to the expansion (1.54) of U_l. One may regret, firstly that it is expressed in terms of k rather than in terms of the energy E, and secondly that in each term of the series only the first part $R_{ln}/(k-k_{ln})$ is a true term of resonance, while the second part has a modulus which is a monotonic function of k.

It is indeed possible to expand U_l in terms of E and at the same time to transfer the contribution of these second parts to the potential scattering. For this purpose, let us regard U_l as a function of the complex variable $E = \hbar^2k^2/2M$ and let us name the corresponding complex plane the E-plane. The scattering matrix has a branch point at $E = 0$; to remove this ambiguity we introduce a cut along the negative real axis of the E-plane. Let us make the

domain defined by

$$-\pi \leqq \arg E \leqq +\pi \tag{2.12a}$$

correspond to the half k-plane in which

$$-\tfrac{1}{2}\pi \leqq \arg k \leqq +\tfrac{1}{2}\pi, \tag{2.12b}$$

a region which contains the poles k_n, but not the poles $-k_n^*$. When there are poles on the imaginary k-axis, these, as well as the corresponding ones on the negative axis of the E-plane, may be included in the half k-plane considered.

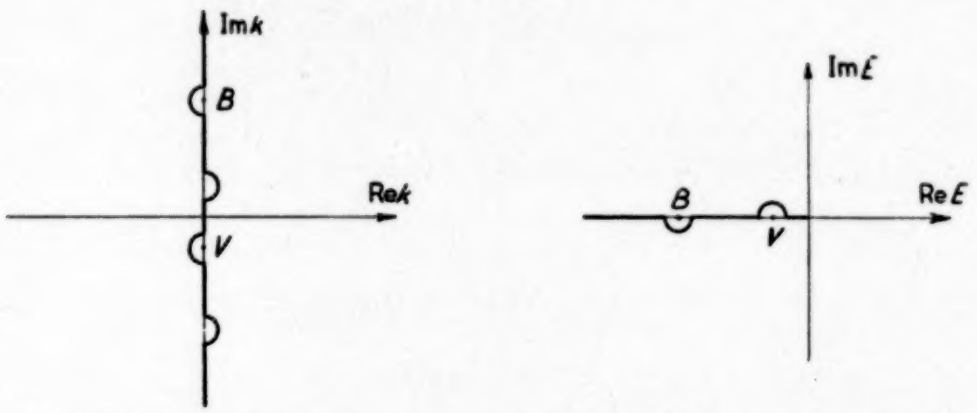

Fig. 1. The half k-plane and the corresponding E-plane when there are poles on the imaginary axis. B = bound state, V = virtual state of deuteron type.

Fig. 1 shows how this can be done. Two poles on the imaginary k-axis will never be symmetrical about the real k-axis; for if $k_n = i\gamma_n$ is a pole of U_l, then $-i\gamma_n$ will be a zero of U_l.

We may now use in the *cut* E-plane expansions of exactly the same form as eq. (1.50); the function $\varepsilon(E)$ is now only defined as a regular function of E in the cut E-plane. The residue of U_l at the pole $\mathscr{E}_{ln}$ is simply related to its residue ρ_{ln} at the pole k_{ln} by the factor $(\hbar^2/2M)2k_{ln}$. Rather than to consider directly an expansion of $U_l - 1$, however, it is convenient to start from expansions of the quantities $\bar{S}_l$ or S_l defined by eq. (1.68): in this way we include in the resulting expansions for the cross sections the factor k^{-2} occurring in their definitions (1.22), (1.23); the expansions of S_l will moreover yield the explicit small-energy behaviour of the cross sections.

For the quantity $\bar{S}_l$, the theorem (1.50) gives for $M = 0$ an expansion of the form

$$\bar{S}_l = \tilde{c}_l(E) + \sum_n \frac{\tilde{r}_{ln}}{E - E_{ln} + \frac{1}{2}i\Gamma_{ln}}, \tag{2.13}$$

where

$$\tilde{r}_{ln} = \frac{\hbar^2}{M} k_{ln} \bar{R}_{ln}; \tag{2.14a}$$

hence

$$U_l = 1 + \left(\frac{2ME}{\hbar^2}\right)^{\frac{1}{2}}\left[\bar{c}_l(E) + \sum_n \frac{\bar{r}_{ln}}{E - E_{ln} + \frac{1}{2}i\Gamma_{ln}}\right], \tag{2.15a}$$

$$\sigma_l = \pi(2l+1)\left|\bar{c}_l(E) + \sum_n \frac{\bar{r}_{ln}}{E - E_{ln} + \frac{1}{2}i\Gamma_{ln}}\right|^2. \tag{2.16a}$$

Applying the theorem (1.50), for $M = 0$, to the expansion of S_l, one gets similarly

$$U_l = 1 + \left(\frac{2ME}{\hbar^2}\right)^{l+\frac{1}{2}}\left(c_l(E) + \sum_n \frac{r_{ln}}{E - E_{ln} + \frac{1}{2}i\Gamma_{ln}}\right), \tag{2.15b}$$

$$\sigma_l = \pi(2l+1)\left(\frac{2ME}{\hbar^2}\right)^{2l}\left|c_l(E) + \sum_n \frac{r_{ln}}{E - E_{ln} + \frac{1}{2}i\Gamma_{ln}}\right|^2, \tag{2.16b}$$

where

$$r_{ln} = \frac{\hbar^2}{M} k_{ln} R_{ln} = \frac{\bar{r}_{ln}}{k_{ln}^{2l}}. \tag{2.14b}$$

Now, the inequality (2.12a) also implies

$$-\pi \leqq \arg E^* \leqq \pi, \tag{2.12c}$$

and we therefore still have, in the cut E-plane, a unitarity relation for U_l in the form

$$U_l(E^*)^* U_l(E) = 1. \tag{2.17}$$

We could therefore introduce in the cross section (1.32) the forms (2.15) of U_l which would give for σ_l expansions similar to that given by eq. (1.63). From eq. (2.17), we also derive the property

$$U_l(E_{ln} + \tfrac{1}{2}i\Gamma_{ln}) = 0, \tag{2.18}$$

which easily leads to the Breit-Wigner approximation discussed in subsection 2.2.

In the cut E-plane there are no relations corresponding to those expressed by eqs. (1.29), (1.28) and (1.56): such relations would introduce arguments of E which do not satisfy the condition (2.12a). However, one may write such relations in an E-plane composed of two Riemann sheets and corresponding to the whole complex k-plane. Then one obtains expansions of the following type †:

$$\bar{S}_l = \bar{Q}_l(k) + \sum_{n=1}^{\infty}\left[\frac{(k + k_{ln})s_{ln}}{E - E_{ln} + \frac{1}{2}i\Gamma_{ln}} + \frac{(k - k_{ln}^*)s_{ln}^*}{E - E_{ln} - \frac{1}{2}i\Gamma_{ln}}\right],$$
$$s_{ln} = \varepsilon_{ln}\rho_{ln}\frac{\hbar^2/2M}{k_{ln}}, \tag{2.19}$$

† See Peierls' paper [6]), particularly p. 21.

where $\bar{S}_l$ and k are double-valued quantities. Clearly, this leads for $U_l - 1$ to an expansion identical with our expansion (1.54) with $M = 1$.

From the foregoing discussion we conclude that in the present case

1) the treatments in a k-plane and in a single E-plane with a cut provide different expansions of the scattering matrix, which are equally well adapted to a description of resonance phenomena;

2) the treatments in a k-plane and in a double E-plane without a cut provide exactly the same expansions.

3. Elastic Scattering of Charged Particles

We now assume that the scattered particles and the target nuclei have the electric charges $Z_1 e$ and $Z_2 e$ respectively. It is well known that in order to be able to define outgoing and incoming waves that are single-valued functions of the complex wave number k, one has to cut off the Coulomb potential at some finite distance $r = b$. We may take this distance b of the order of magnitude of the atomic radius, corresponding to the cut off of the Coulomb field due to the screening effect of the atomic electrons. The radial factor of the partial wave function will then satisfy the equations

$$\left[\frac{d^2}{dr^2} + k^2 - \frac{l(l+1)}{r^2} - v(r)\right] u_l = 0 \qquad \text{for} \qquad 0 \leqq r < a, \tag{3.1a}$$

$$\left[\frac{d^2}{dr^2} + k^2 - \frac{l(l+1)}{r^2} - \frac{2\eta}{r}\right] u_l = 0 \qquad \text{for} \qquad a \leqq r \leqq b, \tag{3.1b}$$

$$\left[\frac{d^2}{dr^2} + k^2 - \frac{l(l+1)}{r^2}\right] u_l = 0 \qquad \text{for} \qquad r > b, \tag{3.1c}$$

$$u_l(0, k) = 0, \tag{3.2}$$

where

$$\eta = Z_1 Z_2 e^2 \frac{M}{\hbar^2}. \tag{3.3}$$

The outgoing and incoming radial waves O_l, I_l are solutions of eqs. (3.1b) and (3.1c). For $r \geqq b$ we may still define them by eqs. (1.12) as in the preceding sections. Consequently, all the considerations and results of sections 1 and 2 are still valid in the present case *provided that b is everywhere substituted for a*. This is true in particular of the expressions (1.19) for the amplitudes, the expression (1.20) for the scattering matrix, the definition (1.33) of the resonant states, and their location in the complex k-plane. The expansion of the scattering matrix in the form (1.54) is also justified without further investigation.

It is not very satisfactory, however, to define the resonant states of a nuclear

system by a boundary condition at the surface of the atom. We shall now see that the appropriate definition of the outgoing and incoming waves in the interval (a, b) makes possible a description of nuclear scattering in terms of physical quantities taken on the "nuclear surface" $r = a$.

Let us introduce in the interval (a, b) two auxiliary Coulomb wave functions $f_l^{(1)}$, $f_l^{(2)}$, defined as solutions of the equation

$$\left[\frac{\mathrm{d}^2}{\mathrm{d}r^2} + k^2 - \frac{l(l+1)}{r^2} - \frac{2\eta}{r}\right] f_l^{(j)} = 0 \qquad (j = 1, 2) \tag{3.4}$$

and satisfying the boundary conditions

$$f_l^{(1)}(a, k) - 1 = f_l^{(1)\prime}(a, k) = 0, \tag{3.5a}$$

$$f_l^{(2)}(a, k) \qquad = f_l^{(2)\prime}(a, k) - 1 = 0. \tag{3.5b}$$

They are real and integral functions of k^2 for $a \leqq r \leqq b$ and consequently have the properties

$$f_l^{(j)}(r, k) = f_l^{(j)}(r, -k), \tag{3.6}$$

$$f_l^{(j)}(r, k)^* = f_l^{(j)}(r, k^*) = f_l^{(j)}(r, -k^*). \tag{3.7}$$

They are linearly independent because

$$W(f_l^{(1)}, f_l^{(2)}; r) = W(f_l^{(1)}, f_l^{(2)}; a) = 1; \tag{3.8}$$

therefore, in the interval (a, b) the outgoing and incoming waves O_l, I_l are necessarily linear combinations of such functions. Matching these linear combinations with the radial waves (1.12) at $r = b$, we immediately see that, for $a \leqq r \leqq b$,

$$O_l(r, k) = -iW(f_l^{(2)}, \mathscr{H}_l^{(1)}; b) f_l^{(1)}(r, k) + iW(f_l^{(1)}, \mathscr{H}_l^{(1)}; b) f_l^{(2)}(r, k), \tag{3.9a}$$

$$I_l(r, k) = iW(f_l^{(2)}, \mathscr{H}_l^{(2)}; b) f_l^{(1)}(r, k) - iW(f_l^{(1)}, \mathscr{H}_l^{(2)}; b) f_l^{(2)}(r, k). \tag{3.9b}$$

But, from the evident relation

$$f_l^{(j)} \mathscr{H}_l^{(k)\prime\prime} - f_l^{(j)\prime\prime} \mathscr{H}_l^{(k)} = -\frac{2\eta}{r} f_l^{(j)} \mathscr{H}_l^{(k)} \tag{3.10}$$

we deduce

$$W(f_l^{(j)}, \mathscr{H}_l^{(k)}; b) = W(f_l^{(j)}, \mathscr{H}_l^{(k)}; a) - 2\eta \int_a^b r^{-1} f_l^{(j)} \mathscr{H}_l^{(k)} \mathrm{d}r, \tag{3.11}$$

and hence

$$O_l(a, k) = -iW(f_l^{(2)}, \mathscr{H}_l^{(1)}; b) = i\left[\mathscr{H}_l^{(1)}(ka) + 2\eta \int_a^b r^{-1} f_l^{(2)} \mathscr{H}_l^{(1)} \mathrm{d}r\right], \tag{3.12a}$$

$$O'_l(a, k) = iW(f_l^{(1)}, \mathscr{H}_l^{(1)}; b) = i\left[\mathscr{H}_l^{(1)\prime}(ka) - 2\eta \int_a^b r^{-1} f_l^{(1)} \mathscr{H}_l^{(1)} \mathrm{d}r\right], \tag{3.12b}$$

$$I_l(a, k) = iW(f_l^{(2)}, \mathscr{H}_l^{(2)}; b) = -i\left[\mathscr{H}_l^{(2)}(ka) + 2\eta \int_a^b r^{-1} f_l^{(2)} \mathscr{H}_l^{(2)} \mathrm{d}r\right], \quad (3.13a)$$

$$I'_l(a, k) = -iW(f_l^{(1)}, \mathscr{H}_l^{(2)}; b) = -i\left[\mathscr{H}_l^{(2)\prime}(ka) - 2\eta \int_a^b r^{-1} f_l^{(1)} \mathscr{H}_l^{(2)} \mathrm{d}r\right]. \quad (3.13b)$$

Defining the function $G_l(r, r')$ by

$$G_l(r, r') = f_l^{(1)}(r, k) f_l^{(2)}(r', k) - f_l^{(1)}(r', k) f_l^{(2)}(r, k), \quad (3.14)$$

we see that the function (3.9a) may also be written as

$$O_l(r, k) = i\left[\mathscr{H}_l^{(1)}(kr) + 2\eta \int_r^b r'^{-1} G_l(r, r') \mathscr{H}_l^{(1)}(kr') \mathrm{d}r'\right], \quad (3.15a)$$

because the function on the right-hand side of eq. (3.15a) satisfies the same differential equation as the function (3.9a) and its value and derivative at $r = a$ are also given by the right-hand sides of eqs. (3.12). Similarly one has

$$I_l(r) = -i\left[\mathscr{H}_l^{(2)}(kr) + 2\eta \int_r^b r'^{-1} G_l(r, r') \mathscr{H}_l^{(2)}(kr') \mathrm{d}r'\right]. \quad (3.15b)$$

From the properties (3.6) and (3.7) of the functions $f_l^{(j)}$ it is evident that the functions O_l, I_l have the following properties for $a \leqq r \leqq b$ as well as for $r > b$:

$$O_l(k^*)^* = I_l(k), \qquad I_l(k^*)^* = O_l(k), \quad (3.16a)$$

$$O_l(-k) = (-1)^l I_l(k), \qquad I_l(-k) = (-1)^l O_l(k), \quad (3.16b)$$

whence also

$$O_l(-k^*) = (-1)^l O_l(k)^*, \qquad I_l(-k^*) = (-1)^l I_l(k)^*. \quad (3.17)$$

In practical calculations, the functions $f_l^{(1)}$, $f_l^{(2)}$ introduced here will be expressed as linear combinations of the usual Coulomb wave functions, i.e., the Whittaker functions corresponding to outgoing and incoming waves, or the regular and irregular functions usually denoted F_l, G_l. The matching of such linear combinations with $f_l^{(1)}$ and $f_l^{(2)}$ is easily made at $r = a$, as a consequence of the conditions (3.5). Further, we still have

$$W(O_l, I_l; r, k) = -2ik. \quad (3.18)$$

The functions O_l, I_l, u_l being solutions of the same equation in the interval $a \leqq r \leqq b$, the Wronskians $W(u_l, O_l; r)$ and $W(u_l, I_l; r)$ are also independent of r, and we have in particular

$$W(u_l, O_l; a) = W(u_l, O_l; b), \qquad W(u_l, I_l; a) = W(u_l, I_l; b). \quad (3.19)$$

These relations have the following consequences: all the results of the preceding sections, such as the expression for the collision matrix

$$U_l = \frac{W(u_l, I_l; a, k)}{W(u_l, O_l; a, k)} \quad (3.20)$$

and the definition of the resonant states

$$W(u_l, O_l; a, k) = 0 \tag{3.21}$$

may be applied to the present case *without substitution of b for a* provided that the expressions (3.15) for the outgoing and incoming radial waves are used instead of those given by eqs. (1.12).

For the discussion of the properties of the resonant states it is important to observe that the property expressed by eq. (1.42) holds in the present case, whether or not a is replaced by b. In fact, if we define

$$L_l(k) \equiv \frac{O'_l(a, k)}{O_l(a, k)}, \tag{3.22}$$

we have

$$L_l(k) - L_l(k)^* = \frac{1}{|O_l|^2} W(O_l^*, O_l; a, k),$$

or, in virtue of the identity

$$W(O_l^*, O_l; b, k) - W(O_l^*, O_l; a, k) = \int_a^b (O_l'' O_l^* - O_l^{*\prime\prime} O_l)\, dr$$
$$= (k^{*2} - k^2) \int_a^b |O_l|^2\, dr$$

and the fact that

$$O_l(b) \equiv i\mathscr{H}_l^{(1)}(b), \qquad O'_l(b) \equiv i\mathscr{H}_l^{(1)\prime}(b), \tag{3.23}$$

the equivalent expression

$$|O_l(a)|^2[L_l(k) - L_l(k)^*] = W(\mathscr{H}_l^{(1)*}, \mathscr{H}_l^{(1)}; b, k) + (k^2 - k^{*2}) \int_a^b |O_l(r)|^2 dr.$$

With the help of eq. (1.42), in which a is replaced by b, this indeed yields a relation of the same form,

$$|O_l(a, k_n)|^2[L_l(k_n) - L_l(k_n)^*] = i(k_n + k_n^*)|\mathscr{H}_0^{(1)}(k_n b)|^2$$
$$+ (k_n^2 - k_n^{*2}) \left[\int_a^b |O_l(r, k_n)|^2 dr + \mathscr{N}_{ln}(b)\right]. \tag{3.24}$$

The same argument as in subsection 1.3 leads for γ_n, when $\kappa_n \neq 0$, to the essentially positive expression

$$2\gamma_n = \frac{|u_{ln}(a)/O_l(a, k_n)|^2 |e^{ik_n b}|^2}{\int_0^a |u_{ln}(r)|^2 dr + \left|\frac{u_{ln}(a)}{O_l(a, k_n)}\right|^2 \left[\int_a^b |O_l(r, k_n)|^2 dr + \mathscr{N}_{ln}(b)\right]}. \tag{3.25}$$

In the expression (3.25), however, the exponential factor $\exp(2\gamma_n b)$ in the numerator seems to give the physically irrelevant parameter b undue influence on the value of γ_n: actually, of course, this factor is compensated by the similar increase with b of the denominator. It is therefore advisable to transform the formula (3.25) so as to remove the explicit occurrence of the factor in question.

This is readily achieved by observing that the decomposition of the right-hand side of eq. (3.24) into two terms respectively proportional to

$$i(k_n+k_n^*) = 2i\kappa_n \qquad \text{and} \qquad k_n^2-k_n^{*2} = -2i\kappa_n \cdot 2\gamma_n$$

is obviously not unique; thus, by writing

$$|\mathscr{H}_0^{(1)}(k_n b)|^2 = |e^{ik_n b}|^2 = 1+2\gamma_n \int_0^b |e^{ik_n r}|^2 dr, \tag{3.26}$$

we get a new decomposition of the same form, from which the terms exhibiting the unwanted increase with b have disappeared:

$$|O_l(a, k_n)|^2[L_l(k_n)-L_l(k_n)^*] = 2i\kappa_n[1-2\gamma_n N_{ln}(a)], \tag{3.27}$$

with

$$N_{ln}(a) = \int_a^b |O_l(r, k_n)|^2 dr - \int_0^b |e^{ik_n r}|^2 dr + \mathscr{N}_{ln}(b). \tag{3.28}$$

This gives for γ_n the new formula, of the same type as (3.25),

$$2\gamma_n = \frac{|u_{ln}(a)/O_l(a, k_n)|^2}{\int_0^a |u_{ln}(r)|^2 dr + \left|\frac{u_{ln}(a)}{O_l(a, k_n)}\right|^2 N_{ln}(a)}; \tag{3.29}$$

it is no longer assured that the coefficient $N_{ln}(a)$ is non-negative, but it is clear that the denominator of the expression (3.29) is still positive. In other words, we use the decomposition (3.24) to prove that γ_n is positive, and we conclude from this result that the equivalent expression (3.29) with the value (3.28) of the coefficient $N_{ln}(a)$ also has the property of being the ratio of two essentially positive quantities.

In conclusion, we may mention explicitly that the "a-independence property" of the resonant states k_n still holds. In fact, for any $x \geqq a$, the solutions of the equation

$$W(u_l, O_l; x, k) = 0 \tag{3.30}$$

are independent of x because u_l and O_l are two solutions of the same equation for such values of x. Of course this presupposes that the potential remains the same for different choices of x: it must be $v(r)$ for $r < a$, $2\eta/r$ for $a \leqq r \leqq b$ and zero for $r > b$.

Part II: THE GENERAL CASE OF NUCLEAR REACTIONS

4. The Configuration Space

4.1. GENERAL ASSUMPTIONS AND NOTATIONS

Our general assumptions will be the same as those made by Lane and Thomas [2] in their review article on the R-matrix formalism: conservation of

probability, time reversibility and causality in the framework of non-relativistic mechanics.

Whenever possible, we shall adopt the same notations as Lane and Thomas [2]) in order to facilitate reference to their paper if more details are wanted about the configuration space, the elimination of the barycentre motion, the channel-spin wave functions, the wave functions of the relative motion, and the definition and properties of the collision matrix. These topics, which are of course independent of the R-matrix formalism, are discussed only briefly in the following.

The discussion of channel wave-functions and boundary conditions in this section is in all essentials also the same as that adopted by C. Bloch [16]).

4.2. REACTION CHANNELS

We shall call *channel* a situation in which the total system of A nucleons we are considering is separated into two fragments, containing A_1 and A_2 nucleons respectively, each of which is in a definite stationary state, while their state of relative motion is also specified. For simplicity, we shall confine the discussion to reactions involving only channels of this restricted type, i.e., reactions in which only two nuclear systems interact to form two other such systems, without any creation or annihilation of particles; photons are also excluded from the discussion.

The state of each fragment A_j is characterized by a total spin quantum number I_j, its projection i_j on some fixed direction in space, and a set of other quantum numbers specifying the energy of the state, which we denote by α_j. Instead of i_1, i_2, we may also use the quantum numbers s, ν specifying the channel spin

$$\mathbf{s} = \mathbf{I}_1+\mathbf{I}_2, \qquad |I_1-I_2| \leqq s \leqq I_1+I_2 \tag{4.1}$$

and its projection ν on the fixed axis. We shall consider states of relative motion of definite orbital momentum $\mathbf{l}$, with quantum numbers l, m. Because of the conservation of the total angular momentum $\mathbf{J} = \mathbf{l}+\mathbf{s}$, of quantum numbers J, M, we may replace the quantum numbers ν, m by J, M in the definition of the channel. We shall thus understand the channel symbol c to represent any one of the sets of quantum numbers

$$\{\alpha_1\alpha_2(I_1I_2)i_1i_2, lm\}, \qquad \{\alpha_1\alpha_2(I_1I_2)s\nu, lm\}, \qquad \{\alpha_1\alpha_2(I_1I_2)sl, JM\}.$$

For each mode of subdivision into two fragments A_1, A_2, we use an appropriate set of coordinates, to which we attach an index chosen as the same letter α by which we denote the states of excitation α_1, α_2 of the fragments. Thus, we shall take for the two fragments sets of internal coordinates q_{α_1}, q_{α_2} (including the spin coordinates of the individual nucleons), and relative position coordi-

nates $\mathbf{r}_\alpha$ of their barycentres. The motion of the barycentre of the total system is, as usual, eliminated.

The possibility of treating the two fragments as separated results from the limited range of the nuclear forces; in other words, if r_α denotes the distance between the barycentres of the two fragments, there exists a distance a_α, the "channel radius", such that for $r_\alpha > a_\alpha$ only non-polarizing forces (in fact, only Coulomb forces) act between the fragments. As in the preceding section, we shall cut off the Coulomb potential at some distance b_α of the order of atomic dimensions. The radii a_α and b_α are, of course, introduced only for mathematical convenience, and will not be allowed to play any essential physical part in our theory.

4.3. INTERIOR AND EXTERIOR REGIONS

The positions of the A nucleons can be represented by a single point in a configuration space of $3A$ dimensions. The region of this space corresponding to the A nucleons being close together in physical space is called the *interior region*; more precisely, under the simplified conditions adopted here (ignoring the possible splitting into more than two fragments), the interior region is defined as the part of the configuration space in which

$$r_\alpha < a_\alpha \qquad \text{for all } \alpha. \tag{4.2}$$

The *boundary surface* of the interior region is then composed of an assembly of parts of the surfaces $r_\alpha = a_\alpha$. Any point which is not in the interior region or on its boundary surface $\mathscr{S}$ is said to be in the *exterior region.*

To be really useful, this distinction of interior and exterior regions must be applied to a configuration space in which one more coordinate, the spin coordinate, is added to the space coordinates of each nucleon. The interior region is then still defined by the conditions (4.2).

Let $\mathscr{S}_\alpha$ denote the portion of the surface $r_\alpha = a_\alpha$ which is part of the boundary surface $\mathscr{S}$. In this sense we think of the surface $\mathscr{S}$ as composed of partial surfaces $\mathscr{S}_\alpha$ such that a point of the configuration space lying in the exterior region just outside $\mathscr{S}_\alpha$ corresponds to the subdivision α of the A nucleons. We shall then have $\mathscr{S} = \sum_\alpha \mathscr{S}_\alpha$, and an element of the surface $\mathscr{S}_\alpha$ will be defined by

$$\mathrm{d}\mathscr{S}_\alpha = a_\alpha^2 \mathrm{d}\Omega_\alpha \mathrm{d}q_{\alpha_1} \mathrm{d}q_{\alpha_2}, \tag{4.3}$$

where $\mathrm{d}\Omega_\alpha$ is the element of solid angle corresponding to the relative angular position of the pair α, and where $\mathrm{d}q_{\alpha_j}$ corresponds to the internal coordinates of the fragment A_j. A symbolic integration over $\mathrm{d}\mathscr{S}_\alpha$ implies not only an integration over the internal space coordinates, but also a summation over the spin coordinates of the individual nucleons.

5. The Wave-function in the Exterior Region

5.1. DECOMPOSITION OF THE WAVE-FUNCTION IN RADIAL AND SURFACE FACTORS

In a channel c, the total wave-function Ψ_c may in the first instance be analysed into two factors, pertaining respectively to the internal state of the fragments and to their relative motion. Owing to the spin degeneracy in the external region, where the fragments only interact through the Coulomb potential, the internal wave-functions $\psi_{\alpha_1 I_1 i_1}$, $\psi_{\alpha_2 I_2 i_2}$ of the fragments may be grouped into a channel-spin wave-function

$$\psi_{\bar{\alpha}sv} = \sum_{i_1+i_2=v} (I_1 i_1, I_2 i_2 | sv) \psi_{\alpha_1 I_1 i_1} \psi_{\alpha_2 I_2 i_2} \tag{5.1}$$

completely characterizing the internal state of the system; in this and later formulae, symbols like $(I_1 i_1, I_2 i_2|sv)$ denote Clebsch-Gordan coefficients and $\bar{\alpha}$ is written for $\alpha_1 \alpha_2$, while indices $I_1 I_2$ are generally omitted.

The states of relative motion of the two fragments may be represented by products of spherical harmonics $i^l Y_m{}^l(\Omega_\alpha)$ and radial components $u_c(r_\alpha)/r_\alpha$. It is convenient to single out the radial factor and to group together the other two into a "surface factor" embodying the dependence of the wave-function on all coordinates except the relative distance r_α. For this surface factor we may write, in the representation $\{\bar{\alpha}sv, lm\}$,

$$\varphi_{\bar{\alpha}sv,\, lm} = i^l Y_m{}^l \psi_{\bar{\alpha}sv}, \tag{5.2a}$$

or in the representation $\{\bar{\alpha}sl, JM\}$,

$$\varphi_{\bar{\alpha}sl,\, JM} = \sum_{v+m=M} (sv, lm|JM) \varphi_{\bar{\alpha}sv,\, lm}. \tag{5.2b}$$

For all channels corresponding to the mode of fragmentation α, the surface functions φ_c may be chosen to form an orthonormal set of the usual kind, which may be assumed to be complete in the subspace of all coordinates except r_α. In this subspace, we write the orthonormality relation in the form

$$\int \varphi_c{}^* \varphi_{c'} \, \mathrm{d}S_\alpha = \delta_{cc'}, \tag{5.3}$$

with

$$\mathrm{d}S_\alpha = \frac{\mathrm{d}\mathscr{S}_\alpha}{a_\alpha{}^2} = \mathrm{d}\Omega_\alpha \mathrm{d}q_{\alpha_1} \mathrm{d}q_{\alpha_2}. \tag{5.4}$$

The completeness of the set φ_c allows us to express the exterior wave-function Ψ_{ext} in its most general form, at any point of the exterior region corresponding to the fragmentation α, as a superposition of all the channel

wave-functions Ψ_c belonging to this mode of fragmentation α:

$$\Psi_{\mathrm{ext}(\alpha)} = \sum_{c(\alpha)} \Psi_c = \sum_{c(\alpha)} \varphi_c \frac{u_c(r_\alpha)}{r_\alpha}, \tag{5.5}$$

where the symbol $\sum_{c(\alpha)}$ indicates a summation over all channels for which the mode of fragmentation of the compound system is α. Moreover, since the very existence of the channels implies that the overlapping of two functions $\Psi_{\mathrm{ext}(\alpha)}$, $\Psi_{\mathrm{ext}(\alpha')}$ is completely negligible, the general form of the total wave function Ψ in the exterior region is

$$\Psi = \sum_{\alpha} \Psi_{\mathrm{ext}(\alpha)} \tag{5.6}$$

or

$$\Psi = \sum_{c} \Psi_c = \sum_{c} \varphi_c \frac{u_c(r_\alpha)}{r_\alpha}; \tag{5.7}$$

in eq. (5.6), only one term can be different from zero at some specified point of the exterior region, while the sums in eqs. (5.7) are extended to all possible channels, irrespectively of the fragmentation.

5.2. WAVE NUMBERS AND RADIAL FACTORS FOR OPEN AND CLOSED CHANNELS

The total energy $\mathscr{E}$ of the compound system is expressed in a given channel c as a sum of the internal energy $E_{\bar{\alpha}} = E_{\alpha_1} + E_{\alpha_2}$ of the fragments and the energy E_c of their relative motion:

$$\mathscr{E} = E_c + E_{\bar{\alpha}}. \tag{5.8}$$

If $E_c > 0$, the channel c is said to be *open*; if $E_c < 0$, it is said to be *closed*. The relative motion in an open channel is characterized by a real positive wave number defined by

$$k_c = + \sqrt{\frac{2M_\alpha E_c}{\hbar^2}}, \tag{5.9}$$

where $M_\alpha = M_{\alpha_1} M_{\alpha_2}/(M_{\alpha_1} + M_{\alpha_2})$ is the reduced mass of the fragments. The corresponding relative velocity is

$$v_c = \frac{\hbar k_c}{M_\alpha}. \tag{5.10}$$

In a closed channel, the wave number defined by eq. (5.9) is imaginary; it will be taken with

$$\mathrm{Im}\, k_c > 0. \tag{5.11}$$

For a state of the system of given energy $\mathscr{E}$, the various channel wave-numbers are not independent, but are connected by the relations of the form (5.8)

expressing the conservation of energy in the processes concerned:

$$\mathscr{E} = \frac{\hbar^2}{2M_\alpha} k_c^2 + E_{\bar{\alpha}} = \frac{\hbar^2}{2M_\alpha} k_{c'}^2 + E_{\bar{\alpha}'} = \ldots . \tag{5.12}$$

The radial factor $u_c(r_\alpha)$ of the channel wave function Ψ_c appearing in eq. (5.7) may be written, as in the single-channel case treated in the first part,

$$u_c(r_\alpha) = x_c O_l(r_\alpha, k_c) + y_c I_l(r_\alpha, k_c), \tag{5.13}$$

where the functions O_l, I_l are again those defined by eqs. (3.15), with the value of the orbital momentum l belonging to the channel c. In this and the following two sections, we consider only the positive and the purely imaginary values of the wave-numbers k_c, which have the direct physical meaning just explained. In sections 8 to 10, when we come to discuss the expansion of the collision matrix, we shall again introduce complex parameters k_c, as we did in part I.

5.3. TIME REVERSAL PROPERTIES

If the usual phase convention for the spherical harmonics is adopted and the phases of the internal wave functions $\varphi_{\bar{\alpha}sv}$ are appropriately fixed [2]), it is easy to see that we have

$$K\varphi_{\bar{\alpha}sl,JM} = (-1)^{J-M} \varphi_{\bar{\alpha}sl,J-M}. \tag{5.14}$$

Since the operator K acts on the radial factors O_l, I_l as the complex-conjugation operator, we simply have, using the relations (3.16),

$$KO_l(k_c) = I_l(k_c^*), \qquad KI_l(k_c) = O_l(k_c^*). \tag{5.15}$$

Hence, for an open channel, we have

$$KO_l(k_c) = I_l(k_c), \qquad KI_l(k_c) = O_l(k_c), \tag{5.16a}$$

while, for a closed channel,

$$\begin{aligned} KO_l(k_c) &= I_l(-k_c) = (-1)^l O_l(k_c), \\ KI_l(k_c) &= O_l(-k_c) = (-1)^l I_l(k_c). \end{aligned} \tag{5.16b}$$

6. Boundary Behaviour of the Interior Wave-function

6.1. THE INTERIOR RADIAL FACTORS

In the case of elastic scattering by a fixed potential, the interior channel wave-functions can be factorized in the same way as the exterior ones, and the boundary conditions can accordingly be expressed in terms of the radial factors only. In the general case, no such factorization of the interior wave-function exists, because of the couplings between the channels, due to the interaction of

all the nucleons in the interior region. Nevertheless, on the boundary surface itself, quantities playing the same part as the interior radial functions $u_l(a)$ and their derivatives $u'_l(a)$ in the simple case can be defined by taking advantage of the following facts: 1) although the "radial" channel coordinates r_α lose their physical meaning in the interior region, they are still mathematically defined in this region; 2) the boundary surface can be decomposed into adjacent parts $\mathscr{S}_\alpha$ corresponding to the various modes of subdivision of the compound system, and 3) on each such part $\mathscr{S}_\alpha$, we may expand any function with the help of the associated orthonormal set of surface functions φ_c.

In particular, at any point of $\mathscr{S}_\alpha$ we can give a definite meaning to the value of the interior wave function Ψ_{int}, multiplied for convenience by r_α, and to the derivative with respect to r_α of this product $r_\alpha\Psi_{\text{int}}$: we simply have to give the coordinates in which $r_\alpha\Psi_{\text{int}}$ and $(\partial/\partial r_\alpha)(r_\alpha\Psi_{\text{int}})$ are expressed values satisfying the condition $r_\alpha = a_\alpha$. We may then expand the surface functions so defined in the form

$$(r_\alpha\Psi_{\text{int}})_{r_\alpha=a_\alpha} = \sum_{c(\alpha)} \Phi_c\varphi_c, \tag{6.1a}$$

$$\left[\frac{\partial}{\partial r_\alpha}(r_\alpha\Psi_{\text{int}})\right]_{r_\alpha=a_\alpha} = \sum_{c(\alpha)} \Phi'_c\varphi_c, \tag{6.1b}$$

where the expansion coefficients are given by

$$\Phi_c = \int \varphi_c^*(r_\alpha\Psi_{\text{int}})_{r_\alpha=a_\alpha}\,dS_\alpha, \tag{6.2a}$$

$$\Phi'_c = \int \varphi_c^* \left[\frac{\partial}{\partial r_\alpha}(r_\alpha\Psi_{\text{int}})\right]_{r_\alpha=a_\alpha} dS_\alpha. \tag{6.2b}$$

It is clear that the quantities Φ_c, Φ'_c reduce to the radial factors $u_l(a)$, $u'_l(a)$ in the single-channel case, and we shall see that they form the natural extension of these factors to the general case. In fact, we shall call Φ'_c the "derivative" of Φ_c and speak of an expression like $\Phi_cO'_c - \Phi'_cO_c$ as the "Wronskian" of Φ_c and O_c at $r_\alpha = a_\alpha$, which we shall denote by $W(\Phi_c, O_c)$.

Because we neglect the overlapping of two functions φ_c corresponding to different fragmentations, we may also give to the expansions (6.1) the following form:

$$(r\Psi_{\text{int}})_{\mathscr{S}} = \sum_c \Phi_c\varphi_c, \tag{6.3a}$$

$$\left[\frac{\partial}{\partial r}(r\Psi_{\text{int}})\right]_{\mathscr{S}} = \sum_c \Phi'_c\varphi_c, \tag{6.3b}$$

where the left-hand side is taken at any point of $\mathscr{S}$, while in the right-hand side

the summation is now extended to all the channels, independently of the fragmentation to which they belong.

6.2. GREEN'S THEOREM

Before discussing the boundary conditions, we shall point out, for later use, a general relation between the product of any two eigenfunctions of different (real) energies $\mathscr{E}$, integrated over the interior region, and a channel sum of Wronskians of the corresponding radial factors defined by eqs. (6.2.). This relation follows from a straightforward application of Green's theorem to the integral of a suitably chosen expression over the interior region.

Let us consider two solutions Ψ_1, Ψ_2 of the wave equation $H\Psi = \mathscr{E}\Psi$, corresponding to two different real energies $\mathscr{E}_1$, $\mathscr{E}_2$. Then, we may write

$$(\mathscr{E}_2-\mathscr{E}_1)\int_\omega \Psi_2^*\Psi_1 \mathrm{d}\omega = \int_\omega [(H\Psi_2)^*\Psi_1-\Psi_2^*(H\Psi_1)]\mathrm{d}\omega, \tag{6.4}$$

where the integration in configuration space is extended to the interior region ω bounded by the surface $\mathscr{S}$. If we assume the potential V to be self-adjoint, i.e.,

$$\int_\omega [(V\Psi_2)^*\Psi_1-\Psi_2^*(V\Psi_1)]\mathrm{d}\omega = 0, \tag{6.5}$$

only the terms of H corresponding to the kinetic energies contribute to the right-hand side of (6.4), and these are transformed by Green's theorem into an integral over the surface $\mathscr{S}$. For the part $\mathscr{S}_\alpha$ of the surface, this integral can be written as

$$-\frac{\hbar^2}{2M_\alpha}\int\left[\frac{\partial\Psi_2^*}{\partial r_\alpha}\Psi_1-\Psi_2^*\frac{\partial\Psi_1}{\partial r_\alpha}\right]_{r_\alpha=a_\alpha}\mathrm{d}\mathscr{S}_\alpha$$

$$=-\frac{\hbar^2}{2M_\alpha}\int\left[\frac{\partial(r_\alpha\Psi_2^*)}{\partial r_\alpha}r_\alpha\Psi_1-r_\alpha\Psi_2^*\frac{\partial(r_\alpha\Psi_1)}{\partial r_\alpha}\right]_{r_\alpha=a_\alpha}\mathrm{d}S_\alpha,$$

or, on account of the expansions (6.1) and the orthonormality relations between the φ_c,

$$-\frac{\hbar^2}{2M_\alpha}\sum_{\mathrm{c}(\alpha)}(\Phi_{2\mathrm{c}}'^*\Phi_{1\mathrm{c}}-\Phi_{2\mathrm{c}}^*\Phi_{1\mathrm{c}}').$$

The integral over the whole surface $\mathscr{S}$ is the sum of similar expressions for the different modes of fragmentation α, and eq. (6.4) thus becomes

$$(\mathscr{E}_2-\mathscr{E}_1)\int\Psi_2^*\Psi_1\mathrm{d}\omega = \sum_\mathrm{c}\frac{\hbar^2}{2M_\mathrm{c}}W(\Phi_{2\mathrm{c}}^*,\Phi_{1\mathrm{c}}), \tag{6.6}$$

where the summation now extends to all channels, and where we have written M_c instead of M_α for the reduced mass in channel c. Eq. (6.6) is the announced general relation, from which we shall derive those we need by an appropriate choice of Ψ_1 and Ψ_2.

6.3. THE BOUNDARY CONDITIONS

With the help of the representation (6.1) of the interior wave-function and its normal derivative on the partial boundary surface $\mathscr{S}_\alpha$, we immediately obtain, by comparison with the expansion (5.5) of the exterior wave-function, the continuity conditions on this surface. Because of the linear independence of the φ_c, these conditions become, with the expression (5.13) for u_c,

$$\Phi_c = x_c O_l(a_\alpha, k_c) + y_c I_l(a_\alpha, k_c), \tag{6.7a}$$

$$\Phi'_c = x_c O'_l(a_\alpha, k_c) + y_c I'_l(a_\alpha, k_c), \tag{6.7b}$$

for all channels c belonging to the mode of subdivision α. Repeating the argument for all the subdivisions, we thus arrive at a complete formulation of the boundary conditions for all channels, which has the advantage of yielding the amplitudes x_c, y_c in explicit form for each channel separately:

$$x_c = -\frac{1}{2ik_c} W(\Phi_c, I_l; a_\alpha). \tag{6.8a}$$

$$y_c = +\frac{1}{2ik_c} W(\Phi_c, O_l; a_\alpha). \tag{6.8b}$$

It is through the factors Φ_c, Φ'_c that a coupling is implicitly established between the amplitudes in the various channels, inasmuch as specification of the incoming amplitudes fixes the interior wave function and all the radial factors Φ_c, Φ'_c which then, by eqs. (6.8a), determine the outgoing amplitudes for all channels.

From now on, when no confusion is to be feared, we shall often find it convenient to use the channel index c instead of more specific indices such as l or α for quantities like O_l, I_l, a_α.

6.4. WAVE-FUNCTIONS WITH A SINGLE ENTRANCE CHANNEL

It is easy to reduce the problem still further by noticing that any interior wave-function specified by any number of incoming amplitudes y_c (which in practice will all belong, of course, to the same mode of fragmentation α) can be expressed as a linear combination

$$\Psi = \sum_c \Psi^{(c)} \tag{6.9}$$

of wave-functions $\Psi^{(c)}$ corresponding to a single entrance channel c, i.e. for which

$$y_{c'} = 0 \qquad \text{for} \qquad c' \neq c, \tag{6.10}$$

or, more explicitly, according to eqs. (6.8b),

$$W(\Phi_{c'}^{(c)}, O_{c'}) = 0 \qquad \text{for } c' \neq c. \tag{6.11}$$

The upper index $^{(c)}$ affecting the various quantities serves to remind us that they refer to the case in which there is no other entrance channel than c. According to eq. (6.9) one also has

$$\Phi_{c'} = \sum_c \Phi_{c'}^{(c)}, \qquad \Phi'_{c'} = \sum_c \Phi_{c'}^{(c)\prime}, \tag{6.12}$$

and therefore, on account of eqs. (6.11),

$$W(\Phi_{c'}, O_{c'}) = \sum_c W(\Phi_{c'}^{(c)}, O_{c'}) = W(\Phi_{c'}^{(c')}, O_{c'}), \tag{6.13}$$

which means, according to (6.8b),

$$y_{c'} = y_{c'}^{(c')}, \tag{6.14a}$$

while on the other hand, by (6.8a),

$$x_{c'} = \sum_c x_{c'}^{(c)}. \tag{6.14b}$$

We therefore see that it is sufficient to treat the case of a single entrance channel.

We may assume that, except for a normalization factor, the solution $\Psi^{(c)}$ of the wave equation is completely defined by the eqs. (6.11) — which may be regarded as boundary conditions on $\mathscr{S}$ — and the condition of finite probability:

$$|\Psi^{(c)}|^2 \text{ finite in the interior region.} \tag{6.15}$$

The latter condition is a generalization of eq. (1.2b) for the elastic scattering; it excludes in particular any wave function whose asymptotic behaviour in channel c would be that of a purely outgoing wave, with no incoming wave in this channel.

In the representation $\{\bar{\alpha}sl, JM\}$, it is clear that, because of the conservation properties of J and M, we have

$$\Phi_{c'}^{(c)} = \Phi_{c'}^{(c)\prime} = 0 \qquad \text{when} \qquad J, M \neq J', M'. \tag{6.16}$$

Moreover, since $\Phi_{\bar{\alpha}'s'l', JM}^{(\bar{\alpha}sl, JM)}$, $\Phi_{\bar{\alpha}'s'l'JM}^{(\bar{\alpha}sl, JM)\prime}$ are scalar products, they are independent of M. In particular, if the notation $-$c is used to designate the channel $\{\bar{\alpha}sl, J-M\}$, we have

$$\Phi_{c'}^{(c)} = \Phi_{-c'}^{(-c)}. \tag{6.17}$$

7. The Collision Matrix

7.1. DEFINITION

Let us return to the general state described by the eigenfunction (6.9). For the component $\Psi^{(c)}$ corresponding to the single entrance channel c we

may write, according to eqs. (6.8),

$$x_{c'}^{(c)} = -U_{c'c}\, y_c^{(c)} \tag{7.1}$$

with

$$U_{c'c} = \frac{W(\Phi_{c'}^{(c)}, I_{c'})/k_{c'}}{W(\Phi_c^{(c)}, O_c)/k_c}. \tag{7.2}$$

From eqs. (6.14) we then derive the relation

$$x_{c'} = -\sum_c U_{c'c}\, y_c, \tag{7.3}$$

showing how in the general case when there are several entrance channels, with given amplitudes y_c, the amplitudes of all exit channels are determined as linear combinations of these incoming amplitudes. The coefficients $U_{c'c}$ of the linear relations (7.3) form a matrix **U** which is fundamental for the computation of the cross-sections for the reactions leading from any one of the entrance channels c to any exit channel c'.

Hitherto no distinction has been made between open and closed channels, and the definition of the matrix **U** is perfectly general in this respect; but of course, only those matrix elements $U_{c'c}$ which refer to open channels c', c, i.e. to real and positive values of the channel wave numbers k_c, $k_{c'}$, are susceptible to a physical interpretation in terms of a reaction leading from channel c to channel c'. If the wave numbers k_c, $k_{c'}$ are real and positive, and v_c, $v_{c'}$ represent the channel velocities according to the definition (5.10), the incoming and outgoing fluxes in the reaction $c \to c'$ are given by $v_c|y_c|^2$ and $v_{c'}|x_{c'}|^2$; it is therefore natural to define the element $\mathscr{U}_{c'c}$ of the *collision matrix* $\mathscr{U}$ by

$$\mathscr{U}_{c'c} = \sqrt{\frac{v_{c'}}{v_c}}\, U_{c'c}; \tag{7.4}$$

the cross section for the reaction $c \to c'$ will then be directly expressed in terms of the amplitude $\mathscr{U}_{c'c}\, y_c^{(un)}$, where $y_c^{(un)}$ is the amplitude corresponding to unit incoming flux. In the following, however, we shall also call **U** "collision matrix" when no confusion is to be feared.

The definition (7.2) of the matrix element $U_{c'c}$ shows that it is entirely determined by the consideration of the wave-function with the single entrance channel c, which was introduced in sub-section 6.4. The most convenient channel designation scheme for representing the matrix **U** is obviously $c \equiv \{\tilde{a}sl, JM\}$: in this scheme, according to eqs. (6.16), the matrix is diagonal with respect to the angular momentum quantum numbers J, M. Moreover, its elements (like the radial factors $\Phi_{c'}^{(c)}$ on which they depend) are independent of M and may therefore be written

$$U_{c'c} = \delta_{M'M}\delta_{J'J}\, U^J_{\tilde{a}'s'l',\tilde{a}sl}. \tag{7.5}$$

One easily passes from the representation $\{\tilde{\alpha}sl, JM\}$ to the scheme $\{\tilde{\alpha}sv, lm\}$, for instance, by relations of the form [2])

$$U_{\tilde{\alpha}'s'v',l'm';\tilde{\alpha}sv,lm} = \sum_{JM} (s'v', l'm'|JM)(sv, lm|JM) U^{J}_{\tilde{\alpha}'s'l',\tilde{\alpha}sl}. \tag{7.6}$$

7.2. GENERAL PROPERTIES

From their very definition, it is clear that the collision matrix elements U_{qp} are independent of any particular normalization adopted for the solution $\Psi^{(p)}$ of the wave equation. The general properties of the collision matrix are most easily established by considering a wave function $\Psi^{(p)}$ for which the normalization $y_p = y_p^{(p)} = 1$ has been adopted. According to eq. (7.1), this yields the following asymptotic behaviour of $\Psi^{(p)}$ in the exterior region:

$$\Psi^{(p)} = \varphi_p \frac{I_p}{r_p} - \sum_c U_{cp}\varphi_c \frac{O_c}{r_c} = \sum_c \frac{\varphi_c}{r_c}(\delta_{cp} I_c - U_{cp} O_c), \tag{7.7}$$

whence for its radial factors the expressions

$$\Phi_c^{(p)} = \delta_{cp} I_c(a_c, k_c) - U_{cp} O_c(a_c, k_c). \tag{7.8}$$

A similar normalization will be adopted in this sub-section for all the wave functions with a single entrance channel we are going to consider.

7.2.1. *Unitarity*

Let us consider two solutions $\Psi_1 = \Psi^{(p)}$, $\Psi_2 = \Psi^{(q)}$ of the wave equation corresponding to the same energy $\mathscr{E}_1 = \mathscr{E}_2 = \mathscr{E}$, for which the channels p, q are both open. According to Green's theorem (6.6), we have

$$\sum_c \frac{\hbar^2}{2M_c} W(\Phi_c^{(q)*}, \Phi_c^{(p)}) = 0, \tag{7.9}$$

where the sum is extended to closed as well as to open channels, which will be respectively denoted by c^- and c^+. Eq. (7.8) is valid for both $c = c^+$ and $c = c^-$, while from eqs. (3.16) we have

$$\Phi_c^{(q)*} = \delta_{cq} O_c(k_c) - U^*_{cq} I_c(k_c) \qquad \text{for } c = c^+, \tag{7.10a}$$

$$\Phi_c^{(q)*} = (-1)^{l_c}[\delta_{cq} I_c(k_c) - U^*_{cq} O_c(k_c)] \qquad \text{for } c = c^-. \tag{7.10b}$$

Introducing the expressions (7.10) into eq. (7.9), and taking eq. (3.18) into account, one obtains

$$\sum_{c^+} \frac{\hbar^2}{2M_c}(-2ik_c\delta_{cp}\delta_{cq} + 2ik_c U^*_{cq} U_{cp}) + \sum_{c^-} \frac{\hbar^2}{2M_c}(-2ik_c\delta_{cq}U_{cp} + 2ik_c\delta_{cp}U^*_{cq})(-1)^{l_c} = 0.$$

All the terms of the latter sum vanish simply because p and q are open channels, and we are left with the identity

$$\sum_{c^+} \frac{\hbar k_c}{M_c} U^*_{cq} U_{cp} = \frac{\hbar k_p}{M_p} \delta_{pq}. \tag{7.11}$$

Using the definition (5.10) of the channel velocity, this may be written

$$\sum_{c^+} v_c U^*_{cq} U_{cp} = v_p \delta_{pq}, \tag{7.12}$$

or, in terms of the collision matrix (7.4),

$$\sum_{c^+} \mathscr{U}^*_{cq} \mathscr{U}_{cp} = \delta_{pq}. \tag{7.13}$$

Eq. (7.13) expresses the unitarity of the collision matrix $\mathscr{U}$ in the subspace of open channels: $\mathscr{U}^\dagger \mathscr{U} = \mathbf{1}$. Eq. (7.11) yields, for p = q,

$$\sum_{c^+} v_c |U_{cp}|^2 = v_p, \tag{7.14}$$

expressing that the total outgoing flux, for all reactions initiated in channel p, is equal to the incoming flux.

7.2.2. *Symmetry*

Let us now adopt the $\{\bar{\alpha}sl, JM\}$ channel designation and let us again use the notation −q to designate a channel identical with q, except for the opposite sign of the angular momentum. If $\Psi^{(q)}$ is an eigenfunction of the Hamiltonian characterized by the single open entrance channel q, two other eigenfunctions are

$$\Psi^{(-q)} = \sum_p \frac{\varphi_{-p}}{r_p} (\delta_{-p-q} I_{-p} - U_{-p-q} O_{-p}) \tag{7.15}$$

and

$$\begin{aligned}(-1)^{J_q+M_q} K\Psi^{(-q)} &= \sum_p \frac{\varphi_p}{r_p} [\delta_{pq} O_p(k_p^*) - U^*_{pq} I_p(k_p^*)] \\ &= \sum_{p^+} \frac{\varphi_p}{r_p} [\delta_{pq} O_p(k_p) - U^*_{pq} I_p(k_p)] - \sum_{p^-} U^*_{pq} O_p(k_p)(-1)^{l_p}; \end{aligned} \tag{7.16}$$

to derive the last formula, use has been made of the properties (5.14) and (5.16), and account has been taken of the fact that the channel q is open.

The wave-function (7.16) is characterized by amplitudes $-U^*_{pq}$ in all open entrance channels p (and zero amplitude in the closed entrance channels); accordingly, it may be represented as a linear combination $-\sum_{c^+} U^*_{cq} \Psi^{(c)}$ of single entrance channel functions of the form (7.7), viz.

$$\sum_{c^+} \sum_{p^+} \frac{\varphi_p}{r_p} U_{pc} U^*_{cq} O_p - \sum_{p^+} \frac{\varphi_p}{r_p} U^*_{pq} I_p + \sum_{c^+} \sum_{p^-} \frac{\varphi_p}{r_p} U_{pc} U^*_{cq} O_p. \tag{7.17}$$

The comparison of the equivalent expressions (7.16) and (7.17) shows, by identification of the coefficients of O_{p^+}, that

$$\sum_{c^+} U_{pc} U^*_{cq} = \delta_{pq}, \tag{7.18}$$

when p and q are two open channels. In the sub-space of open channels, this may be written in the form $\mathbf{U}\mathbf{U}^* = \mathscr{U}\mathscr{U}^* = \mathbf{1}$.

Combining eqs. (7.12) and (7.18) gives for any pair of open channels

$$v_p U_{pq} = v_q U_{qp}, \tag{7.19}$$

i.e.

$$\mathscr{U}_{pq} = \mathscr{U}_{qp}, \tag{7.20}$$

a relation showing that the collision matrix is symmetrical.

8. Complex Wave Numbers

8.1. TIME REVERSAL PROPERTIES

With a view to introducing a definition of the resonant states and an expansion of the collision matrix elements along the same lines as in part I, we shall from now on consider all the channel wave numbers k_c, $k_{c'}$, ... as complex quantities. In this sub-section we provisionally treat them as independent, ignoring the energy conservation relations.

The definition of the functions $\Psi^{(c)}$ is easily extended to this case: it is a solution of the wave equation

$$H\Psi^{(c)} = \left(\frac{\hbar^2}{2M_c} k_c^2 + E_{\bar{\alpha}}\right) \Psi^{(c)}, \tag{8.1}$$

in which the energy is expressed in the form corresponding to the selected entrance channel, and it is completely characterized by the conditions

$$W(\Phi^{(c)}_{c'}, O_{c'}(k_{c'})) = 0 \qquad \text{for } c' \neq c, \tag{8.2a}$$

$$|\Psi^{(c)}|^2 \text{ finite in the interior region,} \tag{8.2b}$$

as a function not only of the space and spin coordinates, but also of all the complex wave numbers.

The choice of the normalization factor for the function $\Psi^{(c)}(k_c, k_{c'}, \ldots)$ is restricted by the specification of its time-reversal behaviour, which has to be compatible with the boundary conditions (8.2). In the $\{\bar{\alpha}sl, JM\}$ channel designation, such a requirement is fulfilled, as we shall see, by the specification

$$K\Psi^{(c)}(k_c, k_{c'}, \ldots) = (-1)^{J-M} \Psi^{(-c)}(-k_c^*, -k_{c'}^*, \ldots). \tag{8.3}$$

For the time-reversal transformation of the radial factor $\Phi_{c'}^{(c)}$ (with $J = J'$, $M = M'$),

$$K\Phi_{c'}^{(c)}(k_c, k_{c'}, \ldots)K^\dagger = \int (K\varphi_{c'})^*(r_\alpha K\Psi_{\text{int}}^{(c)})_{r_\alpha = a_\alpha} \mathrm{d}S_\alpha,$$

we have, according to eqs. (5.14), (6.17) and (8.3),

$$\Phi_{c'}^{(c)}(k_c, k_{c'}, \ldots)^* = \Phi_{c'}^{(c)}(-k_c{}^*, -k_{c'}^*, \ldots). \tag{8.4a}$$

Similarly, we have for the derivatives

$$\Phi_{c'}^{(c)\prime}(k_c, k_{c'}, \ldots)^* = \Phi_{c'}^{(c)\prime}(-k_c{}^*, -k_{c'}^*, \ldots). \tag{8.4b}$$

Together with eqs. (3.17), these equations (8.4) show that the boundary conditions (8.2a), written for the set of wave-numbers $-k_c{}^*, -k_{c'}^*, \ldots$ are just the complex conjugates of the same conditions written for the set k_c, $k_{c'}, \ldots$. This establishes the required compatibility of the time reversal behaviour (8.3) of the function $\Psi^{(c)}$ and the boundary conditions defining this function.

In the same framework of complex independent wave numbers, if the amplitudes $x_{c'}^{(c)}$, $y_c^{(c)}$ and the collision matrix element $U_{c'c}$ are regarded as defined by eqs. (6.8) and (7.2) in terms of the radial factors $\Phi_{c'}^{(c)}(k_c, k_{c'}, \ldots)$, it is clear from eqs. (3.17) that they satisfy the relations †

$$Kx_{c'}^{(c)}K^\dagger = x_{c'}^{(c)}(k_c, k_{c'}, \ldots)^* = (-1)^{l'}x_{c'}^{(c)}(-k_c{}^*, -k_{c'}^*, \ldots), \tag{8.5a}$$

$$Ky_c^{(c)}K^\dagger = y_c^{(c)}(k_c, k_{c'}, \ldots)^* = (-1)^{l}y_c^{(c)}(-k_c{}^*, -k_{c'}^*, \ldots), \tag{8.5b}$$

$$KU_{c'c}K^\dagger = U_{c'c}(k_c, k_{c'}, \ldots)^* = (-1)^{l'-l}U_{c'c}(-k_c{}^*, -k_{c'}^*, \ldots). \tag{8.6}$$

8.2. THE PHYSICAL k_0-PLANE

Let us now impose a restriction upon the range of complex values which we allow for the channel wave-numbers by extending to the complex domain the validity of the energy conservation relations (5.12); the internal energies $E_{\bar{\alpha}}, \ldots$ keep their physical real values. We may then consider all the channel wave-numbers $k_c, k_{c'} \ldots$ to be functions of one of them, which we conveniently choose to be the wave-number k_0 of the channel of lowest internal energy $E_{\bar{\alpha}_0}$, i.e. of highest kinetic energy $\hbar^2 k_0{}^2/2M_0$. Every wave-number k_c is given in terms of k_0 by an expression of the form

$$k_c \equiv k_c(k_0) = \sqrt{k_0{}^2 - K_c{}^2}, \tag{8.7}$$

where K_c is a real quantity defined by

$$K_c{}^2 = E_{\bar{\alpha}_c} - E_{\bar{\alpha}_0}, \tag{8.8}$$

and which we shall take to be positive.

† In the article of Lane and Thomas [2]) sign factors $(-1)^l$ are missing in their eqs. (VI.2.12), with the result that the sign factor is also absent from their relation (VI.2.20), which should be the same as our eq. (8.6).

The values $+K_c$, $-K_c$ of the channel wave-number k_0 are branch-points of the function $k_c(k_0)$ defined by eq. (8.7). To make this function single-valued we must introduce into the complex k_0-plane an appropriate cut joining the two branch-points. We shall draw this cut (fig. 2) below the real axis and symmetrical with respect to the imaginary axis and choose the branch of the function $k_c(k_0)$ which is positive when k_0 is real and positive and larger than K_c.

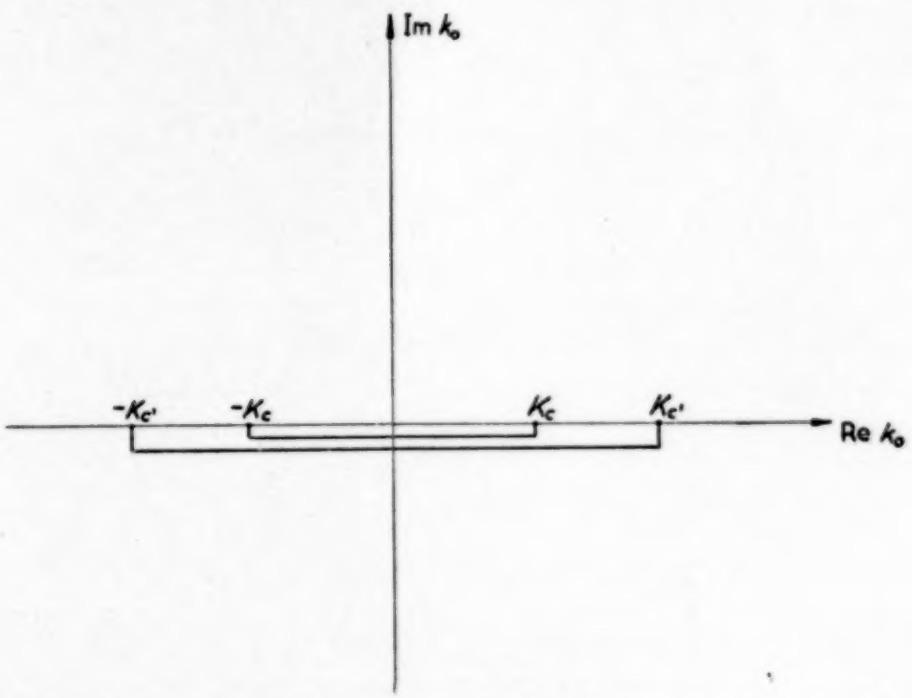

Fig. 2. The physical k_0-plane with typical cuts between channel thresholds.

This ensures that we have in general the important property

$$k_c(-k_0^*) = -k_c(k_0)^*, \tag{8.9}$$

and that the critical values $\pm K_c$ have a simple physical meaning: according as the (real and positive) wave-number k_0 is larger or smaller than K_c, the wave-number k_c is real and positive or purely imaginary with positive imaginary part, which corresponds to the channel c being open or closed; the point $-K_c$ refers to the time-reversed situation. We may therefore call the points $\pm K_c$ the *thresholds* of the channel c in the complex k_0 -plane. The domain obtained by excluding from this plane all the cuts joining the thresholds will be called the *physical k_0-plane.*

It is clear that the formulae of sections 5 and 6 are immediately extended to complex wave-numbers and energies defined in the physical k_0-plane. It must be pointed out, however, that the important formula (6.6) resulting from

Green's theorem has to be slightly modified: it holds in the form

$$(\mathscr{E}_2^*-\mathscr{E}_1)\int_\omega \Psi_2^*\Psi_1 \mathrm{d}\omega = \sum_c \frac{\hbar^2}{2M_c} W(\Phi_{2c}^*, \Phi_{1c}), \tag{8.10}$$

always provided that the hermiticity condition (6.5) is fulfilled.

Thanks to the relations (8.9), the results of sub-section 8.1. also remain valid in the physical k_0-plane. Instead of the relations (8.3), (8.4) and (8.6), we might now simply write

$$K\Psi^{(c)}(k_0) = (-1)^{J-M}\Psi^{(-c)}(-k_0^*), \tag{8.11}$$

$$\Phi_{c'}^{(c)}(k_0)^* = \Phi_{c'}^{(c)}(-k_0^*), \qquad \Phi_{c'}^{(c)\prime}(k_0)^* = \Phi_{c'}^{(c)\prime}(-k_0^*), \tag{8.12}$$

$$U_{c'c}(k_0)^* = (-1)^{l'-l}U_{c'c}(-k_0^*). \tag{8.13}$$

In practice, however, it is also useful to keep the explicit notation $(k_c, k_{c'}, \ldots)$ of sub-section 8.1 in the present case of non-independent complex channel wave-numbers. In particular, for real values of k_0 $(\neq \pm K_c, \pm K_{c'}, \ldots)$, the relations (8.12) and (8.13) are more clearly written in the form

$$\begin{aligned} \Phi_{c'}^{(c)}(k_+, k_-)^* &= \Phi_{c'}^{(c)}(-k_+, +k_-), \\ \Phi_{c'}^{(c)\prime}(k_+, k_-)^* &= \Phi_{c'}^{(c)\prime}(-k_+, +k_-), \end{aligned} \tag{8.14}$$

$$U_{c'c}(k_+, k_-)^* = (-1)^{l'-l}U_{c'c}(-k_+, +k_-), \tag{8.15}$$

where k_+ refers to all the open channels, k_- to all the closed channels. It will be noticed that eqs. (1.25b) and (1.29) are special cases of eqs. (8.12) and (8.13).

9. The Resonant States

9.1. DEFINITION

In this section, we define the resonant states, in direct extension of the procedure of section 1, by boundary conditions expressing the absence of any incoming wave. We formulate these conditions in terms of the channel wave-numbers defined in the physical k_0-plane, and adopt the $\{\tilde{\alpha}sl, JM\}$ channel designation. Because of the conservation properties of the angular momentum, we may discuss separately the states of our nuclear system corresponding to each given set of quantum numbers J, M: in what follows, all channels are understood to correspond to the same set J, M.

We now write down simply the conditions expressing the absence of incoming waves in any channel by arbitrarily selecting some channel c and imposing upon the radial factor $\Phi_c^{(c)}$ of the state with a single entrance channel c the condition

$$W(\Phi_c^{(c)}, O_c) = 0, \tag{9.1a}$$

which, according to (6.8b), indeed means $y_c = 0$. Besides eq. (9.1a), the eigenfunction $\Psi^{(c)}$ under consideration must satisfy the relations

$$W(\Phi_{c'}^{(c)}, O_{c'}) = 0 \qquad \text{for } c' \neq c, \tag{9.1b}$$

expressing that c is the only entrance channel. The conditions (9.1a) and (9.1b) together form a set

$$W(\Phi_c, O_c) = 0 \qquad \text{for all c of given } J, M, \tag{9.2}$$

which is of course independent of the channel selected as entrance channel in the above argument.

Together with the wave equation

$$H\Psi = \left(\frac{\hbar^2}{2M_0} k_0^2 + E_{\bar{\alpha}_0}\right) \Psi \tag{9.3}$$

and the condition of finite probability

$$|\Psi|^2 \text{ finite in the interior region,} \tag{9.4}$$

the boundary conditions (9.2) will therefore characterize a set of eigenfunctions $\Psi_{JM,n}$ which are not related to any particular entrance channel: the corresponding complex wave numbers $k_{J,0n}$ are of course independent of M. The radial factors of the eigenfunction $\Psi_{JM,n}$ are also independent of any entrance channel and may accordingly be designated by $\Phi_{J,cn}$, $\Phi'_{J,cn}$.

To the wave numbers $k_{J,0n}$ of channel 0 are associated, by means of eq. (8.7), a set of wave numbers $k_{J,cn}$ for any other channel c, and a set of complex energy eigenvalues $\mathscr{E}_{J,n}$ satisfying energy conservation relations

$$\mathscr{E}_{J,n} = \frac{\hbar^2}{2M_0} k_{J,0n}^2 + E_{\bar{\alpha}_0} = \frac{\hbar^2}{2M_c} k_{J,cn}^2 + E_{\bar{\alpha}_c} = \dots . \tag{9.5}$$

From eqs. (7.2) and (9.2), we see that *all* the matrix elements $U^J_{\bar{\alpha}'s'l',\bar{\alpha}sl}$ corresponding to a fixed J have the same poles $k_{J,0n}$ in the physical k_0-plane. Since the k_c are single-valued functions of k_0, we need not always refer to the channel 0, but may also say that the poles of the $U^J_{\bar{\alpha}'s'l',\bar{\alpha}sl}$ are the k_{J,c_n}. From now on, we shall usually omit the indices JM in $\Psi_{JM,n}$ and the index J in $k_{J,cn}$ and $\mathscr{E}_{J,n}$.

9.2. PROPERTIES

From eqs. (8.12) and (8.9), it is evident that, as in the one-channel case, with each pole

$$k_{cn} = \kappa_{cn} - i\gamma_{cn} \tag{9.6a}$$

is associated the pole

$$-k_{cn}^* = -\kappa_{cn} - i\gamma_{cn}, \tag{9.6b}$$

and we may therefore take without restriction

$$\kappa_{cn} \geqq 0. \tag{9.6c}$$

The eigenfunction belonging to the eigenvalue $-k_{0n}{}^*$ will be denoted as $\Psi_{JM,-n}$, and its radial factors as $\Phi_{J,c-n}$, $\Phi'_{J,c-n}$. On account of the time-reversal relations (8.12), the latter are related to the radial factors $\Phi_{J,cn}$, $\Phi'_{J,cn}$ by

$$\Phi_{J,c-n} = \Phi^*_{J,cn}, \qquad \Phi'_{J,c-n} = \Phi'^*_{J,cn}. \tag{9.7}$$

Writing $\mathscr{E}_n$ in the form

$$\mathscr{E}_n = E_n - \tfrac{1}{2}i\Gamma_n, \tag{9.8}$$

we have, on account of the energy relations (9.5),

$$E_n = \frac{\hbar^2}{2M_0}(\kappa_{0n}^2 - \gamma_{0n}^2) + E_{\tilde{a}_0} = \frac{\hbar^2}{2M_c}(\kappa_{cn}^2 - \gamma_{cn}^2) + E_{\tilde{a}_c} = \ldots, \tag{9.9a}$$

$$\Gamma_n = \frac{2\hbar^2}{M_0}\kappa_{0n}\gamma_{0n} = \frac{2\hbar^2}{M_c}\kappa_{cn}\gamma_{cn} = \ldots. \tag{9.9b}$$

For a decaying state ($\Gamma_n > 0$), the last relation corresponds to the fact that the rate of decay is the same in all channels, only the branching ratios being different for the various channels.

It may again be shown that

$$\gamma_{cn} \geqq 0 \qquad \text{when} \qquad \kappa_{cn} \neq 0, \tag{9.10}$$

which, by (9.6c) and (9.9b), amounts to proving that

$$\Gamma_n \geqq 0. \tag{9.11}$$

This results from the actual computation of the width Γ_n, carried out by means of the form (8.10) of Green's theorem, applied to $\Psi_1 = \Psi_2 = \Psi_n$. On account of (9.8) we have

$$i\Gamma_n \int_\omega |\Psi_n|^2 \mathrm{d}\omega = \sum_c \frac{\hbar^2}{2M_c} |\Phi_{cn}|^2 \left\{ \frac{\Phi'_{cn}}{\Phi_{cn}} - \frac{\Phi'^*_{cn}}{\Phi^*_{cn}} \right\}. \tag{9.12}$$

In virtue of the conditions (8.2), the quantity between brackets may be written, with the notation (3.22) (in which the channel symbol c is used rather than the quantum number l belonging to it), $L_c(k_{cn}) - L_c(k_{cn})^*$. For this quantity we have the alternative expressions (3.24) and (3.27), which, on account of eqs. (9.6), (9.9b), may be put into the form

$$|O_{cn}|^2[L_c(k_{cn}) - L_c(k_{cn})^*] = 2i\kappa_{cn}|\mathscr{H}_0{}^{(1)}(k_{cn}b_c)|^2$$
$$-i\frac{2M_c}{\hbar^2}\Gamma_n\left[\int_{a_c}^{b_c} |O_c(r_c, k_{cn})|^2 \mathrm{d}r_c + \mathscr{N}_{cn}(b_c)\right], \tag{9.13}$$

$$|O_{cn}|^2[L_c(k_{cn})-L_c(k_{cn})^*] = 2i\kappa_{cn}-i\frac{2M_c}{\hbar^2}\Gamma_n N_{cn}. \tag{9.14}$$

Substituting the expression (9.13) into eq. (9.12), we obtain Γ_n as the quotient of two essentially positive quantities, which proves eqs. (9.11) and (9.10). As in section 3, however, we prefer, for actual use, the expression for Γ_n derived from the substitution of (9.14) into eq. (9.12):

$$\frac{\Gamma_n}{\hbar} = \frac{\sum_c (\hbar\kappa_{cn}/M_c)|\Phi_{cn}/O_{cn}|^2}{\int_\omega |\Psi_n|^2 d\omega + \sum_c N_{cn}|\Phi_{cn}/O_{cn}|^2}, \tag{9.15}$$

in which, by the same argument as in section 3, the denominator is an essentially non-negative quantity.

The classification of the resonant states discussed in section 2 for the single-channel case can be performed by considering the values of k_{cn} which correspond to a given location of k_{0n} in the physical k_0-plane. A state that is "virtual" in the channel 0 (i.e. $\kappa_{0n}^2 < \gamma_{0n}^2$) has the same property in all the other channels (i.e. $\kappa_{cn}^2 < \gamma_{cn}^2$); the proper resonant states ($\kappa_{0n}^2 > \gamma_{0n}^2$), on the other hand, appear as virtual states in the channels c with internal energy $E_{\tilde{a}_c}$ higher than the resonance energy E_n, because then $\kappa_{cn}^2 < \gamma_{cn}^2$.

The occurrence of real wave numbers $k_{0n} = \kappa_{0n} > 0$ may be excluded by the following physical argument: such a solution of the eigenvalue problem would correspond to an actual stationary state of the system with pure outgoing waves in open channels and no incoming wave in any channel; this is in opposition with the condition (9.4). As in section 1, we disregard the very special case corresponding to $k_{0n} = 0$. We may then draw the cuts in the k_0-plane so close to the real axis that they all lie above some line $k_0 = -\Lambda$, where Λ denotes a positive quantity smaller than all the distances γ_{0n} of the points k_{0n} from the real axis. Under such conditions, it may also be seen that k_{0n} is uniquely determined in terms of k_{cn}.

We still have to consider the states of real (negative) energy E_n, corresponding to $\kappa_{0n} = 0$: they have in all channels the property $\kappa_{cn} = 0$. Likewise, the imaginary part γ_{cn} of the channel wave number has the same sign in all channels, and the state in question is thereby unambiguously characterized either as a bound state or as a virtual state of the "deuteron" type.

10. Expansion of the Collision Matrix

10.1 ANALYTICAL PROPERTIES OF THE COLLISION MATRIX

The analytical behaviour of the matrix elements $U_{c'c}$, according to their definition (7.2), depends primarily on that of the radial factors $\Phi_{c'}^{(c)}$, $\Phi_{c'}^{(c)\prime}$ of the interior wave function $\Psi^{(c)}$. Considering the way in which we have derived $\Psi^{(c)}(k_0)$ from $\Psi^{(c)}(k_0, k_c, k_{c'}, \ldots)$ in section 8, we must expect

$\Phi_{c'}^{(c)}(k_0)$, $\Phi_{c'}^{(c)\prime}(k_0)$ to have branch points in the k_0-plane at the thresholds $\pm K_c$, $\pm K_{c'}$, ... We assume that these singularities are the only ones the radial factors have for finite k_0, and that they are not simultaneously zeros of these functions. The absence of zeros at the thresholds is at any rate in agreement with — though of course not a consequence of — the time-reversal relations (8.4). Under such assumptions, in the physical k_0-plane, i.e. the k_0-plane with its cuts, the radial factors are single-valued and regular analytic functions.

It must be observed that the introduction of such a hypothesis of analyticity is made possible in particular by the circumstance that the collision matrix is independent of the normalization of $\Psi^{(c)}$. This assumption about the analytical behaviour of the radial factors is not required (and indeed not fulfilled) when we consider, for instance, the normalization of $\Psi^{(c)}$ to unit incoming flux (cf. eqs. (1.21) and (6.8b)) in order to calculate the cross-sections in terms of the collision matrix; or when we temporarily use some other normalization, such as in eq. (7.8).

Let us now consider the collision matrix element $U_{c'c}$ itself. In the denominator, the function O_c, like $\mathscr{H}_l^{(1)}$, has a pole of order l in $k_c = 0$, and consequently $U_{c'c}$ has a zero of order l at that threshold. Turning to the Wronskian of the numerator, it seems at first sight that it has, like $I_{c'}$, a pole of order l' in $k_{c'} = 0$. It is readily seen, however, that this is not the case. For this purpose, in analogy with what we did in subsection 1.4, let us define the quantity

$$S_{c'c} = \sqrt{\frac{M_c}{M_{c'}}} \frac{1}{k_c^{l+1} k_{c'}^{l'}} (U_{c'c} - \delta_{c'c}), \tag{10.1}$$

which we first consider for $c' = c$. We have

$$S_{cc} = \frac{1}{k_c^{l+1}} \frac{W(\Phi_c^{(c)}, j_c)}{W(\Phi_c^{(c)}, k_c^l O_c)}, \tag{10.2}$$

where, according to eqs. (3.15), we use the function

$$j_c = I_c - O_c = -2i \left[\mathscr{J}_l(k_c a_c) + \eta_c \int_{a_c}^{b_c} r^{-1} G_l(a_c, r) \mathscr{J}_l(k_c r)\, dr \right], \tag{10.3}$$

which, like $\mathscr{J}_l(k_c a_c)$, is the product of k_c^{l+1} by an integral function of k_c^2. It is thus clear that S_{cc} is finite for $k_c = 0$. For $c' \neq c$, on account of eqs. (9.1b), we may again write

$$S_{c'c} = \sqrt{\frac{M_c}{M_{c'}}} \frac{1}{k_c^l k_{c'}^{l'+1}} \frac{W(\Phi_{c'}^{(c)}, I_{c'} - O_{c'})}{W(\Phi_c^{(c)}, O_c)} = \sqrt{\frac{M_c}{M_{c'}}} \frac{1}{k_{c'}^{l'+1}} \frac{W(\Phi_{c'}^{(c)}, j_{c'})}{W(\Phi_c^{(c)}, k_c^l O_c)}, \tag{10.4}$$

and therefore conclude that in any case $S_{c'c}$ is finite in $k_c = 0$ and $k_{c'} = 0$, i.e. that $U_{c'c} - \delta_{c'c}$ behaves according to

$$U_{c'c} - \delta_{c'c} \propto k_c^{l+1} k_{c'}^{l'} \tag{10.5}$$

near these thresholds.

The general conclusion of the preceding analysis is thus that the matrix element

$$\bar{S}_{c'c} = k_c^l k_{c'}^{l'} S_{c'c} = \sqrt{\frac{M_c}{M_{c'}}} \frac{W(\Phi_{c'}^{(c)}, j_{c'}/k_{c'})}{W(\Phi_c^{(c)}, O_c)}, \tag{10.6}$$

which directly governs all the reaction cross-sections, including those for elastic scattering, has no other singularities in the physical k_0-plane than poles corresponding to the resonant states. It can accordingly be expanded in this plane in the form indicated by the Mittag-Leffler theorem. It is more advantageous, however, to use an expansion in the "physical" plane of the total

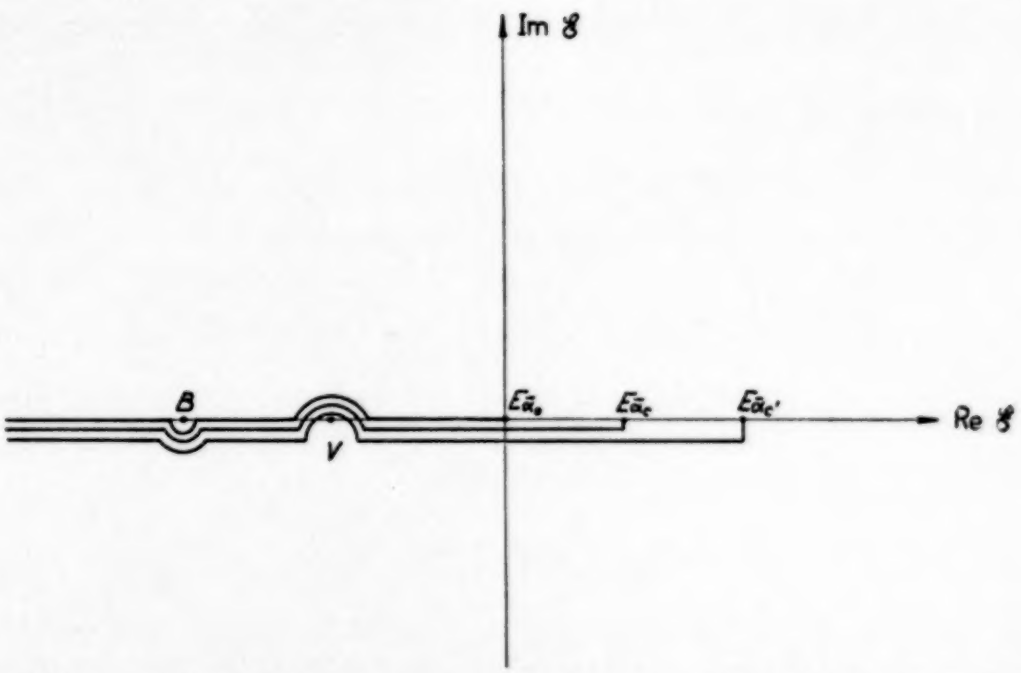

Fig. 3. The physical $\mathscr{E}$-plane with typical cuts from channel thresholds. B = bound state, V = virtual state of deuteron type.

energy $\mathscr{E}$, along the same lines as in subsection 2.3. As functions of $\mathscr{E}$, the matrix elements $S_{c'c}$ have branch-points on the positive real axis at the thresholds $\mathscr{E} = E_{\bar{a}}$ of the various channels. It is convenient to choose as the origin of the energy scale the threshold of channel 0, which amounts to putting $E_{\bar{a}_0} = 0$. The physical $\mathscr{E}$-plane is then defined by drawing cuts from each of the thresholds (including $\mathscr{E} = 0$) along the real axis towards $-\infty$. The resonant states are represented by points in the lower half-plane and possibly also on the negative real axis, the latter corresponding either to bound states or to virtual states of the "deuteron" type. The cuts should pass below the bound-state points and above the "deuteron"-state points and be so close to the real axis that no resonant state should lie on any of them or between two of them (fig. 3).

10.2. EXPANSIONS OF THE COLLISION MATRIX

When the choice of the independent variable has been decided, the arbitrariness in the convergence exponent occurring in the Mittag-Leffler formula still leaves room, in the many-channel theory as well as in the single-channel case, for a variety of expansions of the same general type for the matrix elements $S_{c'c}$, $\bar{S}_{c'c}$. It is reasonable to assume that the asymptotic location of the resonant states will have the same character for the general case of nuclear interaction as for a fixed potential, and that the minimum admissible value of the convergence exponent M will be the same as in the latter case. Here, we shall discuss the expansions of both $S_{c'c}$ and $\bar{S}_{c'c}$ with the convergence exponent $M = 0$; as in sub-section 1.4 the first expansion will bring out explicitly the threshold behaviour, while the other has a somewhat simpler form.

The residue $r_{c'cn}$ of $S_{c'c}$ at $\mathscr{E} = \mathscr{E}_n$ is

$$r_{c'cn} = \sqrt{\frac{M_c}{M_{c'}}} \frac{W(\Phi_{c'n}, j_{c'n})}{k_{cn}^{l} k_{c'n}^{l'+1} \left[\frac{\mathrm{d}}{\mathrm{d}\mathscr{E}} W(\Phi_c^{(c)}, O_c)\right]_{\mathscr{E}=\mathscr{E}_n}}, \tag{10.7}$$

where $j_{c'n} = I_{c'n} - O_{c'n}$. Taking account of eq. (3.18) and of the conditions

$$W(\Phi_{c'n}, O_{c'n}) = 0 \qquad \text{for all } c', \tag{10.8}$$

satisfied by the radial factors $\Phi_{c'n}$, $\Phi'_{c'n}$, we get

$$W(\Phi_{c'n}, j_{c'n}) = -2ik_{c'n} \frac{\Phi_{c'n}}{O_{c'n}}. \tag{10.9}$$

In order to calculate $(\mathrm{d}/\mathrm{d}\mathscr{E})W(\Phi_c^{(c)}, O_c)$, we start from the relation (8.10) derived from Green's theorem, in which we take $\Psi_1 \equiv \Psi^{(c)}(k)$, $\Psi_2 \equiv \Psi^{(c)}(-k_{0n}^*) = \Psi_{-n}$ (the notation k represents the set of channel wave-numbers k_c, $k_{c'}, \ldots$ belonging to the energy $\mathscr{E}$):

$$(\mathscr{E}_n - \mathscr{E}) \int_\omega \Psi_{-n}^* \Psi^{(c)}(k) \mathrm{d}\omega = \sum_{c'} \frac{\hbar^2}{2M_{c'}} W(\Phi_{c'-n}^*, \Phi_{c'}^{(c)}(k)).$$

In virtue of the eqs. (9.7), the Wronskian on the right-hand side is successively transformed into

$$W(\Phi_{c'n}, \Phi_{c'}^{(c)}(k)) = \Phi_{c'n}\Phi_{c'}^{(c)}(k) \left[\frac{\Phi_{c'}^{(c)\prime}}{\Phi_{c'}^{(c)}} - L_{c'n}\right],$$

when account is taken of eqs. (10.8) and the notation (3.22) is used. The last expression may further be split as follows:

$$W(\Phi_{c'n}, \Phi_{c'}^{(c)}(k)) = \Phi_{c'n}\Phi_{c'}^{(c)}(k)[L_{c'}(k) - L_{c'n}] - \frac{\Phi_{c'n}}{O_{c'}(k)} W(\Phi_{c'}^{(c)}, O_{c'}),$$

the last term vanishing, in virtue of the conditions (9.1b), for all channels except c. We therefore get

$$(\mathscr{E}_n-\mathscr{E})\int_\omega \Psi^*_{-n}\Psi^{(c)}(k)\mathrm{d}\omega = -\frac{\hbar^2}{2M_c}\frac{\Phi_{cn}}{O_c(k)}W(\Phi_c^{(c)}, O_c) + \sum_{c'}\frac{\hbar^2}{2M_{c'}}\Phi_{c'n}\Phi_{c'}^{(c)}(k)[L_{c'}(k)-L_{c'n}].$$

We now take the derivative of both sides with respect to $\mathscr{E}$ and let then $\Psi^{(c)}(k)$ coincide with Ψ_n; it is clear, on account of the conditions (10.8) and the special form of the various terms, that the result of this operation is

$$-\int_\omega \Psi^*_{-n}\Psi_n\mathrm{d}\omega = -\frac{\hbar^2}{2M_c}\frac{\Phi_{cn}}{O_{cn}}\left[\frac{\mathrm{d}}{\mathrm{d}\mathscr{E}}W(\Phi_c^{(c)}, O_c)\right]_{\mathscr{E}=\mathscr{E}_n} + \sum_{c'}\frac{\hbar^2}{2M_{c'}}\Phi^2_{c'n}\left.\frac{\mathrm{d}L_{c'}}{\mathrm{d}\mathscr{E}}\right|_{\mathscr{E}=\mathscr{E}_n},$$

whence

$$\frac{1}{\left[\dfrac{\mathrm{d}}{\mathrm{d}\mathscr{E}}W(\Phi_c^{(c)}, O_c)\right]_{\mathscr{E}=\mathscr{E}_n}} = \frac{\hbar^2}{2M_c}\frac{\Phi_{cn}}{O_{cn}}\frac{1}{\nu_n}, \tag{10.10}$$

with

$$\nu_n \equiv \int_\omega \Psi^*_{-n}\Psi_n\mathrm{d}\omega + \sum_c \frac{\hbar^2}{2M_c}\Phi^2_{cn}\frac{\mathrm{d}L_{cn}}{\mathrm{d}\mathscr{E}_n}. \tag{10.11}$$

Inserting the results (10.9) and (10.10) into eq. (10.7), we obtain for the residue $r_{c'cn}$ the symmetrical expression

$$r_{c'cn} = -i\frac{\hbar^2}{\sqrt{M_c M_{c'}}}\frac{1}{\nu_n k^l_{cn}k^{l'}_{c'n}}\frac{\Phi_{cn}}{O_{cn}}\frac{\Phi_{c'n}}{O_{c'n}}. \tag{10.12}$$

We now define by

$$\mathrm{e}^{i\bar{\xi}_{cn}}G_{cn} \equiv \frac{\hbar}{\sqrt{M_c\nu_n}}\frac{\Phi_{cn}}{O_{cn}} \tag{10.13a}$$

the modulus G_{cn} and phase $\bar{\xi}_{cn}$ of one of the typical factors occurring in the expression (10.12). Denoting, moreover, by ζ_{cn} the phase of the complex quantity k^l_{cn}, and defining ξ_{cn} by

$$\xi_{cn} = \bar{\xi}_{cn}-\zeta_{cn}, \tag{10.13b}$$

we have the expansion

$$S_{c'c} = Q_{c'c}(\mathscr{E}) - i\sum_n \frac{\mathrm{e}^{i\xi_{c'n}}}{|k_{c'n}|^{l'}}\frac{G_{c'n}G_{cn}}{\mathscr{E}-\mathscr{E}_n}\frac{\mathrm{e}^{i\xi_{cn}}}{|k_{cn}|^l}. \tag{10.14a}$$

The function $Q_{c'c}(\mathscr{E})$ is regular in the physical $\mathscr{E}$-plane; it is undefined along the cuts, and in particular at the thresholds. A similar expansion is valid for $\bar{S}_{c'c}$, namely

$$\bar{S}_{c'c} = \bar{Q}_{c'c}(\mathscr{E}) - i\sum_n \mathrm{e}^{i\bar{\xi}_{c'n}}\frac{G_{c'n}G_{cn}}{\mathscr{E}-\mathscr{E}_n}\mathrm{e}^{i\bar{\xi}_{cn}}. \tag{10.14b}$$

Since the collision matrix elements and their poles $\mathscr{E}_n$ are a_c-independent quantities, the same property is valid for the residues (10.12) and accordingly also for the quantities G_{cn}, $\bar{\xi}_{cn}$ and ξ_{cn}.

Corresponding to the expansions (10.14), we have for the collision matrix elements

$$\mathscr{U}_{c'c}-\delta_{c'c}=\sqrt{k_{c'}k_c}\left[k_{c'}^{l'}k_c^{l}Q_{c'c}(\mathscr{E})\right.$$
$$\left.-i\sum_n\left(\frac{k_{c'}}{|k_{c'n}|}\right)^{l'}\left(\frac{k_c}{|k_{cn}|}\right)^{l}e^{i\bar{\xi}_{c'n}}\frac{G_{c'n}G_{cn}}{\mathscr{E}-\mathscr{E}_n}e^{i\bar{\xi}_{cn}}\right], \quad (10.15a)$$

$$\mathscr{U}_{c'c}-\delta_{c'c}=\sqrt{k_{c'}k_c}\left[\bar{Q}_{c'c}(\mathscr{E})-i\sum_n e^{i\bar{\xi}_{c'n}}\frac{G_{c'n}G_{cn}}{\mathscr{E}-\mathscr{E}_n}e^{i\bar{\xi}_{cn}}\right]. \quad (10.15b)$$

10.3. PHYSICAL INTERPRETATION OF THE COLLISION MATRIX EXPANSION

Let us return to the expression (9.14) for the *total width* Γ_n. Defining Γ_{cn} by

$$\Gamma_{cn}=\frac{1}{\mu_n}\frac{\hbar^2\kappa_{cn}}{M_c}\left|\frac{\Phi_{cn}}{O_{cn}}\right|^2, \quad (10.16)$$

where

$$\mu_n\equiv\int_\omega|\Psi_n|^2d\omega+\sum_c N_{cn}\left|\frac{\Phi_{cn}}{O_{cn}}\right|^2, \quad (10.17)$$

we may rewrite the equation (9.14) in the form

$$\Gamma_n=\sum_c\Gamma_{cn}; \quad (10.18)$$

clearly, Γ_{cn} has to be interpreted as the *partial width* of the state Ψ_n in channel c.

A *penetration factor* P_{cn} in channel c for the resonant state Ψ_n is appropriately defined by

$$P_{cn}(a_c)=\left|\frac{e^{ik_n a}}{O_c(a_c,k_n)}\right|^2: \quad (10.19a)$$

for an s-neutron channel, it reduces exactly to unity, and in general it remains finite for any choice of the channel radius a_c. Accordingly, the quantity

$$g_{cn}^2=\frac{\Gamma_{cn}}{P_{cn}}=\frac{1}{\mu_n}\frac{\hbar^2\kappa_{cn}}{M_c}e^{-2\gamma_{cn}a_c}|\Phi_{cn}|^2 \quad (10.19b)$$

is the *reduced width* of channel c for the state Ψ_n; the quantity g_{cn} itself, taken as positive, is the corresponding *reduced width amplitude*. The partial width Γ_{cn}, like the total width Γ_n, is an a-independent quantity, i.e. it does not change when any of the channel radii a_c, $a_{c'}$, ... is increased from its smallest possible value (cf. end of section 3). The penetration factor and reduced width of a given channel, on the other hand, are of course dependent on the choice of the corresponding channel radius, except in the case of an s-neutron channel.

The expansions (10.15) are easily rewritten in terms of the above quantities. Introducing the notation

$$q_n = \frac{\mu_n}{|\nu_n|} \tag{10.20}$$

to designate a factor which is channel-independent, we have

$$G_{cn} = q_n \sqrt{\frac{\Gamma_{cn}}{\kappa_{cn}}} = q_n \sqrt{\frac{P_{cn}}{\kappa_{cn}}}\, g_{cn}. \tag{10.21}$$

Hence, instead of the expansions (10.15), we get

$$\mathscr{U}_{c'c} - \delta_{c'c} = k_{c'}^{l'+\frac{1}{2}} k_c^{l+\frac{1}{2}} Q_{c'c}(\mathscr{E}) - i \sum_n q_n \left(\frac{k_{c'}}{|k_{c'n}|}\right)^{l'} \left(\frac{k_c}{|k_{cn}|}\right)^{l} \sqrt{\frac{k_{c'} k_c}{\kappa_{c'n}\, \kappa_{cn}}}\, e^{i\xi_{c'n}} \frac{\Gamma_{c'n}^{\frac{1}{2}} \Gamma_{cn}^{\frac{1}{2}}}{\mathscr{E} - \mathscr{E}_n}\, e^{i\xi_{cn}}, \tag{10.22a}$$

$$\mathscr{U}_{c'c} - \delta_{c'c} = \sqrt{k_{c'} k_c}\, \bar{Q}_{c'c}(\mathscr{E}) - i \sum_n q_n \sqrt{\frac{k_{c'} k_c}{\kappa_{c'n}\, \kappa_{cn}}}\, e^{i\bar{\xi}_{c'n}} \frac{\Gamma_{c'n}^{\frac{1}{2}} \Gamma_{cn}^{\frac{1}{2}}}{\mathscr{E} - \mathscr{E}_n}\, e^{i\bar{\xi}_{cn}}. \tag{10.22b}$$

In these expansions, the factors $\Gamma_{cn}^{\frac{1}{2}}$ may be replaced by $P_{cn}^{\frac{1}{2}}\, g_{cn}$, and the denominators of the resonance terms may be given the familiar form

$$\mathscr{E} - \mathscr{E}_n = E_c - E_{cn} + \tfrac{1}{2} i \Gamma_n = E_{c'} - E_{c'n} + \tfrac{1}{2} i \Gamma_n, \tag{10.23a}$$

where

$$E_c = \frac{\hbar^2}{2M_c} k_c^2, \qquad E_{cn} = E_n - E_{\bar{a}_c} = \frac{\hbar^2}{2M_c} (\kappa_{cn}^2 - \gamma_{cn}^2). \tag{10.23b}$$

The quantities κ_{cn} and γ_{cn} are easily expressed in terms of the resonance energy parameter E_{cn} and the total width Γ_n.

The resonant states, as we define them, have a partial width in each channel c, independently of the sign of E_{cn}, i.e. even if $\mathscr{E}_n$ appears as virtual in the channel c because $E_{cn} < 0$. This corresponds to the fact that the well-defined physical situation represented by a resonant state (with $\Gamma_n > 0$) is by no means a stationary state of definite positive energy $\mathscr{E}$ of the system, but must be regarded as a superposition of all the states $\Psi(\mathscr{E})$ of positive energy. Conversely, in order to represent a single stationary state, we need the whole set of resonant states.

Besides the resonance contributions, all elements of the collision matrix contain in principle background terms $Q_{c'c}(\mathscr{E})$, $\bar{Q}_{c'c}(\mathscr{E})$, which, like the resonance part, are independent of the choice of the channel radii (in the sense explained at the end of section 3). It seems difficult to make any general statement about the relative importance of such background terms. As regards their behaviour as functions of the energy, it is clear that, since they depend on

$\mathscr{E}$ through the channel wave-numbers $k_c \propto (\mathscr{E}-E_{\bar{c}})^{\frac{1}{2}}$, they will exhibit "cusps" at the channel thresholds. In this way, this well-known feature of the reaction cross-sections also finds its natural place in the theory.

Our thanks are due to Prof. R. Peierls and to Dr. H. Weidenmüller for helpful discussions. One of us (J.H.) wishes to express his gratitude to the Copenhagen Institute for Theoretical Physics and the Kellogg Radiation Laboratory at Pasadena, which have offered him excellent opportunities for his work; grants from the University of Liège and the Institut Interuniversitaire des Sciences Nucléaires are gratefully acknowledged.

References

1) H. A. Bethe, Rev. Mod. Phys. **9** (1937) 69;
H. A. Bethe and G. Placzek, Phys. Rev. **51** (1937) 450
2) A. M. Lane and R. G. Thomas, Rev. Mod. Phys. **30** (1958) 257
3) P. L. Kapur and R. E. Peierls, Proc. Roy. Soc. A **166** (1938) 277
4) A. F. J. Siegert, Phys. Rev. **56** (1939) 750
5) J. Humblet, Thesis, University of Liège (1952); Mém. Soc. Roy. Sc. de Liège (8°) **12**, No. 4 (1952)
6) R. G. Newton, J. Math. Phys **1** (1960) 319
7) R. E. Peierls, Proc. Roy. Soc. A **253** (1959) 16
8) K. J. Le Couteur, Proc. Roy. Soc. A **256** (1960) 115
9) L. Rosenfeld, Foundations of the optical model and direct interactions, Hercegnovi Summer meeting, 1959 (NORDITA, Copenhagen, 1960)
10) Proc. Int. Conf. on Nuclear Structure held in Kingston, Ontario, Canada, August 1960; ed. by D. A. Bromley and E. W. Vogt (University of Toronto Press, Toronto and North Holland Publishing Company, Amsterdam, 1960)
11) H. M. Nussenzveig, Nuclear Physics **11** (1959) 499
12) G. Beck and H. M. Nussenzveig, Nuovo Cim. **16** (1960) 416
13) F. J. Shore and V. L. Sailor, Phys Rev. **112** (1958) 191;
E. Vogt, Phys. Rev. **112** (1958) 203
14) E. T. Copson, Theory of Functions of Complex Variables (Oxford University Press, 1935) §6.8
15) J. Humblet, Comptes rendus Acad. Sc. **231** (1950) 1436
16) C. Bloch, Nuclear Physics **4** (1957) 503

2.A.2:
2.E

Nuclear Physics **26** (1961) 594—607; © *North-Holland Publishing Co., Amsterdam*
Not to be reproduced photoprint or by microfilm without written permission from the publisher

THEORY OF NUCLEAR REACTIONS

II. The Foundation of the Optical Model

L. ROSENFELD
NORDITA, *Copenhagen*

Received 15 May 1961

Abstract: An equation determining the optical-model potential in terms of the nuclear interactions is derived from the condition that the model should give the correct shape-elastic scattering, by an argument making direct use of Green's operators, without any expansion in series of orthogonal functions. This method is therefore applicable to the theory in which the resonant states are defined by natural boundary conditions, so that their eigenfunctions are not orthogonal. The computation of the collision matrix for direct interaction processes is performed on the same basis.

1. Introduction

On several occasions during late years, and most recently in a course of lectures given at the 1959 Summer Meeting of Physicists at Hercegnovi [1]), I called attention to the possibility of developing the theory of nuclear reactions on the basis of a "natural"definition of the resonant states, originally proposed by Siegert [2]). Although the set of resonant states defined in this way is not orthogonal, dispersion formulae of the Lorentz type for the elements of the collision matrix can be derived in a simple and rigorous way by a straightforward application of Mittag-Leffler's expansion theorem for meromorphic functions. This important fact was established for the first time by J. Humblet[3]) in the case of elastic scattering by a fixed potential, and the extension to the general case, outlined in the above-mentioned course of lectures, has been developed in detail in a first paper under the same general title as the present one, in collaboration with J. Humblet [4]). The resulting theory is free from the arbitrary elements which mar the other approaches, and is also simpler both conceptually and mathematically.

One point, however, is still in need of elucidation. According to the lucid presentation given by G. Brown [5]), the establishment of the optical model appears to depend on the possibility of comparing the resonant states of the actual nuclear system with those of the model by expanding the ones in terms of the others, a procedure which would seem to succeed only if such resonant states form complete orthogonal systems. In my Hercegnovi lectures I was accordingly led, in discussing the foundation of the optical model, to relinquish

the natural definition of the resonances and reluctantly revert to the Kapur-Peierls one adopted by Brown. On closer inspection, however, it becomes apparent that the orthogonality of the resonant states is quite irrelevant to the argument. In fact, as I intend to show, the argument does not imply any expansion in terms of orthogonal functions at all, but rests essentially on the close relationship between the collision matrix and the Green operator associated with the Hamiltonian and the boundary conditions; therefore it becomes much more transparent if this relationship is expressed directly, without explicit reference to the resonant states. Such a reformulation of Brown's argument is significant inasmuch at it completes the logical framework of a theory of nuclear reactions founded entirely on the natural definition of the resonant states. It may now be concluded that a complete and self-sufficient analysis of the resonance character of the reaction is afforded by the simple approach based on Siegert's resonance conditions and the Mittag-Leffler type of representation of the reaction amplitudes.

2. Implicit Definition of the Optical-Model Potential

For the sake of clarity, we shall briefly recall all the stages of the argument, referring the reader to G. Brown's article [5]) for more details on specific points. In the first place, one expects the optical model to represent the behaviour of the actual nuclear system in the so-called direct interaction processes, the occurrence of which is determined by the average value of the elements of the collision matrix over a suitably chosen distribution of the energy of the system. The choice of this energy distribution (which is part of the definition of the model) is guided by the desirability of upholding the typical resonance structure of the matrix elements; in fact, one expects that the average over a large number of resonance peaks of the Lorentz type of the actual system, contained in a given energy interval, will yield a smooth energy dependence resembling one of the broad "giant" resonances of the same Lorentz type, which pertain to a (complex) potential of the form adopted in the model. As is well known, the desired result is obtained by taking a distribution over the energy E' which is itself of the Lorentz type, viz. $(I/\pi)[(E'-E)^2+I^2]^{-1}\mathrm{d}E'$, and the outcome of the averaging process applied to a function of the energy E' is simply to yield the value of this function for the complex energy value $E+iI$. We have therefore to compare the collision-matrix elements of the actual system, taken for the energy $E+iI$, with those calculated for the model at the energy E. This conclusion is the only part of the argument that makes essential use of the resonance structure of the collision matrix; but obviously, all that is implied is the possibility of representing the matrix elements as sums of resonance terms of the Lorentz type (plus a residual, smoothly varying energy function); the precise way in which the resonant states are defined is irrelevant,

and in particular there is no need for these states to form an orthogonal set. On the contrary, the "natural" definition of the resonant states, leading directly to the required representation of the matrix elements, forms the simplest possible basis for the conclusion just enunciated.

The next step consists in the precise formulation of the comparison between the average behaviour of the actual system and that of the model. In conformity with the nature of the model, we impose identity of behaviour for the shape-elastic scattering; this, as is well known, implies identity for the *total* reaction cross sections as well. Let us restrict ourselves, for simplicity, to two-particle channels, and denote by $\mathscr{U}_{c'c} \equiv (v_{c'}/v_c)^{\frac{1}{2}} U_{c'c}$ the element of the collision matrix corresponding to the reaction that leads from channel c to channel c' (the relative velocity in any channel c being denoted by v_c). Let us distinguish all quantities pertaining to the optical model by a superimposed accent; thus, for the elastic scattering in channel c the model matrix element will be $\hat{U}_{cc}$. The condition that specifies the model may then be written

$$U_{cc}(E+iI) = \hat{U}_{cc}(E) \tag{1}$$

for each channel separately. This equation may be regarded as an implicit definition of the effective (complex) potential $\hat{V}_c$ of the optical model for each channel c. The task is now to extract from it an explicit expression for this potential in terms of the "actual" interaction occurring in the determination of U_{cc}. For this purpose it is clearly desirable to obtain an expression for U_{cc} (and similarly for $\hat{U}_{cc}$) in which the dependence on the Hamiltonian is exhibited explicitly; such an expression will be derived in the two following sections.

3. The Collision Matrix

Let us first recall the definition of the collision matrix in terms of the amplitudes of outgoing and incoming waves in the channels involved. In each channel a radial coordinate r_c can be defined and a channel radius a_c introduced, so that the equation $r_c = a_c$ defines in configuration space the "boundary" of the channel. These boundary surfaces form a total surface $\mathscr{S}$, which divides configuration space into a region Ω interior to all boundaries and its complement, which may be called the exterior region. In the latter, the wave function describing a given physical situation, i.e. a nuclear reaction of a given type, can be expressed as a sum of "channel wave functions" of the form

$$\Psi_c = (x_c O_c + y_c I_c)\frac{\varphi_c}{r_c}, \tag{2}$$

in which O_c/r_c, I_c/r_c are the "radial" components describing an outgoing and an incoming wave respectively, whereas the "surface" factor φ_c includes the dependence on all coordinates other than r_c. The amplitudes y_c of the incoming

waves characterize the given physical situation; the amplitudes x_c of the outgoing waves are then determined by the interior wave function, which embodies the effect of the interactions taking place in the interior region. To relate the amplitudes x_c to the interior wave function, one only has to write down the boundary conditions expressing the smooth joining of the interior and exterior wave functions on the boundary separating the two regions.

The element $U_{c'c}$ of the collision matrix is introduced by considering the special case in which there is only one incoming component, viz. in channel c; the outgoing amplitude $x_{c'}^{(c)}$ in channel c′ is then written in the form

$$x_{c'}^{(c)} = -U_{c'c}\, y_c; \tag{3}$$

this equation defines the matrix element $U_{c'c}$ and allows us to express it in terms of the interior wave function $\Psi^{(c)}$ describing the case in question. More precisely, let us define, on the boundary of each channel c′, the quantity

$$\Phi_{c'}^{(c)} = a_{c'} \int \varphi_{c'}^{*} \Psi^{(c)} \mathrm{d}S_{c'}, \tag{4}$$

where the integration involves all coordinates $Q_{c'}$ other than $r_{c'}$ and is taken over the boundary surface $r_{c'} = a_{c'}$ of channel c′. The first boundary condition on this surface expresses the equality of the quantity $\Phi_{c'}^{(c)}$ with the radial part of the channel wave function given by eq. (2):

$$\Phi_{c'}^{(c)} = x_{c'}^{(c)} O_{c'}(a_{c'}) + y_{c'}^{(c)} I_{c'}(a_{c'}), \tag{5}$$

and accordingly gives $x_{c'}^{(c)}$ in terms of $\Phi_{c'}^{(c)}$ and the incoming amplitude $y_c^{(c)}$ (all amplitudes $y_{c'}^{(c)}$ vanish except that for the entrance channel $c' = c$).

For any channel c′ other than the entrance channel we get, from eqs. (3) and (5),

$$U_{c'c} = -\frac{1}{y_c^{(c)}} \frac{\Phi_{c'}^{(c)}}{O_{c'}(a_{c'})}, \tag{6}$$

and for the entrance channel c,

$$U_{cc} = -\frac{1}{y_c^{(c)}} \frac{\Phi_c^{(c)}}{O_c(a_c)} + \frac{I_c(a_c)}{O_c(a_c)}. \tag{7}$$

The additional term in the last formula (which is the amplitude for "potential scattering") is independent of the dynamical characteristics of the system and therefore plays no part in the comparison between nuclear system and optical model; the quantity of interest is that part of the matrix element (7) which has the same form as the general matrix element (6); accordingly, we shall now discuss the latter. We want to transform it in such a way that its dependence on the Hamiltonian appears explicitly.

4. Green's Operator and Collision Matrix

It will now be advantageous to make use of the algorism introduced by C. Bloch [6]) for expressing eigenfunctions of the Hamiltonian H, satisfying the wave equation

$$(E-H)\Psi = 0 \tag{8}$$

and given boundary conditions, with the help of a Green operator. The method consists in representing the boundary conditions by the action of a suitable operator $\mathscr{L}$ upon the wave function:

$$\mathscr{L}\Psi = \mathscr{F}; \tag{9}$$

both the operator $\mathscr{L}$ and the function $\mathscr{F}$ are built up entirely of *known* quantities and take the form of sums of terms referring to the various channels, each involving a factor $\delta(r_c-a_c)$. It is clear that the wave equation (8) and the boundary conditions (9) are equivalent to the single inhomogeneous equation

$$(E-G)\Psi = -\mathscr{F}, \tag{10}$$

where

$$G = H+\mathscr{L}. \tag{11}$$

The latter can be solved by the Green operator $(E-G)^{-1}$ in the form

$$\Psi = -\frac{1}{E-G}\mathscr{F}, \tag{12}$$

an expression that brings out the role of the Hamiltonian quite explicitly, since the function $\mathscr{F}$ is *independent of this Hamiltonian.*

On account of this last circumstance, we may replace $\mathscr{F}$, in eq. (12), by $\mathscr{L}\hat{\Psi}$, where $\hat{\Psi}$ is the optical-model wave function satisfying the same boundary conditions as the actual wave function Ψ and corresponding to the same energy value E. Eq. (12) then becomes

$$\Psi = -\frac{1}{E-G}\mathscr{L}\hat{\Psi}, \tag{13}$$

thus establishing a definite relation between corresponding wave functions of the actual system and of the optical model. One sees how a direct approach, by means of a Green operator, leads to such a relation without any recourse to expansions in orthogonal functions.

Now, the operator $\mathscr{L}$ may be used to express the matrix element $U_{c'c}$ given by (6) directly in terms of the wave functions $\Psi^{(c)}$ and $\Psi^{(c')}$. To see this, one must consider the explicit form of $\mathscr{L}$, derived in the Appendix, and in particular the relation (A.18), which may be written

$$\varphi^*_{c'}\delta(r_{c'}-a_{c'})\frac{1}{a_{c'}} = -\frac{O_{c'}(a_{c'}, k_{c'})}{i\hbar v_{c'} y^{(c')}_{c'}}[\mathscr{L}(-k^*)\Psi^{(c')}(-k^*)]^*;$$

in this formula, the notation $-k^*$ represents the set of channel wave-numbers $-k^*_c$, $-k^*_{c'}, \ldots$. For the expression (4) of the radial factor $\Phi^{(c)}_{c'}$, which enters into the definition (6) of $U_{c'c}$, we may write

$$\Phi^{(c)}_{c'} = \int \varphi^*_{c'}\delta(r_{c'}-a_{c'})\frac{1}{a_{c'}}\Psi^{(c)}\mathrm{d}\omega,$$

where $\mathrm{d}\omega$ denotes the integration over all variables, and substitute for the first factor its expression just written. This gives us directly the quotient $\Phi^{(c)}_{c'}/O_{c'}$, and consequently

$$U_{c'c} = -i\frac{1}{\hbar v_{c'} y^{(c')}_{c'} y^{(c)}_{c}}\int [\mathscr{L}(-k^*)\Psi^{(c')}(-k^*)]^*\Psi^{(c)}(k)\mathrm{d}\omega.$$

In this formula we may replace $\Psi^{(c')}$ by the corresponding optical-model function $\hat{\Psi}^{(c')}$, and express $\Psi^{(c)}$ in terms of the corresponding $\hat{\Psi}^{(c)}$ by means of eq. (13). Going over to the element $\mathscr{U}_{c'c}$ of the collision matrix, we thus arrive at the expression

$$\mathscr{U}_{c'c} = i\frac{1}{y^{(c')}_{c'}\sqrt{\hbar v_{c'}}}\int [\mathscr{L}(-k^*)\hat{\Psi}^{(c')}(-k^*)]^*\left[\frac{1}{E-G}\mathscr{L}(k)\hat{\Psi}^{(c)}(k)\right]\mathrm{d}\omega\,\frac{1}{y^{(c)}_{c}\sqrt{\hbar v_{c}}}, \tag{14}$$

which has the desired property of exhibiting the explicit dependence of this matrix element on the Hamiltonian of the nuclear system: it shows in fact that the interaction between the nucleons only occurs through the Green operator $(E-G)^{-1}$, everything else being independent of this interaction.

Incidentally, it may be observed that the expression (14) for the matrix element $\mathscr{U}_{c'c}$ also exhibits the complete symmetry between entrance and exit channel $\mathscr{U}_{c'c} = \mathscr{U}_{cc'}$. In fact, according to eqs. (A.9), (A.18) of the Appendix, the integral occurring in eq. (14) is proportional (with a coefficient of proportionality symmetrical in c and c') to the matrix element $(c'|(E-G)^{-1}|c)$ defined by eq. (A.29) of subsection A.3 of the Appendix; and it is shown in this subsection that such a matrix element is also symmetrical in c and c'.

5. Determination of the Optical-Model Potential

We are now prepared to transform the condition (1) imposed upon the optical-model potential so as to derive from it an expression for this potential, in a given channel, in terms of the operator of potential energy V of the nuclear system. To begin with, we may without serious error take the right-hand side

of eq. (1) for the argument $E+iI$ instead of E: for this amounts to adding I to the imaginary part of the model Hamiltonian $\hat{H}$, and the energy interval I must at any rate be chosen appreciably smaller than the half-widths of the resonant states of the model. In this section we shall accordingly keep the notation E for the energy, it being understood that it everywhere represents the complex value $E+iI$.

According to eq. (14), the condition (1) then takes the form

$$\int_{\Omega} [\mathscr{L}(-k^*)\hat{\Psi}^{(c)}(-k^*)]^* \left\{ \left[\frac{1}{E-G} - \frac{1}{E-\hat{G}} \right] \mathscr{L}(k)\hat{\Psi}^{(c)}(k) \right\} d\omega = 0;$$

it is clearly permissible to restrict formally the domain of integration (which is actually the boundary $\mathscr{S}$) to the interior region Ω (including the boundary). Since $\hat{\Psi}^{(c)}$ is a solution of the equation $(E-\hat{H})\hat{\Psi}^{(c)} = 0$, the operator $\mathscr{L}(k)$ in the last formula may be replaced by $-\mathscr{G}(k) \equiv -[E-\hat{H}-\mathscr{L}(k)]$, and $\mathscr{L}(-k^*)$ by the time-reversed operator (cf. Appendix, subsection A.2 and especially eq. (A.21)) $-\mathscr{G}_K(-k^*) \equiv -[E^*-\hat{H}^*-\mathscr{L}(-k^*)]$. Applying eq. (A.26) of the Appendix, we obtain the equivalent equation

$$\int_{\Omega} \hat{\Psi}^{(c)}(-k^*)^* \left\{ (E-\hat{G}) \left[\frac{1}{E-G} - \frac{1}{E-\hat{G}} \right] (E-\hat{G})\hat{\Psi}^{(c)}(k) \right\} d\omega = 0. \quad (15)$$

The operator occurring in eq. (15) is simplified by using the identity

$$\frac{1}{E-G} - \frac{1}{E-\hat{G}} = \frac{1}{E-\hat{G}} \left[\mathscr{V} + \mathscr{V} \frac{1}{E-G} \mathscr{V} \right] \frac{1}{E-\hat{G}}, \quad (16)$$

where

$$\mathscr{V} \equiv V-\hat{V}; \quad (17)$$

eq. (15) then becomes

$$\int_{\Omega} \hat{\Psi}^{(c)}(-k^*)^* \left\{ \left[\mathscr{V} + \mathscr{V} \frac{1}{E-G} \mathscr{V} \right] \hat{\Psi}^{(c)}(k) \right\} d\omega = 0. \quad (18)$$

In this form, our condition involves integrations over the whole interior region, and would thus seem to be unsuited for the determination of the optical-model potential in channel c as a function $\hat{V}_c(r_c)$ of the radial variable r_c. However, we can extract from it another relation allowing this determination, by taking advantage of the fact that the model wave function $\hat{\Psi}^{(c)}$ — in contrast to the corresponding one for the nuclear system — may be decomposed in the interior as well as the exterior region into the product of a radial factor $\hat{u}_c(r_c)/r_c$ and a surface factor $\varphi_c(Q_c)$ depending on all the other channel coordinates Q_c. Integration of an expression of the form

$$\int_{\Omega} \hat{\Psi}^{(c)}(-k^*)\{\mathscr{O}\hat{\Psi}^{(c)}(k)\} d\omega, \quad (19)$$

for any operator $\mathcal{O}$, first over the coordinates Q_c, introduces the matrix element

$$(c|\mathcal{O}|c) = \int \varphi_c^*(Q'_c)dS'_c(Q'_c|\mathcal{O}|Q_c)dS_c\varphi_c(Q_c), \tag{20}$$

which is still an operator with respect to the radial variable r_c. The vanishing of this operator is a sufficient condition for the vanishing of the quantity (19), and it is appropriate, when applied to the operator occurring in eq. (18), to give us the required determination of the optical-model potential $\hat{V}$. Observing that for $r_c \neq a_c$ the operator G becomes H, we accordingly adopt, for the definition of the potential $\hat{V}_c(r_c)$ in any channel c, the equation

$$(c|\mathscr{V}+\mathscr{V}\frac{1}{E-H}\mathscr{V}|c) = 0, \tag{21}$$

which exactly coincides with that derived by Brown [5]).

For the sake of completeness, we shall briefly outline the procedure used by Brown for solving eq. (21). As a first approximation, we may just take $(c|\mathscr{V}|c) = 0$, which directly leads to a real effective potential $\hat{V}_c(r_c) \approx (c|V|c)$ corresponding to the conception of the shell model. We accordingly put

$$\hat{V}_c(r_c) = (c|V|c)+W_c(r_c), \tag{22}$$

and introduce the operator

$$\mathscr{V}_c = V-(c|V|c), \tag{23}$$

which represents the "residual interaction" of the nuclear system in channel c. To find $W_c(r_c)$ we have, according to eqs. (21), (22), (23), to solve the equations

$$W_c = (c|\mathscr{V}\frac{1}{E-H}\mathscr{V}|c), \qquad \mathscr{V} = V_c-W_c. \tag{24}$$

Now, we observe that the condition (21) implies

$$(c|\mathscr{V}\frac{1}{E-H}|c) = 0. \tag{25}$$

Indeed, eq. (21) is readily transformed into

$$(c|\mathscr{V}\frac{1}{E-H}(E-\hat{H})|c) = 0, \tag{26}$$

and since φ_c is an eigenfunction, belonging to the eigenvalue E_α, of the part H_α of the Hamiltonian depending on the Q_c, we may write (denoting by $\hat{H}_r$ the radial part of the Hamiltonian)

$$(E-\hat{H})|c) = (E-H_\alpha-\hat{H}_r)|c) = |c)(E-E_\alpha-\hat{H}_r); \tag{27}$$

combining eqs. (26) and (27), we are immediately led to eq. (25) — which,

incidentally, simply means that $(c|(E-H)^{-1}|c) = (c|(E-\hat{H})^{-1}|c)$.

Taking eq. (25) into account, we derive from eqs. (24)

$$W_c = \frac{(c|\mathscr{V}_c \frac{1}{E-H} \mathscr{V}_c|c)}{1+(c|\frac{1}{E-H}\mathscr{V}_c|c)}. \tag{28}$$

With the help of the density operator Π_c defined by eq. (A.5), this may be written more simply in terms of a modified Hamiltonian

$$H_1 = H-\mathscr{V}_c\Pi_c, \tag{29}$$

in which the residual interaction is removed from the channel c. We then have

$$\frac{1}{E-H} - \frac{1}{E-H_1} = \frac{1}{E-H_1}\mathscr{V}_c\Pi_c\frac{1}{E-H}, \tag{30}$$

from which we easily derive

$$W_c = (c|\mathscr{V}_c \frac{1}{E-H_1+iI}\mathscr{V}_c|c), \tag{31}$$

where we have re-introduced explicitly the complex value $E+iI$ of E. It will be noticed that the operator H_1 is expressed entirely in terms of the residual interaction $\mathscr{V}_c$ as

$$H_1 = T+(c|V|c)+\mathscr{V}_c(1-\Pi_c) \tag{32}$$

(where T denotes the kinetic-energy operator). For the further discussion of the expression (31) the reader is referred to Brown's paper [5]).

6. Direct Interactions

Let us return to the general expression (14) for the matrix element $\mathscr{U}_{c'c}$. If we take its average value over an energy interval I, which amounts to taking its value at the complex energy $E+iI$, we obtain the amplitude for the direct interaction leading from channel c to channel c', immediately expressed in terms of the model wave functions $\hat{\Psi}^{(c)}$, $\hat{\Psi}^{(c')}$ associated with these channels (by the condition that the channel c or c' is the only entrance channel). A simple transformation of the same kind as those used in the preceding argument will now reduce the matrix element $\mathscr{U}_{c'c}$ to the familiar form usually assumed without proof in the treatment of direct interactions in the framework of the optical model. This transformation will thus complete the foundation of the model, by establishing on a firm basis the general prescription for constructing the elements of the collision matrix for the direct interactions.

In the first place, by application of Green's theorem in the form (A.26), the

integral occurring in the expression (14) becomes (apart from the sign)

$$\int_\Omega \hat{\Psi}^{(c')}(-k^*)^* \left\{ (E-\hat{G}) \frac{1}{E-G} \mathscr{L}(k) \hat{\Psi}^{(c)}(k) \right\} d\omega;$$

then, by application of the identity (16), we get

$$\int_\Omega \hat{\Psi}^{(c')}(-k^*)^* \{ \mathscr{L}(k) \hat{\Psi}^{(c)}(k) \} d\omega + \int_\Omega \hat{\Psi}^{(c')}(-k^*)^* \left\{ \left[\mathscr{V} + \mathscr{V} \frac{1}{E-G} \mathscr{V} \right] \frac{1}{E-\hat{G}} \mathscr{L}(k) \hat{\Psi}^{(c)}(k) \right\} d\omega. \quad (33)$$

As shown by the form (A.9) of $\mathscr{L}(k)\hat{\Psi}^{(c)}(k)$, the first term of the expression (33) is proportional to

$$\int_{[\mathscr{S}]} \{ \hat{\Psi}^{(c')}(-k^*)^* \}_{r_c = a_c} \varphi_c \, dS_c,$$

which is either zero (by the orthogonality of φ_c, $\varphi_{c'}$), if the channels c, c′ correspond to the same mode of fragmentation of the nuclear system, or at any rate negligibly small, in other cases. In the second term of the expression (33) we may replace $\mathscr{L}\hat{\Psi}$ by $-(E-\hat{G})\hat{\Psi}$, and further neglect (only for reasons of simplicity) the contribution of $\mathscr{V}(E-G)^{-1}\mathscr{V}$. The matrix element $\mathscr{U}_{c'c}$ then takes the approximate form

$$\mathscr{U}_{c'c} = i \frac{1}{y_{c'}^{(c')} \sqrt{\hbar v_{c'}}} \int_\Omega \hat{\Psi}^{(c')}(-k^*)^* \mathscr{V} \hat{\Psi}^{(c)}(k) d\omega \frac{1}{y_c^{(c)} \sqrt{\hbar v_c}}. \quad (34)$$

If the amplitudes in the entrance channels $y_c^{(c)}$, $y_{c'}^{(c')}$ are normalized to a flux of one particle, i.e.

$$|y_c^{(c)}|^2 = \pi(2l_c+1)/k_c^2, \quad (35)$$

where l_c is the orbital quantum number of the relative motion in channel c, the integrated cross section for the direct reaction c → c′ is given by

$$\sigma_{c'c} = |y_c^{(c)}|^2 |\mathscr{U}_{c'c}|^2, \quad (36)$$

and the probability per unit time of this reaction is $v_c \sigma_{c'c}$. The last factor in the expression for $|\mathscr{U}_{c'c}|^2$ derived from eq. (34), with the normalization (35), may be written $2\pi\rho(k_{c'})/(2l_{c'}+1)$, where

$$\rho(k_c) = \frac{4\pi k_c^2}{(2\pi)^3} \frac{dk_c}{d\varepsilon_c} = \frac{k_c^2}{2\pi^2 \hbar v_c}$$

denotes the density of states per unit of kinetic energy $\varepsilon_c = \hbar^2 k_c^2 / 2M_c$ in channel c. The probability per unit time of the reaction c → c′ thus takes the form

$$v_c \sigma_{c'c} = \frac{2\pi}{\hbar} \left| \int_\Omega \hat{\Psi}^{(c')}(-k^*)^* \mathscr{V} \hat{\Psi}^{(c)}(k) d\omega \right|^2 \frac{\rho(k_{c'})}{2l_{c'}+1}, \quad (37)$$

which is just what one would obtain by considering this reaction as a transition from the state $\hat{\Psi}^{(c)}(k)$ to the state $\hat{\Psi}^{(c')}(-k^*)$ brought about by the interaction $\mathscr{V}$. The state $\hat{\Psi}^{(c)}(k)$ contains an incoming wave in channel c, "distorted" by the optical-model potential $\hat{V}_c$; the state $\hat{\Psi}^{(c')}(-k^*)$, essentially the time reverse of $\hat{\Psi}^{(c')}(k)$ (cf. eq. (A.16)), contains an outgoing wave in channel c' only, "distorted" by the corresponding effective potential $\hat{V}_{c'}$. It must be remembered, in specific cases, that the effective potentials may be different for the two channels involved in the reaction considered. In treating inelastic scattering, in particular, one must be careful to compute the distortion of the outgoing wave by the effective potential corresponding to the excited state of the residual nucleus, which may well be appreciably shallower than that belonging to the ground state.

Appendix

A.1. BOUNDARY CONDITIONS AND THE BLOCH OPERATOR

The boundary conditions which characterize a solution of the equation $(E-H)\Psi = 0$ are those connecting the boundary behaviour of the solution Ψ with the incoming amplitudes in the various channels. They are conveniently expressed, as explained in ref. [4]), section 6, in terms of the radial factors

$$\Phi_c = \int \varphi_c^*(r_c\Psi)_{r_c=a_c} \mathrm{d}S_c, \qquad \Phi'_c = \int \varphi_c^* \left[\frac{\partial}{\partial r_c}(r_c\Psi)\right]_{r_c=a_c} \mathrm{d}S_c, \tag{A.1}$$

and are readily found to be (cf. ref. [4]), subsection 6.3)

$$\Phi'_c - L_c(k_c)\Phi_c = -\frac{2ik_c y_c}{O_c(a_c, k_c)}, \tag{A.2}$$

where k_c denotes the channel wave number, and the notation

$$L_c(k_c) = \frac{O'_c(a_c, k_c)}{O_c(a_c, k_c)} \tag{A.3}$$

is used. The form (A.2) has been chosen, with regard to eqs. (A.1), in order to exhibit the left-hand side as the result of the application of an operator $\mathscr{L}$ to the wave function Ψ. The right-hand side is proportional to the component for channel c of a function $\mathscr{F}$ which may be represented, on the boundary surface of the interior region, by an expansion of the form

$$\sum_c \varphi_c(Q_c)\delta(r_c-a_c)F_c(r_c).$$

The operator $\mathscr{L}$ is accordingly of the form

$$\mathscr{L} = \sum_c \Pi_c \mathscr{D}_c(r_c, k_c), \tag{A.4}$$

where Π_c is the density operator

$$(Q_c|\Pi_c|Q'_c) = \varphi_c(Q_c)\varphi_c^*(Q'_c) \tag{A.5}$$

and $\mathscr{D}_c$ an operator which, applied to Ψ, yields a result proportional to the left-hand side of eq. (A.2). We put

$$\mathscr{D}_c(r_c, k_c) = \frac{\hbar^2}{2M_c a_c}\delta(r_c - a_c)\left[\frac{\partial}{\partial r_c} - L_c(k_c)\right] r_c; \tag{A.6}$$

it is understood that, in the r_c-representation, the operation of $\mathscr{D}_c$ on a wave function $\Psi(r_c)$ is expressed as $\int (r_c|\mathscr{D}_c|r'_c)\mathrm{d}r'_c\,\Psi(r'_c)$ (without the usual weight factor $r_c'^2$). The reason for normalizing the operator $\mathscr{D}_c$ by the factor $\hbar^2/2M_c a_c$ (in which M_c denotes the reduced mass in channel c) will appear presently. With the definitions (A.4) to (A.6) and (A.1) we have (since $v_c = \hbar k_c/M_c$)

$$\mathscr{L}\Psi = \sum_c \frac{\hbar^2}{2M_c a_c}\varphi_c(Q_c)\delta(r_c - a_c)[\Phi'_c - L_c\Phi_c]. \tag{A.7}$$

According to eq. (A.2), the function $\mathscr{F}$ then has to be defined as

$$\mathscr{F} = -\sum_c \varphi_c(Q_c)\delta(r_c - a_c)\frac{i\hbar v_c y_c}{a_c O_c(a_c, k_c)}. \tag{A.8}$$

In particular, for the solution $\Psi^{(c)}$ corresponding to a single entrance channel ($y_{c'}^{(c)} = 0$ for $c' \neq c$), we have

$$\mathscr{L}\Psi^{(c)} = -\varphi_c(Q_c)\delta(r_c - a_c)\frac{i\hbar v_c y_c^{(c)}}{a_c O_c(a_c, k_c)}. \tag{A.9}$$

A.2. TIME-REVERSAL PROPERTIES

In ref. [4]), section 8, it is shown in detail how the time-reversal transformation of all quantities specified by a set of channel wave numbers $k \equiv k_c, k_{c'}, \ldots$ is closely related to the replacement of the set k by $-k^* \equiv -k_c^*, -k_{c'}^*, \ldots$. Thus we have

$$KL_c(k_c)K^\dagger = L_c(k_c)^* = L_c(-k_c^*). \tag{A.10}$$

Besides this substitution, we have to take account of the reversal of angular momentum, which amounts to changing the sign of the projection quantum number M of the total angular momentum (this is denoted by changing the channel index c into $-c$); thus, the time reverse of any surface function φ_c which belongs to the total angular momentum quantum numbers J, M is (cf. ref. [4]), eq. (5.14))

$$K\varphi_c = (-1)^{J-M}\varphi_{-c}, \tag{A.11}$$

implying for the density operator Π_c

$$K\Pi_c K^\dagger = \Pi_{-c}. \tag{A.12}$$

From eqs. (A.10), (A.12) we see that the time reverse of the Bloch operator $\mathscr{L}(k)$, defined by (A.4), (A.6), is given by

$$K\mathscr{L}(k)K^{\dagger} = \mathscr{L}(-k^*). \tag{A.13}$$

For the function $\mathscr{F}(k) = \sum_c \varphi_c(Q_c)\delta(r_c - a_c)F_c(r_c, k)$, we have on account of eq. (A.11)

$$K\mathscr{F}(k) = (-1)^{J-M}\sum_c \varphi_c(Q_c)\delta(r_c-a_c)F_c(k)^*$$
$$= (-1)^{J-M}\sum_c \varphi_c(Q_c)\delta(r_c-a_c)F_c(-k^*) = (-1)^{J-M}\mathscr{F}(-k^*), \tag{A.14}$$

the last transformation following from eqs. (3.17), (8.5) of ref. [4]).

The time reverse of the solution $\Psi_{JM}(k)$ characterized by the boundary conditions

$$\mathscr{L}(k)\Psi_{JM}(k) = \mathscr{F}(k) \tag{9}$$

must therefore satisfy the boundary conditions

$$\mathscr{L}(-k^*)[K\Psi_{JM}(k)] = (-1)^{J-M}\mathscr{F}(-k^*), \tag{A.15}$$

in harmony with the time-reversal behaviour imposed upon it (cf. ref. [4]), eq. (8.3))

$$K\Psi_{JM}(k) = (-1)^{J-M}\Psi_{J-M}(-k^*). \tag{A.16}$$

Instead of eq. (A.15) we may thus write

$$\mathscr{L}(-k^*)\Psi(-k^*) = \mathscr{F}(-k^*). \tag{A.17}.$$

Together with eq. (A.14) this leads, in more explicit form, to the following relation, which is analogous to (A.9) and is used in the text of the paper:

$$[\mathscr{L}(-k^*)\Psi^{(c)}(-k^*)]^* = -\varphi_c^*(Q_c)\delta(r_c-a_c)\frac{i\hbar v_c y_c^{(c)}(k)}{a_c O_c(a_c, k_c)}. \tag{A.18}$$

As regards the wave equation, we have to take account of the possibility that the Hamiltonian H contains a complex (non-hermitian) potential energy, and that the energy eigenvalue E is also complex. The time reverse of the operator $E-H$ is then E^*-H^*. For the operator $G(k) = H+\mathscr{L}(k)$ defined by eq. (11), the most general form of time reversal is therefore

$$G_K(-k^*) = H^*+\mathscr{L}(-k^*). \tag{A.19}$$

For the operator

$$\mathscr{G}(k) = E-H-\mathscr{L}(k) \tag{A.20}$$

(the inverse of Green's operator) the time reverse is

$$\mathscr{G}_K(-k^*) \equiv K\mathscr{G}(k)K^{\dagger} = E^*-H^*-\mathscr{L}(-k^*); \tag{A.21}$$

in the last formulae, the energy value E is that associated with the set of wave numbers k.

A.3. AN EXTENSION OF GREEN'S THEOREM

For any two wave functions Ψ_1, Ψ_2 (not necessarily eigenfunctions of the Hamiltonian H) we may write, with the notation (A.1),

$$\int_\Omega \{(H^*\Psi_2)^*\Psi_1 - \Psi_2^*(H\Psi_1)\}\,\mathrm{d}\omega = \sum_c \frac{\hbar^2}{2M_c}[\Phi_{2c}^*\Phi'_{1c} - \Phi'^*_{2c}\Phi_{1c}], \quad \text{(A.22)}$$

where the integral is extended over the interior region Ω (cf. ref. [4]), subsection 6.2.) On the other hand, it follows from eq. (A.7) that

$$\int_\Omega \{(\mathscr{L}(k_2)\Psi_2)^*\Psi_1 - \Psi_2^*(\mathscr{L}(k_1)\Psi_1)\}\mathrm{d}\omega$$
$$= \sum_c \frac{\hbar^2}{2M_c}\{[\Phi'^*_{2c} - L_c(k_2)^*\Phi^*_{2c}]\Phi_{1c} - \Phi^*_{2c}[\Phi'_{1c} - L_c(k_1)\Phi_{1c}]\} \quad \text{(A.23)}$$

for any two sets of channel wave numbers k_1, k_2. In particular, if $k_2 = -k_1^*$, the terms in L_c on the right-hand side of (A.23) cancel on account of eq. (A.10), and we get

$$\int_\Omega \{(\mathscr{L}(-k^*)\Psi_2)^*\Psi_1 - \Psi_2^*(\mathscr{L}(k)\Psi_1)\}\mathrm{d}\omega = \sum_c \frac{\hbar^2}{2M_c}[\Phi'^*_{2c}\Phi_{1c} - \Phi^*_{2c}\Phi'_{1c}]. \quad \text{(A.24)}$$

Addition of eqs. (A.22), (A.24) yields, with the notation (A.19),

$$\int_\Omega \{(G_K(-k^*)\Psi_2)^*\Psi_1 - \Psi_2^*(G(k)\Psi_1)\}\mathrm{d}\omega = 0. \quad \text{(A.25)}$$

It is in order to obtain this simple result that the normalization factor, of the dimension energy times length, in the expression (A.6) for the operator $\mathscr{D}_c$ has been chosen as $\hbar^2/2M_c a_c$. Eq. (A.25) may also be written in terms of the operator $\mathscr{G}(k)$ defined by (A.20):

$$\int_\Omega \{(\mathscr{G}_K(-k^*)\Psi_2)^*\Psi_1 - \Psi_2^*(\mathscr{G}(k)\Psi_1)\}\mathrm{d}\omega = 0. \quad \text{(A.26)}$$

A.4. SYMMETRY OF GREEN'S OPERATOR

Together with eqs. (A.4), (A.6), eq. (A.13) shows that the operator $\mathscr{L}(-k^*)^*$ only differs from $\mathscr{L}(k)$ by the substitution of Π_c^* for Π_c. Denoting by A^T the result of transposition with respect to the "surface" coordinates only (i.e. $(Q|A^T|Q') = (Q'|A|Q)$ when these matrix elements are calculated on the boundary $\mathscr{S}$ of the interior region), we may therefore write, on account of $\Pi_c^* = \Pi_c^T$,

$$\mathscr{L}(-k^*)^{*T} = \mathscr{L}(k). \quad \text{(A.27)}$$

On the other hand, time-reversal invariance of the real and imaginary parts

of the Hamiltonian operator H implies that $H = H^{\mathrm{T}}$, and the expression (A.21) for the time reverse of $\mathscr{G}(k)$ then shows that

$$\mathscr{G}_K(-k^*)^{*\mathrm{T}} = \mathscr{G}(k). \tag{A.28}$$

The same relation holds for the inverse operators. It means that the matrix element

$$(\mathrm{c}'|\frac{1}{E-G(k)}|\mathrm{c}) = \int_{[\mathscr{S}]} \varphi^*_{\mathrm{c}'} \frac{1}{E-G(k)} \varphi_{\mathrm{c}} \mathrm{d}S \tag{A.29}$$

calculated on the boundary $\mathscr{S}$ has the symmetry property

$$(\mathrm{c}'|\frac{1}{E-G(k)}|\mathrm{c}) = (\mathrm{c}|\frac{1}{E-G(k)}|\mathrm{c}'); \tag{A.30}$$

for this matrix element is equal to the complex conjugate of its time reverse, i.e., in virtue of eq. (A.11) (since it is independent of the quantum number M),

$$(\mathrm{c}'|\frac{1}{E-G(k)}|\mathrm{c}) = (\mathrm{c}|\frac{1}{\mathscr{G}_K(-k^*)^{*\mathrm{T}}}|\mathrm{c}'),$$

and by eq. (A.28) this is the same as

$$(\mathrm{c}|\frac{1}{E-G(k)}|\mathrm{c}').$$

References

1) L. Rosenfeld, Lectures at the Summer Meeting of Physicists, Hercegnovi 1959 (NORDITA 1960)
2) A. F. J. Siegert, Phys. Rev. **56** (1939) 750
3) J. Humblet, Mém. in-8° Soc. Roy. Sc. Liège **12**, no. 4 (1952)
4) J. Humblet and L. Rosenfeld, Nuclear Physics **26** (1961) 529
5) G. Brown, Revs. Mod. Phys. **31** (1959) 893
6) C. Bloch, Nuclear Physics **4** (1957) 503

1.C: 2.I

Nuclear Physics **26** (1961) 594—607; © *North-Holland Publishing Co., Amsterdam*

Not to be reproduced by photoprint or microfilm without written permission from the publisher

CENTRE-OF-MASS INVARIANCE AND THE ENERGY SHIFT IN THE NUCLEAR DIPOLE STATE

STAVROS FALLIEROS

Bartol Research Foundation of the Franklin Institute, Swarthmore, Pennsylvania †

Received 24 March 1961

Abstract: A relation is obtained between the magnitude of the energy shift in the nuclear dipole state and the particle-shell interaction energy which characterizes the single-particle excitations. It is found that the ratio of these two quantities is approximately independent of the strength, the detailed shape and the odd-state coefficients of the nuclear two-body force. A value of about one-half is obtained for this ratio if the customary values for the even-state nuclear force parameters are used.

1. Introduction

The nuclear dipole absorption of γ-rays results, according to the shell model, in the promotion of nucleons from the ground configuration to states of higher excitation and opposite parity [1]). It has been noted [2, 3]) that a particular coherent mixture of such single-particle excitations can be singled out which can be easily interpreted as a simple vibration of the protons and the neutrons in the nucleus against each other. The wave function of this state, which is the equivalent of the original Goldhaber-Teller description of the giant dipole resonance phenomenon, is essentially obtained by the application of the electric dipole operator on the ground-state wave function of the system ††. It is thus the mode into which all the dipole radiative strength for ground-state transitions is concentrated, and is naturally the first stage of the photonuclear excitation.

Since the state of dipole vibration results from a sequence of single-particle excitation events, its characteristic energy should be given by the sum of the average of the single-particle energies involved plus a term representing the effect of the residual nuclear interactions acting between the various configurations. Thus, while the first term includes the interaction of the excired particle

† This research was supported by the United States Office of Naval Research under Contract N6oril44. Reproduction in whole or in part is permitted for any purpose of the United States Government.

†† It should be noted that, although the equivalence between the independent-particle and the collective descriptions of the nuclear dipole excitation has been explicitly demonstrated only by means of wave functions of the harmonic oscillator type, the physical correspondence between the two models should not be expected to be too critically dependent on the detailed radial behaviour of the harmonic oscillator wave functions.

as well as that of the hole created in a previously occupied state by the excitation with the nucleons in the unexcited shells, the second term can be said to represent the interaction between the particle and the hole themselves.

The particle-hole interaction depends sensitively on the detailed properties of the state under consideration. It has been noted [3, 4]) that the particularly pronounced symmetry properties of the state of dipole vibration should result in a significantly large, upward shift of its energy relative to the energies of the single-particle excitations. This effect has also been discussed quantitatively in more detailed theoretical studies of the structure of $J = 1-$, $T = 1$ levels in various nuclei [5, 6]).

The purpose of the present paper † is to obtain a simple estimate of the energy shift caused by the particle-hole interaction in the giant dipole resonance state. What is actually calculated is the ratio of this energy to the potential-energy part of the single-particle excitation. The requirement of translational invariance turns out to be helpful for this purpose. The principal idea here is to note that this requirement imposes restrictions on the relative magnitudes of the particle-hole and particle-shell interaction matrix elements. In particular, the result will be obtained that the spatial parts of the direct and exchange terms of the particle-hole interaction, are equal and opposite to the corresponding terms in the particle-shell interaction. This result is presented in detail in sect. 2. In sect. 3 an approximate estimate of the energy shift is obtained while sect. 4 contains an application to the case of O^{16}. Sect. 5 discusses briefly the question of the purity of the dipole state, i.e. its coupling to other types of excitation. The results of this paper are summarized in sect. 6.

2. The Energy of the Dipole Mode

The results to be obtained in this section will not include the contribution to the energy of the dipole state due to the nuclear spin-orbit force. We shall therefore consider a nuclear system described by the Hamiltonian

$$H = T+V, \tag{1}$$

where T is the kinetic-energy operator and

$$V = \sum_{i<j} V_{ij} \tag{2}$$

describes the internucleon interactions. The two-body nuclear potential V_{ij} is given by

$$V_{ij} = -V_0 P_{ij} V(r_{ij}), \tag{3}$$

where V_0, $V(r_{ij})$ and P_{ij} characterize respectively the strength, shape and exchange nature of the nuclear interaction. The expectation values of the

† A preliminary report of this work has been given in ref. [7]).

exchange operator P_{ij} in two-particle states of spin S and isobaric spin T will be denoted by

$$\langle P_{ij}\rangle_{S,T} = {}^{2T+1,\,2S+1}A. \tag{4}$$

The excitation energy of the dipole state can be written in the general form

$$E_d = \bar{\varepsilon}+M, \tag{5}$$

where $\bar{\varepsilon}$ is the average of the single-particle energies involved in the excitation and M represents the total particle-hole interaction. It will be useful to give somewhat more detailed expressions of the quantities appearing in eq. (5), exhibiting explicitly the effect due to the various terms in the nuclear Hamiltonian. We thus write

$$\bar{\varepsilon} = \Delta T+dJ+eK, \tag{6}$$

$$M = d'J'+e'K', \tag{7}$$

where ΔT is the kinetic energy contribution to the single-particle energy, J and K are the direct and exchange integrals of the particle-shell interaction and J' and K' are the corresponding quantities in the particle-hole interaction. The coefficients d, e, d' and e' are familiar linear combinations of the nuclear force parameters ${}^{2T+1,\,2S+1}A$ and characterize the relative contribution of the various types of two-particle interactions to the total excitation energy. Their calculation is straightforward and gives

$$d = \tfrac{1}{4}[3\,{}^{13}A+3\,{}^{31}A+{}^{11}A+9\,{}^{33}A], \quad e = \tfrac{1}{4}[3\,{}^{13}A+3\,{}^{31}A-{}^{11}A-9\,{}^{33}A], \tag{8}$$

$$d' = \tfrac{1}{4}[-3\,{}^{13}A+{}^{31}A-{}^{11}A+3\,{}^{33}A], \quad e' = \tfrac{1}{4}[-3\,{}^{13}A+{}^{31}A+{}^{11}A-3\,{}^{33}A]. \tag{9}$$

It is worth noticing that the coefficients d and e (and similarly d' and e') are identical to each other as far as even-state forces are concerned. They differ only in the sign of the odd-state force parameters.

We may also give at this point the detailed expressions for the integrals J, K etc. in terms of an appropriate set of individual-particle wave functions ϕ. If primed and unprimed subscripts are used to denote excited and unexcited shell-particles, respectively, and if the amplitudes a_i are introduced to measure the probability for a certain type of single-particle excitation we have

$$J = -V_0\sum_i |a_i|^2 \sum_j \{(\phi_{i'}(1)\,\phi_j(2), V(r_{12})\phi_{i'}(1)\,\phi_j(2)) - (\phi_i(1)\phi_j(2), V(r_{12})\phi_i(1)\phi_j(2))\}, \tag{10}$$

$$K = -V_0\sum_i |a_i|^2 \sum_j \{(\phi_{i'}(1)\phi_j(2), V(r_{12})\phi_j(1)\phi_{i'}(2)) - (\phi_i(1)\phi_j(2), V(r_{12})\phi_j(1)\phi_i(2))\}, \tag{11}$$

$$J' = -V_0\sum_{ij} a_i a_j(\phi_{i'}(1)\phi_j(2), V(r_{12})\phi_i(1)\phi_{j'}(2)), \tag{12}$$

$$K' = -V_0\sum_{ij} a_i a_j(\phi_{i'}(1)\phi_j(2), V(r_{12})\phi_{j'}(1)\phi_{j_i}(2)). \tag{13}$$

The functions ϕ here depend only on the position coordinates of the nucleons since the contributions due to the spin and isobaric spin variables have already been incorporated in the definition of the parameters d, e etc. The notation in the above equations is meant to imply that a nucleon excited in state $\phi_{i'}$ came originally from the corresponding unexcited state ϕ_i.

So far very little reference to the particular properties of the dipole state has been made. Indeed the only thing that was considered in obtaining the above equations was the value of the spin and isobaric spin of this state which determined the particular form of the coefficients d' and e' in eq. (9). We now introduce in more detail the assumed nature of the dipole mode, imposing at the same time the restrictions implied by the requirement of translational invariance. We consider for this purpose the analogy between the dipole operator which generates the dipole state, and the centre-of-mass operator, which, applied on the ground state of a nucleus, creates the well known spurious state first discussed by Elliott and Skyrme [8]). These authors pointed out that in the conventional harmonic-oscillator shell model, there exists a linear combination of single-particle excitations which is in all respects equivalent to a simple change in the centre-of-mass motion of the nucleus. It follows that, since the centre-of-mass excitation does not affect in any way the internucleon separations, it should not involve any change in the potential energy of the nucleus. Since also, this state can be said to result from a sequence of single-particle transitions, its energy could be expressed as a sum of a single-particle excitation term, plus a term representing the particle-hole interaction. It is obvious then that in the spurious state, the particle-hole interaction should exactly cancel the potential part of the single-particle energy.

It is clear that there exists a close formal analogy between the centre-of-mass excitation and the dipole mode. This has already been emphasized by Brink [2]) who pointed out that, if the coordinate that measures the separation between the centres-of-mass of the protons and the neutrons is exhibited explicitly in the nuclear wave function, the dipole mode is seen to correspond to a transition of the proton-neutron system from a 1s to a 1p state of relative motion. The spurious state on the other hand results from a similar change in the part of the wave function which is associated with the centre-of-mass coordinate of the whole system.

The analogy between these two states can be used as a convenient way of expressing the requirement of translational invariance on the matrix elements which determine the energy of the dipole mode. The argument will be that the spatial parts in the matrix elements for particle-hole interaction in the dipole state should be the same with the corresponding terms in the spurious state. A similar relation will also hold between the particle-shell interaction terms. These statements will become more plausible if the detailed from of the centre-of-mass and dipole operators is considered explicitly. The Z-components of

these operators are given by

$$R_Z = \frac{1}{A} \sum_{i=1} z_i, \tag{14}$$

$$D_Z = \tfrac{1}{2} \sum_{i=1} z_i \tau_3(i), \tag{15}$$

where $\tau_3(i)$ is the third component of the isobaric spin operator of the i^{th} nucleon. The only essential difference between the right-hand sides of eqs. (14) and (15) is the presence of the operator $\tau_3(i)$ in the expression for D_Z. It follows that the single-particle processes generated by the operators will be identical as far as the position and spin variables are concerned and will differ only in the relative phases of the amplitudes characterizing proton and neutron configurations.

The particle-shell and hole-shell interactions depend only on the absolute squares of the amplitudes of the configurations involved. The single-particle energies in the centre-of-mass excitation will therefore be given by exactly the same quantity $\bar{\varepsilon}$ that was introduced in eqs. (5), (6) and (8) for the dipole mode. The particle-hole interaction on the other hand is a coherent effect and depends critically on the phases of the various amplitudes. Since, however, the only change in the phases, relevant for the present comparison, is associated with the isobaric spins of the nucleons, the space dependent parts of the particle-hole matrix elements in the centre-of-mass and the dipole excitations will be identical. The difference in isobaric spin can be taken into account by a proper definition of the coefficients involving the nuclear-force parameters. It can be easily verified that these coefficients for the $T = 0$ case are given by expressions identical to those in eq. (8). The total particle-hole interaction in the centre-of-mass excitation is then given by

$$M_{\text{c.m.}} = \mathrm{d}J' + eK', \tag{16}$$

where J' and K' are the same quantities that were introduced in eq. (7) and d and e are given by eq. (8).

We have thus been able to express the excitation energy of the spurious state in terms of quantities that have already appeared in the discussion of the dipole state. In particular, we found that this energy is given by

$$E_{\text{c.m.}} = \bar{\varepsilon} + M_{\text{c.m.}}. \tag{17}$$

If we now remember that this expression should contain no net contribution due to the internucleon interactions, we conclude that, as has already been stated, the terms $M_{\text{c.m.}}$ should cancel exactly with the potential-energy part of $\bar{\varepsilon}$. By imposing this requirement on the right hand sides of eqs. (6) and (16), we obtain the relations

$$J' = -J, \qquad K' = -K, \tag{18}$$

which should be useful for the comparison of the particle-hole and particle-shell interaction energies in the dipole state.

It should be emphasized at this point that the spurious state was introduced in our discussion only as a convenient way of imposing the condition of translational invariance. The relations given by eq. (18) could have been derived without any explicit reference to the rather artificial state that describes changes in the centre-of-mass motion of the nucleus as a whole. One way of doing this would be to note that, if the dipole state is to represent a change in the relative motion of the neutrons with respect to the protons, the components of the nuclear force acting between two nucleons of the same charge should contribute nothing to the total excitation energy. A cancellation similar to the one discussed above should then have to occur, leading again to the relations of eq. (18).

Another way still to obtain the same relations would be of course by explicit calculation of the terms $\bar{\varepsilon}$ and M in eq. (5). In such a calculation one should have to use individual-particle wave functions of the harmonic-oscillator type, in order to avoid introduction of spurious centre-of-mass effects in the total excitation energy.

Before we close this section, it is worth pointing out that although the matrix elements J and J' (and similarly K and K') have been found in eq. (18) to be equal in magnitude, they are by no means identical in nature. Thus for example, in the harmonic oscillator representation the particle-hole matrix elements involve only particles in the outer filled shells whereas the particle-shell matrix elements describe the interaction of an external nucleon with all the particles in the nucleus.

3. The Energy Shift

The results for the energy of the dipole state discussed in the previous section can be summarized by the following equations:

$$\bar{\varepsilon} = \Delta T+\tfrac{1}{4}(3\,{}^{13}A+3\,{}^{31}A)(J+K)+\tfrac{1}{4}({}^{11}A+9\,{}^{33}A)(J-K), \tag{19}$$

$$M = \tfrac{1}{4}(3\,{}^{13}A-{}^{31}A)(J+K)+\tfrac{1}{4}({}^{11}A-3\,{}^{33}A)(J-K), \tag{20}$$

$$E_d = \bar{\varepsilon}+M = \Delta T+\tfrac{1}{2}(3\,{}^{13}A+{}^{31}A)(J+K)+\tfrac{1}{2}({}^{11}A+3\,{}^{33}A)(J-K). \tag{21}$$

Use of eq. (18) has been made in writing eqs. (20) and (21).

We now notice that the matrix elements J and K enter with opposite signs in the terms involving odd-state interactions, whereas in the even-state terms they simply add. This results from the fact that the processes described by K involve an interchange of particles relative to those contained in J. A difference in sign then results whenever the relative state of the particles is odd. Since both J and K are positive quantities, this should lead to a cancellation in

the odd-state terms. Together with the relative unimportance of the odd-state forces in nuclear strucrure problems, this fact would then suggest that the main contribution to the right-hand sides of eqs. (19) to (21) will come from the even-state terms.

It is worth noticing now that the interactions involving nucleons in $T = 0$ relative states are enhanced by the particle-hole contribution by a factor 2. The $T = 1$ interaction terms on the other hand, are decreased by a factor $\frac{2}{3}$. This follows from the fact that the forces between particles with the same charge should have no net effect on the energy of the dipole state. Their contribution to the particle-hole interaction (which is a part of the $T = 1$ terms, ${}^{31}A$ and ${}^{33}A$) will then tend to cancel with the corresponding terms in $\bar{\varepsilon}$. The $T = 0$ components, on the other hand, involve interactions between particles of different charge. The sign of their contribution to the particle-hole energy is determined by the isobaric spin of the state considered. The dipole state has $T = 1$ which implies a repulsive particle-hole interaction for this case.†

In order to obtain an estimate for the magnitude of the energy shift we shall now make an additional approximation and neglect the odd-state terms in eqs. (19) to (21). In addition to the arguments already given, we want to point out here that in the dipole state the integrals J' and K' are comparable in magnitude, a fact which makes the cancellation in the terms containing $J-K$ quite complete. If the nuclear potential $V(r_{ij})$ were of the δ-function type, the integrals J' and K' in eqs. (12) and (13) would be exactly equal. In the artificial limit, on the other hand, of nuclear forces of infinite range, J' tends to zero whereas K' will tend to a constant non-vanishing value††. For a realistic nuclear force range, K' is in general a slowly varying function of the range parameter. What is important for the present discussion is the fact that, in the region of interest, the integral J' is very sensitive to the detailed properties of the state considered. This comes from the fact that the nuclear dynamics described by J' consists of a sequence of virtual annihilations and creations of nucleon-hole pairs. As the range of the nuclear potential increases from zero, these processes become quite similar in structure to electric-dipole transitions,

† In general the interaction in a particle-hole state with spin S and isobaric spin T is given in terms of the particle-particle interaction coefficients by

$$\tfrac{1}{4}\left[(-1)^T \frac{3}{2S+1}\,{}^{13}A+(-1)^S \frac{3}{2T+1}\,{}^{31}A\right](J'+K')+\tfrac{1}{4}\left[(-1)^{S+T}\,{}^{11}A+\frac{9}{(2S+1)(2T+1)}\,{}^{33}A\right](J'-K'),$$

where J' and K' are appropriately defined integrals of the same general form as those given by eqs. (12) and (13).

†† This can be seen by inspection of eq. (13) if the potential $V(r_{ij})$ is replaced by a constant. The reason why K' remains finite is that it contains the so-called "forward scattering" processes, i.e. interactions which do not involve a change in the configurations of the interacting particles. Including these processes in K' rather than in K is particularly convenient if the experimental values for the single particle energies are to be obtained from data on neighbouring nuclei as is done in sec. 4.

but with a nuclear rather than electromagnetic strength. The fact that the dipole-state is characterized by an exceptionally large matrix element for E1, ground-state transitions implies then that the dynamical particle-hole matrix element J' will have a significantly large value for the dipole state. In a state with the same quantum numbers as the dipole-state but small radiative width, on the other hand, J' will, in general, be negligibly small for forces of a realistic range †. Thus, both K' and J' are in our case rather large and not too different from each other. We are therefore justified to neglect the odd-state contributions in eqs. (19) to (21), which can then be rewritten as

$$\bar{\varepsilon} = \Delta T + \tfrac{1}{4}(3\,{}^{13}A + 3\,{}^{31}A)(J+K), \tag{22}$$

$$M = \tfrac{1}{4}(3\,{}^{33}A - {}^{31}A)(J+K), \tag{23}$$

$$E_d = \Delta T + \tfrac{1}{2}(3\,{}^{13}A + {}^{31}A)(J+K). \tag{24}$$

In these simplified expressions however, the detail of the nuclear dynamics is included only in the common factor $J+K$. The ratio of the particle-hole interaction to the potential-energy part of the single-particle energy is then given in terms of the even-state force parameters which are quantities known rather accurately. Indeed we find

$$\frac{M}{\bar{\varepsilon}-\Delta T} = \frac{3\,{}^{13}A - {}^{31}A}{3\,{}^{13}A + 3\,{}^{31}A}, \tag{25}$$

from which we obtain the values $+1$ and $-\frac{1}{3}$ for the two extreme cases of pure singlet-triplet and pure triplet-singlet forces, respectively.

The nuclear force parameters are usually normalized by letting ${}^{13}A = 1$. From the low-lying states of Li^6, the value ${}^{31}A \approx 0.6$ is also obtained [9]). Inserting these numbers on the right hand side of eq. (25) we thus find

$$\frac{M}{\bar{\varepsilon}-\Delta T} \approx \tfrac{1}{2}, \tag{26}$$

the desired ratio of the particle hole to the particle-shell interaction. Since the matrix elements J and K do not appear anywhere in eq. (26) this result is independent of such things as the exact value of the nuclear force strength and range or the detailed radial dependence of the individual particle wave functions.

4. Application to O^{16}

The single-particle excitation energies can, in principle, be obtained by comparison with available experimental data. However, since in the previous discussion the effect of the spin-orbit forces has been omitted, an average over

† A more detailed discussion of this question will be contained in a forthcoming publication.

the spin-orbit splitting must be taken before the experimental energies are introduced in the above equations.

The quantity $\bar{\varepsilon}$ is also an average over the various configurations that participate in the dipole state. In O^{16} the relevant configurations are $(1p)^{-1}$ 1d and $(1p)^{-1}$ 2s and, according to ref. [3]) are weighted by the factors $\frac{5}{6}$ and $\frac{1}{6}$, respectively, i.e.

$$\bar{\varepsilon} = \tfrac{5}{6}\varepsilon_{1d} + \tfrac{1}{6}\varepsilon_{2s}. \tag{27}$$

The quantities ε_{1d} and ε_{2s} contain the energies of a 1d or 2s nucleon in interaction with the O^{16} core plus the interaction energy of a 1p hole with the same core. From the experimentally known [10] levels in O^{17} and O^{15}, one easily obtains after averaging over the spin-orbit slittings in both nuclei the values

$$\varepsilon_{1d} = 17.8 \text{ MeV}, \qquad \varepsilon_{2s} = 16.4 \text{ MeV}, \tag{28}$$

which inserted into eq. (27) yield

$$\bar{\varepsilon} = 17.5 \text{ MeV}. \tag{29}$$

The kinetic energy part of $\bar{\varepsilon}$ can be evaluated by the conventional shell-model methods. With a proper radial parameter consistent with electron-scattering experiments one obtains

$$\Delta T = 7.3 \text{ MeV}. \tag{30}$$

Consequently we have

$$\bar{\varepsilon} - \Delta T = 10.2 \text{ MeV}. \tag{31}$$

According to the results of sect. 3, the particle-hole shift is approximately equal to one-half of the particle-shell interaction energy which is given by eq. (31), i.e.

$$M = 5.1 \text{ MeV}. \tag{32}$$

Substitution of eqs. (29) and (32) in eq (5) finally gives

$$E_d = 22.6 \text{ MeV}. \tag{33}$$

It is interesting to compare this estimate with the results of the intermediate coupling calculations of Elliott and Flowers [5]). Among the $J = 1-$ $T = 1$ states obtained by these authors, the one † that possesses most of the radiative groundstate width lies at 22.6 MeV. The comparison with our result of eq. (33) is only too good in view of the fact that the spin-orbit forces have not been included in our calculation and the dipole state has been treated as a completely pure mode.

† The state found by Elliott and Flowers at 25.2 MeV contains mostly $S = 1$ configurations and has properties somewhat different from those of the dipole state discussed here.

5. The Purity of the Dipole State

The discussion in this section is limited only to considerations which follow from the requirement of centre-of-mass invariance. What we want is to obtain an idea about the strength with which the dipole mode is coupled to another state of some intrinsic excitation. If we denote these states by Ψ and Ψ', respectively, and assume that the configurations contained in Ψ' are the same with those involved in the dipole excitation we can we rite

$$\Psi = \sum_i a_i \Phi_i, \tag{34}$$

$$\Psi' = \sum_i a'_i \Phi_i. \tag{35}$$

Here Φ_i is the wave function of a particular configuration characterized by a single particle excitation energy ε_i and the coefficients a_i are the same amplitudes as those appearing in eqs. (10) to (13). Since Ψ and Ψ' are different states we obviously have

$$\sum_i a_i a'_i = 0. \tag{36}$$

The nuclear off-diagonal matrix element connecting the states Ψ and Ψ' will consist of two terms of different nature: one resulting from possible differences in the various single particle energies ε_i and another which contains the effect of the particle-hole interaction. Thus in general we have

$$(\Psi, H\Psi') = \sum_i a_i a'_i \varepsilon_i + \sum_{ij} a_i a'_j M_{ij}, \tag{37}$$

the first term vanishing whenever all the single particle energies ε_i are equal to each other. If we now also assume that the kinetic energy parts in the various ε_i are the same, we can in analogy with eqs. (6) and (7) write

$$\sum_i a_i a'_i \varepsilon_i = dI + eL, \tag{38}$$

$$\sum_{ij} a_i a'_j M_{ij} = d'I' + e'L', \tag{39}$$

where d, e, d' and e' are the coefficients defined by eqs. (8) and (9) and I, L etc. are again some appropriate direct and exchange integrals. We now note again that if the states considered had isobaric spin $T = 0$ instead of $T = 1$ (in which case Ψ would be the spurious centre-of-mass excitation rather than the dipole mode), eqs. (38) and (39) would still hold; the only difference is that the coefficients d' and e' would be identical to d and e, respectively, rather than be given by eq. (9). Since, however, the spurious state cannot be coupled to a state that does not contain any excitation in its centre-of-mass motion, it follows that in the $T = 0$ case, the particle-hole contribution should cancel with the single particle term. This in turn suggests that

$$I' = -I, \quad L' = -L. \tag{40}$$

These relations should also hold for the case of $T = 1$. Taking now into account the results of eqs. (38), (39) and (40), we can rewrite eq. (37) as follows

$$\begin{aligned}(\Psi, H\Psi') &= (d-d')I+(e-e')L \\ &= \tfrac{1}{2}(3\,{}^{13}A+{}^{31}A)(I+L)+\tfrac{1}{2}({}^{11}A+3\,{}^{33}A)(I-L).\end{aligned} \tag{41}$$

It is worth comparing this result with the expression for the total energy of the dipole state given by eq. (21). It is seen that exactly the same combinations of the nuclear force parameters ${}^{2T+1,2S+1}A$ enter in these two formulae. This is hardly surprising since the coefficients $3\,{}^{13}A+{}^{31}A$ and ${}^{11}A+3\,{}^{33}A$ measure precisely the strength of the total proton-neutron interaction in even and odd states, respectively. In the simple scheme we are considering here the dipole excitation consists simply of a motion of protons against neutrons. The p-n forces should then obviously be the only ones to contribute both to the total excitation energy and to the coupling of this mode with any other type of excitation †.

It is of interest now to compare also the result of eq. (41) with the right-hand side of eq. (38) which can be rewritten as

$$\sum_i a_i a'_i \varepsilon_i = \tfrac{1}{4}(3\,{}^{13}A+3\,{}^{31}A)(I+L)+\tfrac{1}{4}({}^{11}A+9\,{}^{33}A)(I-L). \tag{42}$$

If the odd state forces were to be neglected again, eqs. (41) and (42) would imply that

$$(\Psi, H\Psi') = \frac{2(3\,{}^{13}A+{}^{31}A)}{3\,{}^{13}A+3\,{}^{31}A}\sum a_i a'_i \varepsilon_i, \tag{43}$$

i.e. the coupling between Ψ and Ψ' would be determined by the differences in the various single particle energies and would vanish if all the ε_i involved were equal. We conclude, therefore, that in a model in which the odd state interactions are neglected and the single particle energies are all equal, the nuclear matrix element that couples the states Ψ and Ψ' vanishes. We should remember that the single-particle excitation energies considered here represent averages over the spin-orbit force effects. The assumption therefore that the main configurations which enter in our discussion have almost the same energy would not be too unreasonable. On the other hand, the assumption that the odd state forces are negligible does not seem to be as well justified in the present case as it was in the case considered in sect. 3. The exceptionally small contribution to the energy of the dipole state due to the odd-state forces was a consequence of the fact that the matrix element J had a significantly large value there.

† It follows from these considerations that an interaction acting only between nucleons of the same charge, such as the Coulomb interaction, could not possibly induce an excitation in the relative motion of the protons against the neutrons in the nucleus. Thus the coupling of the dipole mode to low lying $T = 0$ states can in general take place only through higher order processes of smaller probability [11]).

This was associated with the particularly pronounced symmetry properties of the dipole state and should not be expected to be true in general. Moreover, in the case of an off-diagonal matrix element involving states of intrinsic excitation there is no reason for the quantities I and L to have even the same sign. From eq. (42) we then see that in such a case the odd state forces might have a relatively more important contribution. The simple result of eq. (43) could not therefore be expected to be true in general. One can still argue however, that when the single-particle excitation energies are not too different from each other both matrix elements I and L in eq. (42) will be small. This would then in turn imply the relative smallness of the off-diagonal matrix element $(\Psi, H\Psi')$ as shown by eq. (41). It should be noted that the magnitude of the terms discussed above is considered only in relation to the corresponding diagonal matrix elements. The particularly pronounced energy shift in the dipole state should thus tend to decrease the relative importance of the off-diagonal terms.

Looking also directly at the matrix elements I' and L' (rather than their respectively equal terms I and L) one can see that there are good reasons to expect them to be relatively small. Although the understanding of the detailed dynamics of this problem is outside the scope of this paper †), we can argue in general that the relative unimportance of these terms should be associated with the basically different symmetry properties that characterize the two states Ψ and Ψ'. This is particularly well illustrated by the behaviour of the integral I' which, in analogy to what has already been noted for the integral J' in sect. 3, represents processes quite similar in structure with a sequence of electric dipole transitions. The same reasons that caused J' to be unusually large, namely the fact that in the dipole state the dipole transitions are exceptionally effective, would now make I' a small quantity since it involves the state Ψ' which is unable to decay by an E1 transition to the ground state.

6. Summary

The main purpose of this work † is to demonstrate that a relation exists between the particle-shell and the particle-hole interaction energies. The first of these quantities is defined as the interaction of the excited particle and that of the associated hole with all the nucleons in the nucleus considered. The particle-hole term then contains all the interactions between the various configurations which are conveniently described as interactions between the particle and the hole themselves. It is natural to expect that since the same effective nuclear forces are responsible for both these terms some relation should exist between their magnitudes. For example, a weaker nuclear force

† A detailed discussion of this question will be contained in a forthcoming publication.

† Considerations similar to those discussed in this paper are contained in recent work by J. M. Soper and J. P. Elliott (private communication from J. P. Elliott).

would not only result in a smaller energy shift due to the particle-hole interaction but would also reduce the single particle excitation energies accordingly. These remarks are rather obvious and are automatically satisfied in any consistent calculation. It may be useful, however, keeping them in mind in cases where the information on the magnitude of the single particle energies is obtained from experimental data and only the particle-hole interaction terms are calculated. Since both terms involve the interaction between particles in different shells this consistency requirement can be of some importance.

In the case of the dipole mode of nuclear excitation the relation between the particle-hole shift and the particle-shell interaction is found to be significantly simple. The argument leading to the relation between these two terms found in sect. 2 can be summarized as follows:

(a) Along with the dipole mode which represents an out-of-phase oscillation of the protons against the neutrons in the nucleus, consider the in-phase mode in which the protons and the neutrons move together.

(b) Notice that the change of phase of the proton-neutron oscillation can be performed simply by changing the isobaric spin from $T = 1$, to $T = 0$.

(c) Since a change of phase will affect the amplitudes that characterize the various nuclear configurations but not their absolute squares, the single particle energies will not be affected at all by this transformation.

(d) The particle-hole matrix elements in the $T = 0$ case are different from those in the $T = 1$ case but this change is reflected only in the particular combination of the nuclear force coefficients which will characterize the strength of the interaction. The spatial parts of the matrix elements will be the same in both cases.

(e) Notice that the $T = 0$ mode is simply an excitation of the centre of-mass of the nucleus as a whole. This implies that there can be no potential energy change associated with this excitation, i.e. that in this case the particle-hole and the particle-shell interactions cancel each other. It then follows that the spatial parts of the direct and exchange particle-hole matrix elements are respectively equal and opposite to those of the particle-shell interaction.

(f) If, in addition, the contribution of the odd-state forces is neglected (an assumption particularly well justified in the present case) and the customary vaiue of 0.6 is used for the ratio of the triplet-singlet to the singlet-triplet nuclear force parameters, the above results are seen to imply a value of about one-half for the ratio of the particle hole shift to the particle-shell energy in the dipole state. As we have already noted, this result refers only to the contributions due to the central part of the nuclear forces and should be compared with experiment only after an average has been taken over the effect of the spin-orbit interactions.

In our discussion we have considered the simple proton-neutron vibration alone, essentially assuming that it is a true eigenstate of our system. Our results

therefore would not be very useful if this mode is strongly mixed with other types of excitation. Although the detailed study of this problem was outside the purpose of this work we have argued in sect. 5 that this coupling should be rather small. In particular, based only on the requirement of centre-of mass invariance we have proved that if all the single particle energies involved in the dipole excitation are exactly equal and if the contribution due to the odd-state forces can be neglected, the coupling between the dipole state and any other state consisting of the same basic configuration should be zero. In conclusion, we may repeat that, although the relations obtained in this work cannot be considered as a substitute for more detailed calculations, they show quite clearly that the required energy shift in the dipole state is only a natural consequence of a consistent shell-model description and provide a reasonable first idea about the magnitude of this quantity.

Note added in proof: After this work was completed, it came to the author's attention that a systematic treatment of the spurious state in nuclei, in which the effect of ground state correlations is also taken into account, has recently been published by D. M. Thouless (Nuclear Physics **22** (1961) 78). We wish to thank Dr. G. E. Brown for informing us of Thouless's work as well as for a communication on related matters.

References

1) D. H. Wilkinson, Ann. Rev. Nucl. Sci. **9** (1959) 1
2) D. M. Brink, Nuclear Physics **4** (1957) 215
3) S. Fallieros, R. A. Ferrell and M. K. Pal, Nuclear Physics **15** (1960) 363
4) G. E. Brown and M. Bolsterli, Phys. Rev. Lett. **3** (1959) 472.
5) J. P. Elliott and J. W. Flowers, Proc. Roy. Soc. **242** (1957) 57
6) G. E. Brown, L. Castillejo and J. A. Evans, Nuclear Physics **22** (1960) 1
7) S. Fallieros, Bull. Am. Phys. Soc. **6** (1961) 79
8) J. P. Elliott and T. H. R. Skyrme, Nuovo Cim. **4** (1956) 164
9) D. Kurath, Lectures on nuclear structure, University of Maryland tech. report no. 135 p. 5
10) F. Ajzenberg and T. Lauritsen, Nuclear Physics **11** (1959) 1.
11) S. Fallieros and W. M. MacDonald, Bull. Am. Phys. Soc. **5** (1960) 55 and to be published

2.B

Nuclear Physics **26** (1961) 608—615; © *North-Holland Publishing Co., Amsterdam*

Not to be reproduced by photoprint or microfilm without written permission from the publisher

A SEARCH FOR FINE STRUCTURE IN THE REACTIONS $B^{10}(d, \alpha_0)Be^8$ AND $B^{10}(d, \alpha_1)Be^{8*}$

G. J. F. LEGGE

Department of Physics, University of Melbourne

Received 10 March 1961

Abstract: The excitation functions for the reactions $B^{10}(d, \alpha_0)$ Be^8 and $B^{10}(d, \alpha_1)Be^{8*}$ have been measured in 10 keV steps of deuteron energy from 400 to 900 keV. The alpha particles were detected at 45° with a thin CsI(Tl) crystal and photomultiplier. No fine structure is observed in either reaction. The absolute values of the differential reaction cross sections at 45° (laboratory) angle are found to be 0.24 ± 0.05 mb/sr for the ground state group and 1.25 ± 0.4 mb/sr for the group going to the first excited state in Be^8, both cross sections being measured at a deuteron energy of 780 keV. The alpha particle spectrum, as measured with $5^1/_2$ % energy resolution and $1^1/_2$ % statistics, shows no sign of any Be^8 state between 3 and 5 MeV.

1. Introduction

The level structure of light nuclei in the region of excitation 20—30 MeV is of particular interest because of the discovery of "breaks" in photonuclear yield curves, and the attribution of these to compound nucleus levels in the intermediate nucleus [1]). Information is most required on the closed shell nucleus O^{16} and the closed sub-shell (on *jj* coupling) nucleus C^{12}. Here we might expect the level densities to be somewhat smaller than in neighbouring light nuclei, and indeed it is just the above two nuclei that have provided the major evidence for breaks. The high Q value for B^{10}+d reactions allows the examination of level structure in C^{12} at excitations of over 25 MeV, with the use of only a low energy deuteron source. It may well be argued that such excitations are well above the 22 MeV of the giant photonuclear resonance in C^{12}, and consequently compound nucleus effects are less likely to be discernible; however, it is hoped that fairly stringent selection rules will thin out the excited levels to some extent if we choose the (d, α) reactions. In particular, there is a double requirement that the isobaric spin T of any C^{12} state excited by these reactions be zero, since all other components of the reaction have this value of T. The isobaric spin conservation laws may still hold at such excitations if the compound nucleus levels are wide, because then, as indicated by Lane and Thomas [2]), the states are too short lived to allow time for isobaric spin mixing to occur. Another feature of these reactions is that compound nucleus effects are likely to predominate, too great a rearrangement of nucleons being required for

direct processes to be major contributors. Two previous determinations of the excitation functions for B^{10} (d, α_0)Be^8 and Be^{10} (d, α_1)Be^{8*} have been reported for the present region of excitation [3, 4]), but the variation of deuteron energy in steps of 100 keV or greater was too coarse to have shown fine structure.

2. Targets

Because of the difficulty in obtaining pure highly uniform targets of boron by evaporation [5, 6]) or electromagnetic separation [6]) techniques, the procedure adopted was that of "cracking" diborane (B_2H_6) onto tantalum foils [7]), which were inductively heated to 900° C in a vacuum of 10^{-4} mm of mercury. The 150 μm tantalum foils, which were out-gassed before and after the cracking process, were stored in a hydrogen atmosphere until use, thus preventing reabsorption of air by the foils or oxidation of the boron films — the (d, p) reactions on oxygen and nitrogen have large cross sections and tend to produce pulse pile-up in the counter. The very nature of the diborane preparation and cracking processes is a guarantee of pure boron targets. The backing material was untouched surgical tantalum supplied by Ethicon.

During the experiment, the formation of carbon on the target was inhibited by the use of liquid air traps in both the beam and pumping line, and by allowing the beam to heat the target to a dull red, thus preventing condensation and subsequent cracking of oil vapour on the target. The targets used proved to be free from any troublesome impurities, and stood up well to several days of bombardment with beams of up to 20 μA. The uniformity was assumed from repeatability measurements to be about 1 % or better for the $\frac{1}{4}$ cm^2 area over which the beam wandered. The target thickness was estimated by comparing the yield from it with that from a B^{10} target of known thickness supplied by Harwell. The estimated layer of 16 $\mu g \cdot cm^{-2}$ of natural boron was assumed to be entirely on the surface of the tantalum; if penetration occurred [8]), then an estimate of about 6 keV for the energy equivalent would be too low.

3. Experimental Procedure

An analysed and collimated beam of deuterons from the University of Melbourne Van de Graaff generator struck a target with an incident angle of 60° as shown in fig. 1. The beam current was measured to an accuracy of 0.1 % by means of an integrator [9]) connected to the target and to a Faraday cage surrounding it. Secondary electrons from the collimators, from the target and from ionization of residual gas were suppressed with a potential of −2000 V. To keep ionization down to a minimum, the target chamber was maintained at a pressure of 2×10^{-5} mm of mercury or less. Alpha particles emitted at an angle of 45° (laboratory co-ordinates) were detected in a CsI(Tl) crystal of

diameter 2.5 cm (machined down from a larger diameter) and thickness 130 μm. The crystal was supplied by Harshaw Chemical Co. already cemented to a plastic cylinder of thickness 1.3 cm; this was optically coupled to a 5 cm Dumont 6292 photomultiplier tube by means of "Nugol" (pure paraffin oil). A collimator of diameter 1 cm in front of the crystal was found to be necessary for good energy resolution; this was probably due to uneven polishing of the crystal face at some stage of its life. A 10 μm thick aluminium foil served as a light reflector over the crystal, as a light seal to block light emanating from the target and as a means of stopping a high flux of scattered

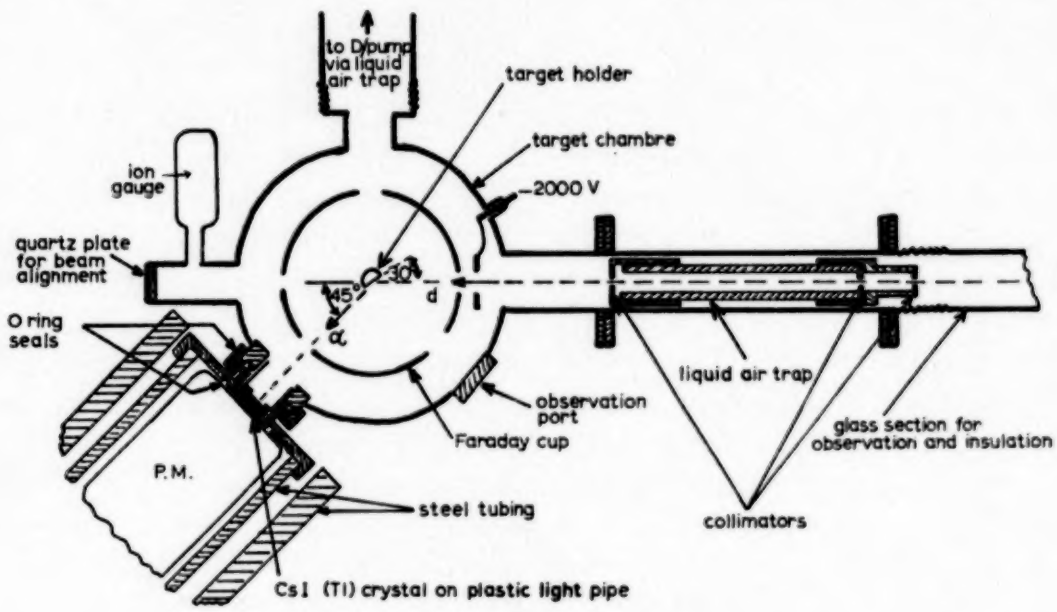

Fig. 1. Experimental arrangement.

deuterons, thus preventing pulse pile-up in the electronics. Pulses from the photomultiplier were fed through a head amplifier to a cathode follower which drove pulses having a maximum height of 20 V through a long 72 Ω line to the counting room. Here the pulses were fed to two single-channel analysers. The arrangement described gave a resolution of $4^1/_2$% for the ground state alpha group which entered the crystal with an energy of about $12^1/_2$ MeV.

The large percentage (82) of B^{11} in the target was unimportant, because the Q values for both (d, α) and (d, p) reactions on B^{11} are low. Any protons from the target could lose a maximum energy of only about 4 MeV in the thin CsI(Tl) crystal. Thus their pulse heights were below those of the two alpha groups under investigation, despite the greater response of CsI (Tl) to protons than to alpha particles. The choice of a forward angle of observation was dictated by the requirement of high alpha particle energies.

The alpha spectrum is shown in fig. 2. The α_1 peak is very broad because of the natural width of the first excited state of Be^8, but the α_0 peak is narrow and

sits on a high energy tail, possibly due to three-body break up of C^{12}. Because of the tail, the cross section on the low energy side of the α_0 peak does not fall below 20 % of the peak height. Consequently it is important to prevent the relative shift of α_0 peak and α_0 channel, if good counting statistics are required. Considerable effort was made to stabilize the gain of the system: a large amount of negative feed-back (feed-back factor $\beta = -\frac{1}{17}$) was applied between output of the cathode follower and input of the high gain amplifier, thus also eliminating the non-linearity of the cathode follower (a consequence of the large output pulse requirement) and giving an overall non-linearity of less than 1% for the output range 0 to 30 V. All electronic equipment concerned with the experimental measurements was run off manually stabilized mains from the counting room and no electronic earths were made in the Van de Graaff pit;

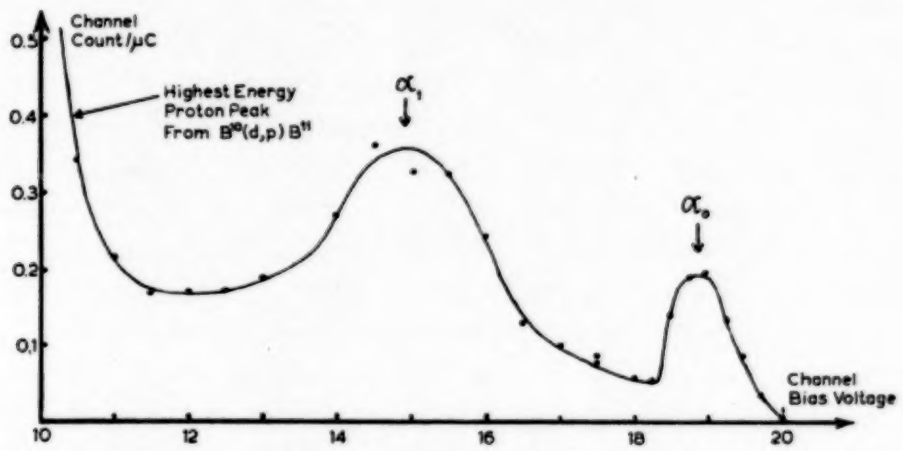

Fig. 2. Spectrum of α-particles from B^{10} (d, α) Be^8.

the target chamber, which had a common earth with the photomultiplier was therefore insulated from all other Van de Graaff metal work. Long term drifts tend to take place in photomultiplier gain, and, to a lesser extent, in single channel analyser bias, but not to any extent in analyser channel width. Therefore the following method was devised for keeping the channels on the peaks, particularly on the very narrow α_0 peak. The first analyser had its bias and channel width adjusted to roughly cover the lower half of the narrow α_0 peak. The gain of the amplifier system was then manually controlled, by means of a potentiometer across the 72 Ω line matching resistor, so that the count rates in the channel output and the top level output (all counts above the channel, and therefore the top half of the α_0 peak) were the same, allowing of course for statistical fluctuations when the counting rates were low. The sum of the two outputs is then the total α_0 count. A small drift in the α_0 peak relative to the α_0 channel will now cause a large change in the relative count rates for the two α_0 outputs, although only a small change appears in their sum. Thus, for

the case in point, where the peak height is five times the low energy background, and where the width at half height is about 5 % of the mean pulse height for the peak, then a drift in amplifier gain or analyser bias of 0.1 % leads to a change in the total α_0 count rate of 0.4 %, but this is easily detected by the resultant swing of 8 % in the (α_0 channel)/(α_0 top level) count rate ratio. The second analyser was used in the normal manner to cover the broad α_1 peak. Note that if the bias of only one analyser were to drift, then the above procedure would stabilize for α_0 pulses, but not for α_1 pulses; however, this is not serious, because the α_1 peak is much broader than that for α_0; consequently the α_1 count is much less sensitive to electronic drifts. It should be pointed out that the above method of stabilization is only suitable in the case of a narrow resonance occurring at the maximum pulse height. In this experiment there were no background counts in the region of the two alpha peaks.

The yields of α_0 and α_1 particles were measured for deuterons of energy 400 to 890 keV in steps of 10 keV. Counting statistics were maintained at about $1\frac{1}{2}$ % for the α_1 group and 3 % for the α_0 group, except in the range of deuteron energies 500 to 600 keV; here the difficulties of machine operation forced an increase in these figures to about 4 % and 7 % respectively. Since the magnetic analyser employed could not be stabilized to much better than 10 keV and, as will be seen from the results, the α_0 and α_1 yields both increase at rates of between 5 and 10 % per 10 keV throughout the region investigated, it was pointless to attempt any improvement in counting statistics.

Two runs were done at 780 keV on a thick (90 $\mu g \cdot cm^{-2}$) separated B^{10} target from Harwell and the spectra were recorded on a 100-channel kicksorter. The data was used to estimate the absolute values of the 45° differential cross sections for the two alpha groups.

4. Results and Discussion

The excitation functions for both reactions are shown in fig. 3. There is no evidence for any resonance structure in either reaction. All deviations from smooth curves are less than 10 % and most are less than 5 %, except between 500 and 600 keV, where statistics are inferior. If any of the deviations do represent structure, then the half widths of such deviations (though not necessarily of the levels they represent) are no greater than 10 keV. An investigation of the $B^{11}(p, n)C^{11}$ reaction[8]) in 10 keV steps of proton energy also showed no evidence for narrow resonances in C^{12} over the same region of excitation; however, it did show a wide resonance centred around the C^{12} excitation energy 26.0 MeV, which corresponds to a deuteron energy of about 950 keV. This resonance possibly corresponds to the maximum observed in the $B^{10}(d, \alpha_0)$ Be^8 cross section at about 1 MeV deuteron energy[3,4]). It would then appear that any resonances in the $B^{10}(d, \alpha_0)Be^8$ and $B^{10}(d, \alpha_1)$ Be^{8*}

reactions are either very broad, or else overlapping to a great extent. As was indicated in the introduction, we might hope for a lower level density in the (d, α) reactions than in the (d, p) or (d, n) reactions; however, there is no reason why any (d, α) resonances should be narrow. The width for deuteron or alpha

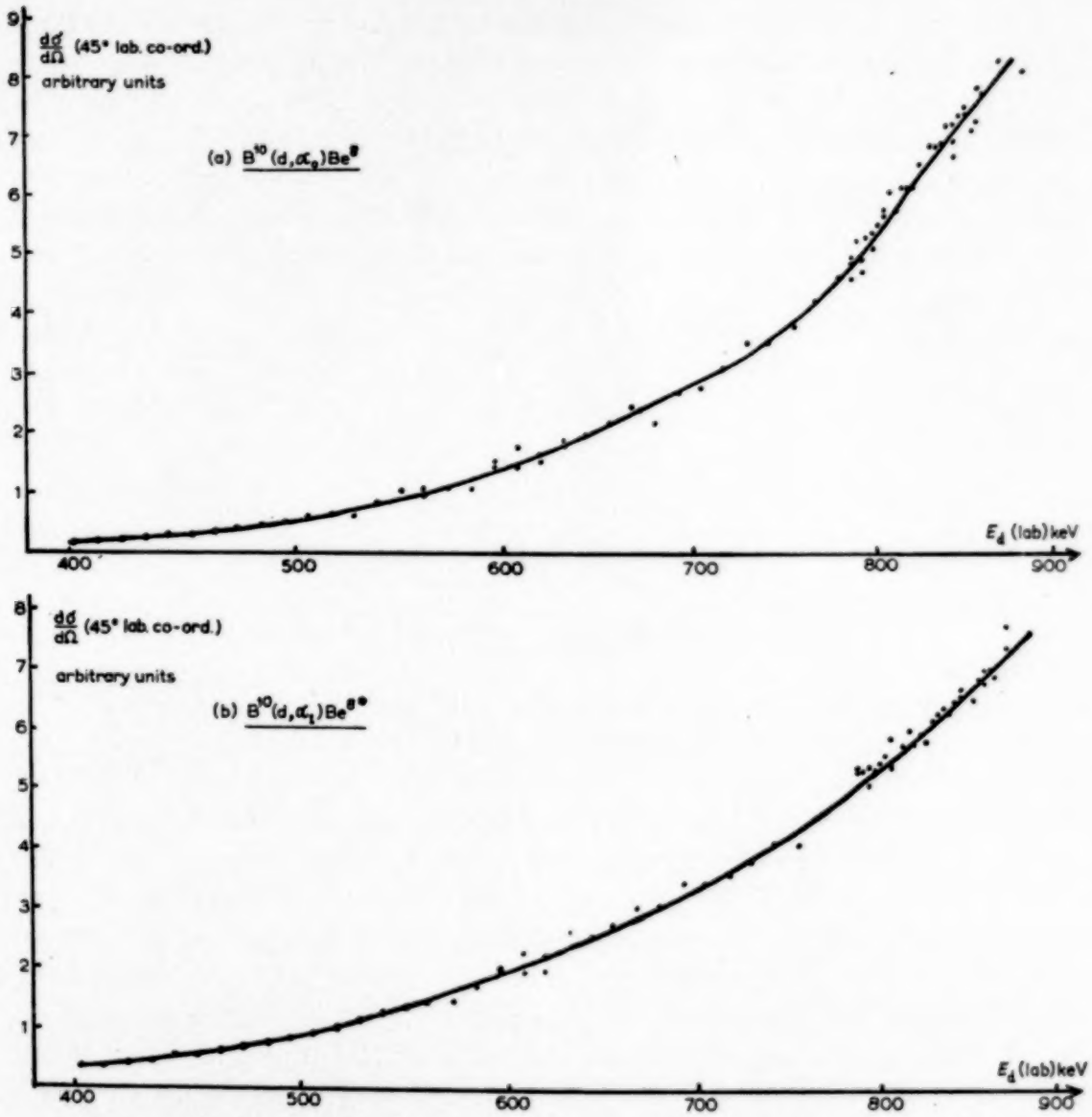

Fig. 3. Excitation functions at 45° (lab) for (a) $B^{10}(d, \alpha_0)\ Be^8$ and (b) $B^{10}(d, \alpha_1)\ Be^{8*}$.

emission for such resonances could well be narrow, but very probably all would be broadened by their ability to emit protons and neutrons. Several experimenters have investigated the (d, p) and (d, n) reactions[10]), though generally with thicker targets and larger energy steps than those used in this experiment. Again there are no suggestions of narrow resonance structure in this energy region.

The absolute values of the differential cross sections have been estimated for the two reactions. They are 0.24 ± 0.05 mb/sr for the ground state group, and 1.25 ± 0.4 mb/sr for the first excited state group — both measured at 780 keV deuteron energy and 45° detection angle (all in laboratory co-ordinates). In each case there is a 10 % error ascribed to the target thickness and the remainder arises mostly from an estimate of area under the resonance. The large error in the α_1 cross section is due to uncertainty in fitting a Gaussian curve to the low energy side of the α_1 peak. In point of fact, this Gaussian cannot be justified, because it has been shown by Treacy[11]) that the yield on the low energy side of this peak is probably at least partly due to a long tail of unknown length and height. Part of this low energy yield and also part of the area contained by the Gaussian is probably due to three-body break up of C^{12} and

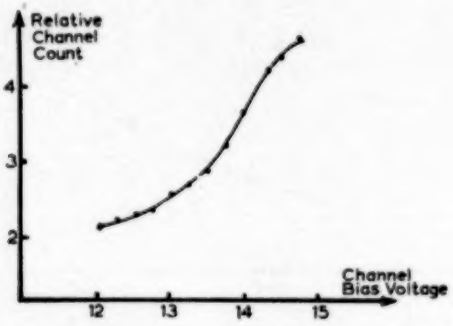

Fig. 4. Low energy slope of $B^{10}(d, \alpha_1)$ Be^{8*} peak.

to break up of Be^8. Thus the error in the α_1 differential cross section may be even greater than shown; however, the above estimate is at least made of a defined quantity approximating the true quantity, the latter being ill-defined.

When the spectrum of fig. 2 was first taken, there was some suggestion of a peak at 13.75 V on the low energy side of the α_1 resonance peak; this would correspond to a level in Be^8 of about 3.7 MeV excitation energy. Since there had been some evidence for and against levels [12]) in Be^8 at about 4.1 and 4.9 MeV, this region was investigated with better statistics before deciding on the channel limits for the α_1 count. The result of this investigation is shown in fig. 4. There is no further evidence for the doubtful peak, the curve being perfectly smooth within the $1\frac{1}{2}$ % variation allowed by counting statistics. The region of excitation covered in this investigation was roughly 3 to 5 MeV, the energy resolution being about $5\frac{1}{2}$ % for these alpha energies.

I wish to thank Professor Sir Leslie Martin, Associate Professor C.B.O. Mohr, Professor D. N. F. Dunbar and Dr. B. M. Spicer for their interest in this work. I thank my fellow team members of the Van de Graaff Generator, especially Mr. W. R. Graham and Mr. J. L. Black for all their assistance. I am deeply grateful to Professor A. S. Buchanan and his assistants of the Chemistry Department for the time and care taken in preparation of pure diborane.

References

1) L. Katz *et al.*, Phys. Rev. **95** (1954) 464;
J. Goldemberg and L. Katz, Phys. Rev. **95** (1954) 471;
B. M. Spicer and A. S. Penfold, Phys. Rev. **100** (1955) 1375;
A. S. Penfold and B. M. Spicer, Phys. Rev. **100** (1955) 1377;
I. M. Thorson and L. Katz, Proc. Phys. Soc. A **77** (1961) 166
2) A. M. Lane and R. G. Thomas, Revs. Mod. Phys. **30** (1958) 257
3) W. D. Whitehead, Phys. Rev. **82** (1951) 553
4) R. L. Becker, Phys. Rev. **119** (1960) 1076
5) J. K. Bair, J. D. Kington and H. B. Willard, Phys. Rev. **100** (1955) 21;
J. H. Gibbons and R. L. Macklin, Phys. Rev. **114** (1959) 571
6) R. W. McIlroy, private communication
7) R. W. Dodson *et al.*, in Nat. Nuc. Energy Series Div. 5, vol. 3, ed. by A. C. Graves and D. K. Froman (McGraw-Hill Book Co., New York, 1952) p. 20
8) G. J. F. Legge and I. F. Bubb, Nuclear Physics **26** (1961) 616
9) G. J. F. Legge, to be published
10) C. H. Paris, F. Valckx and P. Endt, Physica **20** (1954) 573;
W. H. Burke, J. R. Risser and G. C. Phillips, Phys. Rev. **93** (1954) 188
11) P. B. Treacy, Phil. Mag. **44** (1953) 325
12) P. Cuer and J. J. Jung, Compt. Rend. **236** (1953) 2401;
P. Cuer, J. J. Jung and R. Bilwes, Compt. Rend. **238** (1954) 1405;
R. E. Holland *et al.*, Phys. Rev. **99** (1955) 92

2.C. *Nuclear Physics* **26** (1961) 616—633; © *North-Holland Publishing Co., Amsterdam*
Not to be reproduced by photoprint or microfilm without written permission from the publisher

C^{12} LEVEL STRUCTURE IN THE EXCITATION REGION 20.5—26.5 MeV

G. J. F. LEGGE and I. F. BUBB
Department of Physics, University of Melbourne

Received 10 March 1961

Abstract: The absolute cross-section for total neutron emission in the reaction B^{11} (p, n) C^{11} has been found by an activation technique over the range of proton energies 4.9 MeV to 11.4 MeV. The excitation function for this reaction is plotted in 10 keV steps of proton energy. Eleven resonances are resolved at proton energies of 5.065, 5.48, 6.03, 7.28, 7.73, 8.25, 8.64, 9.24, 9.79, 10.13 and 10.91 MeV. None of the resonances has an estimated width at half height of less than 70 keV. The cross section has a maximum value of 430 ± 45 mb at 6.03 MeV, at which energy the excitation function is fitted by assuming the existence of a single particle state having $J^{\pi} = 4^{-}$. Direct interaction and compound system modes of reaction appear to contribute to the cross section roughly in the ratio 2 : 1 throughout the region of excitation covered. There is some evidence for interference between the two modes. A comparison with other experimental results is made.

1. Introduction

Since the observation of "breaks" in the yield curves for photonuclear reactions in light nuclei in the region of the so called "giant resonances" [1, 17]), there has been much speculation as to the composition of these resonances [2]). Several experimenters have attempted to show the presence or otherwise of fine structure in them, particularly [3]) in C^{12}; however, severe limitations are imposed by the lack of a suitable monoenergetic gamma ray source and the difficulty in absolute energy calibration of betatrons at such energies. Recent work by Carroll and Stephens [4]) using gamma rays from the H^3+p reaction has given strong support to suggestions of fine structure in C^{12}. However, here again there is a lack of a sufficiently intense monochromatic γ ray beam. An obvious answer is to investigate the inverse reaction B^{11} (p, γ) C^{12}. This has been done by Gemmell, Morton and Titterton at Canberra [5]) and by Gove, Litherland and Batchelor at Chalk River [6]) and roughly again by Jones and Gemmell [7]) at Harwell. The results are indecisive, there being only a suggestion of possible fine structure within the main resonance. The main difficulties here are probably the preparation of thin, uniform and preferably self-supporting targets, and the elimination of background radiation — particularly if a target backing is found to be necessary. In view of the above difficulties, it was decided to investigate the level structure of C^{12} by means of the reaction

$B^{11}(p, n)\,C^{11}$, using an activation technique. This reaction should excite more levels than those seen in the B^{11} $(p, \gamma)\,C^{12}$ reaction or its inverse; however, it was hoped that the increased level density would not mask all fine structure. The technique has decided advantages over previous ones in that besides the good energy resolution of less than 10 keV, excellent counting statistics may be achieved for short bombardment times with very low backgrounds and backed targets.

2. Target Preparation and Uniformity

In an experiment designed to surpass 1 % in relative cross section measurements, non-uniformity over the area of a target can be a large source of error. Boron is a difficult element to evaporate successfully [8–10]), and it was not possible to obtain an electromagnetically separated target of uniformity guaranteed better than ± 20 %. Consequently considerable effort was expended in producing satisfactory targets by the cracking [11, 12]) of diborane (B_2H_6) on to 6.4 μm tantalum backing. Targets of dimensions 0.5 cm $\times$ 1.5 cm were cut from a prepared target foil of dimensions 3.6 cm $\times$ 1.5 cm. The non-uniformity over a single target was estimated to be of the order of ± 1 %, and less over the region bombarded. Each target holder carried six targets, attached by means of "glyptal", and individual targets were positioned at the target station by means of a ball-locator working on the target holder. Because of this precise location, and because the current distribution over the energy analysing slit was fairly uniform, the beam spot could not seriously wander, and hence target non-uniformity should have been only a few tenths of 1 %. This was borne out by repeated measurements of target thickness during the course of the experiment. Since the 6.4 μm tantalum backing was readily transparent to the proton beam, the activity yields were compared for each of the 36 targets for three different energies. The relative yields were the same for each energy. This suggested that there was little, if any, boron on the back of the tantalum — an occurrence which could have badly distorted the excitation function and upset the energy resolution. The boron films were highly tenacious, and extremely pure from the very nature of their formation. The purity was tested by plotting a C^{11} decay curve. This was linear, on a logarithmic scale, within 0.5 % over a period of 200 min ($\approx$ 10 half lives). This curve also demonstrated the negligible background due to tantalum activity from such thin foils, a feature that was verified by activating a thick tantalum target at a proton energy $E_p = 9.6$ MeV. The targets used ranged in thickness from 5 to 9 keV for $E_p = 5$ MeV, and from $2\frac{1}{2}$ to $4\frac{1}{2}$ keV for $E_p = 11$ MeV. In order to inhibit oxidation of the targets, their holders were kept in an atmosphere of hydrogen when not in use.

3. Apparatus

3.1. ACTIVATION APPARATUS

The target geometry is shown in fig. 1. The beam diverged from the slits A and B, but the geometry was such that no beam could hit the cylinder G except that which passed through the transparent target F. In order to minimize the secondary ionization of gases within the Faraday cup from which some positive ions might have been extracted by the suppressor, and at the same time to prevent the formation of a carbon layer on the targets, the Faraday cup was held at a pressure of less than 10^{-5} mm Hg by an oil diffusion pump working through a liquid air trap.

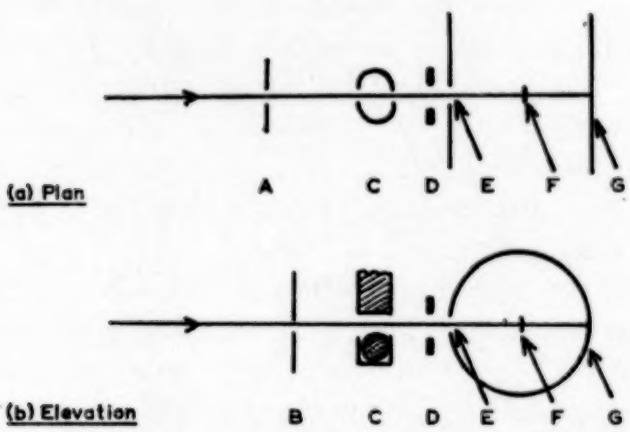

Fig. 1. Target geometry. (A) Energy analysing slit (vertical). (B) Horizontal slit. (C) Chopper. (D) Suppressor ring at − 4 kV. (E) Slit in cylinder (G) which acts as a Faraday cup and surrounds the target (F). (F) and (G) are electrically connected and are insulated from (C) and (D).

The target chamber and the holder are shown in fig. 2. The chamber, fig. 2(b), had a 2.5 cm hole through the centre, left to right in the figure, enabling the beam to pass through to a further target station if desired. The target holder, fig. 2(c), was of 0.32 cm steel plate, having a slot milled most of its length and right through except for a ledge as shown in the figure; this ledge was used to support the targets C in the centre of the 0.32 cm holder. Targets were accurately positioned by means of the slot A formed by two half cylinders, and by means of a ball locator B. The locating holes are visible on the right hand side of the holder. The castellated copper cylinders D and E shown in fig. 2(a) were made to slide up the gap F, visible in fig. (2b). E was rigidly fixed at the top of this gap, so that D might (i) be pushed right home to make a vacuum tight seal around the chamber by means of the 0 ring seals G, H and J of fig. 2(b), (ii) be partially withdrawn and turned hard clockwise so as to bring the slit K of fig. 2(a) centrally into the beam path or (iii) be further withdrawn and turned so as to clear the 2.5 cm diameter hole through the chamber.

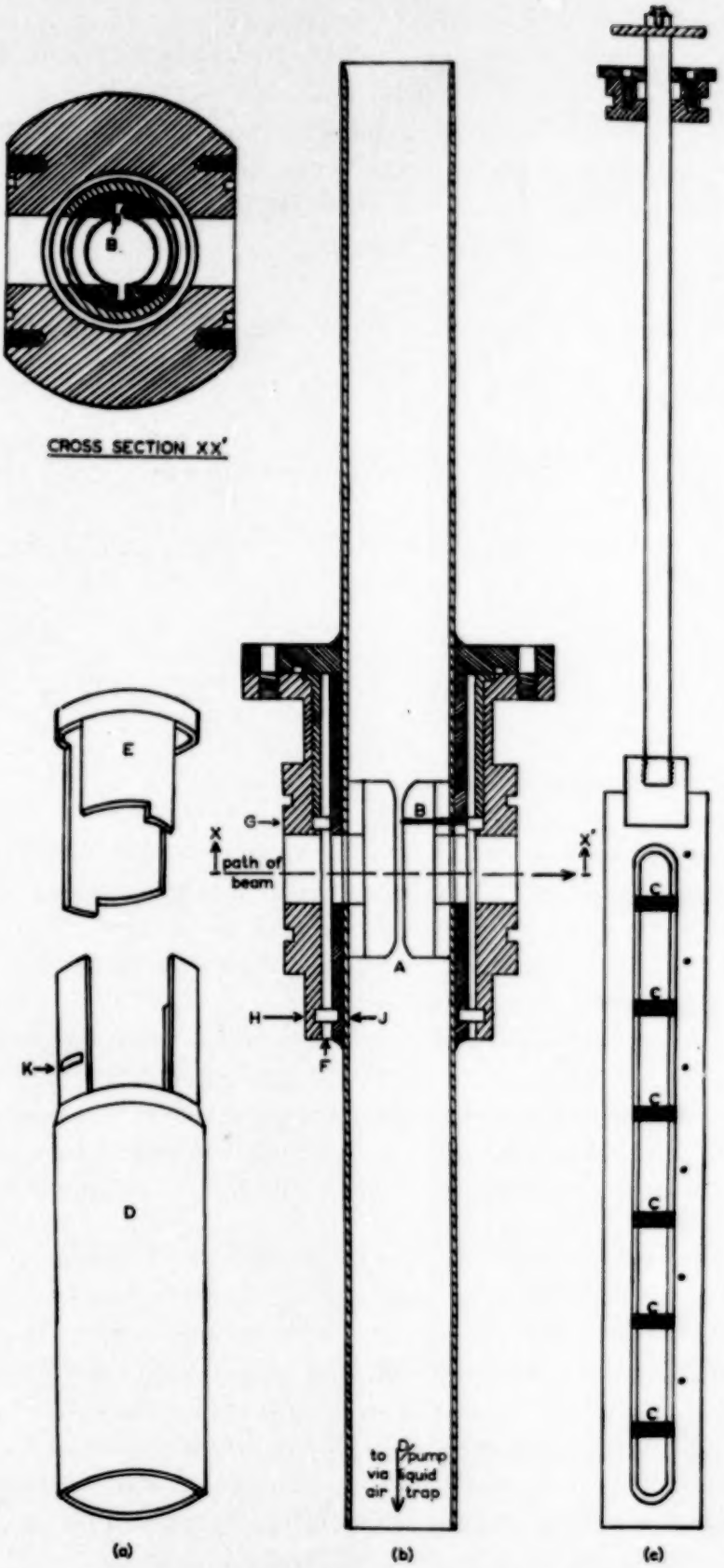

Fig. 2. Activation chamber and target holder.

3.2. COUNTING APPARATUS

After bombardment, the target holder, containing six activated targets, was slid between two 2.5 cm diameter anthracene crystals which were 0.5 cm apart. Again the position of each target when counted was rigidly determined by a ball locator. The crystals were viewed by two EMI type 9536B 5 cm diameter photomultiplier tubes, and, as shown in fig. 3, the outputs from two

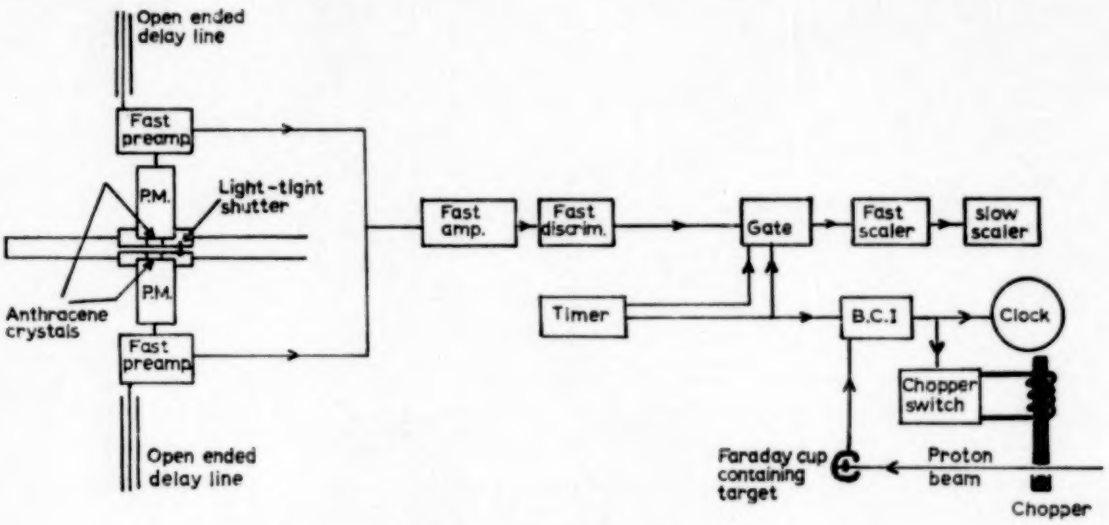

Fig. 3. Counting and timing apparatus.

fast pre-amplifiers were summed and fed through a fast amplifier to a discriminator; the pulses from this discriminator were gated and finally counted by a fast scaler followed by a slow scaler. The dead time of the whole chain was limited by the discriminator to 0.3 μsec. The discriminator was triggered by 97 % of all positons entering the crystals.

The two photomultipliers were shielded against stray magnetic fields by thick steel housings; the vicinity of crystals and photomultipliers was covered by about 6 cm of lead, which decreased the background count rate by a factor of 3, to less than 3/sec. The counting and timing equipment was situated in a departmental counting room which was well clear of machine backgrounds.

3.3. TIMING PROCEDURE AND BEAM CURRENT MEASUREMENT

The start of each bombardment and the start and finish of each count were controlled by a timer, the two outputs of which were 170 sec apart with a period of 200 sec. The above two outputs were used to operate the gate (a simple flip-flop circuit) giving a 170 sec counting interval for each target, and allowing a 30 sec interval for the operator to record counts, zero scalers and move the target holder to a new position. The pulse which started the count was also used to start the beam current integrator; this in turn dropped the chopper and started an electric clock. When the integrator had received some

predetermined charge (1, 2 or 4 μC), it automatically raised the chopper, stopped the clock, and gave a reading of excess charge collected during the turn-off process. Since the time between the activation start and the count start was always an integral number of 200 sec intervals, roughly synchronised clocks in the machine control room and in the counting room were sufficient to fix this interval accurately. The beam current integrator was adjusted to have a leakage time constant equal to the C^{11} decay constant; consequently the important time interval was that between the end of bombardment and the start of counting — hence the necessity for the electric stop clock giving the time of run.

The integrator was a fedback, vibrating reed electrometer type designed by D. E. Caro. Bombardment usually took about 100 sec, allowing time between runs to move the target holder to a new position, and change the machine energy by 10 keV. The beam could be optimised before each run by observing the current on the insulated chopper. The spread in beam energy from the University of Melbourne's variable energy cyclotron is such that six targets could be irradiated at 10 keV intervals, swinging only the analyser magnetic field and trimming the main magnetic field for optimum beam. Major energy changes, involving a shift of the cyclotron radio frequency, were made while target holders were being changed over and the target chamber evacuated.

3.4. ENERGY CALIBRATION OF THE BEAM ANALYSER

The magnetic analyser has an energy resolution of better than ± 0.1 % (width at half height < 0.1 %), and the field is measured and stabilised by means of the signal from a nuclear magnetic resonance probe. Despite this use of field stabilization rather than current stabilization, hysteresis effects can upset the calibration. To eliminate this risk the analyser magnet current was always raised continuously. The instrument has been calibrated against a 5.3007 MeV Po^{210} α source, against a 5.800 MeV Al^{27} (p, n) Si^{27} threshold and against a 7.016 MeV Ni^{60} (p, n) Cu^{60} threshold. Although the calibration is incomplete, it may safely be claimed that with respect to the above reference energies the energy scale used in this experiment has an accuracy of better than ± 20 keV in the region of proton energies 5 to 7 MeV. Because the magnet was designed for minimum saturation effects, the absolute calibration error is probably well below 50 keV even at a proton energy of 11.4 MeV. This is borne out by a comparison between experiments on other machines and those on the Melbourne machine.

4. Results

The excitation function is shown in fig. 4 as a function of proton energy in the laboratory system (lower scale) and of C^{12} excitation energy (upper scale).

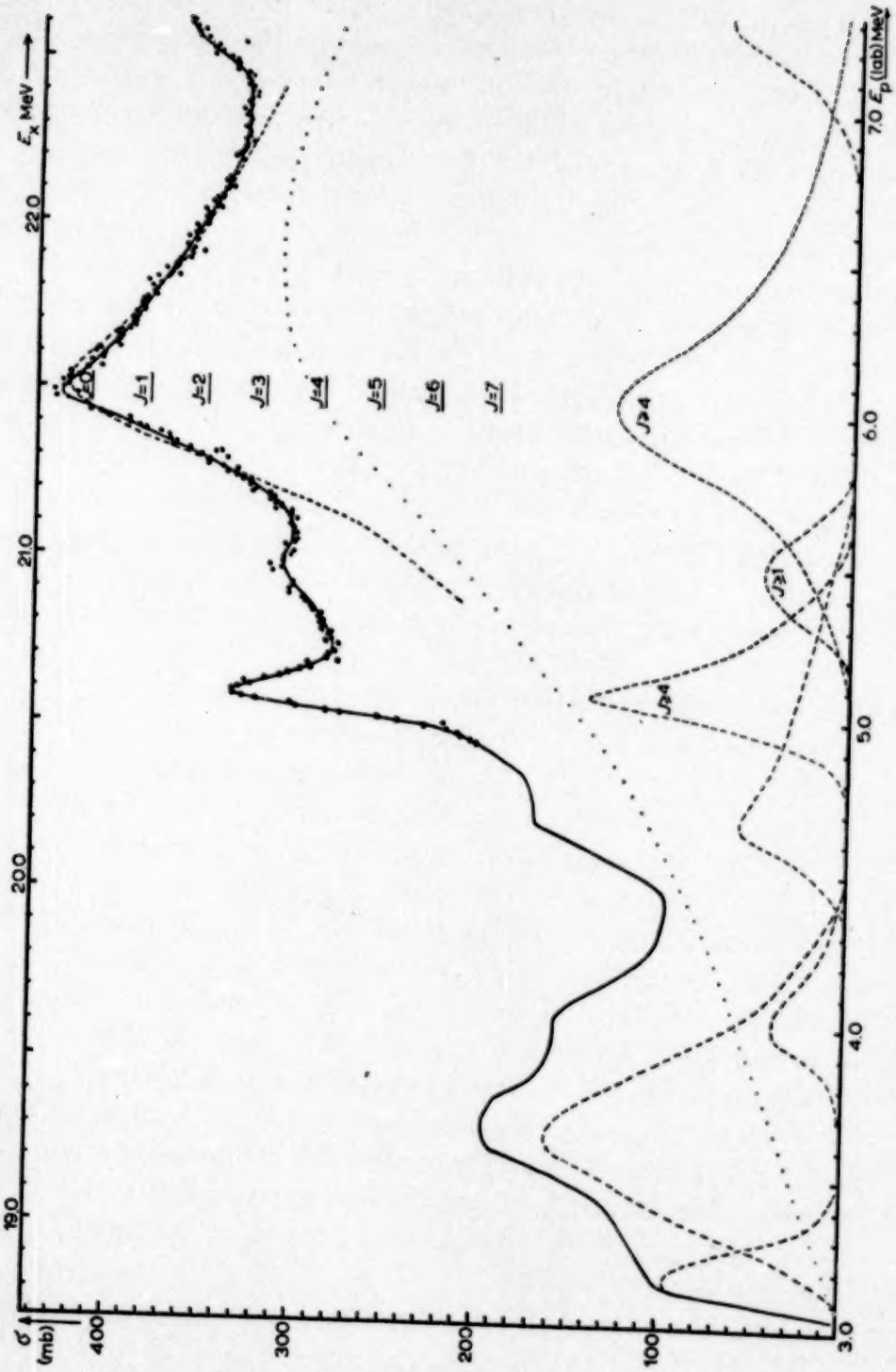

Fig. 4a. Excitation function of B^{11} (p, n) C^{11}. Proton energies < 7.3 MeV.

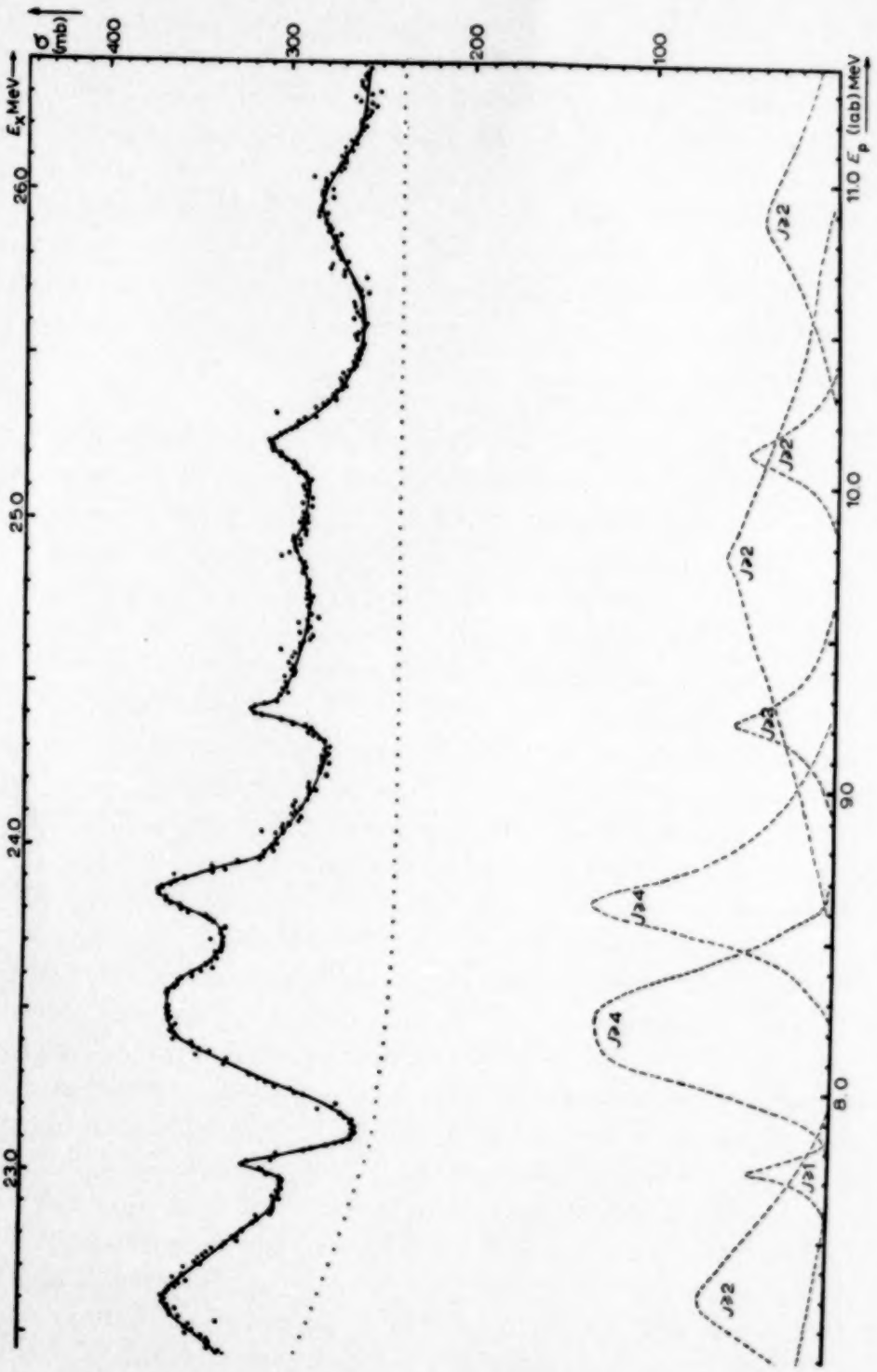

Fig. 4b. Excitation function of B^{11} (p, n) C^{11}. Proton energies 7.1—11.4 MeV.

These results have been corrected for natural background (≈ 0.1 %), background from neighbouring targets (≈ 4 %), lag between finish of run and start of count (varied by ≈ 2 % over any one target holder and by much more for different holders), the charge "spillover" on the current integrator (≈ 0.4 %), the integrator calibration and the target thickness, in that order. The dead time of the counting apparatus was about 0.3 μsec and yielded a roughly constant error of about 0.1 %. The large corrections were known very accurately and, considering the counting statistics of about 0.1 to 0.2 %, the overall accuracy for short energy intervals should be about ± 0.5 % (standard deviation). This figure is in agreement with the fall of points about the smooth curve as shown. The data below 4.9 MeV are the results of Gibbons and Macklin [9]), normalized to this experiment by means of a common peak at about 5.1 MeV.

There are eleven apparent resonances in the excitation function for this experiment as displayed in fig. 4. These occur for proton energies 5.065, 5.48, 6.03, 7.28, 7.73, 8.25, 8.64, 9.24, 9.79, 10.13 and 10.91 MeV. The resonance at 5.065 MeV has been observed previously by Bair, Kington and Willard [8]), who assigned to it a proton energy of 5.12 MeV for the reactions B^{11} (p, γ_0) C^{12} and B^{11} (p, γ_1) C^{12*} and 5.13 MeV for the reaction B^{11} (p, p' γ) B^{11}. The same level was also seen by Gibbons and Macklin [9]), who measured the total neutron emission from the reaction B^{11} (p, n) C^{11} by means of BF_3 counters. Their result of 5.10 MeV may yet be high because of an unknown target thickness. Blaser, Boehm, Marmier and Scherrer [13]), for the same reaction but poorer resolution, observed a level at 5.2 MeV; and the 0^0 neutron data of Marion, Bonner and Cook [14]) suggests a value of 5.35 MeV. Allowing then for apparent shifts due to angular distributions, and for target thickness and energy resolution, none of the above results is in disagreement with the value of 5.065 MeV suggested by this experiment.

Above this excitation energy there is little agreement amongst the B^{11}(p, n) C^{11} experiments (see table 1). If the last two points in the excitation function plotted by Gibbons and Macklin have any significance, then there is some support for the weak level found in the present experiment at 5.48 MeV. The levels found at 5.87 and 6.37 MeV by Blaser are difficult to explain in terms of energy calibration errors on their part, because their calibration elsewhere is only 50 keV off Bair's. Also it is doubtful whether their level at 5.87 could be the weak level at 5.48 MeV in this experiment; and yet their largest peak at 6.37 MeV could scarcely be identified with any level in this experiment save that at 6.03 MeV. The results of Kalinin *et al* [15]) could be made to agree if reduced in energy by about 0.6 MeV. As they stand, the only agreement reached is for a fairly weak resonance at 10.1 MeV.

Turning to the results of B^{11} (p, γ) C^{12} experiments, we find good agreement at 7.2 MeV; and, if we take account of "excrescences" on the side of this peak

TABLE 1

Maxima in yields of $B^{11}(p, n)C^{11}$ and $B^{11}(p, \gamma)C^{12}$

Blaser *et al.* E_p(MeV)	Kalinin *et al.* E_p(MeV)	Gibbons *et al.* E_p(MeV)	This exp. E_p(MeV)	Gemmell *et al.* E_p(MeV)	Gove *et al.* E_p(MeV)	Excitation in C^{12} (MeV) (this exp.)
5.18		5.10	5.065			20.60
		(5.45)	5.48			20.98
5.87						
			6.03	(5.95)	(6.09)	21.49
6.37						
	6.6			(6.75)		
			7.28	7.2	7.21	22.63
			7.73			23.04
			8.25			23.52
					(8.45)	
	8.8		8.64			23.88
			9.24			24.43
			9.79			24.93
	10.1		10.13			25.24
			10.91			25.96

TABLE 2

Levels in C^{12} as found in this experiment and in photonuclear experiments

This exp.		Thorson and Katz $C^{12}(\gamma, n)C^{11}$		Sadeh $C^{12}(\gamma, n)C^{11}$		Carroll and Stephens Total γ absorption		Cohen *et al.* $C^{12}(\gamma, p)B^{11}$	Jones *et al.* $C^{12}(\gamma, 3\alpha)$
E_x (MeV)	Γ (MeV)	Break (MeV)	E'_x (MeV)	Break (MeV)	E'_x (MeV)	E_x (MeV)	Γ (MeV)	E_x (MeV)	E_x (MeV)
20.60	0.21	20.29	20.50	20.37	20.58	20.46	(0.14)		
20.98	0.30	20.62	20.92	20.75	21.05	20.92	(0.29)	20.8	
21.49	0.61	20.90	21.51					21.5	(21.5)
		21.08							
		21.22							
		21.58							
22.63	0.42	22.02	22.44					22.6	22.7
23.04	0.07	22.88	22.95					23.1	
23.52	0.41								
23.88	0.23								
24.43	0.14								24.3
24.93	1.0								(25.0)
25.24	0.15								
25.96	0.48								

at about 25.9 to 26.0 MeV. This is in good agreement with the highest resonance observed by Gemmell *et al.* [5]) and also by Gove *et al.* [6]), then there is good agreement at 6.0 MeV. A further excrescence seen by Gemmell at 6.75 MeV was undetectable in the present experiment or in that of Gove. The results of Gemell do not extend to 8.45 MeV where another excrescence seen by Gove is midway between two peaks in the present experiment. A further investigation by Gemmell, in collaboration with Jones at Harwell [7]), lends support to the results of Gove, but also suggests a possible level around 6.55 MeV.

In order to compare the results of the present experiment with photonuclear results, the excitation function has been fitted with a number of rough Gaussian curves sitting on a large background contribution. These Gaussian curves are shown at the base of fig. 4 and will be further discussed in sect. 6. In table 2 are listed the excitation energies for each peak together with the estimated width of the corresponding Gaussian curve. The levels found in five photonuclear experiments [4, 16, 27]) are also listed. Calculations by Penfold and Spicer [17]) on test cross sections have shown that "breaks" in a photonuclear yield curve occur at a distance below the resonance roughly equal to the level width. Following the lead of Thorson and Katz, to each photonuclear break energy has been added the width of its assumed parent resonance, as determined by the present experiment. These corrected energies E'_x are shown after the break energies in table 2. The agreement between all the sets of data is quite good, and certainly within experimental errors if we consider uncertainties in the various machine calibrations and in estimates of resonance width Γ. It should also be remembered that the calculations of Penfold and Spicer were based on non-overlapping resonances. The only serious discrepancy in table 2 is the absence of any data which will substantiate the evidence of Thorson and Katz for breaks at 21.08, 21.22 and 21.58 MeV. There is no apparent explanation for the failure of corresponding resonances to show up in the B^{11} (p, n) C^{11} experiment. The excitation regions of 21.2 to 21.4 MeV, 21.6 to 22.4 MeV and 25.3 to 26.4 MeV were the only regions not covered at least twice in the present experiment. The first two regions would probably contain the three missing resonances, if they exist; however, there was no suggestion of their presence, whereas all repeated sections of the excitation function showed excellent reproducibility, including the weak resonances at 20.98 and 24.93 MeV. Possibly the "swamping" effect of the large resonance at 21.49 MeV in the present experiment obscured the missing resonances; however, the effect of a corresponding large (γ, n) resonance could be to produce a yield curve which was concave up between the break and the resonance. Such a curve might be mistaken for further breaks. The bracketed results of Jones *et al.* correspond to two wide but fairly weak possible resonances for which statistics are poor.

The excitation functions for B^{10} (d, p) B^{11}, B^{10} (d, n) C^{11}, B^{10} (d, γ) C^{12} (ref. [18])), and B^{10} (d, α_0) Be^8 (ref. [19])) all suggest the presence of a wide resonance in C^{12}

energy of the present experiment. Also, a careful search for narrow resonance structure was made for the B^{10} (d, α_0) Be^8 and B^{10} (d, α_1) Be^{8*} reactions, in deuteron energy steps of 10 keV or less, over the region [12]) of excitation energy 25.53 to 25.94 MeV. No evidence for such fine structure was found, which again is in agreement with the present experiment.

5. Absolute Cross Section

5.1. TARGET THICKNESS

As mentioned previously, the boron was first deposited on foils of moderate area which were then cut up to form the targets. One such foil, from which some targets had been cut, was used in a measurement of target thickness. Since for any given foil, the surface density of boron was fairly uniform, as

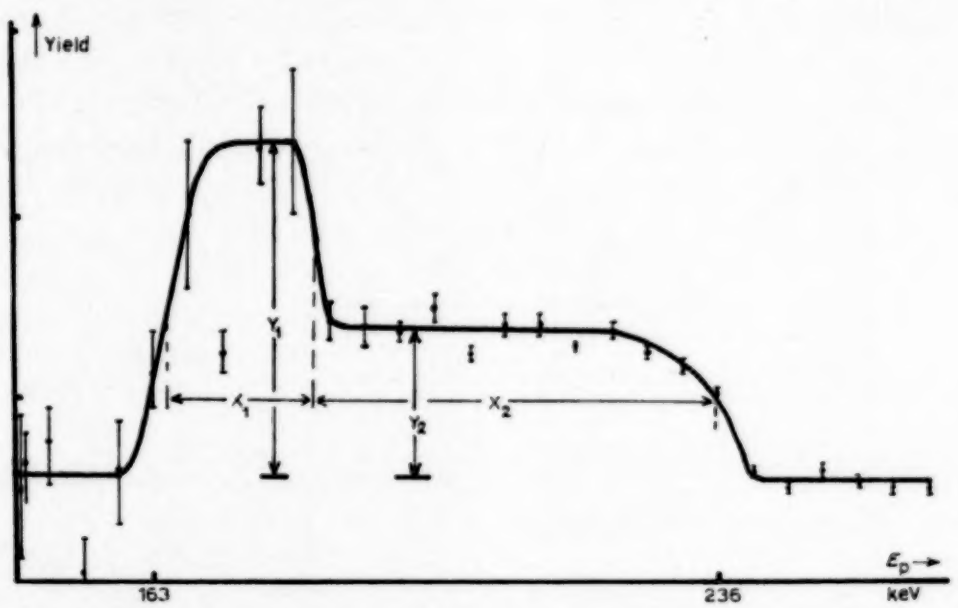

Fig. 5. Thick target measurement of the B^{11} (p, γ) C^{12} excitation function.

shown by comparative target thickness measurements, it was not necessary to use one of the experimental targets. This provided a larger target area which was free of oxide, nitride and any oil or carbon films, having been stored in a hydrogen atmosphere since its preparation.

The selected foil was bombarded with the proton beam from a Van de Graaff generator. Gamma rays emitted at 90° from the B^{11} (p, γ) C^{12} resonance at 163 keV were observed with a 7.6 cm NaI (Tl) crystal. The excitation function sketched in fig. 5 has a sharp rise as the resonance " hits" the front of the target, but drops to less than half height at 184 keV and then falls to background level at about 236 keV. There are two possible explanations of the first drop: either the boron reacted with or penetrated the tantalum surface or the

boron coating was uneven, possibly due to a pitted tantalum surface. In either case the effective boron thickness is estimated by multiplying the maximum width (width of total peak at half height) by the ratio $(X_1+X_2Y_2/Y_1)/(X_1+X_2)$, where the letters refer to fig. 5. This yields a value of 44 ± 2 keV, which for protons of this energy represents 35 μgm · cm^{-2}. If no penetration of the backing is assumed, the thickness is estimated to be 71 ± 2 keV or 90 μg · cm^{-2}, taking the maximum width referred to above, and ignoring the apparent uneven heights.

5.2. COUNTING EFFICIENCY AND ABSOLUTE CROSS SECTION

The total neutron emission has been estimated, and corrections have been made for counting geometry assuming a point source, for finite size of source, for absorption of positons in the tantalum foil and scattering of positons from the crystal surfaces and for loss of low energy positons due to discrimination. These corrections are listed in table 3 with a rough estimate of the uncertainty each contributed to the total cross section. The only sizeable correction was that due to counting geometry, and this was relatively well defined. The count of annihilation gamma rays from positons which escaped the crystals was thought to be very small.

TABLE 3

Sources of counting loss

Nature of correction	% loss	% uncertainty contributed to absolute cross section
Geometry loss	21	±2
Finite source size	3	±1
Foil absorption and total scattering	4	±1
Discriminator threshold	2.5	±1
Total loss	30%	±5% (maximum error)

From the above data the cross section at the peak of the 5.06 MeV proton resonance was estimated to be 335 ± 35 mb, of which half the uncertainty is in the target thickness. The maximum thickness assumption would yield a cross section at the same energy of 210 ± 20 mb.

The value of 335 mb is not in agreement with that of Blaser *et al.* [13]) if the peak value of 110 mb from their 5.2 MeV proton resonance is taken. Bair *et al.* [8]) did not quite cover the peak of this resonance; however, taking their estimate of about 70 mb for the cross section at 3.55 MeV, assuming an isotropic neutron distribution †, it is most unlikely that their rising cross section just above 5 MeV would attain a peak value of anything like 335 mb. This is substantiated

† Bair measured neutrons emitted in the forward direction over almost 2π sr.

by the rough agreement in relative cross section below 5 MeV of the data of Blaser and those of Bair. Blaser also gives a value of about 55 mb at 3.55 MeV. However, although there is rough agreement between these two experiments, Marion *et al.* [14]) have measured the cross section for neutrons emitted in the forward cone of half angle 10°. If an isotropic distribution is assumed, their total cross section becomes 188 mb, measured at a proton energy of 3.46 MeV. This would give a value of roughly 380 mb for the resonance at 5.1 MeV, in good agreement with the estimate of 335 ± 35 mb from the present experiment. The possibility that Bair's targets were not metallic boron as assumed, but B_2O_3 has been suggested by Bonner and acknowledged by Bair [8]). The targets used by Blaser for the absolute measurement were of metallic boron deposited on aluminium. Again the possibility of oxidation arises, and if evaporation was used, the possibility of impurities [9]). A final piece of evidence is provided by an activation done earlier in this laboratory, in which a target on a thick tantalum backing was irradiated and the activity measured with a Geiger counter. This yielded absolute values of cross section of 400 ± 100 mb at 5.8 MeV and 300 ± 100 mb at 9.6 MeV, in rough agreement with the present experiment. In this early investigation, the error was mostly in the beam current measurement, the solid angle of counting could only have been overestimated, yielding a low value of cross section, and the target thickness was determined by comparison with a Harwell separated target in the reaction B^{10} (d, α) Be^8, by proton scattering and roughly by weighing and by counting interference fringes; all estimates were in rough agreement. No allowance was made for scattering from the thick backing or from the air or the counter window.

6. Analysis of the Excitation Curve

The excitation curve of fig. 4 has the appearance of resonance structure superimposed on a continuous background. The latter rises rapidly from threshold to about $3\frac{1}{2}$ MeV above, and thereafter remains fairly constant. Presumably this background, which contributes about $\frac{2}{3}$ the total cross section over the entire energy range, is due to direct interaction mechanisms. The only available information on direct interaction cross sections in this region is the accumulated data on the reaction C^{12} (p, p') C^{12*} used by Levinson and Banerjee [20]). In the above reaction, the cross section attains a maximum value of 240 mb at 8 MeV above the threshold. This figure is in good agreement with the estimated background plateau for this experiment; however, even allowing for the lesser effect of the Coulomb barrier in the (p, n) reaction than in the (p, p') reaction, it seems unlikely that the direct interaction cross section could peak at only $3\frac{1}{2}$ MeV above the threshold. It is more likely that the direct interaction terms interfere constructively with single particle resonance terms, and the background then consists of direct interaction plus interference terms.

If the large, fairly isolated peak at a proton energy E_p of 6.03 MeV is the product of a single resonance of total angular momentum J, then the maximum possible value of the resonance cross section is

$$\sigma_{max} = \frac{\pi}{k_p^2} \frac{2J+1}{(2I_1+1)(2I_2+1)},$$

where k_p is the wave number of the protons outside the compound system and I_1 and I_2 are the angular momenta $\frac{1}{2}$ and $\frac{3}{2}$ of the proton and the B^{11} nucleus. Substituting $k_p^2 = 24.4\,b^{-1}$ at $E_p = 6.03$ MeV gives $\sigma_{max} = 16.1$ $(2J+1)$ mb. The various possible values of J then give corresponding values of σ_{max}, and, if these are subtracted from the total cross section at the peak, each will give a minimum value of the background cross section immediately under the peak for a given value of J. These values are shown as horizontal lines under the 6.03 MeV peak in fig. 4.

The width and height of this peak suggest the presence of a single-particle resonance, in which case the J value is unlikely to exceed 4. Even this value of J requires the background to have a pronounced peak at about $E_p = 6\frac{1}{2}$ MeV. If reference is again made to the data of Levinson and Banerjee, direct interaction probably contributes less than 180 mb at 3 MeV above the threshold (for C^{12} (p, p′) C^{12*} the figure is nearer 120 mb). Therefore the interference term must be large. If the direct interaction is assumed to contribute 180 mb and the single particle resonance to contribute the maximum possible cross section, then a J value of 2 is possible, though less likely than 3 or 4. The value of $J = 4$ was chosen as requiring the least interference contribution and hence the smoothest background. The requirements for direct and single particle contributions are also easier to fulfil.

The only possible single particle state with $J = 4$ for this excitation of C^{12} is, in jj coupling, that formed by coupling a $d_{\frac{3}{2}}$ proton or neutron to the ground state of B^{11} or C^{11} which are thought to have $J^\pi = \frac{3}{2}^-$. The configuration would then be $(1s)^4(1p_{\frac{3}{2}})^7(1d_{\frac{3}{2}})$ and the J^π value 4^-. This could well be a fairly pure state, since the only other possible 4^- state of any strength in this vicinity would be that having the configuration $(1s)^4(1p_{\frac{3}{2}})^6(1p_{\frac{1}{2}})(2s)$ which involves 2-particle excitation. Consider now the manner in which a 4^- state in C^{12} at 21.49 MeV excitation energy could decay. The first excited state in B^{11} is known to be $\frac{1}{2}^-$ and therefore unavailable; the corresponding state [21]) in C^{11} is probably also $\frac{1}{2}^-$. Higher states in C^{11} are energetically unattainable; the second excited state in B^{11} (probably $\frac{5}{2}^-$) requires about 1 MeV d waves, and the state above ($\frac{3}{2}^-$ to $\frac{7}{2}^-$) about $\frac{1}{2}$ MeV s or d waves. The most likely alpha decay is by 11 MeV f waves to the 2^+ first excited state of Be^8 or by 2 MeV p waves to the 4^+ second excited state. Gamma emission is unlikely to compete seriously. All these modes of decay will have small penetration factors, and therefore small partial widths. Thus, though there may be some

contribution from other decay modes to the reduced width sum, the total width is likely to comprise mainly the partial widths for decay via proton and neutron emission to the ground states of B^{11} and C^{11} respectively; both require d wave emission, but both protons and neutrons have large penetration factors for these energies. On the above arguments, the reduced widths for d wave emission of protons and neutrons should be large, and their partial widths roughly equal, together providing almost the full width.

Employing the notation of Lane and Thomas [22]), and assuming penetration factors of $P = \rho A^{-2}$ and an interaction radius of $a = 1.45\ (11^{\frac{1}{3}}+1)$ fm, a rough fit to the experimental data was sought of the Breit-Wigner one level formula

$$\sigma_{p,n} = \frac{\pi}{k_p^2} \frac{2J+1}{(2I_1+1)(2I_2+1)} \frac{\Gamma_{\lambda p}\Gamma_{\lambda n}}{(E_\lambda+\Delta_\lambda-E)^2+\frac{1}{4}\Gamma_\lambda^2}.$$

The proton and neutron partial widths and level shifts were estimated as functions of energy by the use of graphs of proton A and B functions by Sharp, Gove and Paul [23]) and tables of neutron penetrabilities and shift functions by Monahan, Biedenharn and Schiffer [24]). Assuming that the background curve would pass close to but above the $J = 4$ line of fig. 4 it was possible to predict values for the proton and neutron reduced widths of $\gamma_p^2 \approx \gamma_n^2 \approx \frac{1}{4}$ MeV. A smooth background curve (shown dotted) was then sketched by eye on fig. 4. The calculated resonance shape for $\gamma_p^2 = \gamma_n^2 = \frac{1}{4}$ MeV was added to this, giving a fairly good fit (shown dashed) to the total cross section over this peak. No attempt was made to obtain a better fit by changing the background or reduced width assumptions, since the approximations and assumptions made did not warrant it. For this choice of J, the sharpness of the experimental peak could not be fitted unless a much sharper interference peak was included in the background. The partial widths for proton and neutron emission at resonance according to the above theory are $\Gamma_p = 0.46$ MeV and $\Gamma_n = 0.25$ MeV giving a total width of $\Gamma = 0.71$ MeV. The dimensionless reduced widths are $\theta_p^2 = \gamma_p^2\ (\hbar^2/Ma^2)^{-1} = 0.125$ and $\theta_n^2 = \gamma_n^2\ (\hbar^2/Ma^2)^{-1} = 0.125$ giving a sum of $\sum\theta^2 = 0.25$. Lane [25]) estimates the single particle reduced width for d waves to be 0.6, as calculated with a harmonic oscillator well, though this value may be slightly high.

If the background shown dotted in fig. 4 is assumed, then the remaining resonant cross section may be fitted with the approximate Gaussian curves shown dashed along the base of fig. 4. It must be emphasized that such a smooth background would be incompatible with further interference terms. Therefore any predictions of minimum J values must be regarded as only a rough guide. Within each Gaussian curve is the corresponding minimum value of J, if no additional interference terms contribute; however, in view of the singular apparent scarcity of levels with low J values, there would

appear to be a great deal of such interference. In particular a large interference term is needed to explain the height of the peak at 22.6 MeV excitation. This occurs at the peak of the giant photonuclear dipole resonance and is therefore probably a 1^- level, whereas a smooth background predicts $J \geqq 2$. The smooth background of fig. 4 also predicts a rough distribution of 0 : 2 : 5 : 0 : 4 for the relative numbers of levels having $J = 0$, 1, 2, 3 and 4 in the excitation region of 20 to 25 MeV. The presence of more interference terms could modify these predictions sufficiently to make them compatible with a rough distribution of 3 : 7: 7: 4: 2 predicted by the level density formulae of Newton [26]).

7. Conclusion

In contrast to the above predictions of J values, the surprising manner in which most of the levels seen in the present experiment appear to be capable of gamma emission to the ground state would suggest that the majority of them are 1^- levels, or at least that their J values are small. Certainly, all levels participating in the $C^{12}(\gamma, n)\ C^{11}$ and $C^{12}(\gamma, p)\ B^{11}$ reactions should also participate in the B^{11} (p, n) C^{11} reaction; but the converse should be far from the truth. Thus the apparent agreement on level density between the present experiment and photonuclear experiments is an enigma. Although unsupported by the present experiment, the photonuclear giant resonance may be due to a singularly propitious grouping of 1^-, $T = 1$ levels around $22\frac{1}{2}$ MeV excitation. Thorson and Katz [27]) have suggested that the onset of the giant resonance may be associated with an observed increase in integrated cross section with increase in level excitation. Although the data of Ajzenberg and Lauritsen [28]) up to 20 MeV and the results from the present experiment above this energy show an increase of average level width with excitation energy, there is poor correlation between the integrated cross sections found by Thorson and Katz and the corresponding level widths as determined in this experiment. Therefore the increase in integrated cross section is presumably due to an increase in the reduced width for electric dipole emission to the ground state of C^{12}, there being no gross increase in reduced width for neutron emission apparent in the present experiment. Thus, whilst some agreement is attained between photonuclear and particle experiments, there are still many questions unanswered, and in particular there is a need for information on the spins, parities and isobaric spins of levels in the region of the giant photonuclear resonance.

We wish to express our appreciation of the interest in this work shown by Associate Professor C. B. O. Mohr and also by Dr. B. M. Spicer, whom we thank for stimulating discussion of the photonuclear work. Mr. D. Robson was of great assistance on the subject of direct interactions. We thank Dr. D. S. Gemmell of A.E.R.E., Harwell for providing details of his preliminary in-

vestigations. We are deeply indebted to Professor A. S. Buchanan and his assistants of the Chemistry Department for the time and care taken over preparation of pure diborane. Finally we express our appreciation of the work done and interest shown by all fellow members of the cyclotron team headed by Professor D. E. Caro.

References

1) L. Katz *et al*, Phys. Rev. **95** (1954) 464;
J. Goldemberg and L. Katz, Phys. Rev. **95** (1954) 471;
B. M. Spicer and A. S. Penfold, Phys. Rev. **100** (1955) 1375
2) R. N. H. Haslam *et al*, Can. J. Phys. **31** (1953) 210;
A. K. M. Siddiq and R. N. H. Haslam, Can. J. Phys. **36** (1958) 963;
A. S. Penfold and E. L. Garwin, Phys Rev. **114** (1959) 1324, **116** (1959) 120
3) M. M. Wolf and W. E. Stephens, Phys. Rev. **112** (1958) 890;
L. D. Cohen and W. E. Stephens, Phys. Rev. Lett. **2** (1959) 263
4) E. E. Carroll and W. E. Stephens, Phys. Rev. **118** (1960) 1256.
5) D. S. Gemmell, A. H. Morton and E. W. Titterton, Nuclear Physics **10** (1959) 33
6) H. E. Gove, A. E. Litherland and R. Batchelor, Phys. Rev. Lett. **3** (1959) 177
7) D. S. Gemmell, private communication
8) J. K. Bair, J. D. Kington and H. B. Willard, Phys. Rev. **100** (1955) 21
9) J. H. Gibbons and R. L. Macklin, Phys. Rev. **114** (1959) 571
10) R. W. McIlroy, private communication
11) R. W. Dodson *et al*, in Nat. Nuc. Energy Series Div. 5, vol **3**., ed. by A. C. Graves and D. K. Froman (McGraw-Hill Book Co., New York, 1952) p. 20
12) G. J. F. Legge, Nuclear Physics **26** (1961) 608
13) J. P. Blaser *et al.*, Helv. Phys. Acta **24** (1951) 465
14) J. B. Marion, T. W. Bonner and C. W. Cook, Phys. Rev. **100** (1955) 91, Los Alamos Report LA—2014 (1956)
15) S. P. Kalinin, A. A. Ogloblin and Y. M. Petrov, Soviet J. Atomic Energy **2** (1957) 193.
16) E. J. Jones, Proc. Glasgow Conf. (Pergamon Press, London 1955) p. 147;
L. Cohen, *et al.*, Phys. Rev. **104** (1956) 108;
D. Sadeh, Compt. Rend **249** (1959) 531
17) A. S. Penfold and B. M. Spicer, Phys Rev. **100** (1955) 1377
18) W. H. Burke, J. R. Risser and G. C. Phillips, Phys. Rev. **93** (1954) 188
19) J. B. Marion and G. Weber, Phys. Rev. **103** (1956) 1408;
R. L. Becker, Phys. Rev. **119** (1960) 1076
20) C. A. Levinson and M. K. Banerjee, Ann. Phys. **3** (1958) 67
21) J. A. McDonell *et al*, Aust. J. Phys. **13** (1960) 99;
D. G. Sargood, private communication
22) A. M. Lane and R. G. Thomas, Revs. Mod. Phys. **30** (1958) 257
23) W. T. Sharp, H. E. Gove and E. B. Paul, Graphs of Coulomb functions 2nd ed. (1955) TPI—70 A.E.C.L. report no. 268
24) J. E. Monahan, L. C. Biedenharn and J. F. Schiffer, A.E.C. report (1958) ANL—5846
25) A. M. Lane, Revs. Mod. Phys. **32** (1960) 519
26) T. D. Newton, Can. J. Phys. **34** (1956) 804
27) I. M. Thorson and L. Katz, Proc. Phys. Soc. A **77** (1961) 166
28) F. Ajzenberg-Selove and T. Lauritsen, Nuclear Physics **11** (1959) 1

7.C:9.A

Nuclear Physics **26** (1961) 634—648; © *North-Holland Publishing Co., Amsterdam*

Not to be reproduced by photoprint or microfilm without written permission from the publisher

THE PRODUCTION AND PROPERTIES OF MESONS AT HIGH ENERGIES

F. A. BRISBOUT, C. GAULD, J. LEHANE, C. B. A. McCUSKER, J. MALOS, K. NISHIKAWA and L. G. VAN LOON

The F.B.S. Nuclear Department, School of Physics, University of Sydney, Sydney, N.S.W. †

Received 12 May 1961

Abstract: Results from a 10 l stack of Ilford K5 emulsion flown to 38.4 km are presented. It is shown that the transverse momentum spectrum of the secondary particles of jets has two peaks at about 0.4 and 2.0 GeV/c respectively, and possibly a third peak at about 8 GeV/c; that the interaction cross section of secondary pions is considerably smaller than the geometric value; that the interactions they produce in emulsions have a lower average multiplicity than proton produced interactions in the same energy range; and that the number of particles per interaction close to the forward direction is less than that expected from extrapolation from slightly greater angles. The results are compared with those of other experiments and their meaning discussed.

1. Introduction

The majority of particles produced in nuclear interactions of primary energy greater than 500 GeV are π mesons [1]). In this paper the distributions in angle and momentum of these particles at production are studied, their mean free path for further interactions found and the character of these interactions compared with those produced by protons.

2. Flight and Scanning

The interactions discussed in this paper occurred in a 10 l block of Ilford K5 emulsion flown for $4\frac{1}{2}$ h at 38.4 km over Texas in the autumn of 1959. The emulsion was developed at the new plant, built for the ICEF project, in the University of Chicago. The flight was carried out by units of the U.S.A.F. and both flying and processing were supervised by Dr. A. J. Herz.

Scanning began early in 1960. Two methods were used, the first was an area scan using a stereomicroscope with $\times$ $12\frac{1}{2}$ eyepiece and $\times 2$ objectives, the second was a line scan with a $\times$ 20 objective. Two lines were used, the first 1 cm form the bottom of the stack; the second 14 cm from the bottom (i.e. about halfway up). In the line scan, all events resulting in four or more parallel

† This work has been supported by the Nuclear Research Foundation within the University of Sydney and by the Office of Scientific Research of the Air Research and Development Command of the USAF.

tracks in one field of view were accepted. From the events found so far six, with energies greater than 5000 GeV per nucleon have been selected.

3. Methods of Analysis

3.1. ANGULAR DISTRIBUTION AND ENERGY DETERMINATION

For each jet a reference track was chosen near to the shower axis and the spatial separations (both in and perpendicular to the plane of the emulsion) of all other shower tracks were measured relative to this at suitable distances from the jet origin. This and other relevant data (e.g. shrinkage factors and so on) were fed into the Sydney University digital computer SILLIAC which was programmed to print out:

(i) the true space angles and target diagram coordinates of each track,

(ii) γ_p determined from $\gamma_p = 2/\tan^2\eta$, where η is the median angle of the shower particles,

(iii) γ_C obtained from the formula of Castagnoli *et al.* [2]),

(iv) the coordinates for a Walker-Duller plot [3]).

Using γ_p and n_s the event was then examined using the method of Roesler and McCusker [4]) to determine the nature of the collision (i.e. whether nucleon-nucleon or more complex) and the true primary energy estimated.

3.2. SECONDARY INTERACTIONS

Cones of constant half angle were scanned for electron pairs and secondary interactions. Bremsstrahlung electron pairs were distinguished from parent electron pairs according to the method of Brisbout *et al.* [1]). Secondary and tertiary interactions were distinguished by the method described in appendix 1.

The total path length of all charged secondaries was determined for each jet by multiplying the distance from the parent jet origin to the edge of the stack by the number of charged secondaries which did not interact and adding to this the total distance from primary to secondary interactions of all secondaries which did interact. In this determination great care was taken a) to correct n_s for electron pairs and b) to distinguish between secondary and tertiary interactions. Details are given in appendix 1.

For each secondary interaction the angular distribution and energy were obtained in a manner similar to that for primary events. In this case however no correction for cascading within the struck nucleus was used for a reason to be detailed later. In order to get the transverse momentum of the secondary interaction, its angle to the shower axis must be found with considerable accuracy. Details of the methods used to determine this are given in appendix 2, and of the extracting of electron pairs from amongst the shower tracks measured in the angular distribution are given in appendix 4.

4. Analysis of Electromagnetic Cascades

As described by Pinkau [5]), "cuts" were made at intervals of approximately 1 cascade unit along the paths of jets α1, α4, S1 and S2. The positions of all the electron tracks were measured. Their angular coordinates as calculated by SILLIAC were then plotted on transparent paper. Superposition of these on the angular target diagram of the shower tracks and parent electron pairs enabled the nature of the origins of individual γ ray cascades to be determined. Cascades due to π^0 mesons produced in secondary interactions were detected firstly because they did not correspond to any of the parent electron pairs from the original jets and secondly because they did not maintain a constant angle from cut to cut †. The numbers of electron tracks within a suitable radius from the individual cascade cores were corrected for background effects due to shower tracks and intermixing of cascades. The details of this background correction are given in appendix 3. The energies of the individual γ rays were determined from both the radial electron distributions and the longitudinal cascade development.

5. Results

5.1. GENERAL

Details of the primary jets are given in table 1 and of the secondary jets in

TABLE 1
Primary jets

Jet	γ_p	$2\gamma_c^2$	Outgoing energy per nucleon (GeV)	Tunnel theory energy estimate per nucleon (GeV)	Free path before interacting (cm)	Path length for analysis (cm)
S1($x+>3$)x			>20 000		0	9
S2(0+6p)	2 000 000	280 000 with 6th track and 2 300 000 without 6th track		2 000 000	3.5	6
α1(12+116)α	1 800	1 900	8 000	7 000	8.2	23
α4(18+131)α	5 000	7 500	11 000	19 000	6.9	11
α2(15+ 81)α	7 400	7 000		15 000	22.5	4
α5(0 + 47)α	22 000	18 000		28 000	8.2	8

The sum of the outgoing energies was calculated in the manner of Brisbout and McCusker [6]), allowing for the fact that in these cases, the inelasticity was not unity.

† The base line employed in converting the positions of the electron tracks into angular coordinates was given, in each case, by the distance of the "cut" from the parent jet origin.

table 2. A comparison of the γ_p values of primary and secondary interactions brings out a point which has been made before [6, 7]), namely that in many cases γ_p (and γ_c) gives a gross underestimate of the primary energy but that an estimate based on the tunnel theory is accurate within the experimental limits.

TABLE 2

Secondary interactions

Secondary interaction	Distance from origin (cm)	Angle of emission (10^{-3} rad)	γ_p	P_T (GeV/c)
S1S1 (0+11p)	2.0		20 000	
S1S2 (4+ 9n)	4.3	5.0	540	2.4
Jet S1S1 (cone half angle 6.5×10^{-3} rad)				
S1S1S1 (8+9p)	1.3	2.1	800	1.6
Jet S2 (cone half angle 10^{-2} rad)				
S2S1 (18+15p)	2.2	3.0	500	1.5
Jet α1 (cone half angle 6×10^{-3} rad)				
α1S1 (28+13p)	2.5	6.0	300	1.8
α1S2 (0+10p)	4.1	0.9	300	0.27
α1S3 (32+16p)	6.0	0.9	60	0.05
α1S4 (4+14p)	12.4	0.4	38 000	2.8[a])
α1S5 (2+16n)	12.4	0.4	5 000	1.9
α1S6 (4+ 5n)	11.2	0.4	300	0.12
α1S7 (6+ 7n)	16.8	2.1	1 000	2.1
α1S8 (8+ 3p)	9.5	0.8	20	0.16
α1S9 (0+13p)	15.5	0.4	6 000	2.4
α1S10 (7+ 7n)	14.1	5.5	500	2.7
α1S11 (4+ 9n)	14.7	1.2	600	0.48
Jet α4 (cone half angle 6.5×10^{-3} rad)				
α4S1 (3+11n)	1.8	0.6	4 300	2.6
α4S2 (4+ 4p)	2.6	1.2	160	0.19
α4S3 (22+ 8p)	3.1	5.5	120	0.66
α4S4 (22+21n)	3.5	0.6	1 200	0.7
α4S5 (19+18p)	3.4	6.5	70	0.45
α4S6 (11+ 9p)	6.8	1.6	20	0.04
α4S7 (0+ 8p)	9.6	0.6	10 000	6.0
α4S8 (15+15n)	9.8	1.5	20	0.03
α4S9 (3+11n)	6.8	4.9	2 000	9.8
α4S10 (21+18n)	9.7	4.2	100	0.42

[a]) It is believed from a comparison of this value of γ_p with that for the other secondaries of α1 and with α1 itself that this value is an overestimate of the energy. The value of P_T is based on an estimate 7000 GeV for the energy of α1S4.

5.2. TRANSVERSE MOMENTUM

Detailed results employed in the determination of the transverse momentum of the π^0 mesons are given in table 3. Here, those γ rays most likely to arise from the decay of the same π^0 meson are bracketed together. The value R gives the ratio of the π^0 meson energy, as determined from the opening angle

TABLE 3

γ rays and π^0 mesons

Electron pairs	γ-ray energy (GeV)	R	π^0 meson energy (GeV)	Angle of emission (10^{-3} rad)	P_T of π^0 meson (GeV/c)
Jet S1 (within angle of 3×10^{-3} rad)					
0	$\leqq$50		$\leqq$100	2.2	$\leqq$0.2
Jet S1S1 (within angle of 4×10^{-3} rad)					
3 a	140 60	1.0	200	1.3	0.26
4	130		260	1.2	0.31
c c′	40 40	1.0	80	3.2	0.25
3 4	140 130	0.8			
Jet S2 (within angle of 1×10^{-2} rad)					
1 3	3 60	1.3	60	3.0	0.18
4	150		300	1.2	0.36
Jet α1 (within angle of 6×10^{-3} rad)					
a′ 00′	150 100	0.6	400	1.4	0.56
i d	150 350	0.9	450	0.8	0.36
a‴ a″	100 100	1.0	200	2.0	0.40
0′ 0‴	150 100	0.8	200	1.6	0.32
d d′	350 200	0.9	500	0.95	0.47
d′ c′	200 400	0.6	370		
c′ c″	400 200	0.8	450	1.2	0.55
d″ d‴	250		370	2.3	0.85

TABLE 3 (continued)

Electron pairs	γ-ray energy (GeV)	R	π^0 meson energy (GeV)	Angle of emission (10^{-3} rad)	P_T of π^0 meson (GeV/c)
Jet $\alpha 4$ (within angle of 6×10^{-3} rad)					
c 0	400 400	1.0	800	0.4	0.32
c′ A	350 350	0.7	500	0.55	0.28
A″ A″″	150 200	1.1	400	2.4	0.96
A‴ K′	150	1.0	300	1.8	0.54
B B′	100 100	1.5	300	1.8	0.54
L N	120 50	1.2	200	1.7	0.34
D	40		80	6.0	0.48
J J′	70 70	1.0	150	3.2	0.47
F	$\leqq$20		40	2.8	0.11

R is the ratio of π^0 energy estimated from the opening angle to that obtained from the sum of its γ-ray energies.

between the two γ rays, to that of the sum of the energies of the two γ rays as determined by cascade analysis. With few exceptions (which are probably due to fluctuations) these values of R are close to unity indicating that the γ rays have been paired off satisfactorily.

The values of the transverse momenta for the secondary interactions are included in table 2.

The distribution of the transverse momenta for π^0 mesons and secondary interactions are shown in figs. 1 and 2 for jets S1 s1, S2, $\alpha 1$ and $\alpha 4$, together with jets P_4 and P_8 from a previous publication [6]), respectively. (In the former case $P_T = E_{\pi^0} \sin\theta$, where E_{π^0} is the energy of the π^0 meson and θ its angle of emission. In the latter case P_T is given by $\gamma_p \sin\theta$.)

The distribution in transverse momentum for the π^0 mesons is well fitted by a Poissonian of mean value

$$0.37^{+0.05}_{-0.03}\ \text{GeV/c}.$$

This value is in particularly good agreement with that of the Japanese emulsion group [10]).

The distribution in transverse momentum of the secondary interactions, unlike that for the π^0 mesons, appears to have a secondary peak at about

2.4 GeV/c and, in addition, three points with very large P_T. Using the Poissonian from the π^0 distribution, the probability that 14 out of 39 events from such a distribution should have momenta greater than 1 GeV/c is less than 10^{-12}. The statistical reality of this effect is thus established. Two possible physical explanations of these high P_T values are a) that in many cases gross overestimates of the energy are made when this is equated to γ_p and b) that,

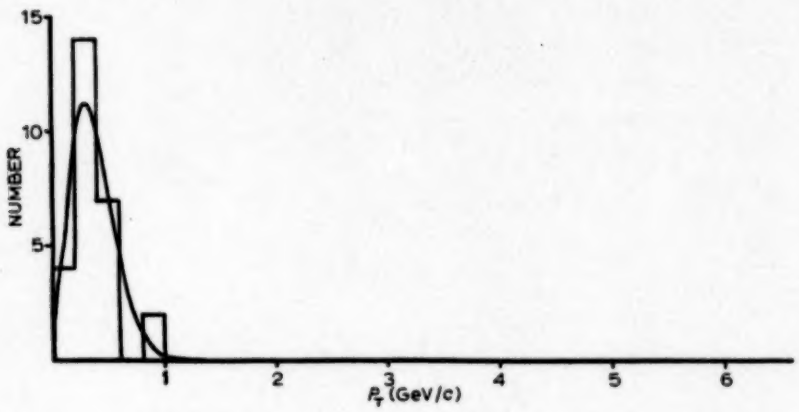

Fig. 1. This shows the distribution in transverse momentum for π^0 mesons from jets S1s1, S2, α1, α4, P_4 and P_8.

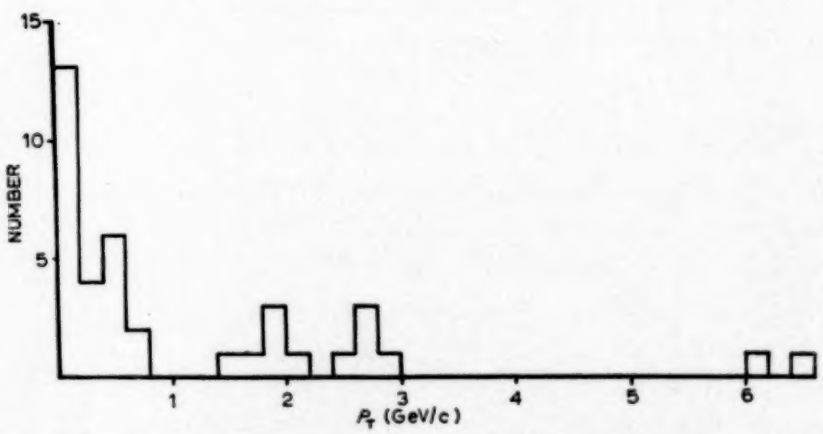

Fig. 2. This shows the distribution in transverse momentum obtained from secondary interactions of the jets S1s1, S2, α1, α4, P_4 and P_8.

commonly particles other than π mesons have values of P_T in the region of 2.0 GeV/c.

There are a number of difficulties in the way of accepting the first of these two hypotheses.

In the first place a series of overestimates of the energy would be expected to produce a smoothed distribution with a long tail at higher momenta rather than the two distinct peaks seen. Secondly, it has been shown elsewhere and also in this paper that for primary jets, γ_p is generally an *underestimate* of the

energy. Hence it seems very likely that this second peak is a real physical phenomenon, rather than an effect of measurement and its absence in the π^0 distribution as well as the considerable number of cases where the particle concerned is neutral lead us to believe that it is concerned with particles other than pions.

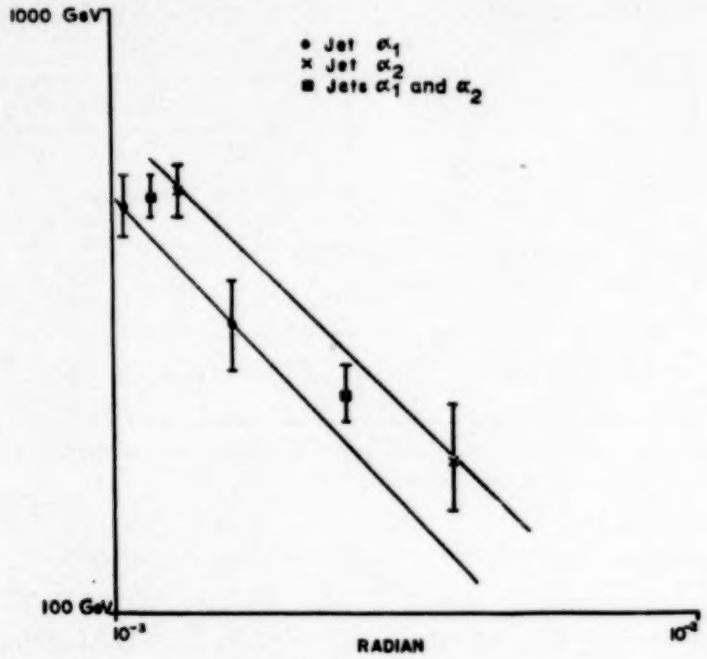

Fig. 3. This gives the variation of E_{π^0} with θ for the π^0 mesons from jets $\alpha 1$ and $\alpha 4$.

The three very high values of P_T add to the previous evidence both from air shower [6, 8, 11]) and emulsion work [8]) suggesting the reality of such large values.

Fig. 3 shows the variation of E_{π^0} with θ for jets α_1 and α_4. The line to which these points are fitted has a slope of about minus unity.

5.3. MEAN FREE PATH

For a total track length of 675 cm 14 secondary interactions with charged primaries were observed giving a value for the interaction mean free path of 48^{+17}_{-10} cm. Combining these results with those of Edwards *et al.*, a value of 37^{+5}_{-4} cm is obtained as compared to a value of 27 cm if the interaction cross section were geometric. As pointed out previously by Edwards *et al.* [8]), the difference may be explained by assuming that π mesons which constitute 80% of the shower particles, have an interaction cross section in nuclear matter considerably less than the geometric value.

If this small value for the cross section is correct then a pion will generally make only one collision in traversing a nucleus in the emulsion in which any collisions take place. The successful predictions of the tunnel theory of jets

suggests that for proton primaries the average number of collisions is at least two. Thus it would seem that a comparison of the average multiplicities of primary and secondary jets might be of great interest. Such a comparison has been made in table 4 for two different energy ranges (as determined by γ_p).

TABLE 4

The average number of shower particles per jet for primary and secondary jets in two different ranges of γ_p

	Primary jets				Secondary jets			
Range of γ_p	Mean γ_p	Total n_s	Number of events	$\overline{n_s}$	Mean γ_p	Total n_s	Number of events	$\overline{n_s}$
49—300	120	458	22	20.8	166	189	18	10.5
301—2 000	1 010	680	29	23.6	600	218	16	13.6

The slow increase in $\overline{n_s}$ with energy for each type of jet and the large difference in $\overline{n_s}$ between types in the same energy range can be seen.

The events for the primary jets in the lower energy range were obtained from the paper of Daniel *et al.* [9]), those for the higher energy range from various sources summarised by McCusker and Roesler [7]). The values for the secondary interactions were obtained from our own results together with those of Edwards *et al.* [8]). It can be seen that whereas the mean multiplicity of either group shows only a slow increase with energy, there is in both cases, a large and statistically significant difference in the mean multiplicities of primary and secondary jets in the same energy group.

It is obvious that these two observations, namely, the small interaction cross section of the pions and the large difference of primary and secondary multiplicities can be explained on the assumption of a pion-nuclear cross section about one third of a nucleon-nucleon cross section which has a value equal to or slightly greater than the geometric value. However, two other explanations must also be considered.

The first is that the difference in multiplicities is due to scanning bias. This assumes that since the secondary interactions are found in cone scans there is less likelihood of events of low multiplicity being missed than in the case of primary interactions. Two arguments make this hypothesis unlikely. The overall average multiplicity of the secondary events is 12.0 ± 0.6 and for primary events is 22.3 ± 0.7. If we believe that a value of the latter of 14.0 would be, statistically, equivalent to the former, then, assuming the average multiplicity of the 'missed' events to be 6, we could have to suppose that these events made up 50 % of the total and that none were missed in the cone scan for

secondaries. Not only is such a large scanning loss difficult to credit, but also one finds that in the secondary events the proportion with average multiplicity 6 is only 25 % of the total. The second argument is that for the primary events, those in the low γ_p range were mostly found by a volume scan; those in the higher range by a line scan for cascades. For the argument to hold not only must both methods be very inefficient but both must be equally inefficient.

The other explanation is that the average multiplicity in pion-nucleon encounters is considerably less than in nucleon-nucleon encounters at the same γ_p. If this is taken in conjunction with the hypothesis that the pion-nucleon and nucleon-nucleon cross sections are the same, one encounters two difficulties. The first is that it is difficult to reconcile a nucleon-nucleon cross section of only a third the the geometric value with the successful predictions of the tunnel theory based on the assumption of about geometric cross section. With this theory it has been possible to explain the variation of n_s with γ_p at all energies from 500 to 100 000 GeV, to predict an average n_s in nucleon-nucleon encounters at 1000 GeV which has been since confirmed by cloud chamber measurements [12, 13]), to obtain the variation of n_s with Atomic weight A at 5000 GeV found experimentally and to explain the frequent occurrence of stars with few or no heavy prongs at high energies. The second difficulty is that if one assumes a 'fireball' model of nucleon-nucleon collisions, then a smaller multiplicity in pion-nucleon collisions is plausibly explained by the assumption that in this case only one fireball is produced, more or less attached to the struck nucleon. Meson emission will mostly take place from this fireball which is moving rather slowly in the laboratory system. Thus an energy estimate based on γ_p will be a considerable underestimate. This is hard to reconcile with the present determined ratio of primary to secondary energies and even more difficult to reconcile with the present good agreement between the P_T distributions for charged and neutral pions. However, the distinct possibility exists that some part of the difference in $\overline{n_s}$ is due to a difference in the pion-nucleon and nucleon-nucleon collisions.

5.4. ANGULAR DISTRIBUTIONS OF PARENT JETS

The angular distribution of the shower tracks of the primary jets are shown in figs. 4 and 5 and the Walker-Duller plots in fig. 6. In fig. 5 the shower particles densities are plotted against angle of emission. The points show the number of shower tracks within a given angular zone divided by the solid angle of that zone. If θ_2 and θ_1 are the upper and lower limits of these zones then the shower particle densities are given by

$$\frac{N_{(\theta_2-\theta_1)}}{\pi\,(\theta_2{}^2-\theta_1{}^2)}.$$

Straight lines with slopes varying from -1.5 to -2.0 can be drawn through

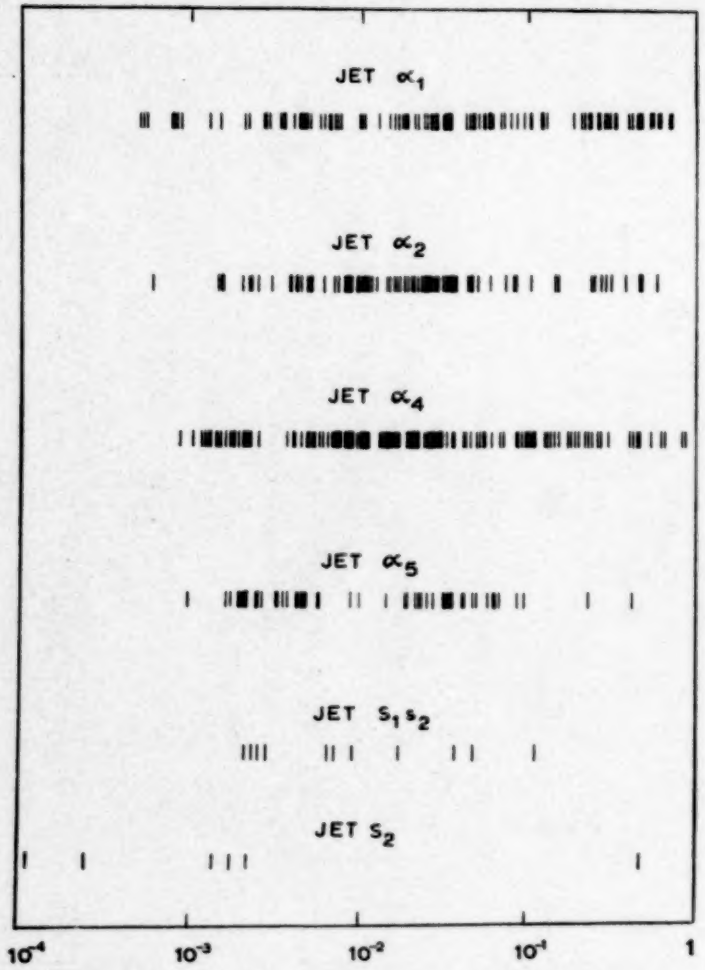

Fig. 4. The angular distribution of shower tracks from the jets.

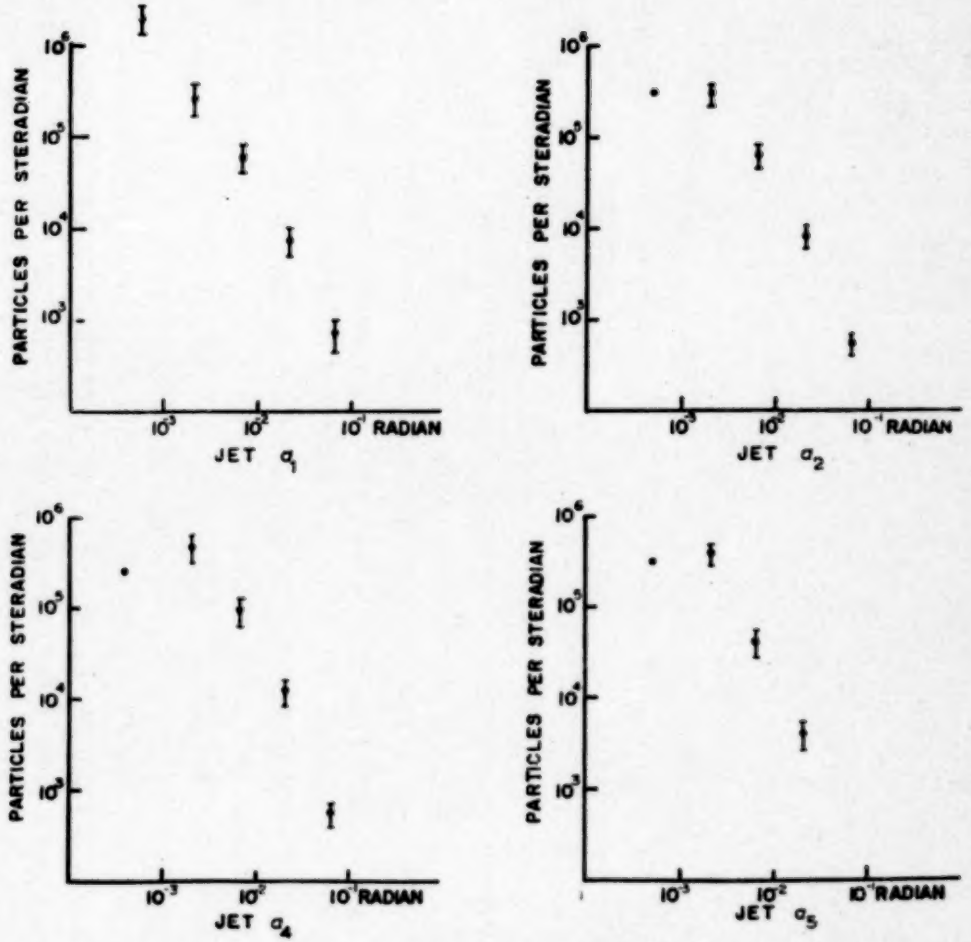

Fig. 5. The density of shower tracks against angle of emission for four jets with α primaries

all the points except for the central zone. Here the observed shower track densities fall significantly below that predicted by the power law fitting the outer regions. This effect is partly to be expected from the Lorentz transformation from the c.m. system to the laboratory system. Various models likely to explain the results of the angular distributions are being investigated.

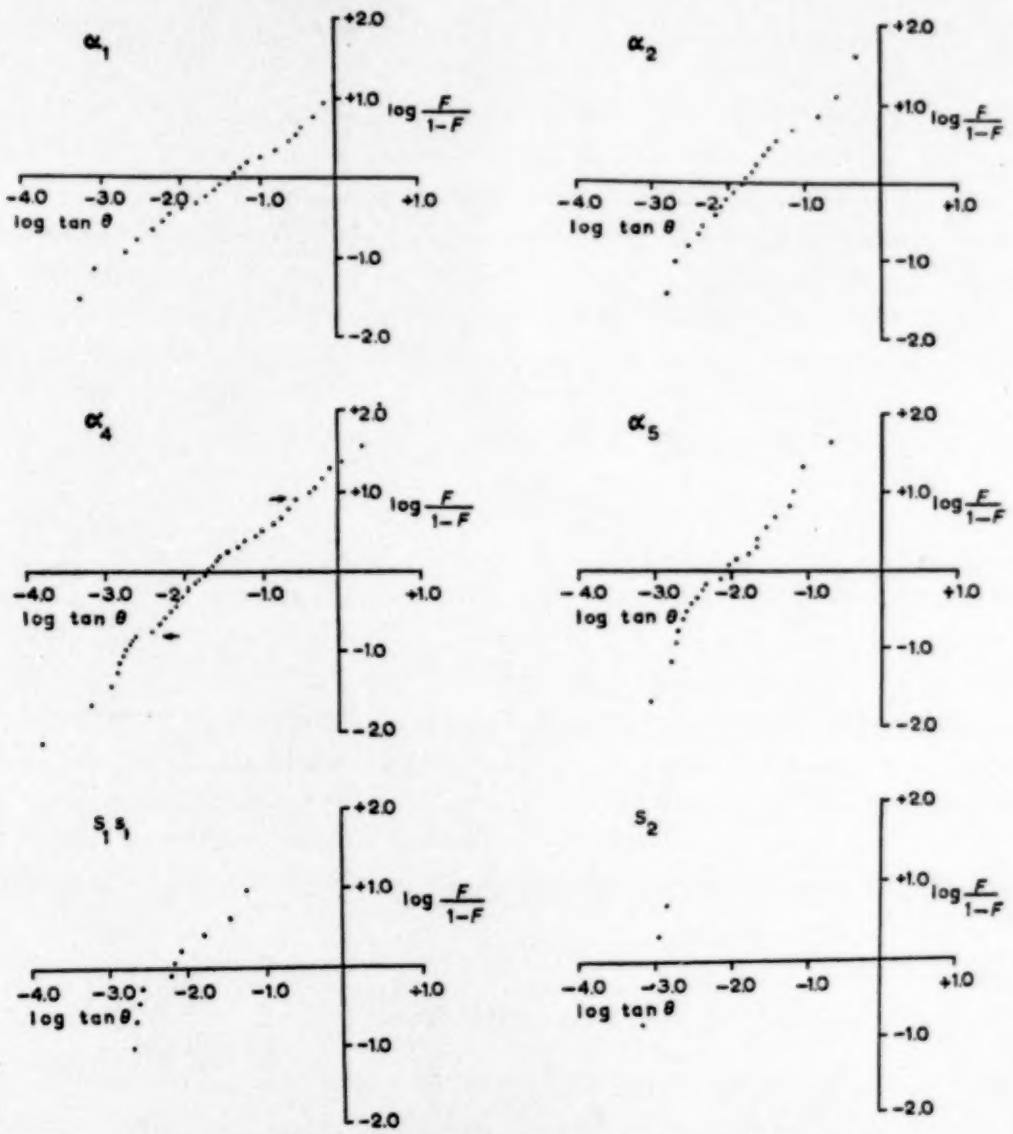

Fig. 6. The Walker-Duller plots for jets S1s1, S2, α1, α2, α4 and α5.

6. Conclusions

We give here a summary of the results obtained in the present paper.

The transverse momentum of the charged shower tracks from the jets has two peaks — one centred about 0.37 GeV/c corresponding to π mesons and one centred about 2.4 GeV/c corresponding to non-pions. It is to be noted that

those secondary interactions produced by neutral shower particles, which are certainly of a secondary rather than a tertiary nature, fall into the latter group. A few particles of much higher transverse momentum have been seen.

The transverse momentum does not appear to increase appreciably with angle of emission in the laboratory system within the angular range under observation.

The interaction cross section for π mesons is considerably less than the geometric value. The ratio of the average n_s in primary and secondary jets suggests that the interaction cross section for protons is a good deal bigger although it cannot be excluded that part of the difference is due to the inherent difference of pion-nucleon and nucleon-nucleon collisions.

In the case of nucleon-nucleus collisions it has again been found that taking γ_p (or Castagnoli's γ_c) leads to an underestimate of the primary energy.

For all zones except that closest to the shower axis, particle density decreases markedly, with angle. Part at least of the fall off from a power law seen in the central zone is due to the Lorentz transformation. A closer study of this effect is expected to throw light on the differential cross section of meson production in the forward cone in the centre-of-mass system.

The authors wish to thank the U.S.A.F. for carrying out the balloon exposure of our stack, the I.C.E.F. for the facilities for its processing and Dr. A. J. Herz for his supervision of the flight and developing of the stack. We also wish to acknowledge the help given by Mr. F. Irons in arranging the computer programs used in the course of analysis, to Mr. A. Gray for the measurements of emulsion distortion needed to improve the accuracy in the determination of the angles of emission of the electron pairs and the primaries of secondary interactions and to Miss Rosemary Roberts for her supervision of the scanning. Finally the authors wish to thank Professor H. Messel for providing the excellent facilities of the Department.

Appendix 1.

Differentiation between Secondary and Tertiary Events

1) The spatial coordinates of each parent electron pair were carefully measured with respect to the reference track in a number of plates. These were then extrapolated back towards the parent jet origin. In this way the true origin of each parent electron pair could be determined as being either that of the parent jet itself or that of some secondary interaction.

2) In the case of secondary or tertiary interactions produced by charged particles the coordinates of the primary shower track were extrapolated back in a similar manner. In some cases where the spatial separation between the primary shower tracks and the reference track was not large compared with

experimental errors. In such cases the primary shower tracks were followed all the way back to origin.

Appendix 2

Determination of Shower Axis of Parent Jets

In the case of jets produced by singly charged particles the energies of the charged and neutral shower particles were determined where possible. The shower axis was then altered from the reference track to a position such that the energies of the secondary events fell off with angular distance in all directions.

In the case of jets produced by α-particles the above method could be checked in the following way. Amongst the secondary interactions observed, several (always less than four) appeared to have energies distinctly above the rest. These occurred within very narrow angles to each other ($< 6\times10^{-4}$ rad). The most likely interpretation is that these interactions are due to the fragmentation products of the original primary α particle. Three such interactions in the cases of both jets α_1 and α_4 indicated the position of the shower axis to within an accuracy of 2×10^{-4} rad. In these cases the two methods of determining the shower axis were in agreement.

Appendix 3

The Background Correction

In the cases where a number of π^0 mesons are emitted from the same jet the resulting electromagnetic cascades tend to intermix one with another. One cascade thus produces a "background" effect upon another. A nominal energy was first assigned to each γ-ray cascade from the numbers of electrons observed within given radii from the cascade's core. Several regions free from parent electrons were then examined to determine the background effect of each cascade as a function of distance from each of these cores. By varying the position from which the "background asmple" was taken the effects of each cascade could be determined. The energies of all the γ rays were then recalculated taking background into account. The background effects due to cascades which were not adjacent to regions free from parent electrons were assumed to be similar to those of cascades of the same nominal energy and longitudinal distance. Further regions, which were themselves free of parent electron pairs, but which were surrounded on all sides by γ ray cascades were then selected. The background correction for the neighboring γ rays was then applied to observe whether the central region would then be depleted of electron tracks. If so the background correction was assumed to be satisfactory. In eliminating the background, shower tracks and effects from secondary interactions were naturally taken into account.

Appendix 4

Elimination of Electrons from the Angular Distribution of Shower Tracks

In order to distinguish the separate tracks in high energy jets, the angular distribution has to be measured at a distance of about 1 cm from the jet origin. In this length some electron pairs are usually expected to materialise. Often their origins are not distinguishable amongst the dense core of the shower tracks. For this reason each track of the central core is followed out for about 4 cm and electron tracks identified by their bremsstrahlung. Electron pairs occurring at wider angles in the angular distribution can be readily observed by following back all the tracks in this angular region. This can be done to within quite a small distance of the jet origin so that the probability of a track being due to an electron is correspondingly small.

References

1) F. A. Brisbout, C. Dahanayake, A. Engler, Y. Fujimoto and D. H. Perkins, Phil. Mag. **1** (1956) 603
2) C. Castagnoli, G. Cortini, C. Franzinetti, A. Manfredini and D. Moreno, Nuovo Cim. **10** (1953) 1539
3) N. M. Duller and W. D. Walker, Phys. Rev. **93** (1954) 215
4) F. C. Roesler and C. B. A. McCusker, Nuovo Cim. **10** (1953) 127
5) K. Pinkau, Phil. Mag. **2** (1957) 1389
6) F. A. Brisbout and C. B. A. McCusker, Nuovo Cim. **11** (1959) 484
7) C. B. A. McCusker and F. C. Roesler, Nuovo Cim. **5** (1957) 1136
8) B. Edwards, J. Losty, D. H. Perkins, K. Pinkau and J. Reynolds, Phil. Mag. **3** (1958) 237
9) R. R. Daniel, J. H. Davies, J. H. Mulvey and D. H. Perkins, Phil. Mag. **43** (1952) 753
10) O. Minakawa, Y. Nishimura, M. Tsuzuki, H. Yamanouchi, H. Aizu, H. Hasegawa, Y. Ishii, S. Tokunaga, Y. Fujimoto, S. Hasegawa, J. Nishimura, K. Niu, K. Nishikawa, K. Imaeda and M. Kazuno, Suppl. Nuovo Cim. **11** (1959) 112
11) T. E. Cranshaw and W. Galbraith, Proc. Oxford Conf. (1956) A.E.R.E. report
12) W. B. Fretter and L. F. Hausen, Proc. Moscow Conf. vol. I (1960) p. 136
13) C. B. A. McCusker and F. C. Roesler, Phys. Rev. **91** (1953) 769

3.B:4.E *Nuclear Physics* **26** (1961) 649—657; © *North-Holland Publishing Co., Amsterdam*
Not to be reproduced by photoprint or microfilm without written permission from the publisher

THE DECAY OF Se^{75}

W. F. EDWARDS † and C. J. GALLAGHER, Jr. ††
California Institute of Technology, Pasadena, California †††

Received 24 March 1961

Abstract: Using the DuMond bent-crystal gamma-ray spectrometer, the DuMond iron-free ring-focusing beta-ray spectrometer and an iron free low-field semi-circular spectrometer, the energies and relative intensities of the gamma radiations and of the conversion electrons following the decay of Se^{75} into As^{75} have been measured. The conversion coefficients and transition multipolarities deduced from this information are given and discussed. Comparisons are made with measurements by other investigators. Inconsistencies between reported values of the mixing parameter of the 279.57 keV M1 + E2 transition are reconciled and the best value determined is 0.50 ± 0.06.

1. Introduction

Within the last few years the Se^{75} decay scheme, which was previously in considerable doubt, has been well established. Metzger [1]), in a study of the resonance fluorescence of several of the transitions, pointed out some inconsistencies in the decay scheme proposed by Schardt [2]). In addition to our preliminary report [3]), the published work of numerous groups has served to confirm the decay scheme proposed by Schardt, and the inconsistencies in the gamma-ray multipolarities reported by Schardt and Welker [4]) have generally been cleared up. Gamma-ray energies, gamma-ray intensities, conversion electron intensities and conversion coefficients reported by many investigators are discussed in this paper; included are the results of Metzger and Todd [5]), Grigorev *et al.* [6]), Bashilov and Il'in [7]) and De Croës and Bäckström [8]). The last mentioned also report precise transition energies. Pertinent data from angular correlation measurements have been reported by Schardt and Welker [4]), Kelly and Wiedenbeck [9]) and Van den Bold *et al.* [10]).

2. Instruments and Sources

Radioactive sources for the gamma-ray spectrometer were made by neutron irradiation of SeO_2 with the selenium enriched in the isotope Se^{74} (isotopic abundance 12.3 %) at the Materials Testing Reactor, Arco, Idaho. The DuMond

† Present address: Utah State University, Logan, Utah.
†† Present address: Institute of Theoretical Physics, Copenhagen, Denmark.
††† Work supported by the United States Atomic Energy Commission.

bent-crystal gamma-ray spectrometer was used to measure gamma-ray energies and intensities. The source for the gamma-ray spectrometer consisted of approximately 3 mg of the SeO_2 enclosed in a quartz capillary of internal diameter 0.02 cm. With the present source conditions the energy resolution of the gamma-ray spectrometer was $\Delta E/E = 2.3\times10^{-5}E$, where E is the gamma-ray energy in keV and ΔE is the full width of the line profile at half-maximum. For strong lines the errors in the gamma-ray energy measurements were assigned either as $\frac{1}{20}$ of the full width of the line at half maximum or 10 eV, whichever was greater. For weak lines the assigned error was sometimes as great as $\frac{1}{5}$ the line width.

The gamma-ray spectrometer was recently calibrated to permit precise relative intensity measurements [11]). The intensities were taken to be proportional to the total number of counts in the photo peak of the NaI(Tl) detector with the crystal spectrometer set at an energy corresponding to the centre of the diffracted line. The relative intensities were then corrected for absorption due to the presence of quartz, air, and aluminium in the gamma-ray beam, for the detector efficiency and for the energy dependent reflectivity of the curved crystal, which has been shown [11]) to have $E^{-1.987\pm0.022}$ dependence. The statistical error was 1 % or less for most lines and was never greater than 6 %.

The conversion electrons were measured with the DuMond iron-free ring-focusing spectrometer operating at 0.7 % optimum-match momentum resolution and an iron-free semicircular low-field spectrometer at 1 % resolution. The sources for the beta spectrometer were prepared from activities produced by irradiating Se metal and had specific activities of $\approx 10\mu$Cur/μg. Sources of thickness between 5 and 30μg/cm^2 were prepared by vacuum evaporation of this material into aluminized mica backings. The Geiger-Müller counter in the ring-focusing spectrometer had a 0.96 mg/cm^2 mica window, which caused considerable absorption at electron energies below approximately 80 keV. As a consequence, the intensities of conversion electrons whose energies were below 120 keV were also measured with the semicircular spectrometer in which the G. M. counter had only a 30 μg/cm^2 formvar window, which did not absorb electrons above approximately 10 keV.

3. Results

The gamma-ray energies are reported in table 1. They were obtained by converting the measured wavelength in x-units to keV by using the factor $E(\text{keV}) = 12372.44/\lambda$ x units as reported by DuMond and Cohen [12]). Some disagreement exists between our transition energies and those reported by de Croës and Bäckström [8]), whose values are generally approximately 0.08 % lower. A systematic error is indicated. Transition energies establish levels as

TABLE 1

Data for transitions in As^{75}

Gamma-ray energy (keV)	Gamma-ray relative intensity	Internal conversion coefficients				Multipolarity assignment	Decay fraction [c] (%)
		α_K [a]	K/(L+M)	α_{total}	$\frac{\alpha_K \text{ measured}}{\alpha_K \text{ theoretical}}$ [b]		
24.3	<0.3		[d]			(M2)	
66.05±0.01	1.63±0.06	0.36 ±0.05	[e]	0.42		M1+E2	1.4±0.1
96.74±0.01	5.57±0.18	0.81 ±0.07	6.5	0.95	1.10±0.10	E2	6.5±0.3
121.12±0.01	28.0 ±0.6	(0.0406) [a]	10.5	0.0445	(1.10) [a]	E1	17.4±0.4
135.99±0.02	95.5 ±1.8	(0.0240) [a]	7.6	0.0272	(0.91) [a]	E1	58.5±1.1
198.60±0.06	2.4 ±0.1	0.018 ±0.002		0.018		M1+E2	1.5±0.1
264.62±0.07	100	0.0060±0.0005	9.5	0.0067	0.97±0.08	M1	60.1
279.57±0.08	42.2 ±0.6	0.0076±0.0009	7.9	0.0086		M1+E2	25.4±0.4
304.0 ±0.3	2.29±0.14	0.045 ±0.006	6.1	0.052	0.99±0.13	E3	1.4±0.1
400.7 ±0.2	19.5 ±0.6	0.0011±0.0001	8.8	0.0012	0.94±0.09	E1	11.6±0.4

[a]) The conversion coefficients were normalized to the best fit of the coefficients of the 121.12 keV and 135.99 keV transitions with theoretical E1 values.

[b]) The theoretical coefficients are those given by Rose [13]) based upon the multipolarity assignments in column 7.

[c]) The decay fraction is proportional to $(1 + \alpha_{total})$ and is normalized to 100 % feeding of the ground state neglecting any beta branching to that level.

[d]) K : L : M = 3.7 : 1 : 0.24.

[e]) K : L : M = 8.3 : 1 : 0.2.

shown in fig. 1 at the following energies (in keV); 198.60±0.04, 264.66±0.04, 279.53±0.04, 303.91±0.04 and 400.65±0.04.

Gamma-ray intensities are reported in table 1. Conversion electron intensities are reported as normalized conversion coefficients. The conversion coefficients, also given in table 1, were normalized to the best fit of the 121.12 keV and 135.99 keV K conversion coefficients to the theoretical E1 values. The multipolarity assignments, based on the conversion coefficients and the theoretical values of Rose [13]), are as indicated.

The 24.3 keV gamma ray was not detected. Using a thin window NaI(Tl) scintillation spectrometer the upper limit of its gamma-ray intensity was estimated to be $\frac{1}{5}$ the intensity of the 66.05 keV gamma ray. A 24.3 keV M2 transition has a theoretical K-conversion coefficient of 160. From this and the known ratio of K-conversion electrons, the expected intensity was found to be 0.02 relative to a value of 100 for the 264.62 keV transition, and it is therefore not surprising that the gamma ray was not observed. The K : L : M ratios are as theoretically expected assuming an M2 assignment.

TABLE 2

Log *ft* values for electron capture transitions from Se^{75} to As^{75}

Energy of level	Electron capture branching (%)	Transition	log *ft*
0	<0.01 [a])	$\frac{5}{2}+ \rightarrow \frac{3}{2}-$	>9.6
198.61	<0.5	$\frac{5}{2}+ \rightarrow \frac{1}{2}-$	>9.4
264.62	2.9±1.1	$\frac{5}{2}+ \rightarrow \frac{3}{2}-$	7.8
279.57	≲ 1±1	$\frac{5}{2}+ \rightarrow \frac{5}{2}-$	≳8.3
304.0	≲ 1±1	$\frac{5}{2}+ \rightarrow \frac{3}{2}+$	≳8.2
400.7	94±1.3	$\frac{5}{2}+ \rightarrow \frac{5}{2}+$	6.0
575 [b])	0.04 [b])	$\frac{5}{2}+ \rightarrow \frac{7}{2}-$	9.0 [b])

[a]) The percentage branchings were calculated assuming no branching to the ground state.
[b]) Reported by H. Langevin-Joliot and M. Langevin (ref. [14]) and included for completeness.

The decay fractions of the transitions indicate weak beta branching to some of the excited levels. With the decay fractions normalized to 100 %, and assuming no primary beta branching to the ground-state, the feeding of the 264.62 keV level appears to be (2.9±1.1)%. There is also some feeding, of the order of 1 or 2 %, to either the 279.53 keV level or the 303.91 keV level or both. With the present spin assignments a 1st forbidden beta transition to the 279.53 level is expected, whereas the transition expected to the 303.91 keV level is 2nd forbidden. Log *ft* values have been calculated using these branching ratios or limits on branching ratios and the previously reported electron capture decay energy [14, 15]) with the aid of Moszkowski's nomograph [16]). The results are shown in table 2. The sign of the Gamow-Teller to Fermi matrix element ratio

for the transition to the 400.65 keV state has been measured by Boehm and Gallagher and found to be negative [17]).

4. Comparison with Previous Results

The decay scheme of Se^{75} originally proposed by Schardt and Welker (see fig. 1) is now well established with the original discrepancies removed.

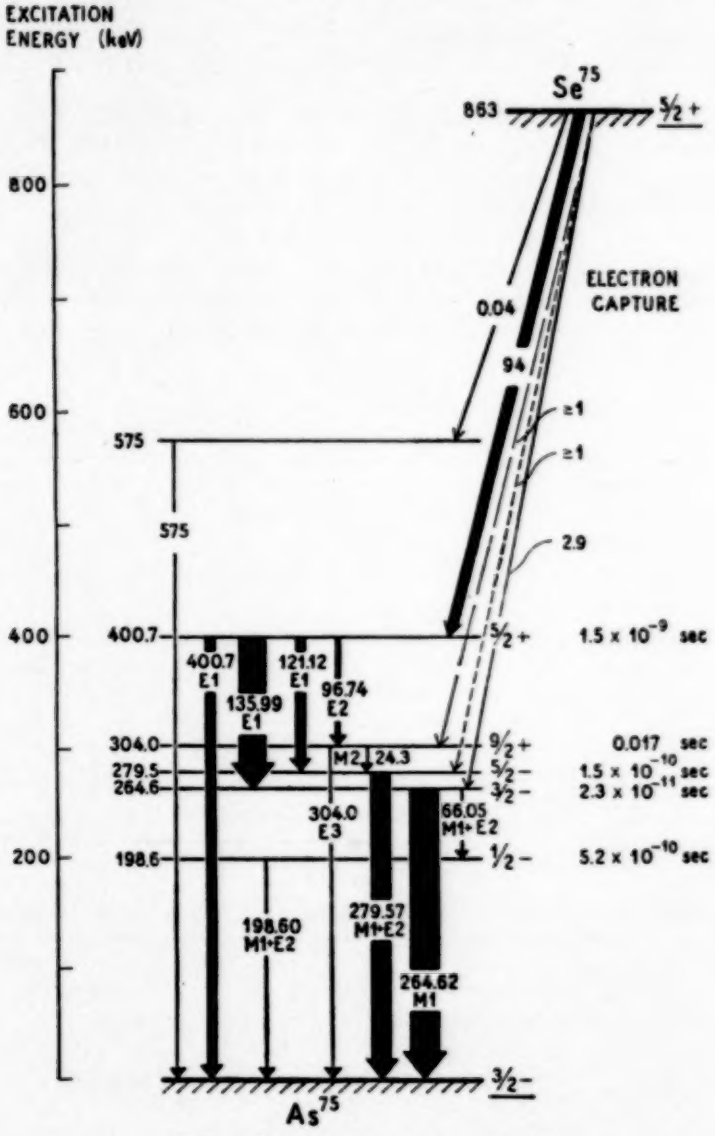

Fig. 1. The decay scheme of Se^{75}.

In the course of the many independent studies of this decay scheme several other apparent discrepancies have appeared, however, and we attempt to resolve these in the following discussion.

TABLE 3

Half-lives of levels in As^{75}

Energy of level (keV)	Reported $t_{\frac{1}{2}}$ (sec)	Ref.
198.60	5.2×10^{-10} a)	19)
264.62	2.3×10^{-11}	18)
	1.65×10^{-11}	1)
	2.5×10^{-11}	1)
279.57	1.5×10^{-10} b)	19)
304.0	0.017	2)
400.7	1.5×10^{-9}	18)

a) Calculated from the average value $B(E2) = 0.022$ reported by Alder *et al.* (ref. [19]), where we have used the values $(1+\alpha_{total})_{199} = 1.018$ and $|\delta|_{199} = 0.38$ calculated from the conversion coefficient of the 199 keV transition reported in the present paper.

b) Calculated from the average value $B(E2) = 0.060$ reported in ref. [19]), where we have used the values $(1+\alpha_{total})_{280} = 1.0086$, $|\delta|_{280} = 0.50$ and the 95 % branching from the 280 keV level through the 280 keV transition reported in the present paper. In using the total $B(E2)$ for the calculation of the half-life of the 280 keV level we have assumed no Coulomb excitation of the 264.62-keV level.

TABLE 4

Relative gamma-ray intensities following Se^{75} decay

Transition energy (keV)	Schardt and Welker	Grigorev *et al.*	Metzger and Todd	de Croës and Bäckström	Our results
66.05	1.8± 1	1.53±0.15			1.6 ±0.6
96.74	6.6± 1.5	5.5 ±0.3			5.6 ±0.2
121.12	28 $\pm^{6}_{3}$	27.9 ±1.3		28 ± 5	28.0 ±0.6
135.99	94 ±12	96 ±5		86 ±15	95.5 ±1.8
198.60	3	2.6 ±0.2			2.4 ±0.1
264.62	100	100	100	100	100
279.57	45.7± 4	41 ±2.5	47 ±1	42.5 ±2	42.2 ±0.6
304.0	2.0±0.5	2.5 ±0.3	2.1±0.3	2.15±0.3	2.29±0.14
400.7	24.8± 2.5	22.3 ±2.3	19 ±2	23 ±2	19.5 ±0.6

TABLE 5

Relative K conversion electron intensities following Se^{75} Decay

Transition energy (keV)	Schardt and Welker	Grigorev *et al.*	Metzger and Todd	de Croës and Bäckström	Our Result
66.05		73.7 ± 4.4		80 ±12	99 ±12
96.74	715	645 ±25		940 ±60	753 ±60
121.12	173	154 ±2.3		180 ±12	187 ±15
135.99	420	384 ±5	377 ±20	450 ±30	378 ±30
198.60	6.4±0.7	7.3 ±0.3		6.8±1	7 ± 1
264.62	100 ±8	100 ± 3	100	100	100
279.57	53 ±7	49.2 ± 3	53.6± 1.6	63 ± 5	53 ± 5
304.0	15.6±1.3	16.1 ± 0.8	15.4± 0.9	16.0± 1	17.2± 1.7
400.7	3.6±0.6	3.76±0.26	3.6± 0.4	3.8± 0.3	3.7± 0.4

Although no half-life determinations have been made in the present study, the half-lives of all the strongly populated states in As^{75} have now been either directly measured [1, 2, 18]), or the levels have been Coulomb excited [19]); for the sake of completeness half-lives of the levels are shown in fig. 1. and listed in table 3. The total electron capture energy obtained from the data reported by Trail and Johnson [14]) and Gossett and Butler [15]) is also given in fig. 1. We have observed the 577 keV gamma-ray reported by Langevin-Joliot and Langevin [18]) but only in the NaI spectrum.

The gamma-ray intensities and conversion electron intensities reported by the various groups are compared in tables 4 and 5. The conversion electron intensities reported by the various investigators do not vary beyond the experimental errors, with the exception of the values reported for the 96.74 keV transition and the value reported by Grigorev *et al.* for the 121.12 keV transition. The relative gamma-ray intensity measurements are generally in very good agreement; the only exception to this is the measurement of the intensity of the 279.57 keV line by Metzger and Todd, their value of 47 ± 1 differing considerably from the present value of 42.2 ± 0.06 as well as from the values 41 ± 2.5 and 42.5 ± 2 measured by Grigorev *et al.* and de Croës and Bäckström respectively. Because this line is very close in energy to the 264.62 keV line, relative to which its intensity was measured, absorption corrections and the curved crystal reflectivity correction were very small; therefore the magnitude of our reported error is almost entirely due to counting statistics. Furthermore, the intensity of this line was remeasured four times. The highest value measured was 42.7 and the mean 42.2. For these reasons we feel that the value of Metzger and Todd is high.

A point still open to discussion is the M1+E2 mixing ratio of the 279.57 keV transition. Metzger and Todd [5]) and later Manning and Rogers [20]) have

TABLE 6

Conversion coefficient data for the 279.57 keV transition in As^{75}

Investigators	Gamma-ray intensity	K conversion electron intensity	K conversion coefficient ($\times 10^3$)	Mixing parameter $\lvert\delta\rvert$
Schardt and Welker	45.7 ± 4	$53\ \pm8$		
Grigorev *et al.*	$41\ \pm2.5$	49.2 ± 3	7.6 ± 0.8	$0.51^{+0.12}_{-0.13}$
Bashilov and Il'in			7.6 ± 1.0	$0.51^{+0.15}_{-0.16}$
Metzger and Todd	$47\ \pm1$	53.6 ± 1.6	7.0 ± 0.4	$0.42^{+0.06}_{-0.07}$ [a])
de Croës and Bäckström	42.5 ± 2	$63\ \pm5$	9.9 ± 1	$0.88^{+0.19}_{-0.17}$
Present investigators	42.2 ± 0.6	$53\ \pm5$	7.6 ± 0.9	$0.51^{+0.14}_{-0.15}$

[a]) This value differs from that reported in the original paper [21]).

commented upon the disagreement between the mixing parameters δ_1 as determined by conversion coefficient information and those determined by angular correlation. Table 6 gives the mixing parameters calculated from conversion coefficients assuming the theoretical coefficients of Rose [13]). The agreement is rather good in spite of the apparently high gamma-ray intensity of Metzger and Todd which lowers their value for the mixing parameter. The agreement is better than reported previously [5, 20]) because a calculation error in Metzger and Todd's value for the mixing parameter has been corrected [21]).

The angular correlation data for this transition are summarized in table 7.

TABLE 7

Angular correlation data for the 279.57 keV transition in As^{75}

Investigators	a_2	δ
Schardt and Welker	-0.42 ± 0.03	-0.44 ± 0.11
Kelly and Wiedenbeck	-0.41 ± 0.03	-0.41 ± 0.08
van den Bold *et al.*	-0.466 ± 0.02	$-0.74^{+0.26}_{-0.21}$ [a])

[a]) This value differs from that reported in the original paper, the error limits having been incorrectly assigned [22]).

The agreement among the various values for the mixing parameter is now reasonable, primarily because the error limits on the value -0.74 ± 0.10 previously reported by van den Bold *et al.* were in error and have now been corrected in such a way as to improve the agreement [22]).

The mean of the eight values for the mixing parameter is 0.47. The deviation of the individual values from the mean is certainly reasonable as reflected by the χ^2-test. The expected value of χ^2 which is equal to the number of degrees of freedom or amount of over-determination of the system, is 7. The calculated value is 8.0. The probability that χ^2 be equal to 8.0 or more by random deviation alone is 0.33, indicating consistency of the data. If Metzger and Todd's value is eliminated from the set, the mean is 0.50 and χ^2 is 7.2 (the expected value in this case is 6); the probability of the value 7.2 or greater by random deviation is 0.30. We conclude that the determinations of the mixing ratios of the 279.57 keV transition are in satisfactory agreement and that the best value for the mixing parameter is 0.50 ± 0.06 which indicates an 80 % M1+20 % E2 mixture for this transition.

We are grateful to Professor J. W. M. DuMond and Professor F. Boehm for their interest and to Dr. G. Manning for helpful discussions.

References

1) F. R. Metzger, Phys. Rev. **110** (1958) 123
2) A. W. Schardt, Phys. Rev. **108** (1957) 398
3) W. F. Edwards, C. J. Gallagher, Jr. and J. W. M. DuMond, Bull. Am. Phys. Soc. **4** (1959) 279
4) A. W. Schardt and J. P. Welker, Phys. Rev. **99** (1955) 810
5) F. R. Metzger and W. B. Todd, Nuclear Physics **10** (1959) 220
6) Grigorev, Zolotavin, Klementev and Sinitzyn, Izvestia Akad. Nauk SSSR **23** (1959) 159
7) A. A. Bashilov and V. V. Il'in, Izvestia Akad. Nauk SSSR **23** (1959) 159
8) M. DeCroës and G. Bäckström, Ark. för Fys. **16** (1960) 567
9) W. H. Kelly and M. L. Wiedenbeck, Phys. Rev. **102** (1956) 1130
10) H. C. Van den Bold, J. Van de Geijn and P. M. Endt, Physica **24** (1958) 24
11) W. Edwards, Ph. D. Thesis, California Institute of Technology, 1960 (unpublished)
12) Cohen, DuMond, Layton and Rollett, Rev. Mod. Phys. **27** (1955) 363
13) M. E. Rose, Internal conversion coefficients (North-Holland Publishing Co., Amsterdam, 1958)
14) C. C. Trail and C. H. Johnson, Phys. Rev. **91** (1953) 474
15) C. R. Gossett and J. W. Butler, Phys. Rev. **113** (1959) 246
16) S. A. Moszkowski, Phys. Rev. **82** (1951) 25
17) F. Boehm and C. J. Gallagher, Jr., Phys. Rev. **119** (1960) 258
18) H. Langevin - Joliot and M. Langevin, J., Phys. Rad. **19** (1958) 765
19) Alder, Bohr, Huus, Mottelson and Winther, Revs. Mod. Phys. **28** (1956) 432
20) G. Manning and J. Rogers, Nuclear Physics **15** (1960) 166
21) F. R. Metzger, private communication
22) H. C. van den Bold, private communication

7.C

Nuclear Physics **26** (1961) 658—669; © *North-Holland Publishing Co., Amsterdam*

Not to be reproduced by photoprint or microfilm without written permission from the publisher

THE STRUCTURE OF THE NUCLEON CORE BY THE HARTREE APPROXIMATION

YASUSHI TAKAHASHI

Dublin Institute for Advanced Studies, Dublin, Ireland

Received 6 March 1961

Abstract: A method is proposed to investigate the structure of the nucleon core. A set of equations is derived to define the nucleon core and the meson cloud simultaneously. The equations are formulated by a variational method which enables us to find an approximate solution. The size of the nucleon core is estimated for a non-relativistic nucleon interacting with a neutral scalar meson. The coupling constant between nucleon and meson is given by the ratio of the sizes of the core and the cloud. It is shown that for $f^2/4\pi \approx 1$, the core size may be about half that of the meson cloud, where the number of mesons around the nucleon is about one. The generalization to a more realistic case is also suggested. The renormalization is not considered in this paper.

1. Introduction

It has become almost certain that the interaction of elementary particles may be classified into three groups, namely, strong, electromagnetic and weak interactions. Reliable conclusions can be drawn for processes through weak and electromagnetic interactions, since the perturbation approach may be justified in these cases, as is seen in the weak V-A theory and the quantum electrodynamics based on the renormalization technique. It is noticed, however, that even these processes are disturbed by strong interactions in some cases and the quantitative understanding is not always satisfactory. For example, although they are likely to be an effect of strong interactions, the electromagnetic structure of the nucleon and the G_A/G_V ratio in the V-A interaction have not been explained satisfactorily, due to the lack of an appropriate approximation method for the strong interactions [1, 2]).

In this connection, it is quite interesting to recall that Yennie *et al.* suggested a large nucleon core to interpret the electromagnetic structure of the nucleon and Takeda also analysed difficulties in present meson theory from the viewpoint that the bare mass of the nucleon is as small as that of the muon †). The main objection to this speculation consists in the fact that it seems unlikely that present meson theory can lead to such a large core. A possible explanation has been put forward by Tamm, who stresses the importance of the nucleon-antinucleon pair creation in the meson cloud [3]).

† Private communication.

In this paper, we would like to examine the problem of strong interactions from the viewpoint of an approximation method by taking a simple model, i.e. a system consisting of a non-relativistic nucleon and the neutral meson field via scalar interaction. This model has been examined in the fixed source approximation, in which the nucleon is held fixed at the origin and is replaced by a c-number source function, and further the recoil of the nucleon is entirely neglected [4]). However, such an approximation is apparently unjustified in high energy processes. We treat this system by the Hartree approximation without introducing any ad hoc c-number function. This way of treating the interaction proves useful for invariance considerations.

Sect. 2 is devoted to a formulation by which the nucleon-meson system can be treated "consistently". We derive a set of differential equations which defines the structure of the nucleon and the meson cloud simultaneously. The equations are non-linear and cannot be solved exactly except in trivial cases. We therefore reformulate the matter in terms of a variational principle, which enables us to apply the approximation method of Ritz.

In sect. 3, we evaluate the nucleon wave function by the method of Ritz. It will be shown that the size of the nucleon is not much smaller than that of the meson cloud for the coupling constant $f^2/4\pi \approx 1$. The number of mesons in the cloud is also calculated.

We discuss in sect. 4 the possibility of generalizing our method to more realistic cases, where we again obtain a set of equations the same as those discussed in sect. 2.

2. Formulation

For the sake of simplicity, we take a one-body non-relativistic nucleon interacting with the neutral meson field through scalar coupling. Such a system is described by the Schrödinger equation

$$i\frac{\partial}{\partial t}\Psi(\mathbf{x},t) = H\Psi(\mathbf{x},t), \tag{2.1}$$

where

$$H = \frac{1}{2M}\mathbf{p}^2 + f\phi(\mathbf{x}) + H_\pi, \tag{2.2}$$

$$H_\pi = \tfrac{1}{2}\int \mathrm{d}^3x\{\pi(\mathbf{x})\pi(\mathbf{x}) + \nabla\phi(\mathbf{x})\cdot\nabla\phi(\mathbf{x}) + \mu^2\phi(\mathbf{x})\phi(\mathbf{x})\}. \tag{2.3}$$

The notation is conventional.

We first review the ordinary cut-off theory. In the cut-off theory the Hamiltonian (2.2) is replaced by

$$H_{(\text{fixed})} = f\int \mathrm{d}^3x U(\mathbf{x})\phi(\mathbf{x}) + H_\pi. \tag{2.4}$$

where $U(\mathbf{x})$ is a c-number source function satisfying

$$\int d^3x U(\mathbf{x}) = 1. \tag{2.5}$$

The stationary states are determined by the eigenvalue equation

$$H_{(\text{fixed})}\Phi = E_{(\text{fixed})}\Phi. \tag{2.6}$$

The canonical transformation

$$\phi(\mathbf{x}) = \phi'(\mathbf{x})+V(\mathbf{x}), \qquad \pi(\mathbf{x}) = \pi'(\mathbf{x}), \tag{.7}$$

with a c-number function $V(\mathbf{x})$ defined by

$$(\Delta-\mu^2)V(\mathbf{x}) = fU(\mathbf{x}), \tag{2.8}$$

is introduced to diagonalize the Hamiltonian as

$$H_{(\text{fixed})} = H'_{\pi}+\tfrac{1}{2}f\int \mathrm{d}^3x V(\mathbf{x})U(\mathbf{x}), \tag{2.9}$$

where

$$H'_{\pi} = \tfrac{1}{2}\int \mathrm{d}^3x\{\pi'(\mathbf{x})\pi'(\mathbf{x})+\nabla\phi'(\mathbf{x})\cdot\nabla\phi'(\mathbf{x})+\mu^2\phi'(\mathbf{x})\phi'(\mathbf{x})\}. \tag{2.10}$$

The lowest eigenvalue is obviously

$$E_{(\text{fixed})} = -\frac{f^2}{8\pi}\int \mathrm{d}^3x\int \mathrm{d}^3y U(\mathbf{x})\,U(\mathbf{y})\,\frac{\mathrm{e}^{-\mu|\mathbf{x}-\mathbf{y}|}}{|\mathbf{x}-\mathbf{y}|}, \tag{2.11}$$

apart from the zero-point energy.

In order to take the nucleon recoil into account, we introduce a unitary S such that

$$\phi'(\mathbf{x}) = S\phi(\mathbf{x})S^{-1}, \qquad \pi'(\mathbf{x}) = S\pi(\mathbf{x})S^{-1}, \tag{2.12}$$

$$S = \exp[-iF], \qquad F = \int \mathrm{d}^3x V(\mathbf{x})\pi(\mathbf{x}). \tag{2.13}$$

The total energy is

$$\begin{aligned} H &= \frac{1}{2M}\mathbf{p}^2+H_{(\text{fixed})}\cdot \\ &= \frac{1}{2M}\mathbf{p}^2+SH_{\pi}S^{-1}+\tfrac{1}{2}f\int \mathrm{d}^3x V(\mathbf{x})U(\mathbf{x}) \\ &= S\left\{\frac{1}{2M}\mathbf{p}^2+H_{\pi}+\tfrac{1}{2}f\int \mathrm{d}^3x V(\mathbf{x})U(\mathbf{x})+S^{-1}\left[\frac{1}{2M}\mathbf{p}^2, S\right]\right\}S^{-1}. \end{aligned} \tag{2.14}$$

The last term of (2.14) is the nucleon recoil which is usually treated as a perturbation [5]). Incidentally, the eigenstate Φ_0 belonging to (2.11) satisfies

$$(\Phi_0, \phi'(\mathbf{x})\Phi_0) = 0, \qquad (\Phi_0, \pi'(\mathbf{x})\Phi_0) = 0. \tag{2.15}$$

The higher energy states are

$$\Phi(\mathbf{k}_1, \mathbf{k}_2, \ldots, \mathbf{k}_n) = \frac{1}{\sqrt{n!}} \prod_{m=1}^{n} a^+(\mathbf{k}_m)\Phi_0, \tag{2.16}$$

where

$$a^+(\mathbf{k}) = \frac{-i}{(2\pi)^{\frac{3}{2}}} \int \mathrm{d}^3x[\pi'(\mathbf{x}) - i\omega(\mathbf{k})\phi'(\mathbf{x})]\mathrm{e}^{i\mathbf{k}\mathbf{x}} \frac{1}{\sqrt{2\omega(\mathbf{k})}}, \tag{2.17}$$

$$\omega(\mathbf{k}) = (\mathbf{k}^2+\mu^2)^{\frac{1}{2}}.$$

In the cut-off theory reviewed above, we introduced an ad hoc source function $U(\mathbf{x})$, which cannot be determined by the theory.

In order to overcome this unsatisfactory feature of the cut-off theory, we propose to treat the original Schrödinger eq. (2.1) by the Hartree method. The equation to be investigated is

$$H\Psi(\mathbf{x}) = E\Psi(\mathbf{x}), \tag{2.18}$$

with the Hamiltonian (2.2) instead of (2.5). We assume $\Psi(\mathbf{x})$ is a product of the nucleon wave function $\varphi(\mathbf{x})$ and the meson wave function Φ, namely

$$\Psi(\mathbf{x}) = \varphi(\mathbf{x})\Phi. \tag{2.19}$$

They are normalized so that

$$\int \mathrm{d}^3x\varphi^*(\mathbf{x})\varphi(\mathbf{x}) = 1, \qquad (\Phi, \Phi) = 1. \tag{2.20}$$

Eq. (2.18) now implies

$$[H_\pi + f\int \mathrm{d}^3x\varphi^*(\mathbf{x})\varphi(\mathbf{x})\phi(\mathbf{x})]\Phi = E_1\Phi, \tag{2.21}$$

$$\left[\frac{1}{2M}\mathbf{p}^2 + f(\Phi, \phi(\mathbf{x})\Phi)\right]\varphi(\mathbf{x}) = E_{II}\varphi(\mathbf{x}), \tag{2.22}$$

where

$$E_1 = E - \frac{1}{2M}\int \mathrm{d}^3x\varphi^*(\mathbf{x})\mathbf{p}^2\varphi(\mathbf{x}), \tag{2.23}$$

$$E_{II} = E - (\Phi, H_\pi\Phi), \tag{2.24}$$

or

$$E = E_1 + E_{II} - f\int \mathrm{d}^3x\varphi^*(\mathbf{x})\varphi(\mathbf{x})(\Phi, \phi(\mathbf{x})\Phi). \tag{2.25}$$

We shall hereafter refer to eqs. (2.21) and (2.22) as the first and the second eigenvalue equations, respectively.

We notice that the first eigenvalue eq. (2.21) is of the same form as that in the cut-off theory. The difference is that the source function $\varphi^*(\mathbf{x})\varphi(\mathbf{x})$ in our equation is to be determined by the second eigenvalue equation, whereas the source function $U(\mathbf{x})$ in the cut-off theory is introduced ad hoc.

The above consideration can be formulated by a variational method which is useful for obtaining an approximate solution of (2.21) and (2.22). For this purpose, we define a quantity

$$I=\int \mathrm{d}^3x\varphi^*(\mathbf{x})(\Phi, H\Phi)\varphi(\mathbf{x})-E'_{\mathrm{I}}\{(\Phi,\Phi)-I\}-E'_{\mathrm{II}}\left\{\int \mathrm{d}^3x\varphi^*(\mathbf{x})\varphi(\mathbf{x})-1\right\}, \tag{2.26}$$

and minimize it, i.e.

$$\frac{\delta I}{\delta\Phi^*}=0\rightarrow\left[H_\pi+f\int \mathrm{d}^3x\varphi^*(\mathbf{x})\varphi(\mathbf{x})\phi(\mathbf{x})\right]\Phi=E_{\mathrm{I}}\Phi, \tag{2.27}$$

$$\frac{\delta I}{\delta\varphi^*(\mathbf{x})}=0\rightarrow\left[\frac{1}{2M}\mathbf{p}^2+f(\Phi,\phi(\mathbf{x})\Phi)\right]\varphi(\mathbf{x})=E_{\mathrm{II}}\varphi(\mathbf{x}), \tag{2.28}$$

where E'_{I} and E'_{II} are the Lagrange multipliers, and we have

$$\begin{aligned}
E_{\mathrm{I}} &= E'_{\mathrm{I}}-\frac{1}{2M}\int \mathrm{d}^3x\varphi^*(\mathbf{x})\mathbf{p}^2\varphi(\mathbf{x}),\\
E_{\mathrm{II}} &= E'_{\mathrm{II}}-(\Phi, H_\pi\Phi),\\
E'_{\mathrm{I}} &= E'_{\mathrm{II}}=E=\frac{1}{2M}\int \mathrm{d}^3x\varphi^*(\mathbf{x})\mathbf{p}^2\varphi(\mathbf{x})+(\Phi, H_\pi\Phi)+f\int \mathrm{d}^3x\varphi^*(\mathbf{x})(\Phi,\phi(\mathbf{x})\Phi)\varphi(\mathbf{x}).
\end{aligned} \tag{2.29}$$

Eq. (2.27) can be solved in exactly the same way as (2.6) in the cut-off theory. The transformation

$$\begin{aligned}
&\phi(\mathbf{x})=\phi'(\mathbf{x})+V(\mathbf{x}), \qquad \pi(\mathbf{x})=\pi'(\mathbf{x}),\\
&(\Delta-\mu^2)V(\mathbf{x})=f\varphi^*(\mathbf{x})\varphi(\mathbf{x}),
\end{aligned} \tag{2.30}$$

brings (2.27) into the form

$$\left[H'_\pi+\tfrac{1}{2}f\int \mathrm{d}^3x\varphi^*(\mathbf{x})\varphi(\mathbf{x})V(\mathbf{x})\right]\Phi=E_{\mathrm{I}}\Phi. \tag{2.31}$$

The lowest energy is, therefore,

$$E_{\mathrm{I}}^0=\tfrac{1}{2}f\int \mathrm{d}^3x\varphi^*(\mathbf{x})\varphi(\mathbf{x})V(\mathbf{x})=-\frac{f^2}{8\pi}\int \mathrm{d}^3x\int \mathrm{d}^3y|\varphi(\mathbf{x})|^2|\varphi(\mathbf{y})|^2\frac{\mathrm{e}^{-\mu|\mathbf{x}-\mathbf{y}|}}{|\mathbf{x}-\mathbf{y}|} \tag{2.32}$$

in the state Φ_0. It also follows that

$$(\Phi_0,\phi(\mathbf{x})\Phi_0)=V(\mathbf{x}). \tag{2.33}$$

The second eigenvalue equation becomes, therefore,

$$\left[\frac{1}{2M}\mathbf{p}^2+fV(\mathbf{x})\right]\varphi(\mathbf{x})=E_{\mathrm{II}}\varphi(\mathbf{x}). \tag{2.34}$$

This is the equation which determines the nucleon state in the absence of real mesons.

For the meson state Φ_0, we have

$$\begin{aligned} I_0 &= \frac{1}{2M}\int \mathrm{d}^3x\varphi^*(\mathbf{x})\mathbf{p}^2\varphi(\mathbf{x})+\tfrac{1}{2}f\int \mathrm{d}^3x\varphi^*(\mathbf{x})\varphi(\mathbf{x})V(\mathbf{x}) \\ &\quad -E_{\mathrm{II}}\left\{\int \mathrm{d}^3x\varphi^*(\mathbf{x})\varphi(\mathbf{x})-1\right\}, \\ &= \frac{1}{2M}\int \mathrm{d}^3x\varphi^*(\mathbf{x})\mathbf{p}^2\varphi(\mathbf{x})-E_{\mathrm{II}}\left\{\int \mathrm{d}^3x\varphi^*(\mathbf{x})\varphi(\mathbf{x})-1\right\} \\ &\quad -\frac{f^2}{8\pi}\int \mathrm{d}^3x\int \mathrm{d}^3y|\varphi(\mathbf{x})|^2|\varphi(\mathbf{y})|^2\frac{\mathrm{e}^{-\mu|\mathbf{x}-\mathbf{y}|}}{|\mathbf{x}-\mathbf{y}|}. \end{aligned} \tag{2.35}$$

We can also formulate (2.25) in terms of $\varphi(\mathbf{x})$ and $V(\mathbf{x})$ by

$$\begin{aligned} I_0 &= \frac{1}{2M}\int \mathrm{d}^3x\varphi^*(\mathbf{x})\mathbf{p}^2\varphi(\mathbf{x})+f\int \mathrm{d}^3x\varphi^*(\mathbf{x})\varphi(\mathbf{x})V(\mathbf{x}) \\ &\quad +\tfrac{1}{2}\int \mathrm{d}^3x\{\nabla V(\mathbf{x})\cdot\nabla V(\mathbf{x})+\mu^2V(\mathbf{x})V(\mathbf{x})\} \\ &\quad -E_{\mathrm{II}}\left\{\int \mathrm{d}^3x\varphi^*(\mathbf{x})\varphi(\mathbf{x})-1\right\}, \end{aligned} \tag{2.36}$$

treating now $\varphi(\mathbf{x})$ and $V(\mathbf{x})$ independently.

As can easily be verified, the minimum value of I_0 is the minimum total energy, i.e. if $\varphi(\mathbf{x})$ and $V(\mathbf{x})$ satisfy (2.34) and (2.30), respectively, then

$$\begin{aligned} I_0 &= E_{\mathrm{II}}-\tfrac{1}{2}f\int \mathrm{d}^3x\varphi^*(\mathbf{x})\varphi(\mathbf{x})V(\mathbf{x}) \\ &= E_{\mathrm{II}}+E_{\mathrm{I}}{}^0-f\int \mathrm{d}^3x\varphi^*(\mathbf{x})\varphi(\mathbf{x})V(\mathbf{x}) = E^0. \end{aligned} \tag{2.37}$$

We conclude this section by the remark that our eqs. (2.21) and (2.22) are invariant under space translation, while the ordinary cut-off eq. (2.6) does not fulfil this condition owing to the introduction of an ad hoc function $U(\mathbf{x})$.

3. The Nucleon Wave Function in the Ground State

We examine the equations

$$\begin{gathered} (\Delta+\varepsilon)\varphi(\mathbf{x}) = 2MfV(\mathbf{x})\varphi(\mathbf{x}), \qquad (\Delta-\mu^2)V(\mathbf{x}) = f\varphi^*(\mathbf{x})\varphi(\mathbf{x}), \\ \int \mathrm{d}^3x\varphi^*(\mathbf{x})\varphi(\mathbf{x}) = 1, \end{gathered} \tag{3.1}$$

$$\varepsilon = 2ME_{\mathrm{II}}. \tag{3.2}$$

We observe that the plane wave solution exists, namely,

$$\varphi(\mathbf{x}) = \frac{1}{\sqrt{\Omega}}\mathrm{e}^{i\mathbf{k}\mathbf{x}}, \qquad fV(\mathbf{x}) = -\frac{f^2}{\Omega}\frac{1}{\mu^2}. \tag{3.3}$$

These equations satisfy (3.1) and we get

$$E_{II} = \frac{1}{2M}\mathbf{k}^2 - \frac{f^2}{\mu^2}\frac{1}{\Omega}, \tag{3.4}$$

$$E = \frac{1}{2M}\mathbf{k}^2 - \frac{1}{2}\frac{f^2}{\mu^2}\frac{1}{\Omega}, \tag{3.5}$$

where Ω is the normalization volume.

We next seek a solution corresponding to a nucleon at rest at the origin surrounded by the meson cloud. In this connection it is instructive to consider the one-dimensional model. The equations are

$$\left(\frac{\mathrm{d}^2}{\mathrm{d}x^2} + \varepsilon\right)\varphi(x) = 2MfV(x)\varphi(x), \qquad \left(\frac{\mathrm{d}^2}{\mathrm{d}x^2} - \mu^2\right)V(x) = f\varphi^*(x)\varphi(x),$$
$$\int_{-\infty}^{\infty}\mathrm{d}x\varphi^*(x)\varphi(x) = 1. \tag{3.6}$$

Introducing a new variable

$$\xi = \cosh \alpha x, \qquad 1 \leqq \xi \leqq \infty,$$

we obtain

$$\left\{(\xi^2-1)\frac{\mathrm{d}^2}{\mathrm{d}\xi^2} + \xi\frac{\mathrm{d}}{\mathrm{d}\xi} + \frac{\varepsilon}{\alpha^2}\right\}\varphi(\xi) = \frac{2Mf}{\alpha^2}V(\xi)\varphi(\xi),$$
$$\left\{(\xi^2-1)\frac{\mathrm{d}^2}{\mathrm{d}\xi^2} + \xi\frac{\mathrm{d}}{\mathrm{d}\xi} - \frac{\mu^2}{\alpha^2}\right\}V(\xi) = \frac{f}{\alpha^2}\varphi^*(\xi)\varphi(\xi), \tag{3.7}$$
$$\frac{4}{\mu}\int_1^{\infty}\mathrm{d}\xi\frac{\varphi^*(\xi)\varphi(\xi)}{\sqrt{\xi^2-1}} = 1.$$

One can easily verify that the first two equations of (3.7) are fulfilled by

$$\varphi(\xi) = \left(\frac{9}{8}\frac{\mu^4}{Mf^2}\right)^{\frac{1}{2}}\xi^{-2}, \qquad V(\xi) = -\frac{3}{4}\frac{\mu^2}{Mf}\xi^{-2},$$
$$\alpha^2 = \tfrac{1}{4}\mu^2, \qquad \varepsilon = -\mu^2. \tag{3.8}$$

The third equation is satisfied only when

$$f^2 = 3\frac{\mu^3}{M}. \tag{3.9}$$

In x-space, the solution is

$$\varphi(x) = \left(\frac{9}{8}\frac{\mu^4}{Mf^2}\right)^{\frac{1}{2}}\frac{1}{\cosh^2\frac{1}{2}\mu x}, \qquad V(x) = -\frac{3}{4}\frac{\mu^2}{Mf}\frac{1}{\cosh^2\frac{1}{2}\mu x},$$
$$\varepsilon = -\mu^2, \qquad f^2 = 3\frac{\mu^3}{M}, \qquad \min I_0 = E^0 = -\frac{1}{5}\frac{\mu^2}{M}. \tag{3.10}$$

It is quite interesting to notice that the normalization condition is satisfied only when the coupling constant is given by the last relation in (3.10) and the nucleon state does not depend on M but on μ only, i.e.

$$\varphi(x) = (\tfrac{3}{8}\mu)^{\frac{1}{2}} \frac{1}{\cosh^2 \frac{1}{2}\mu x}. \tag{3.11}$$

We do not know whether or not (3.10) is the only solution. There may be solutions for an arbitrary value of f.

Returning to the three dimensional case, we can so far only treat it by the method of Ritz. In order to evaluate the energy roughly, assume functions

$$\varphi(\mathbf{x}) = \frac{1}{\sqrt{\pi}} (\tfrac{1}{2}K)^{\frac{3}{2}} e^{-\frac{1}{2}Kr}, \qquad V(\mathbf{x}) = N e^{-\beta r}, \qquad (r = |\mathbf{x}|) \tag{3.12}$$

with parameters K, β and N to be determined. The substitition of (3.12) into (2.36) gives us

$$I_0(K, \beta, N) = \frac{1}{8M} K^2 + f \frac{NK^3}{(K+\beta)^3} + \tfrac{1}{2}\pi N^2 \left(\frac{1}{\beta} + \frac{\mu^2}{\beta^3}\right). \tag{3.13}$$

The minimum I_0 is given by

$$\frac{1}{M} + 12fN \frac{K\beta}{(K+\beta)^4)} = 0, \tag{3.14.1}$$

$$6\frac{f}{\pi} \frac{K^3}{(K+\beta)^4} + N\left(\frac{1}{\beta^2} + \frac{3\mu^2}{\beta^4}\right) = 0, \tag{3.14.2}$$

$$\frac{f}{\pi} \frac{K^3}{(K+\beta)^3} + N\left(\frac{1}{\beta} + \frac{\mu^2}{\beta^3}\right) = 0. \tag{3.14.3}$$

Expanding K, β and N in powers of $\mu^2/M^2 \equiv m$, we have

$$\begin{gathered} K = K_0 + mK_1 + O(m^2), \qquad \beta = \beta_0 + m\beta_1 + O(m^2), \\ N = N_0 + mN_1 + O(m^2), \end{gathered} \tag{3.15}$$

with

$$K_0 = \frac{f^2 M}{\pi} \frac{5^5}{6^5}, \qquad \beta_0 = \frac{f^2 M}{\pi} \frac{5^4}{3 \cdot 6^5}, \qquad N_0 = -\frac{f}{\pi} \frac{f^2 M}{\pi} \frac{5^7}{6^9}, \tag{3.16}$$

$$K_1 = -15M^2 K_0^{-1}, \qquad \beta_1 = \tfrac{9}{5} M^2 \beta_0^{-1}, \qquad N_1 = \frac{M}{f} \frac{6^3}{5}. \tag{3.17}$$

Notice that the coefficients K_1, β_1 and N_1 are singular at $f=0$. We remark in this connection that the analogy with quantum electrodynamics should not be taken too seriously on analysing meson phenomena.

If we neglect μ^2-terms, we have

$$I_0(K_0, \beta_0, N_0, \mu^2 = 0) = -M \frac{f^2}{2\pi^2} \frac{5^{10}}{6^{12}}. \tag{3.18}$$

In order to see how the meson mass alters the above values, we consider m-terms. We then get

$$I_0 = -M \frac{f^2}{2\pi^2} \frac{5^{10}}{6^{12}} + \frac{\mu^2}{M} \frac{65}{4} + \mathrm{O}(m^2), \tag{3.19}$$

which indicates that the meson mass raises the minimum energy. The size of the nucleon core becomes large due to the meson mass, while that of the meson cloud becomes smaller, as is seen in (3.17).

The quantities K, β and N appearing in (3.14) are expressed with a parameter D as

$$\begin{aligned} K &= \sqrt{3} \frac{\mu}{D} \left(\frac{1-D}{5D-1}\right)^{\frac{1}{2}}, \qquad \beta = \sqrt{3}\mu \left(\frac{1-D}{5D-1}\right)^{\frac{1}{2}}, \\ N &= -\frac{3\sqrt{3}}{4} \frac{f}{\pi} \frac{\mu}{D} \frac{1}{(1+D)^4} \frac{(1-D)^{\frac{3}{2}}}{(5D-1)^{\frac{1}{2}}}, \end{aligned} \tag{3.20}$$

where

$$\frac{f^2}{4\pi} = \frac{1}{24\sqrt{3}} \frac{\mu}{M} \frac{(1+D)^8}{D^3} \frac{1}{(5D-1)^{\frac{1}{2}}(1-D)^{\frac{1}{2}}} \qquad (0.2 < D < 1). \tag{3.21}$$

The number of mesons in the meson cloud is, on account of (2.33),

$$\begin{aligned} \langle n_{\mathrm{meson}} \rangle &= (\Phi_0, \int \mathrm{d}^3k a^+(\mathbf{k}) a(\mathbf{k}) \Phi_0) \\ &= \frac{2}{\pi} (2\pi)^3 \beta^2 N^2 \int_0^\infty \mathrm{d}k \frac{k^2}{(k^2+\beta^2)^{\frac{7}{2}}} = \frac{4\pi}{5\sqrt{3}} \frac{\mu}{M} \frac{1}{D^3} \frac{(1-D)^{\frac{3}{2}}}{(5D-1)^{\frac{1}{2}}}. \end{aligned} \tag{3.22}$$

Numerical values of K, β, $f^2/4\pi$ and $\langle n_{\mathrm{meson}} \rangle$ are given in table 1.

TABLE 1

Numerical values of the parameters ($\mu/M = 0.15$)

D	0.25	0.30	0.35	0.40	0.45	0.50
K/μ	12.0	6.83	4.61	3.23	2.55	2.00
β/μ	3.00	2.05	1.61	1.29	1.15	1.00
$f^2/4\pi$	3.18	1.84	1.33	1.12	0.933	0.854
$\langle n_{\mathrm{meson}} \rangle$	17.6	6.68	3.71	1.64	0.871	0.503
Sign of I_0	+	+	−	−	−	0

The parameter D has a simple physical significance. From (3.20), we observe

$$D = \beta/K,$$

which is roughly the ratio of the sizes of nucleon core and meson cloud. The table shows that if $f^2/4\pi \approx 1$, the quantity D is about 0.4 and the meson number in the cloud is about unity. We also notice that the minimum energy becomes positive for certain values of $f^2/4\pi$. These values should be rejected, since the state corresponding to them are unstable. The values given in table 1 should not be taken too seriously in view of our crude initial trial functions. We shall improve the trial functions in a separate paper.

4. Discussion

We have obtained equations which define the nucleon state in its own scalar field

$$\begin{aligned} &\left[\frac{1}{2M}\,\mathbf{p}^2+fV(\mathbf{x})\right]\varphi(\mathbf{x}) = E_{\mathrm{II}}\varphi(\mathbf{x}), \\ &(\Delta-\mu^2)V(\mathbf{x}) = f\varphi^*(\mathbf{x})\varphi(\mathbf{x}). \end{aligned} \tag{4.1}$$

It is, however, quite difficult to solve these. The perturbation approximation would not work, for the solution may not be analytic at $f = 0$, as was seen in (3.17). We are thus led to an approach by a variational method. According to the rough extimate carried out in sect. 3, the size of the nucleon core in the ground state is close to that of the meson cloud for a normal magnitude of the coupling constant. This fact is in conformity with the electromagnetic structure of the nucleon, [1, 3]) although our simple model should be refined for more realistic cases to compare with experiment. The basic eqs. (4.1) in our model seem to hold, however, even for charge independent interaction without derivatives.

Let us take a Hamiltonian

$$H = \frac{1}{2M}\,\mathbf{p}^2+f\tau^a\phi^a(\mathbf{x})+H_\pi, \tag{4.2}$$

where τ^a is the isospin matrix. Assuming the state vector is a product of a nucleon spatial function $\varphi(\mathbf{x})$ and a Φ, which depends on the meson variables and the nucleon spin and isospin, we obtain

$$\begin{aligned} &\left[H_\pi+f\int \mathrm{d}^3x\varphi^*(\mathbf{x})\varphi(\mathbf{x})\tau^a\phi^a(\mathbf{x})\right]\Phi = E_{\mathrm{I}}\Phi, \\ &\left[\frac{1}{2M}\,\mathbf{p}^2+f(\Phi,\tau^a\phi^a(\mathbf{x})\Phi)\right]\varphi(\mathbf{x}) = E_{\mathrm{II}}\varphi(\mathbf{x}). \end{aligned} \tag{4.3}$$

Here we have split the total state vector in the manner mentioned above,

but we could also assume $\Psi(\mathbf{x}) = \varphi_{\text{spin}}(\mathbf{x})\Phi$, where Φ depends on the meson variables only. The reason for the former choice lies in the fact that the first equation of (4.3) is closest to the ordinary fixed source model.

The first eigenvalue equation is treated, for example, by Tomonaga's method [6]). We introduce a complete orthonormal set of functions

$$U_0(\mathbf{k}), U_1(\mathbf{k}), U_2(\mathbf{k}), \ldots, \tag{4.4}$$

with

$$U_0(\mathbf{k}) = \frac{1}{N_0^{\frac{1}{2}}} \frac{\sqrt{2}}{\omega^{\frac{1}{2}}(\mathbf{k})} \frac{1}{(2\pi)^{\frac{3}{2}}} \int_{-\infty}^{\infty} \mathrm{d}^3x \varphi^*(\mathbf{x})\varphi(\mathbf{x}) \mathrm{e}^{-i\mathbf{k}\cdot\mathbf{x}}, \tag{4.5}$$

where

$$N_0 = \int \mathrm{d}^3x \int \mathrm{d}^3y |\varphi(\mathbf{x})|^2 G(\mathbf{x}-\mathbf{y}) |\varphi(\mathbf{y})|^2,$$

$$G(\mathbf{x}-\mathbf{y}) = \frac{2}{(2\pi)^3} \int \frac{\mathrm{d}^3k}{\omega^3(\mathbf{k})} \mathrm{e}^{i\mathbf{k}\cdot(\mathbf{x}-\mathbf{y})} = \frac{1}{\pi^2} K_0(\mu|\mathbf{x}-\mathbf{y}|).$$

The creation and annihilation operators of the meson can be expanded in terms of (4.4) as

$$a^{\alpha\dagger}(\mathbf{k}) = \sum_{s=0}^{\infty} A_s^{\alpha\dagger} U_s^*(\mathbf{k}), \qquad a^{\alpha}(\mathbf{k}) = \sum_{s=0}^{\infty} A_s^{\alpha} U_s(\mathbf{k}). \tag{4.6}$$

The meson field corresponding to the first term in (4.6) is

$$\begin{aligned} \phi_0^{\alpha}(\mathbf{x}) &= \frac{1}{(2\pi)^{\frac{3}{2}}} \int \frac{\mathrm{d}^3k}{\sqrt{2\omega(\mathbf{k})}} \{A_0^{\alpha} U_0(\mathbf{k}) \mathrm{e}^{i\mathbf{k}\cdot\mathbf{x}} + A_0^{\alpha\dagger} U_0^*(\mathbf{k}) \mathrm{e}^{-i\mathbf{k}\cdot\mathbf{x}}\}, \\ &= -\frac{1}{fN_0^{\frac{1}{2}}} V(\mathbf{x}) \{A_0^{\alpha} + A_0^{\alpha\dagger}\}, \end{aligned} \tag{4.7}$$

where

$$(\Delta - \mu^2) V(\mathbf{x}) = f\varphi^*(\mathbf{x})\varphi(\mathbf{x}). \tag{4.8}$$

The second eigenvalue equation turns out to be

$$\left[\frac{1}{2M} \mathbf{p}^2 + f' V(\mathbf{x})\right] \varphi(\mathbf{x}) = E_{\text{II}} \varphi(\mathbf{x}), \tag{4.9}$$

with

$$f' = -\frac{2}{N_0^{\frac{1}{2}}} (\Phi, (A_0^{\alpha} + A_0^{\alpha\dagger}) \tau^{\alpha} \Phi), \tag{4.10}$$

which is only a number. Notice that eq. (4.9) differs from (4.1) by the factor f'. If one changes the normalization of $V(\mathbf{x})$ by a factor $(f/f')^{\frac{1}{2}}$, eqs. (4.8) and

(4.9) become

$$\left[\frac{1}{2M}\,\mathbf{p}^2+gV(\mathbf{x})\right]\varphi(\mathbf{x}) = E_{II}\varphi(\mathbf{x}),$$
$$(\Delta-\mu^2)V(\mathbf{x}) = g\varphi^*(\mathbf{x})\varphi(\mathbf{x}), \tag{4.11}$$

with

$$g^2 = ff', \tag{4.12}$$

which are the same as (4.1). The quantity ff' must be positive, otherwise bound states do not exist.

It would be of interest to pursue further research on the structure of the nucleon along the line described in this paper. In particular, the effect of the nucleon core on the scalar part of the anomalous magnetic moment of the nucleon and on the scattering process must be carefully investigated in view of the success of the simpe cut-off theory of Chew and Low.

The author wishes to thank Professor J. L. Synge for many stimulating discussions regarding the non-linear equations. He is also indebted to Professor C. Lanczos, Professor L. O'Raifeartaigh, Dr. S. Kamefuchi, Rev. J. Spelman and Rev. C. Ryan for their interest and pertinent comments.

References

1) D. R. Yennie, M. M. Lévy and D. G. Ravenhall, Rev. Mod. Phys. **29** (1957) 144
2) M. Gell-Mann and M. M. Lévy, Nuovo Cim. **16** (1960) 705 and related papers
3) I. E. Tamm, JETP **5** (1957) 154
4) S. Tomonaga, Prog. Theor. Phys. **2** (1947) 2
5) K. M. Watson and E. W. Hart, Phys. Rev. **79** (1950) 918
6) Z. Maki, M. Sato and S. Tomonaga, Prog. Theor. Phys. **9** (1953) 607

3.A: 6A

Nuclear Physics **26** (1961) 670—680; © *North-Holland Publishing Co., Amsterdam*

Not to be reproduced by photoprint or microfilm without written permission from the publisher

AN INTENSITY CALIBRATION OF THE TWO METRE CURVED-CRYSTAL SPECTROMETER

W. F. EDWARDS †, J. W. M. DUMOND and F. BOEHM

California Institute of Technology, Pasadena ††

Received 6 March 1961

Abstract: The 2 m curved-crystal diffraction spectrometer at the California Institute of Technology was calibrated to permit precise relative intensity measurements of gamma rays or X-rays over the energy range 60 keV to 400 keV. The curved quartz crystal (2 mm thick, (310) planes) was found to have a dependence of reflectivity I/I_u upon energy E given by

$$I/I_u = (E_0/E)^{1.987\pm0.022},$$

where E_0 is a reference energy within the range of the calibration. The relative intensity uncertainty, from sources other than counting rare statistics, is now of the order of 3% or less for gamma rays differing in energy up to a factor of four.

1. Introduction

The uncertainty in the energy dependence of the gamma ray or X-ray reflection coefficient in a bent crystal has long been the factor limiting the precision of intensity measurements using a bent-crystal spectrometer. To find the relative intensities of gamma rays or X-rays, a knowledge of the relative efficiency for reflection at each energy is necessary. Lind, West and DuMond [1, 2]) have reported that the (310) planes in an unstressed quartz crystal have a reflection coefficient that varies more slowly than E^{-1} and approximately as $E^{-0.58}$. When the crystal is stressed by bending, however, they found that this relationship changes. They reported that a 1 mm thick, stressed quartz crystal lamina bent from an initially flat state to a cylindrical radius of 2 m at its neutral plane in the curved-crystal spectrometer at the California Institute of Technology exhibited a dependence of reflection coefficient near E^{-2}. Using the same spectrometer Hatch found that this relationship also seemed to hold for a 2 mm thick crystal [3]). However, the uncertainty in the exponent has heretofore been so great as to introduce an intensity uncertainty factor of the order of two for gamma rays differing in energy by a factor of four.

Other investigators have reported on the reflection properties of bent quartz crystals, giving more precise values of the exponent. Sumbaev [4]) gives the value -1.85 ± 0.04 and Bergvall [5]) reports the exponent -1.99 ± 0.05. Both were using the (310) planes.

† Present address: Utah State University, Logan, Utah.

†† This work was supported by the U.S. Atomic Energy Commission and was submitted by W. F. Edwards as part of a Ph. D. Thesis, California Institute of Technology, 1960.

In the present determination a unified calibration of the whole spectrometer was actually performed. This provided an empirical curve for correcting relative intensities without an appeal to individual corrections; then known absorption and efficiency corrections were used to reduce the data, resulting in information regarding the reflectivity-energy dependence. It is apparent that to use the instrument for precise intensity measurements a unified calibration is all that is necessary, nevertheless, information regarding the reflectivity of the crystal will be useful to other research groups using crystal spectrometers of different geometries as well as to those studying the reflection properties of crystals. As it turns out, compared with the reflectivity correction, other corrections are small with the consequence that a unified calibration does primarily determine the reflectivity. Other correction factors include absorption in the air path, in the bent quartz crystal, in the aluminium window of the scintillation crystal detector and in the source holder, self absorption in the source, and "photo" efficiency of the detector. These corrections are well-known and seldom comprise a correction factor greater than 2, whereas the factor arising from crystal reflectivity has been as great as 16 and occasionally as large as 100 depending upon the energy difference of the gamma rays. Thus the reduction from a curve representing the unified instrument calibration to one representing the crystal reflectivity results in almost no loss in the precision of the information.

Two independent methods were used to find the spectrometer calibration and the crystal reflectivity. The first was a comparison of intensities measured using the curved-crystal spectrometer with intensities measured using other instruments which give accurate intensity measurements. The second was a method which takes advantage of the over-determination which can be achieved when information about the populating and de-populating of excited nuclear levels is available. We shall call the latter the "decay scheme method".

2. Instruments and Sources

The sources used in the experiments to be described were radioactive Se^{75} and Hf^{180m}.

In addition to the curved-crystal spectrometer, a ring-focusing magnetic spectrometer [6]) and a semicircular magnetic spectrometer [7]) were used to measure relative intensities of internally converted electrons in the Hf^{180} experiment. The ring-focusing spectrometer was operated at 0.7 % optimum-match resolution and was used to measure the relative intensities of internal conversion electrons having energies greater than 24 keV. The detector is a Geiger counter having a mica window of thickness 0.9 mg/cm^2. Electrons having energies below 120 keV were measured with the semi-circular spectro-

meter operating at 1% momentum resolution. Its detector window was Formvar with a thickness of approximately 20 $\mu g/cm^2$. Sources for these two spectrometers were prepared by vacuum evaporation of the activated material onto aluminium backings.

The curved-crystal spectrometer with the sources enclosed in quartz capillaries of internal diameter 0.02 cm and height 2 cm was operated at an energy resolution $\Delta E/E = 2.3\times10^{-5}\ E$, where E is the gamma ray energy in keV. Gamma ray relative intensities were found by setting the diffraction spectrometer on the maximum position of the line profiles and recording the photopeaks of the NaI(Tl) detector with a 100-channel analyzer. A background curve below the photopeak profile was also recorded on the multi-channel analyzer by setting the bent-crystal spectrometer sufficiently off the position for diffraction maximum to avoid appreciable effect from the "tails" of the line. About 1 X-unit (or about 1 mÅ) usually suffices for this. The relative intensities were taken to be equal to the areas of the photopeaks above this background after being corrected for the effects already noted.

The Se^{75} source was produced by neutron irradiation of SeO_2 in the Materials Testing Reactor, Arco, Idaho. The selenium was enriched in the isotope 74 (isotopic abundance 12.3 %). The Hf^{180m} sources were produced by neutron irradiation of HfO_2 enriched in the isotope 179 (abundance 83.6 %). The neutron flux in both cases was approximately $2\times10^{14}/cm^2\cdot sec$.

3. Comparison of Intensities of Transitions Following Se^{75} Decay

Studies recently made of the decay scheme of Se^{75} offer gamma ray intensity measurements which can be used to check the calibration of the curved-crystal spectrometer. The isotope Se^{75} decays by electron capture to As^{75}. In decaying to the ground state, the excited As^{75} nucleus emits 9 gamma rays with intensities strong enough to be studied by the crystal diffraction method. These gamma rays range in energy from 66.05 keV to 400.7 keV, covering well the most useful range of the Mark I curved-crystal spectrometer.

Three other research groups have measured these same relative gamma-ray intensities, two of them by external conversion and one by sodium-iodide pulse-height spectroscopy. Schardt and Welker[8]) made important initial measurements of relative gamma-ray intensities by means of a sodium-iodide crystal detector. More recently, Grigorev, *et al.*[9]) studied the gamma rays using external conversion measuring the conversion electrons with a lens spectrometer. Metzger and Todd[10]) have measured the relative intensities of 5 of the gamma rays by using external conversion. The relative intensities reported by these groups are given in table 1.

The values measured here, corrected for crystal reflectivity assuming an exact E^{-2} law, are shown in column 6 of the table. The actual reflectivity

TABLE 1

As^{75} gamma-ray intensity data

Gamma-ray energy, present measurement (keV)	Gamma-ray intensity					
	With other instruments				With the curved-crystal spectrometer	
	Schardt and Welker [8])	Grigorev *et al.* [9])	Metzger and Todd [10])	Mean value	Corrected [a]) with $E^{-2.000}$	Corrected [b]) with $E^{-1.987\pm0.022}$
66.05±0.01	1.8±1	1.53+0.15		1.53±0.15	1.60±0.03	1.63±0.06
96.74±0.01	6.6±1.5	5.5 ±0.3		5.6 ±0.3	5.50±0.09	5.57±0.18
121.12±0.01	29 ±4	27.9 ±1.3		28.0 ±1.2	27.7 ±0.4	28.0 ±0.6
135.99±0.02	94 ±12	96 ±5		95.6 ±4.6	94.7 ±1.0	95.5 ±1.8
198.60±0.06	3	2.6 ±0.2		2.6 ±0.2	2.4 ±0.1	2.4 ±0.1
264.62±0.07	100	100	100	100 46.2 ±0.9	100	100
279.57±0.08	45.7±4	41 ±2.5	47 ±1	42.2 ±2.1 [c])	42.2 ±0.6	42.2 ±0.6
304.0 ±0.3	2.0±0.5	2.5 ±0.3	2.1±0.3	2.25±0.20	2.29±0.14	2.29±0.14
400.7 ±0.2	24.8±2.5	22.3 ±2.3	19 ±2	21.6 ±1.3	19.6 ±0.6	19.5 ±0.6

[a]) These intensities were obtained assuming a curved-crystal reflectivity correction proportional to $E^{-2.000}$. The errors do not include a reflectivity uncertainty.

[b]) These intensities were obtained in accordance with the present spectrometer intensity calibration which indicates a curved-crystal reflectivity proportional to $E^{-1.987\pm0.022}$.

[c]) This value is the mean of the values obtained by the first two groups. For a discussion of this see text.

correction was determined as follows: The mean of the values measured by other groups was found, weighting the measurements inversely as the square of reported errors. Our present bent-crystal intensity, uncorrected for crystal reflectivity, was then divided by the mean of the other measurements to give values which then represented the curved-crystal reflectivity in relative units normalized to unity for the 264.62 keV line. When plotted on double logarithmic paper, the reflectivity as a function of energy shows a straight-line nature which indicates that the function does indeed follow a power law. This curve is shown in fig. 1.

To determine the best value of the exponent and its uncertainty, a least-squares adjustment was performed. The intensity, normalized to a particular energy is

$$I/I_u = (E_0/E)^{2+x} \tag{1}$$

or

$$\log I/I_u = (2+x)\log(E_0/E), \tag{2}$$

where E is the energy of the line, E_0 is the reference energy (where the relative correction is arbitrarily taken equal to unity) and I_u and I are the uncorrected and corrected relative intensities, respectively. The only parameter to fit to the input data is x, the correction to the exponent 2 in the reflectivity law. The quantity $(2+x)$ is the slope of the adjusted line plotted in log-log units.

By examining table 1, one can see that the agreement between the experimental data is, indeed, very good. There does, however, exist a discrepancy between various sources as to the reported intensities of the 279.57-keV line. All other Se^{75} data indicate a crystal reflectivity relationship very close to E^{-2} (as also does the calibration by the decay scheme method). Assuming the E^{-2} law, the intensity of the 279.57 keV line relative to the 264.62 keV line could be measured with considerable accuracy with the resulting relative intensity 42.2 ± 0.6. As the energy difference is small, the uncertainties due to energy dependent corrections were negligible so the error is almost entirely due to counting statistics. The present value overlaps that of Grigorev *et al.* and also that of Schardt and Welker; however, it is about seven standard deviations from that of Metzger and Todd. Because of this great difference, the point was carefully remeasured until the total number of measurements on this line was four (the other lines were measured twice). The reproducibility was good, the highest value being 42.7 and the mean 42.2. The lines were entirely resolved and very strong. It was therefore felt that the value of Metzger and Todd was in error and, hence, this value was not used. This did not, however, have a great effect on the output value of the exponent. The difference in the exponent, if the value by Metzger and Todd has been used, would have amounted to less than 0.3%. The adjusted value of x was found to be 0.000 ± 0.032, giving an exponent in the reflectivity law of 2.000 ± 0.032 over the range 60 keV $\leqq E \leqq$

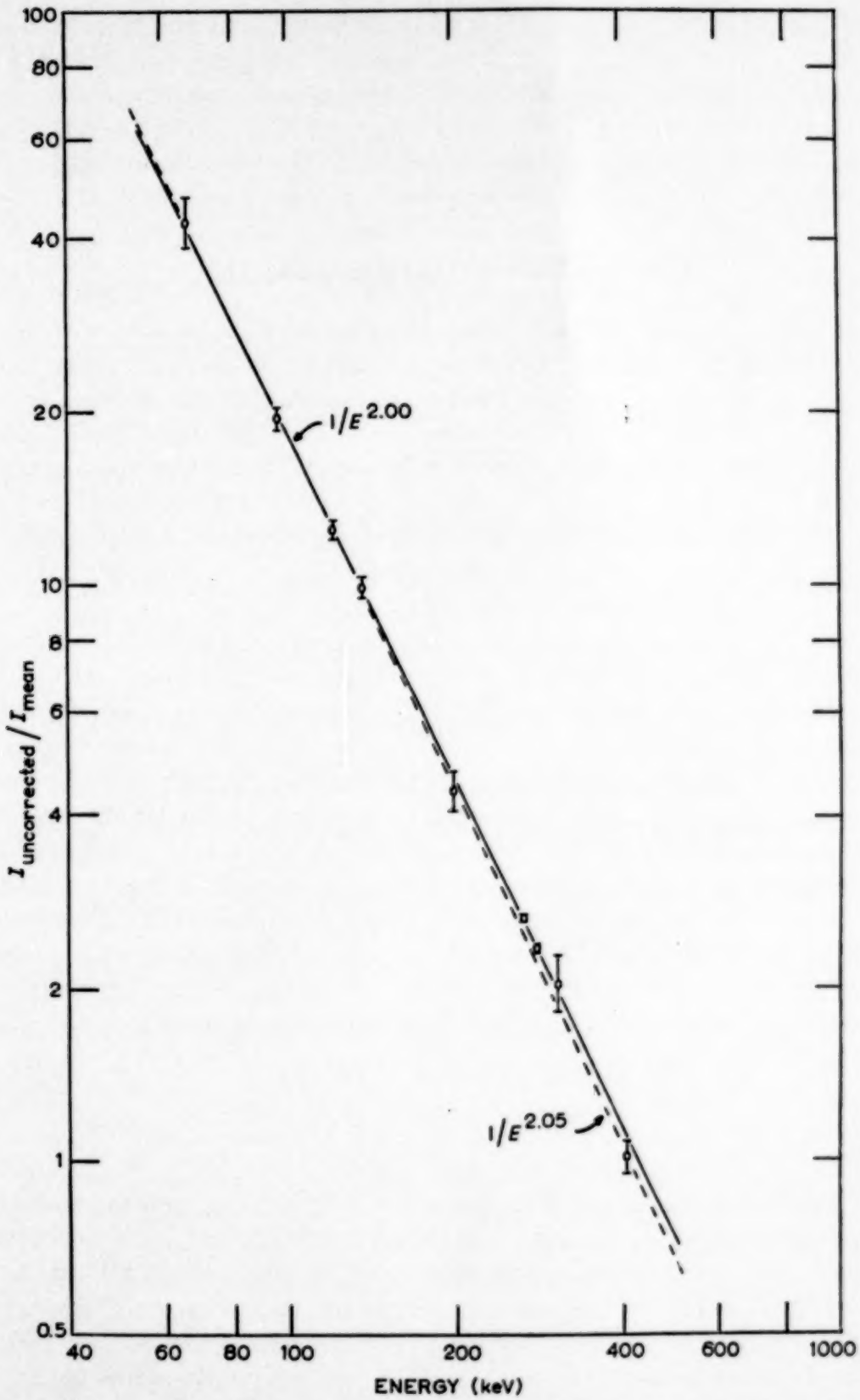

Fig. 1. The determination of the quartz-crystal reflection coefficient using measurements of the intensities of gamma-rays following the decay of Se^{75}. The intensities measured with the curved-crystal spectrometer are compared with those measured by several other authors. $I_{uncorrected}$ is the present intensity uncorrected for reflection coefficient variation. I_{mean} is the mean value of the determinations by other investigators. A least squares adjustment indicated a $E^{-2.000\pm0.032}$ relationship.

400 keV. The quoted error is the standard deviation σ_i reflecting the accuracy of the original measurements or the "internal" error. The consistency of the data is good for the standard deviation σ_e based on the spread of the observations ("external" error) is 0.024 giving $\sigma_e/\sigma_i = 0.75$. This corresponds to a χ^2 of only 3.94 with 7 degrees of freedom, indicating that the accuracy of the original measurements probably was better than the estimates assigned.

4. Decay Scheme Method using Hf^{180m}

The second method for calibrating the spectrometer already very briefly alluded to in an earlier paper [11], requires (1) knowledge of a nuclear decay scheme, (2) knowledge of the relative intensities (uncorrected for crystal reflectivity) of gamma rays emitted as a result of transitions in said decay scheme and (3) knowledge of the relative beta-ray intensities of the conversion electrons associated with these transitions. The latter were measured with the homogeneous magnetic field spectrometer and the semi-circular spectrometer. The decay scheme can in fact provide over-determination of the experimental data in the following manner.

The decay fraction of a transition is the percentage of the total decay rate contributed by a particular electromagnetic transition (in the form of either conversion electrons or gamma rays) and is proportional to $(1+\alpha_t)I_\gamma$, where α_t is the total conversion coefficient of the transition (the ratio of the conversion electron intensity to the gamma-ray intensity) and I_γ is the relative intensity of the gamma ray. If no primary beta branching or other non-electromagnetic feeding of a particular intermediate energy level exists, then the sum of the electromagnetic decay fractions of transitions populating that level must equal the sum of the electromagnetic decay fractions of transitions depopulating it. Now the conversion coefficient of any transition can be written in terms of (1) the conversion coefficient of any other transition, and (2) the ratios of relative beta-intensities and of relative gamma-ray intensities by means of the obvious identity

$$\alpha(2) = \alpha(1)\,\frac{I(2)_e}{I(1)_e}\,\frac{I(1)_\gamma}{I(2)_\gamma}, \tag{3}$$

wherein the numbers (1) and (2) label any two different transitions in the scheme. Using eq. (3), the former equation expressing the balance between the feeding and bleeding of any level can be written in terms of relative beta-ray intensities, relative gamma-ray intensities and only one arbitrarily selected absolute conversion coefficient in the entire decay scheme. When precise intensity measurements are available, the only unknown is then that absolute conversion coefficient, the determination of which thus establishes an absolute scale for all others in the sample. The over-determination of a set

of level equations in such a case is thus equal to $n-1$, where n is the number of equations. In the present experiment, however, this over-determination was lessened by including in the equations correction factors to the relative gamma-ray intensity scale to take care of a possible small deviation x (see eq. (1)) in the exponent of the law of crystal reflectivity. These correction factors, all functions of the known gamma-ray energies and of x, thus introduced one extra unknown.

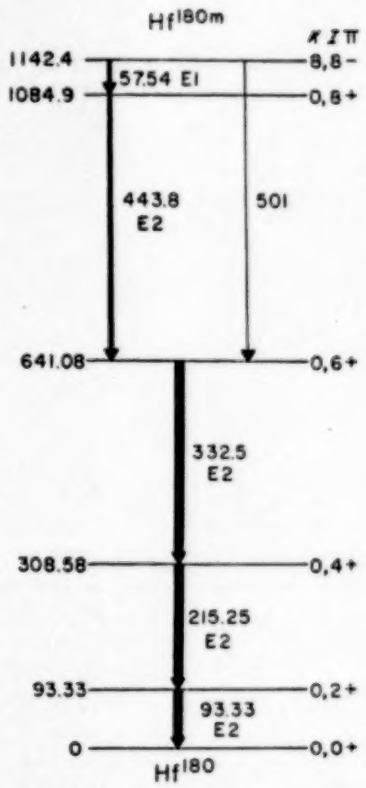

Fig. 2. The decay scheme of Hf^{180m}.

As shown in fig. 2, Hf^{180m} has four levels for which equations can be written, the 2+, 4+, 6+ and 8+ levels. The gamma-ray intensity of the 501 keV transition was not, however, determined with sufficient accuracy. Furthermore, the uncertainties of the 443.8 keV transition intensities were quite large. For these reasons, the equation for the 6+ level was rejected. The unknown absolute conversion coefficient, in terms of which the equations were written, was that of the 93.33 keV transition.

To determine the deviation from E^{-2} law, the raw gamma-ray intensity data were corrected for all known correction factors and for $E^{-2.000}$ crystal reflectivity. These relative intensities (indicated by primes in the following equations) were then multiplied by a correction function with the parameter x, indicating the deviation from a pure E^{-2} reflectivity law. As x was expected to be small,

the exponential was expanded in a power series neglecting higher terms. We have

$$\frac{I(i)_\gamma}{I(j)_\gamma} = \frac{I'(i)_\gamma}{I'(j)_\gamma}\left[\frac{E(i)}{E(j)}\right]^x \approx \frac{I'(i)_\gamma}{I'(j)_\gamma}\left[1+x\ln\frac{E(i)}{E(j)}\right]. \tag{4}$$

This was then substituted for the relative gamma-ray intensities in the equations for levels 2+, 4+ and 8+, which then became the three observational equations with two unknown quantities as follows:

$$\left[\frac{I(2)_e}{I(1)_e}-1\right]\alpha(1)-\frac{I'(2)_\gamma}{I'(1)_\gamma}\ln\left(\frac{E_2}{E_1}\right)x = 1-\frac{I'(2)_\gamma}{I'(1)_\gamma}, \tag{5}$$

$$\left[\frac{I(3)_e}{I(1)_e}-1\right]\alpha(1)-\frac{I'(3)_\gamma}{I'(1)_\gamma}\ln\left(\frac{E_3}{E_1}\right)x = 1-\frac{I'(3)_\gamma}{I'(1)_\gamma}, \tag{6}$$

$$\left[\frac{I(5)_e}{I(1)_e}-\frac{I(4)_e}{I(1)_e}\right]\alpha(1)+\left[\frac{I'(5)_\gamma}{I'(1)_\gamma}\ln\frac{E_5}{E_1}-\frac{I'(4)_\gamma}{I'(1)_\gamma}\ln\frac{E_4}{E_1}\right]x = \frac{I'(4)_\gamma}{I'(1)_\gamma}-\frac{I'(5)_\gamma}{I'(1)_\gamma}. \tag{7}$$

The transitions, having energies 93.33, 215.25, 332.5, 443.8 and 57.54 keV, are identified by the numbers 1, 2, 3, 4 and 5, respectively. The experimental data are found in table 2.

TABLE 2

Hf^{180} transition data used in the calibration of the curved-crystal spectrometer and in obtaining absolute conversion coefficients

Gamma-ray energy (keV)	Total conversion electron intensity (relative units) [a]	Gamma-ray intensity [b] corrected with $E^{-2.000}$	Gamma-ray intensity [c] corrected with $E^{-1.987\pm0.022}$
57.54±0.01	0.378 ±0.013	289± 6	291± 7
93.33±0.02	0.956 ±0.023	100± 2	100± 2
215.25±0.13	0.221 ±0.010	506±10	500±14
332.5 ±0.3	0.0634±0.0025	557±17	567±24
443.8 ±0.6	0.0227±0.0012	502±20	491±26
501.3 ±0.6 [d]			

[a] The electron intensities should be multiplied by 5.38 to put them on the same scale as the gammay-ray intensities. They include the total of all subshell conversion electron intensities for each transition. For the 215.25, 332.5 and 501.0 keV transitions, all of the subshell lines were not measured and a small correction was applied to account for the unmeasured lines.

[b] These intensities were obtained assuming a curved crystal reflectivity correction proportional to $E^{-2.000}$. The errors do not include the reflectivity uncertainty.

[c] These intensities were obtained in accordance with the present spectrometer intensity calibration which indicates a curved-crystal reflectivity proportional to $E^{-1.987\pm0.022}$.

[d] The energy of this crossover transition was determined from the sum of the 57.54 keV and 443.8 keV cascade gamma rays.

The equations are of the form

$$a_i\alpha(1)+b_ix+c_i = 0, \qquad i = 1, 2, 3, \tag{8}$$

where a_i, b_i and c_i are imprecise parameters which are functions of the primitive, uncorrelated data. A least-squares procedure was applied to these equations, taking into account the correlations between the parameters †. The resulting values for the unknowns are $x = -0.026 \pm 0.032$ and $\alpha(1) = 5.05 \pm 0.29$. The internal errors are given. The ratio of the external and internal error is 1.1. This corresponds to $\chi^2 = 1.13$ with one degree of freedom indicating good internal consistency of the data.

5. Conclusions

The values of x obtained from the two calibration methods are in reasonable agreement. That obtained from the Se^{75} experiment alone is 0.000 ± 0.032, which overlaps the value obtained from the Hf^{180m} experiment above. A more precise value of x was found by combining the results of the two experiments. This amounts to adding to eqs. (5), (6) and (7), a fourth equation

$$x = c_4,$$

where c_4 is the value for x obtained from the Se^{75} experiment. The least-squares adjusted values of the variables from this new set of equations are $x = -0.013 \pm 0.022$ and $\alpha_{93} = 5.14 \pm 0.24$. In this case, the ratio of external and internal error is 0.8, and we have $\chi^2 = 1.29$ with two degrees of freedom, again indicating that the accuracy of the measurements is probably better than the estimates assigned.

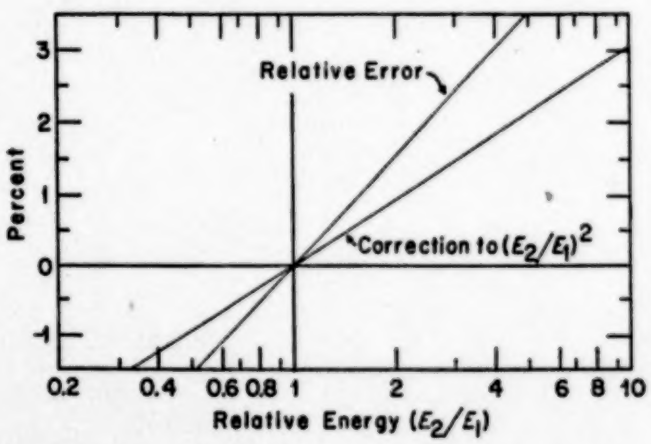

Fig. 3. Results of the curved-crystal spectrometer calibration showing the percentage deviation of the intensities of two gamma rays having energies E_2 and E_1 when corrected for the $(E_2/E_1)^{1.987 \pm 0.022}$ relationship from those corrected with a pure $(E_2/E_1)^2$ law. Also given is the uncertainty in relative intensity measurements arising from the uncertainty in the reflectivity law.

Thus the energy dependence of the peak reflection coefficient of the (310) planes in the 2 mm thick quartz slab bent to a 2 m radius of curvature used

† We wish to acknowledge the kind assistance of Dr. E. R. Cohen who outlined the proper least-squares procedure to use in solving the equations.

in the curved-crystal spectrometer over the range 60 keV $\leqq E \leqq$ 400 keV is $E^{-1.987\pm0.022}$. It is interesting to note that the uncertainty in the value of the exponent includes the number 2.000 within a standard deviation. The E^{-2} law predicted by Lind *et al.* does not disagree with the present result. Fig. 3 gives a graph of the correction to a pure E^{-2} law. It also gives the error introduced when correcting relative gamma-ray intensities for the curved-crystal reflectivity. From fig. 3, it can be seen that the relative uncertainty due to the reflectivity correction when comparing intensities of gamma rays whose energies differ by a factor of four has now been reduced to ± 3 %.

References

1) D. A. Lind, Ph. D. thesis, California Institute of Technology (1948) unpublished
2) D. A. Lind, W. J. West and J. W. M. DuMond, Phys. Rev. **77** (1950) 475
3) E. M. Hatch, Ph. D. thesis, California Institute of Technology (1956) unpublished
4) O. I. Sumbaev, JETP (Soviet Physics) **5** (1957) 170
5) P. Bergvall, Ark. f. Fys. **17** (1960) 125
6) J. W. M. DuMond, Ann. Phys. **2** (1957) 283
7) H. E. Henrikson, Report no. 24, USAEC, California Institute of Technology (1956)
8) A. W. Schardt and J. P. Welker, Phys. Rev. **99** (1955) 810
9) Grigorev, Zolotavin, Klementev and Sinetzyn, Izvestia Akad. Nauk, SSSR **23** (1959) 159
10) F. R. Metzger and W. B. Todd, Nuclear Physics **10** (1959) 220
11) W. F. Edwards and F. Boehm, Phys. Rev. **121** (1961) 1499

7.C

Nuclear Physics **26** (1961) 681—692; © *North-Holland Publishing Co., Amsterdam*

Not to be reproduced by photoprint or microfilm without written permission from the publisher

DISPERSION RELATIONS FOR PHOTOPRODUCTION OF π^0-MESONS ON DEUTERONS

VLADIMÍR ŠACHL

Laboratory of Theoretical Physics, Joint Institute for Nuclear Research, Dubna, USSR †

Received 16 February 1961

Abstract: The dispersion relations for the process of photoproduction of neutral mesons on deuterons are derived with the aid of impulse approximation. The unobservable region begins here with the state of a free proton and neutron and contains no other poles. The calculations including the recoil in the Breit system are carried out in a two-nucleon approximation and are specialized for the value of the momentum $\frac{1}{4}\mu^2 M/(M+\mu)$, where they are valid up to a maximum photon energy of 236 MeV. The derivation of the results without the spin-flip part is given for the case of deuterons perpendicularly polarized to the direction of propagation of mesons and photons.

1. Introduction

Although dispersion relations have been constructed for some few different types of reactions, non-elastic processes containing bound states were not hitherto considered. In formulating a consistent relativistic theory of processes of this type, we restrict ourselves, as we are always constrained by dispersion relations, to one process of this sort — the photoproduction of π-mesons on deuterons.

At first there arises the question of the treatment of the bound state. Because so far there exists no satisfactory method of general validity in quantum field theory applicable also to the vertex parts of the bound states, we are compelled to treat the deuteron with the aid of the impulse approximation. The impulse approximation is characterized in this case: 1) by the interactions with the separate nucleons as if they were unbounded, 2) by the fact that the interactions of the separate free nucleons in the intermediate state are negligible in comparison with the other interactions. Good results with the aid of the impulse approximation in the phenomenological theory of the photoproduction of π-mesons on deuterons have been obtained by Chew and Lewis and by Lax and Feshbach [1]).

From the general point of view of field theory and from the causality condition it is necessary to treat the interaction of wave fields with the individual nucleons separately, i.e. locally, and this leads through the composition of the local interactions for both nucleons to a certain non-locality.

† Permanent address: Czechoslovak Academy of Sciences, Prague, Czechoslovakia.

Success in using the method of dispersion relations has been achieved especially in reactions involving interactions of mesons and photons with nucleons. The dispersion relations for non-forward scattering, which will appear also in our case, were first proved for the scattering of mesons on nucleons† by N. N. Bogolyubov [3]). Dispersion relations of this type for the photoproduction of π-mesons on nucleons were in particular established in a paper by A. A. Logunov, A. N. Tavchelidze and L. D. Solovyev [4]).

The deuteron has no other bound state than a spin triplet and isobaric singlet state. In dispersion relations for forward scattering it was treated with the aid of impulse approximation for scattering of π-mesons on deuterons in a paper by F. Kaschluhn [5]). From the point of view of dispersion relations we get in the intermediate state as a first approximation, the "two-nucleon" approximation, two free nucleons. The unobservable region beginning with these nucleons contains no other poles. To the two nucleons, to which as a system we assign the relative momentum $\mathbf{p}_r$, belongs a continuous spectrum. In view of the complicated form of general results for the photoproduction amplitude, the dispersion relations will only be given for deuterons perpendicularly polarized†† to the direction of the propagation of mesons and photons.

2. Photoproduction Amplitude

Let us consider the process of photoproduction of neutral mesons on deuterons. We denote the final and initial momenta of the system of nucleons

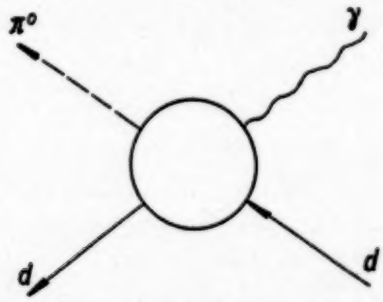

Fig. 1. Graph of the process of photoproduction of π^0-mesons on deuterons.

by $\mathbf{p}'$ and $\mathbf{p}$, their spinor field operator by ψ, their quantum numbers by m' and m; the momenta of π-meson and photon by $\mathbf{q}$ and $\mathbf{k}$, their field operators by $\varphi_{\rho'}(x)$ pseudoscalar meson field) and $A_\mu(x)$ (electromagnetic field); their quantum numbers are denoted by ρ' for the π^0-meson and μ for the photon.

Then we write the matrix element of the S-matrix expressing the photoproduction amplitude

$$S(\omega, \mathbf{q}'; \alpha, \mathbf{k}) = \langle \mathbf{p}', m'; \mathbf{q}', \rho' | S | \mathbf{k}, \mu; \mathbf{p}, m \rangle. \tag{1}$$

† For a survey about proofs for the other types of processes, see ref. [2]).

†† Since this was written, two other cases of polarization have been studied which lead to simplification; those will be discussed in a following paper.

To include the recoil we choose Breit's coordinate system, in which

$$\mathbf{p}+\mathbf{p}' = 0. \tag{2}$$

On account of the laws of conservation of momentum and energy this gives us the possibility of expressing the momentum of the photon $\mathbf{k}$ and of the meson $\mathbf{q}$ in the form

$$\begin{aligned} \mathbf{k} &= \lambda\mathbf{e}-(1+t)\mathbf{p}, \\ \mathbf{q} &= \lambda\mathbf{e}+(1-t)\mathbf{p}, \end{aligned} \tag{3}$$

where $t = \mu^2/4\mathbf{p}^2$, λ is an arbitrary parameter and the unit vector $\mathbf{e}$ is orthogonal to the momentum $\mathbf{p}$. For a fixed momentum $\mathbf{p}$ we get in this way the energy of the π-meson ($E = q^0$) as

$$E^2 = \lambda^2+(1+t)^2\mathbf{p}^2. \tag{4}$$

Turning back to the matrix element (1), by using the creation and annihilation operators of meson and electromagnetic field with their commutation relations with the S-matrix, we can rewrite the matrix element in the form

$$S(\omega, \mathbf{q}'; \alpha, \mathbf{k}) = \sum_{\mu} e_{\mu}{}^{\lambda}(\mathbf{k}) S_{\mu\rho'}, \tag{5}$$

$$S_{\mu\rho'} = \frac{1}{2\sqrt{k^0 q^0}} \int e^{i(qx-ky)} \langle \mathbf{p}', m' | \frac{\delta^2 S}{\delta\varphi_{\rho'}(x)\,\delta A_{\mu}(y)} S^{+} | \mathbf{p}, m\rangle \,dx\,dy. \tag{5a}$$

The radiation operator of the second order H_2 between the bra and the ket in the matrix element ocurring in eq. (5a) can be expressed by the hermitian current operators of the meson $j^{\rho'}(x)$ and the electromagnetic $i^{\mu}(y)$ field, usually denoted by

$$j^{\rho'}(x) = i\frac{\delta S}{\delta\varphi_{\rho'}(x)} S^{+}, \quad i^{\mu}(x) = i\frac{\delta S}{\delta A_{\mu}(x)} S^{+}; \tag{6}$$

then, the radiation operator H_2 is simply expressed by

$$H_2 = -j^{\rho'}(x) i^{\mu}(y) - i\frac{\delta j^{\rho'}(x)}{\delta A_{\mu}(y)} = -i^{\mu}(y) j^{\rho'}(x) - i\frac{\delta i^{\mu}(y)}{\delta\varphi_{\rho'}(x)}. \tag{7}$$

Using the same notation in our case of deuterons as in the case of photoproduction of π-mesons on nucleons [5]), we can pass in the physical region of the plane of complex energies from the causal matrix element in (5a), denoted by $V^{\rho'\mu}_{\mathbf{p}', m; \mathbf{p}, m}(x)$, to the retarded one, which we denote by $W^{\rho'\mu}_{\mathbf{p}', m'; \mathbf{p}, m}(x)$, and to the advanced one: these matrix elements are identical with $V^{\rho\mu}_{\mathbf{p}', m'; \mathbf{p}, m}(x)$, in the upper or lower half-plane, respectively, and on the real axis (with the exception of a finite number of points and lines of discontinuity on the real axis).

Using the Fourier transformation we pass from the quantities $V(x)$, $W(x)$ to the transformed quantities $T(k)$, $M(k)$. For example for $M(k)$ we have

$$M^{\rho'\mu}_{\mathbf{p}',m';\mathbf{p},m}(k) = \int \mathrm{d}x e^{ikx} W^{\rho'\mu}_{\mathbf{p}',m';\mathbf{p},m}(x), \tag{8}$$

where instead of $M(k)$ and $W(x)$ the causal $T(k)$ and $V(x)$, or the advanced quantities, or any product of the currents occurring in the expression (7), can be substituted as well. As usual it suffices to consider only the retarded parts, in view of the quite analogous properties of the advanced parts in the lower half plane. In the expression for the function $W^{\rho'\mu}_{\mathbf{p}',m';\mathbf{p},m}(x)$ according to eq. (7), there occur terms which are formed as products of meson and electromagnetic currents and which can be split spectrally [6]) as products of two matrix elements. In other words, we split the function $M^{\rho'\mu}_{\mathbf{p}',m';\mathbf{p},m}(k)$ in an obvious way into a dispersive part D and an absorptive one A, which we can define either by means of our functions $W(x)$ or of the products of currents from eq. (7). In this way we get the matrix element (5a) expressed in the upper half plane of complex energies and on the real axis in the form

$$S_{\mu\rho'} = \frac{i(2\pi)^4}{\sqrt{4k^0q^0}}\,\delta(p'+q-p-k)\left\{D^{\rho'\mu}_{\mathbf{p}',m;\mathbf{p},m}\left(\frac{k+q}{2}\right)+iA^{\rho'\mu}_{\mathbf{p}',m';\mathbf{p},m}\left(\frac{k+q}{2}\right)\right\}. \tag{9}$$

Owing to the fact that only the absorptive part — defining in the form (5) the photoproduction amplitude of π^0-mesons on deuterons — is necessary for determining dispersion relations, we introduce only this part explicitly. Thus, after the indicated integrations, we have, in our coordinate system (2),

$$\begin{aligned}
&A^{\rho'\mu}_{\mathbf{p}',m';\mathbf{p},m}(E,\lambda\mathbf{e}) \\
&= \pi\sum_n \langle\psi^*_{-\mathbf{p},m'},\, J^{\rho'}(0)\psi_{n,\lambda\mathbf{e}-t\mathbf{p}}\rangle\langle\psi_{n,\lambda\mathbf{e}-t\mathbf{p}} I^{\mu}(0)\psi_{\mathbf{p},m}\rangle\delta(\sqrt{M^2+\mathbf{p}^2}+E-\sqrt{M_n{}^2+\lambda^2+t^2\mathbf{p}^2}) \\
&- \pi\sum_n \langle\psi^*_{-\mathbf{p},m'},\, I^{\mu}(0)\psi_{n,-\lambda\mathbf{e}+t\mathbf{p}}\rangle\langle\psi^*_{n,-\lambda\mathbf{e}+t\mathbf{p}} J^{\rho'}(0)\psi_{\mathbf{p},m}\rangle\delta(\sqrt{M^2+\mathbf{p}^2}-E-\sqrt{M_n{}^2+\lambda^2+t^2\mathbf{p}^2}),
\end{aligned}$$

where all quantities in the matrix elements are expressed in Heisenberg's picture, and where one has

$$\lambda\mathbf{e}-t\mathbf{p} = \mathbf{q}-\mathbf{p} = \mathbf{k}+\mathbf{p}.$$

3. Isobaric Structure

On the basis of isobaric invariance the isobaric structure of the process of photoproduction of π^0-mesons on deuterons is reduced to a particularly simple case: third component of a vector in isobaric space. The only possible intermediate states, for a process involving a change of the isobaric spin by 1, are, in our case of a free neutron and a free proton, only the states with isobaric spin 1.

For the process $\gamma+\mathrm{d}\to\mathrm{n}+\mathrm{p}$, in which the initial isospin state $|I, I_z\rangle$ is $|0, 0\rangle$ and the final isospin state either $\langle 0, 0|$ for a scalar wave function in the isobaric space, or $\langle 1, I_z|$ with $I_z = 0$ for a vector wave function, the S-matrix may be written in the form of a scalar $\mathscr{S}^{(2)}$ and the third component of a vector $V_3^{(2)}$:

$$S^{(2)} = \mathscr{S}^{(2)}+V_3^{(2)} = c_s+c_+v_3, \qquad c_s^2+c_+^2 = 1. \tag{11}$$

Analogously, for the process $\mathrm{p}+\mathrm{n}\to\mathrm{d}+\pi^0$ with the initial state $|0, 0\rangle$ or $|1, I_z\rangle$ with $I_z = 0$, and the final state $\langle 1, I_z'|$ for $I'_z = 0$, the $S^{(3)}$ matrix is a scalar $\mathscr{S}^{(3)}$:

$$S^{(3)} = \mathscr{S}^{(3)} = \mathbf{v}\cdot\boldsymbol{\pi}. \tag{12}$$

The resulting wave function will be the third component of a vector only:

$$S = S^{(2)}S^{(3)} = c_+v_3\,\mathbf{v}\cdot\boldsymbol{\pi}, \qquad c_+^2 = 1. \tag{13}$$

4. Two-Nucleon Approximation

From the laws of conservation of energy (in our coordinate system $k^0 = q^{0\prime}$) and from the condition that the quantity $\lambda^2 \geqq 0$, we obtain the energy of the photoproduction threshold E_{thr} in the form

$$E_{\mathrm{thr}} = (1+t)|\mathbf{p}|, \quad t = \frac{\mu^2}{4\mathbf{p}^2}. \tag{14}$$

If we consider in eq. (10) as intermediate states

$n = 0$: the deuteron or two nucleons,

$n = 1$: the deuteron and a π-meson, or two nucleons and a π-meson,

$n = 2$: the deuteron and two π-mesons,

we get for the energies of these states

$$E_i^{(n)} = \pm\frac{\frac{1}{2}\{M_n^2-M^2-\mu^2\}-\mathbf{p}\cdot\mathbf{q}}{\sqrt{M^2+\mathbf{p}^2}}, \qquad \begin{matrix} n = 0, 1, 2 \\ i = 1, 2, \end{matrix} \tag{15}$$

where M_n represents, for $n = 0$ the mass of deuteron M or the mass of two nucleons M_s, for $n = 1$ the mass $M_1 = M+\mu$ or $M_{1s} = M_s+\mu$), for $n = 2$ the mass $M_2 = M+2\mu$. The energies (15) are symmetrically placed on the real axis: $E_1^{(n)} = -E_2^{(n)}$, and (see fig. 2) $E_1^{(0)} < E_1^{(0s)} < E_1^{(1)} < E_1^{(1s)} < E_1^{(2)}$.

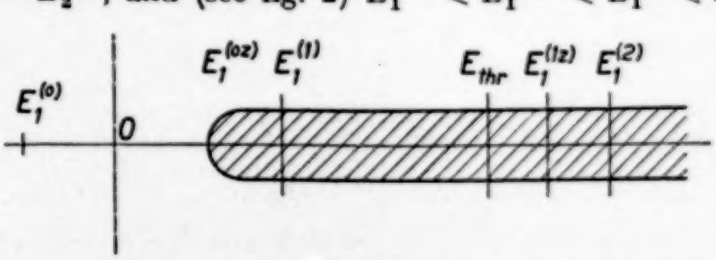

Fig. 2. Energy spectrum of the photoproduction of π^0-mesons.

We find by comparison with the energy of the threshold E_{thr} of the photoproduction process that always $E_1^{(1)} \leqq E_{\text{thr}}$, and that for energies of γ-quanta in the interval from 10 MeV up to 236.25 MeV one also has always $E_1^{(2)} > E_{\text{thr}}$. We obtain the equality $E_1^{(1)} = E_{\text{thr}}$ for the values of the momentum $\mathbf{p}$ given by

$$\mathbf{p}^2 = \tfrac{1}{4}\frac{M\mu^2}{M+\mu}, \tag{16}$$

which is a non-forward scattering ($|\mathbf{p}| \neq 0$).

We see that at least for one absolute value of the momentum, given by eq. (16), the contributions of the terms in the expansion (10) belonging to the higher quantum states are negligible. We limit ourselves to the first term in the expansion (10) which includes the deuteron or two free nucleons in the intermediate state. On account of the relations given by the isobaric structure in our process, which permit the lowest intermediate states with isobaric spin 1 — owing to the emission of neutral π-mesons — we see that the deuteron, which is an isobaric spin singlet, cannot exist as an intermediate state. Therefore, we only retain intermidiate states of the type of one neutron and one proton.

Further we shall use the relative momentum $\mathbf{p}_r$, of these two free nucleons so that for the relative mass $M_n = M_{0z}$ in (15) we simply have

$$M_{0z}^2 = M_z^2 + 4\mathbf{p}_r^2. \tag{17}$$

In terms of $M = M_z - \varepsilon$, the beginning of the continuous spectrum, we get from eq. (15), with the aid of eq. (3), the energy in the form

$$E_1^{0z} = E_p = -\frac{M\varepsilon + \beta' - \mathbf{p}^2 + 2\mathbf{p}_r^2}{\sqrt{M^2+\mathbf{p}^2}}, \quad \beta' = \frac{\varepsilon^2}{2} - \frac{\mu^2}{4}. \tag{18}$$

For these two-nucleon terms the δ-functions can be expressed in the form

$$\delta\left(\sqrt{M^2+\mathbf{p}^2} \mp E - \sqrt{M_{0z}^2+\lambda^2+t^2\mathbf{p}^2}\right) = \left|\frac{MM_z+\beta'+2\mathbf{p}_r^2}{M^2+\mathbf{p}^2}\right| \delta\left(E \pm \frac{M\varepsilon+\beta'-\mathbf{p}^2+2\mathbf{p}_r^2}{\sqrt{M^2+\mathbf{p}^2}}\right). \tag{19}$$

For our photoproduction amplitude with polarized photons we obtain in two-nucleon approximation

$$\begin{aligned} Y^{\rho'\lambda}_{\mathbf{p}',m';\mathbf{p},m}(E,\lambda\mathbf{e}) &= \sum_{\mu} e_\mu{}^{\lambda}(k) A^{\rho'\mu}_{\mathbf{p}',m';\mathbf{p},m}(E,\lambda\mathbf{e}) \\ &= \pi\left|1 - \frac{E_p}{\sqrt{M^2+\mathbf{p}^2}}\right| \sum_{\mu} \{\langle \psi^*_{-\mathbf{p},m'} J^{\rho'}(0)\psi_{0z,\lambda\mathbf{e}-t\mathbf{p}}\rangle\langle\psi^*_{0z,\lambda\mathbf{e}-t\mathbf{p}} I^{\mu}(0)\psi_{\mathbf{p},m}\rangle\delta(E+E_p) \\ &\quad - \langle\psi^*_{-\mathbf{p},m'} I^{\mu}(0)\psi_{0z,-\lambda\mathbf{e}+t\mathbf{p}}\rangle\langle\psi^*_{0z,-\lambda\mathbf{e}+t\mathbf{p}} J^{\rho'}(0)\psi_{\mathbf{p},m}\rangle\delta(E-E_p), \end{aligned} \tag{20}$$

where $A^{\rho'\lambda}_{\mathbf{p}',m';\mathbf{p},m}$ is given by the first term of the expansion (10) and can be expressed with the aid of eq. (19).

We now calculate the separate matrix elements in the photoproduction amplitude (20). Going over from Heisenberg's to Schrödinger's representation we rewrite the expression (20) in the form

$$Y^{\rho'\lambda}_{\mathbf{p}',m';\mathbf{p},m}(E,\mathbf{q}-\mathbf{p})$$
$$=\pi\left|1-\frac{E_p}{\sqrt{M^2+\mathbf{p}^2}}\right|\sum_{\mu}\{\langle-\mathbf{p},m'|j^{\rho'}(x)|\mathbf{q}-\mathbf{p},l\rangle\langle\mathbf{q}-\mathbf{p},l|i^{\mu}(x)|\mathbf{p},m\rangle\delta(E+E_p)$$
$$-\langle-\mathbf{p},m'|i^{\mu}(x)|\mathbf{p}-\mathbf{q},l\rangle\langle\mathbf{p}-\mathbf{q},l|j^{\rho'}(x)|\mathbf{p},m\rangle\delta(E-E_p). \tag{21}$$

We derive the following formula as a first approximation for the matrix elements containing the meson current, using the impulse approximation from the definition of the S-matrix [5]):

$$\langle\mathbf{q}''_{\text{in}},l|j(x)|\mathbf{p},s\rangle$$
$$=-i\frac{g\sqrt{2}}{M_z}\Big\{\int d\mathbf{x}_2\chi_z^*(\mathbf{x},\mathbf{x}_2,t)Y_lX_L\tau^1\boldsymbol{\sigma}_1\cdot\mathbf{q}'_{\text{in}}\chi_d(\mathbf{x},\mathbf{x}_2,t)Y_sX_S \tag{22}$$
$$+\int d\mathbf{x}_1\chi_z^*(\mathbf{x}_1,\mathbf{x},t)Y_lX_L\tau^1\boldsymbol{\sigma}_2\cdot\mathbf{q}'_{\text{in}}\chi_d(\mathbf{x}_1,\mathbf{x},t)Y_sX_S\Big\},$$

where

$$\mathbf{q}'_{\text{in}}=\mathbf{q}''_{\text{in}}-\mathbf{p}$$
$$\chi_d(\mathbf{x}_1,\mathbf{x}_2,t)=e^{i\mathbf{p}\cdot\mathbf{x}_c}\psi_d(\mathbf{x}_r)e^{-ip_0t},\qquad p_0=\sqrt{\left(\frac{M_z}{2}\right)^2+\mathbf{p}^2}$$
$$\chi_z(\mathbf{x}_1,\mathbf{x}_2,t)=e^{i\mathbf{q}''_{\text{in}}\cdot\mathbf{x}_c}\psi_z(\mathbf{x}_r)e^{-iq''_{0_{\text{in}}}t},\quad q''_{0_{\text{in}}}=\sqrt{M_{0z}^2+\mathbf{q}''^2_{\text{in}}}, \tag{23}$$
$$\mathbf{x}_c=\tfrac{1}{2}(\mathbf{x}_1+\mathbf{x}_2);\ \mathbf{x}_r=\mathbf{x}_1-\mathbf{x}_2.$$

The wave functions of the intermediate state, symmetrical or anti-symmetrical respectively, are given by

$$\psi_z(\mathbf{x}_r)=\frac{1}{\sqrt{2}}\{\psi'_z(\mathbf{x}_r)\pm\psi'_z(-\mathbf{x}_r)\}=\frac{1}{4\pi\sqrt{\pi}}(e^{-i\mathbf{p}_r\cdot\mathbf{x}_r}\pm e^{i\mathbf{p}_r\cdot\mathbf{x}_r}). \tag{24}$$

(19 We introduce the wave function of the deuteron in the reliable form

$$\psi_d(\mathbf{x}_r)=\left(\frac{\alpha\beta(\alpha+\beta)}{2\pi(\alpha-\beta)^2}\right)^{\frac{1}{2}}\frac{1}{|\mathbf{x}_r|}(e^{-\alpha|\mathbf{x}_r|}-e^{-\beta|\mathbf{x}_r|}), \tag{25}$$

which appears to be a good approximation for the choice of constants $\beta=6\alpha$. The individual symbols in the expressions (22), (23), (24) and (25) mean: $\mathbf{x}_r$ the relative coordinates, $\mathbf{x}_c$ the coordinates of the centre of mass, z the indices of the intermediate state, 1 the first and 2 the second nucleon, l, s the quantum numbers of the intermediate and final state respectively, $\mathbf{q}''_{\text{in}}$ the momentum of the intermediate state, Y and X the spin- and isospin functions of the state; M_z is the mass of two nucleons and $\alpha=0.32\,\mu_0$, where μ_0 is the mass of the π_0-meson.

For the matrix elements with the electromagnetic current we obtain on the basis of the impulse approximation, with the aid of the S-matrix, as a first approximation analogously the formula †

$$\begin{aligned}\langle \mathbf{q}''_{\mathrm{in}}, l|i^{\mu}(x)|\mathbf{p}, s\rangle &\approx \langle \mathbf{q}''_{\mathrm{in}}, l|i^{j}(x)|\mathbf{p}, s\rangle \\ &= i\int \mathrm{d}\mathbf{x}_2 \chi_z^*(\mathbf{x}, \mathbf{x}_2, t) Y_l X_L \left\{\frac{2e}{M_z}\frac{\partial}{\partial x_j}\left(\tfrac{1}{2}-t_{\zeta_1}\right)+[\boldsymbol{\sigma}_1\times\mathbf{k}]_j\mu_1\right\} \\ &\times \chi_d(\mathbf{x}, \mathbf{x}_2, t) Y_s X_S + i\int \mathrm{d}\mathbf{x}_1 \chi_z^*(\mathbf{x}_1, \mathbf{x}, t) Y_l X_L \\ &\times \left\{\frac{2e}{M_z}\frac{\partial}{\partial x_j}\left(\tfrac{1}{2}-t_{\zeta_2}\right)+[\boldsymbol{\sigma}_2\times\mathbf{k}]_j\mu_2\right\} \chi_d(\mathbf{x}_1, \mathbf{x}, t) Y_s X_S, \quad j=1,2,3,\end{aligned} \tag{26}$$

where

$$\begin{aligned}\mu_1 &= \mu_{\mathrm{p}}\left(\tfrac{1}{2}-t_{\zeta_1}\right)+\mu_{\mathrm{n}}\left(\tfrac{1}{2}+t_{\zeta_1}\right), \\ \mu_2 &= \mu_{\mathrm{p}}\left(\tfrac{1}{2}-t_{\zeta_2}\right)+\mu_{\mathrm{n}}\left(\tfrac{1}{2}+t_{\zeta_2}\right),\end{aligned} \qquad t_{\zeta_i} = \begin{cases} \tfrac{1}{2} \text{ for a neutron,} \\ -\tfrac{1}{2} \text{ for a proton.}\end{cases} \tag{27}$$

Here, t_{ζ_i} denotes the eigenvalue of the z-component of the isobaric spin of the i-th nucleon, $j = 1, 2, 3$, and other symbols have the same meaning as in eq. (22).

Inserting the expressions (22) and (26) in the photoproduction amplitude (21), for $x = 0$, after performing the operation of the spin matrices $\boldsymbol{\sigma}(\sigma_{+1}\sigma_{-1}\sigma_0)$

$$\sigma_0{}^{1,2}Y_{1,0} = Y_{0,0}\cdots \tag{28}$$

and of the matrices of isobaric spin

$$\tau_0{}^{1,2}X_{0,0} = \pm X_{1,0}, \tag{29}$$

we sum over the spin-functions Y and isospin-functions X. We obtain simpler results, to which we restrict ourselves, in the case of deuterons with spin perpendicularly polarized to the direction of the propagation of meson and photon. The first expressions between braces in eq. (26) vanish in this case after summing over spin- and isospin-functions. Physically this case is realizable by placing the deuteron target in a magnetic field. We shall not take into account the polarization of the deuteron spins in the direction of propagation of the π^0-mesons. Then the photoproduction amplitude of deuterons with spin perpendicularly polarized ro the direction of propagation of mesons is obtained after carrying out the above operations and summing over μ, in the form

$$Y^{\rho'\lambda}_{\mathbf{p}', m'; \mathbf{p}, m}(E, \lambda\mathbf{e}) = \pi\left|1-\frac{E_p}{\sqrt{M^2+\mathbf{p}^2}}\right| B^0(E, \mathbf{p}-\mathbf{q})(\delta(E+E_p)-\delta(E-E_p)), \tag{30}$$

† The non-relativistic interaction Hamiltonian was used as a starting point for the dirvation of this formula in ref. [7]). For the possibility of deriving the formula (26) in the form indicated, the author is indebted to Dr. F. Kaschluhn.

where

$$B^0(E, \mathbf{p}-\mathbf{q}) = \frac{2g\sqrt{2}}{M_s}\mathbf{q}(-\mathbf{i}^2k_y+\mathbf{j}^2k_x)(\mu_p-\mu_n)I(\mathbf{q})I(\mathbf{k})$$

and

$$I(\mathbf{u}) = \int \psi_d(\mathbf{x}_r)\psi_{s\,sym}(\mathbf{x}_r)\cos(\tfrac{1}{2}\mathbf{u}\cdot\mathbf{x}_r)d\mathbf{x}_r, \tag{31}$$

where E_p denotes the energy given by the expression (18) with the only difference that the quantity β' is now equal to

$$\beta' = \frac{\varepsilon^2}{2} - \frac{\tau}{4} \tag{32}$$

with analytical continuation on the real axis ($\tau \to \mu^2$). In the argument of the function B^0 (where ^{0} means the value of the projection of the spin on the direction of propagation of the meson), the difference of momenta $\mathbf{p}-\mathbf{q}$ will go over into the difference $t\mathbf{p}-\lambda\mathbf{e}$.

The value of the integral (30) is given by

$$I(\mathbf{u}) = \frac{(\frac{1}{2}\alpha\beta(\alpha+\beta))^{\frac{1}{2}}}{\pi(\alpha-\beta)}\left\{\frac{1}{\alpha^2+g_+^{\,2}} - \frac{1}{\beta^2+g_+^{\,2}} + \frac{1}{\alpha^2+g_-^{\,2}} - \frac{1}{\beta^2+g_-^{\,2}}\right\}, \tag{33}$$

$$g_\pm^{\,2} = |\mathbf{p}_r \pm \tfrac{1}{2}\mathbf{u}|^2. \tag{34}$$

5. Dispersion Relations

In order to derive † the dispersion relations we pay closer attention to the photoproduction amplitude (30) for deuterons perpendicularly polarized to the direction of mesons, which is an odd function and which we shall use in the following.

For negative values of the energy E_p only the first δ-function contributes to the expression (30), and for positive values only the second δ-function. The energy E_p reaches its maximum for the value $\mathbf{p}_r = 0$ of the relative momentum:

$$E_p^{\max} = \frac{M\varepsilon+\beta-\mathbf{p}^2}{\sqrt{M^2+\mathbf{p}^2}}. \tag{35}$$

For the value of the momentum

$$\mathbf{p}_r^{\,2} = \tfrac{1}{2}(M\varepsilon+\beta-\mathbf{p}^2) = P'^2 \tag{36}$$

the energy E_p vanishes.

† See ref. [3]), chapter VI.

For the values of the momentum $\mathbf{p}_r^2$ in the interval

$$0 < \mathbf{p}_r^2 < P'^2$$

the energy E_p runs through positive values in the interval

$$E_p^{\max} > E_p > 0$$

and therefore only the second δ-function makes a contribution.
For the values $\mathbf{p}_r^2 > P'^2$, the quantity E_p is negative and therefore only the first δ-function contributes in the whole region

$$E_{\text{thr}} < E_p < 0,$$

while the relative momenta $\mathbf{p}_r^2$ run through values in the interval

$$P'^2 < \mathbf{p}_r^2 < P^2,$$

where P^2 is the value of the relative momentum $\mathbf{p}_r^2$ for which

$$E_{\text{thr}} = -E_p. \tag{37}$$

For the special case of the deuteron momentum

$$\mathbf{p}^2 = \tfrac{1}{4}\mu^2 \frac{M}{M+\mu}$$

we obtain the above values of the momenta P and P' in the form

$$\begin{aligned} P'^2 &= -\tfrac{1}{4}\mu^2 \frac{2M+\mu}{M+\mu} + \tfrac{1}{2}\varepsilon(M+\varepsilon) \\ P^2 &= \frac{\mu-\varepsilon}{2}\left(M + \frac{\mu+\varepsilon}{2}\right) = 7.0797\,\mu_0^2. \end{aligned} \tag{38}$$

On account of the fact that there always exists an interval of definite length on the boundary of the region, Im $E = 0$ (the real axis), we can regard the function Y as the only one with a branch line on the real axis. The dispersion relations for the photoproduction of π^0-mesons on deuterons perpendicularly polarized to the direction of propagation of the mesons can then be written

$$\begin{aligned} D^0(E,\tau) - D^0(E_0,\tau) = \frac{2}{\pi}(E^2-E_0^2)\mathrm{P}\Bigg[&\int_{|E_{\min}(\tau)|}^{\infty} \mathrm{d}E' \frac{E'Y(E',\tau)}{(E'^2-E^2)(E'^2-E_0^2)} \\ &+ \int_{|E_{\max}(\tau)|}^{E_{\min}(\tau)|} \mathrm{d}E' \frac{E'Y(E',\tau)}{(E'^2-E^2)(E'^2-E_0^2)}\Bigg], \end{aligned} \tag{39}$$

where

$$E_{\min}(\tau) = \frac{\tau-\mu^2}{4\sqrt{M^2+\mathbf{p}^2}} - \frac{\mathbf{p}^2+\frac{1}{4}\mu^2}{|\mathbf{p}|}, \tag{40a}$$

$$E_{\max}(\tau) = -\frac{M\varepsilon+\beta'-\mathbf{p}^2}{\sqrt{M^2+\mathbf{p}^2}}, \tag{40b}$$

and where the other symbols denote: D^0 the hermitic part of the amplitude for deuterons, $Y(E', \tau)$ the antihermitic part (the odd function), P the principal value of the integral, E_0 the energy, which we choose equal to the mass of the π^0-meson μ. The first integral is related to the observable region from the energy $E_{\min}$ to infinity. The second integral falls into the unobservable region with imaginary momenta and may be expressed by means of the Bogolyubov method. This integral is a function of the energy E only and can be determined separately.

For the special value of the deuteron momentum given by eq. (16), for which the expression for the photoproduction amplitude in the two-nucleon approximation is valid, the dispersion relations for photoproduction of mesons on deuterons perpendicularly polarized to the direction of propagation of the π^0-mesons takes the form

$$D(E)-D(\mu) = \frac{2}{\pi}\,\mathbf{q}^2\,\mathrm{P}\int_{\mu}^{\frac{2M+\mu}{2\sqrt{M^2+M\mu}}\infty} \mathrm{d}E'\,\frac{E' Y^{\rho'\lambda}_{\mathbf{p}',m;\,\mathbf{p},m}(E')}{(E'^2-E^2)(E'^2-\mu^2)} + J(E), \tag{41}$$

where

$$\mathbf{q}^2 = E^2-\mu^2$$

and where the photoproduction amplitude $Y^{\rho'\lambda}_{\mathbf{p},m;\,\mathbf{p},m}(E')$ is given by the expression (30).

The expression $J(E)$ which comes from the unobservable region is given by the integral

$$J(E) = \frac{g4\sqrt{2}}{M_s}\,(\mu_{\mathrm{p}}-\mu_{\mathrm{n}})\,\mathbf{q}^2\,\mathrm{P}\int_0^P (-\mathbf{i}^2 k_y+\mathbf{j}^2 k_x)\left|1-\frac{E_p(\tau)}{\sqrt{M^2+\mathbf{p}^2}}\right| \times \frac{\mathbf{q}''}{\mathbf{q}'^2}\,\frac{E_p(\tau)}{E^2-E_p^{\,2}(\tau)}\,I(\mathbf{q})I(\mathbf{k})\mathrm{d}\mathbf{p}, \tag{42}$$

where g is the coupling constant,

$$\mathbf{q}'^2 = E_p^{\,2}(\tau)-\mu^2, \quad \mathbf{q}''^2 = E_p^{\,2}(\tau)-\tau > 0, \tag{43}$$

$P = 2.6608\,\mu_0$ and $I(\mathbf{q})$ and $I(\mathbf{k})$ are given by the expression (33).

In conclusion the author would like to thank Prof. N. N. Bogolyubov for his interest throughout the work, Dr. A. A. Logunov and J. Fischer for numerous useful remarks. The author is especially indebted to Dr. F. Kaschluhn for longer discusions and criticism.

References

1) G. F. Chew, H. W. Lewis, Phys. Rev. **84** (1951) 779;
H. Fesbach and M. Lax, Phys. Rev. **88** (1952) 509
2) D. V. Shirkov, Annual International Conference on High Energy Physics (Interscience Publishers, New York 1959)
3) N. N. Bogolyubov, B. V. Medvedev and M. L. Polivanov, Problems of the Theory of Dispersion Relations (Gosizdat phys. mat. lit. ,Moscow 1958); abridged German translation by F. Kaschluhn, Fortschr. d. Phys. **6** (1958) 169
4) A. A. Logunov, A. M. Tavchelidze and L. D. Solovyev, Nuclear Physics **4** (1957) 427; see also E. Corinaldesi, Nuovo Cim. **4** (1956) 1384
5) F. Kaschluhn, Zeitschr. f. Naturforschung 13a (1958) 183; Nuclear Physics **5** (1958) 303
6) N. N. Bogolyubov and D. V. Shirkov, Introduction to the Quantum Field Theory (GITTL, Moscow 1957) p. 383; see also G. F. Chew, F. E. Low, M. L. Goldberger and Y. Nambu, Phys. Rev. **106** (1957) 1345
7) W. M. MacDonald, Phys. Rev. **98** (1955) 60

10.D *Nuclear Physics* **26** (1961) 693—698; © *North-Holland Publishing Co., Amsterdam*

BOOK REVIEWS

A. M. BALDIN, V. I. GOL'DANSKII and I. L. ROZENTHAL, *Kinematics of nuclear reactions* (Pergamon Press, Oxford 1961, xiii–303 p. 42s.)

This book is a translation (by W. E. Jones) of the original russian volume: Kinematika yadernykh reaktsii (Moskva, Fizmatgiz, 1959). The reproduction is made by photo-lithography of a typed text with letter press setting of the formulae. The book is by this way of reproduction rather heavy to read. Since, however, the general character of the book is that of a handbook, which one does not read from beginning to end, this is no serious drawback. The text and the formulae are legible except perhaps in one or two places.

The book covers a subject which is more extensive than one would think from the title. In fact it is a rather comprehensive treatment of the consequences of the conservation laws on reactions and decays of elementary particles.

The subject is divided into three almost equal parts. The first part is an exposition of the consequences of energy and momentum conservation for interactions between relativistic particles. In the first chapters one finds the general theory including the important transformation formulae between the laboratory system and the centre of mass system. Then a large number of examples are treated in detail. These are conveniently classified according to the number of secondary particles and include also an exposition of Fermi's statistical theory of multiple processes.

The second part of the book is devoted to the quantal description of non-relativistic nuclear reactions. The treatment is based on the S-matrix formalism. The first chapters in this part deal with the definition and the properties of the S-matrix. In the following chapters the theory is applied to collisions between particles possessing spin, to polarization of particles and finally to processes involving photons.

The third part of the book is an appendix containing a large number of graphs and tables which are important for the practical application of the formulae and theory of the text to specific problems of nuclear reactions.

The book is especially written for experimental physicists and will probably prove to be a very useful source of reference. The force of the treatment lies in the wealth of explicit calculations which are carried through to the bitter end, and also in the graphical construction methods which are presented. A small drawback is the lack of an index.

Aage Winther.

A. B. MCINTOSH and T. J. HEAL (Editors), *Materials for Nuclear Engineers* (Temple Press Limited, London, 1960. ix-373 p. 75s.)

The basis of this book is a number of articles on nuclear materials formerly published in 'Nuclear Engineering Magazine'.

Since the first publication of these articles, volumes of new information have been made available, especially from the Second Geneva Conference. This relatively new information has been incorporated; thus the book is considered to cover the engineering properties of specially selected nuclear materials up to mid 1959. Since the book is prepared by competent authorities connected with the United Kingdom Nuclear Energy Programme, only nuclear materials of direct interest to the present British programme are discussed, with particular emphasis on materials for gas cooled reactors.

The following topics are treated: Uranium, Plutonium, Thorium, Ceramic Fuels, Graphite, Magnesium, Beryllium and Zirconium. These materials are discussed according to the following scheme; occurrence and extraction, physical and mechanical properties, compatibility, fabrication and behaviour under reactor conditions. Each chapter is followed by an appendix surveying in

tables the properties of the materials. Due to this presentation, the book appears very readable and gives a clear view of the materials themselves plus a comparison between them.

The book in general can be considered as a good engineering reference source for the materials selected. Besides the basic data, limited theoretical discussions are included, which greatly advance the interest and usefulness of the book.

Niels Hansen

C. R. TIPTON, JR. (Editor), *Reactor Handbook*, Second edition, revised and enlarged, vol. 1: Materials (Interscience Publishers, Inc. New York, 1960. xv–1207 p. $ 36.50)

Reactor Handbook is a revised and enlarged edition of "General Properties of Materials, The Reactor Handbook, vol. 3", published in 1955 by U. S. AEC as AECD–3647.

In fact, the new handbook can be regarded as an original publication due to the expansion of nearly all subjects together with the addition of many new topics. Many new authors selected among the specialists in the United States have contributed to the work.

In contrast to the first handbook, the new edition is divided into chapters covering the materials after their function in the reactor, thus fuel materials, cladding and structural materials, and control, moderator, coolant and shielding materials. Due to this concept, the handbook includes gases, liquids and solids, contrary to the former handbook, which exclusively treated solids. This new concept makes the handbook valuable as an overall introduction to the field of nuclear materials.

The handbook is current up to spring 1958, thus references to the Second Geneva Conference have not been made. The lack of such references must be regarded as a drawback, but apart from this lack, the handbook includes satisfactory lists of references.

Another objection is the lack of summary tables covering the general physical properties of materials. As an appendix, a compilation of constitutional diagrammes of binary alloy systems is included.

Apart from the above mentioned objections, the handbook can be regarded as an extremely well-planned and well-written contribution to the literature in the field of nuclear materials.

The handbook can be considered useful for those working in the field, and as an overall introduction, due to its coverage of nuclear engineering data, its general topics and its extended reference information.

Niels Hansen

J. H. SANDERS, *The Fundamental Atomic Constants* (Clarendon Press: Oxford University Press, London, 1961. vi–88 p. 10s.)

The present monograph, belonging to the Oxford Library of the Physical Sciences, gives an up-to-date summary of the measurements of the fundamental constants of atomic physics, and of the methods of adjustment by which a consistent set of values for these constants can be derived (or, as was the case at early stages, inconsistencies can be disclosed and tracked down to their origin). The author modestly confines himself to the reporting of the methods and results, while refraining from independent criticism. A valuable feature of the booklet is the very complete survey (with accurate references) of the early measurements.

L. R.

J. E. DRUMMOND, *Plasma Physics* (McGraw-Hill Book Co., New York, 1961. xiv–386 p. 97s.)

This book is a collection of essays written by eminent specialists on the various aspects of plasma physics. Most of the contributors describe work mainly carried out in the United States, but there is an important chapter on the brilliant contribution of the Soviet physicists, written especially for this book by two of them. The book is very carefully edited by Dr. Drummond, who has supplied an introductory chapter surveying the history and present status of the whole field. As a result, as Dr. Drummond points out in the preface, the material here assembled, when read

in a definite sequence, provides a suitable text for graduate students. Altogether an authoritative, excellently produced, introduction into the most fundamental aspects and latest developments of the subject.

L. R.

C. SANCHEZ DEL RIO, *Fundamentos teóricos de la física atómica y nuclear* (Servicio de Publicaciones de la Junta de Energia Nuclear, Madrid, 1960. viii–167 p.)

A competently written, but very elementary introduction into the main ideas and methods of theoretical nuclear physics. The author says it contains the matter of a course he has to give to engineers and other groups of non-physicists engaged in nuclear energy work, as well as to university students in physics. It is refreshing to see that the pressure of the times is so great as to force for modern science a modest entrance even into those parts of the world which had remained closed to it. In comparison with the high level attained by the literature is this domain in Latin America, a book like this is, indeed, a revealing testimony to the backwardness in which obscurantism and tyranny have plunged the unhappy country from which it comes.

L. R.

J. B. MARION, 1960 *Nuclear Data Tables*, part III (U.S. Government Printing Office, Washington D.C., 1960. xi–181 p. $ 1.25)

The general programme of this series was outlined in the review of the first issue (this journal **12** (1959) 220). In 1960, four parts have been published, of which this is the third. The material it contains has been compiled by J. B. Marion, of the University of Maryland, from widely scattered sources. It thus assembles in a most convenient form a large variety of auxiliary graphs used in the interpretation of nuclear reaction data.

In the review quoted above, I pointed out the desirability for the Nuclear Data Group, which is rendering such excellent service to the community of physicists, to conform in the use of symbols and units to the recommendations of the SUN Commission, whose efforts are no less praiseworthy. This appeal is here repeated as a *delenda Carthago*.

L. R.

Summer course in plasma physics (Danish Atomic Energy Commission, Roskilde, Denmark. 1960. viii–645 p. D. kr. 60.00)

In this bulky report the essential material of the lectures held at the International Summer Course in Plasma physics in 1960 has been collected and published in a very efficient way. In particular, we are not only given transcripts of the lectures (reproduced as typescripts) but also reproductions of published papers bearing on the matters treated in the course. This enhances the usefulness of this publication as a source of reference.

The domain covered by the course is very wide indeed: one may well wonder in what degree of exhaustion the most conscientious participants emerged from the ordeal. An enumeration of the main headings will give an idea of the wealth of information packed in this report: single particle motion, magneto-hydrodynamics, fundamental equations, stability, relaxation, radiation, thermonuclear aspects, pinch and shock, apparatus concepts, plasma waves and diagnostics. Each topic is discussed in a series of lectures of varying length (often by different lecturers) and the treatment is detailed and accurate.

The organizers of the course, headed by Prof. O. Kofoed-Hansen, and the editor of the report, Dr. C. F. Wandel, must be congratulated for a most successful contribution to the survey of a rapidly expanding new field of fundamental research.

L. R.

J. L. DELCROIX, *Introduction to the Theory of Ionized Gases* (Interscience Publishing Co., London, 1960. xi–149 p.).

J. F. DENISSE et J. L. DELCROIX, *Théorie des ondes dans les plasmas* (Dunod, Paris, 1961. xii–167 p. 16 NF)

Two excellent pocket-books which will be valuable not only to students, but also to research workers. With admirable concision and clarity they manage to present a remarkably complete view of the essential phenomena in weakly or strongly ionized gases, and a systematic discussion of the various types of plasma oscillations over the whole frequency range, which is especially illuminating.

The American book, an Interscience tract, is a translation of a French original belonging to the same series as the second book (which would equally deserve to be translated). The latter series (the "Monographies Dunod") renders to the French readers the same outstanding service as the Interscience tracts to the English-reading public.

Spitzer's earlier tract on fully ionized gases is supplementary to Delcroix' treatise.

L. R.

J. GORTER (Editor), *Progress in Low Temperature Physics*, Vol. III (North-Holland Publishing Company, Amsterdam, 1961. xii–495 p. 48 guilders)

The third volume of this well-known series is packed with material of fascinating interest. The three first chapters discuss special problems regarding liquid He II, the next two are concerned with He^3. Then comes a long chapter on recent developments in superconductivity, followed by others on electron resonances in metals, orientation of atomic nuclei, solid state masers, the equation of state and transport properties of H^2 and some solid-gas equilibria. All the authors are well-known experts in their respective fields who, as well as the editor, deserve our gratitude for their unselfish devotion in providing us with a most helpful guidance in a many-sided domain of active research.

L. R.

Reactors of the World (second series) (Temple Press Ltd., London, 1961. 13 cutaway drawings, 17s. 6d).

The literature of nuclear engineering in its many-sided expansion has reached the stage of including also picture-books. The present one is a collection (the second to be issued) of drawings of 13 typical reactors originally published in Nuclear Engineering. These large perspective drawings, although very detailed, are amazingly clear and most of them also aesthetically pleasing. In some cases, use has been made of gaudy colouring to enhance the intelligibility. To each drawings a data sheet is appended. This technique of synthetic representation of complicated assemblies is highly successful in helping the layman to vizualize them, and is no doubt also a useful auxiliary for the design engineers.

L. R.

S. D. DRELL and F. ZACHARIASEN, *Electromagnetic Structure of Nucleons* (Clarendon Press: Oxford University Press, London, 1961. 110 p. 12/6)

This monograph is a valuable addition to the Oxford Library of the Physical Sciences. It gives a clear and complete survey of the present state of the problem of nucleon structure, including a detailed account of the use of dispersion relations in this problem.

The notes, many of which are essential to the intelligence of the text (and would have better been incorporated into it) are printed at the end of the volume, mixed up with mere bibliographical references. This is a thoroughly bad procedure, which the Oxford Press ought not to have tolerated.

L. R.

INSTRUCTIONS TO CONTRIBUTORS

In order to facilitate the preparation of typescripts, we show on pp. 706 and 707 two model pages of such a typescript. In a general way, contributors are invited to follow the recommendations of the Document U.I.P. 6 (1955) (Symbols and Units) of the S.U.N. Commission of the I.U.P.A.P. (published in *Nuclear Physics* **1** (1956) 539) with the subsequent additions and corrections. For their convenience, the main conventions to which attention should be paid are repeated in the following instructions.

GENERAL

Manuscripts may be written in English, French or German. They should be *typewritten first copies* (or *very clear* preprints) with a wide margin and ample space between the lines, also in abstracts, footnotes and references. *All* pages should be numbered (also those containing references, tables and figure captions).

In the text, no reference should be made to page numbers; if necessary, one can refer to section or subsection numbers.

TITLE

Avoid long titles. In the typescript ordinary lettertype should be used as shown in the model; the printer is instructed how to proceed. After a title (or a subtitle) there should be *no period.*

SUBTITLES

Sections and subsections should *always* have a *number* (use arabic numerals) and a *title* (use ordinary typescript, not capitals), except when the manuscript is a very short note. These subtitles should again be short, but should normally not contain only symbols. E.g. one should write as the title of a section:

4. Experimental results, and as the title of a subsection: 4.1. The nucleus Zn^{69} (in preference to: 4.1. Zn^{69}).

ABSTRACT

The text of a paper should *always* be preceded by an abstract, which should be written *in English*, irrespectively of the language used in the main body of the paper. The abstract should be *short*, but should mention all essential points of the paper. It should contain important new quantitative results, but no extensive tables or complicated formulae.

FOOTNOTES AND REFERENCES

A sharp distinction should be made between footnotes and references. While the former are printed at the foot of the page, the latter will appear in a list at the end of the paper. Such a list may only contain bare references to publications, and **no comment or remark on these publications;** any such remark should be either included in the text or put in a footnote.

FOOTNOTES

Avoid footnotes as far as possible. In any case, they should be short and *never* contain any important part of an argument or any complicated formulae. Footnotes must *not* be numbered, but indicated by the following signs: †, ††, ‡, ‡‡ (starting anew on each page). **Avoid appending a footnote sign to a symbol, a formula, a formula number, or a title or subtitle**. In the typescript, footnotes must be typed (as shown in the model) on the sheet to which they belong and in the same wide spacing as the text.

REFERENCES

All references to the literature must be listed on separate sheets (wide spacing!). They must be numbered in the way indicated in the model. Note the style (and punctuation) adopted for journals [*n*) author, journal volume (year) page], and for books [*m*) author, title (publisher, place, year) chapter, page]; no capitals or italics should be used and initials of names should come first. In the list there should be no period at the end of each number; a semicolon is inserted between references under the same number. Reference *n*) of the list is quoted in the text or the footnotes explicitly as: ref. [n]), or implicitly as: [n]). If several references are quoted simultaneously, one should use: refs. [n, m]), or: [n, m]).

Do not append reference numbers to a number, a symbol, a formula, or a title or subtitle. Thus, do not write: the quantity Q[5]), but: the quantity[5]) Q, or: the quantity Q (ref. [5])).

FIGURES

The drawings for the figures must be on separate sheets, drawn in Indian ink in large size and carefully lettered. The lettering as well as all other details should be *of properly proportionate dimensions*, so as not to become illegible or unclear when the drawings are reduced in size for printing. In the lettering, special

attention should be paid to the rules for indicating units; do not unnecessarily use capitals or italics. The utmost care should be taken in the preparation of drawings, as changes in proof cause delay, confusion and costly new printing plates!

The drawings should not contain any text that is not an essential part of the figure. The title of the figure and all relevant explanations should be collected in a figure caption (see below). However, brief explanations of symbols not usually found among printing types may be included in the drawing.

All drawings should have wide margins, so as to enable the editorial staff to give the necessary indications; each drawing should be marked with the number of the figure and an (abbreviated) mention of authors and title of the paper.

All figures must have a number and a caption. **The captions must be typed on a separate sheet,** and never on the sheets containing the drawings.

In the text of the manuscript, figures are referred to as: See fig. 1, or: In figs. 2 and 3 . . ., etc. (*no capitals*), whereas the approximate place of the figures should be indicated in pencil in the margin.

TABLES

The exact place of tables, just as that of the figures, cannot be fixed in advance; therefore, they should not be part of the running text of the manuscript, but **must be typed on separate sheets.** Tables must have a number (in arabic numerals) and a title. In the text of the manuscript, they are referred to as: In tables 4 and 5, . . . (no capitals); their approximate place should be indicated in pencil in the margin.

Footnotes to a table, to be printed directly below the table, are not indicated with the ordinary footnote signs, but rather as: [a]), [b, c]), etc.

FORMULAE IN THE TEXT

Avoid superposition of symbols (fractions or complicated exponents) which would necessitate increased spacing of lines; when superposition cannot be avoided, place the expression on a separate line. The following list contains the most usual cases.

Use	Do *not* use
a/b, $\mathrm{d}x/\mathrm{d}t$	$\frac{a}{b}$, $\frac{\mathrm{d}x}{\mathrm{d}t}$
$\sum_{i=1}^{n} A_i$	$\sum_{i=1}^{n} A_i$
$\int_a^b y\mathrm{d}x$	$\int_a^b y\mathrm{d}x$
$(a^2-b^2)^{\frac{1}{2}}$ or $\sqrt{(a^2-b^2)}$	$\sqrt{a^2-b^2}$
$\exp(-x^2)$	e^{-x^2}

In using the solidus, care should be taken to avoid ambiguities by inserting brackets.

There are special rules for numerical fractions (see below).

DISPLAYED FORMULAE

Do not type displayed formulae. Write them in *large size* and *very distinctly.* (Please instruct your typist to leave a large amount of space for the filling in of formulae.) The "solidus" and "exp" rules may be relaxed, in order to secure easier legibility. *Punctuation* should be used after a displayed formula as if the formula were not displayed; do not put superfluous colons(:) at the end of the text preceding a displayed formula. *Please define symbols and notation in a careful and orderly manner!*

Long and complicated formulae should be carefully written on a separate sheet, like tables or figures. *Remember that the compositor cannot guess any illegible symbol, since he does not understand the formula!* If you cannot write legibly, let somebody else do it for you!

NUMERICAL FRACTIONS

In numerical fractions, both in formulae in the text and in displayed formulae, the solidus should never be used. These fractions are always printed in small type as $\frac{1}{2}$, $\frac{3}{4}$, $\frac{171}{2349}$, etc.

Write	Do *not* write
$\frac{1}{2}\pi$	$\frac{\pi}{2}$ or $\pi/2$
$\frac{8}{27}\ln x$	$\frac{8\ln x}{27}$ or $8\ln x/27$
$\frac{1}{2}(n-1)$	$\frac{n-1}{2}$ or $(n-1)/2$
$2s_{\frac{1}{2}}$	$2s_{1/2}$

NUMBERED FORMULAE

The numbers of formulae should be placed at the right-hand end of the line or lines containing the formula.

Formulae **must not be referred to by the number alone,** but by this number preceded by eq. (not Eq.) for equation (or some other word, such as formula, expression, etc., if equation is inappropriate), e.g.: Substituting expression (12) into eqs. (5) and (6), ...

SYMBOLS

(1) Symbols of scalar quantities are printed in *italics* and must be underlined in the text of the typescript. In displayed formulae, however, this is not necessary.

(2) Vectors are printed in clarendon (bold face), indicated by wavy underlining in the typescript (both in the text and in displayed formulae!), as is shown in the model typescript. *Do not use arrows* to indicate vectors.

(3) All letters or groups of letters indicating *standard functions* or *mathematical operations* (exp x, e^x, sin x, log x, ln x, dx, . . .), *units* (cm, GeV, . . .), *chemical symbols*, *abbreviations* or *anything not a quantity* (n = neutron, p = proton, d = deuteron; E2, M1 and other multipole symbols, $^2S_{\frac{1}{2}}$-state, s-, p-, d-shell, etc.) are printed in ordinary type and must be left in the typescript without any abbreviation mark.

Symbols or names of units should never have the plural mark.

Use	Do *not* use
The quantities Q are . . .	The Q's are . . .
5 cm	5 cm., 5 cms
7 V	7 V., 7 volts

(4) The same rules apply also to superscripts and subscripts.

(5) Conform to recommendations of international scientific bodies. **A list of units in frequent use is printed below.**

(6) In the description of apparatus and experimental arrangements all dimensions and other quantitative indications should be given *in metric units* (do *not* use inches).

(7) **Do not begin a sentence with a symbol:** phrase the sentence in such a way that the symbol be preceded by some appropriate word. Thus, do *not* write: J is the angular momentum, but : Here, J denotes the angular momentum, or some such phrase not beginning with J. Likewise, instead of: N reaches a maximum . . ., write: The quantity N reaches . . ., or: The function N reaches . . . . Avoid monstrosities like: In P, f is a factor. . ., or: For Ca^{45}, $T_{\frac{1}{2}} = 160$ d.

Also, do not use superfluous commas; write: The proton energy E_p is . . ., instead of: The proton energy, E_p, is . . . .

(8) All Greek letters should be underlined in red in the manuscript. Explain unusual symbols (e.g., script letters) in pencil in the margin. If necessary, supply a list of symbols with explanations on a separate sheet. In writing,

be especially careful to avoid confusion between Greek letters and italics, or between capitals and lower-case letters, such as:

$K\ k\ \kappa\ h$	$\Psi\ \psi$
$V\ v\ \nu$	$\Phi\ \phi$
$U\ u\ \mu$	$\Theta\ \theta$
$W\ w\ \omega$	$S\ s$
$P\ p\ \rho$	$C\ c$
$X\ x\ \chi$ × (times)	$O\ o$ 0(zero)
δ ∂(partial differential)	$Z\ z$ 2
α ∝(proportional to)	l 1(one)
$I\ \mathcal{I}\ J\ \mathcal{J}$	$x^1\ x'$

(9) In decimal numbers use a point (*not* a comma) to mark the position of the units. To facilitate the reading of large numbers some extra-space (but no comma or point) may be inserted between groups of three numerals. Thus, one should write: 5102.9 or 5 102.9, *but in no case*: 5,102.9 or 5.102,9. Note also: 0.67, not: .67!

(10) Although the officially recommended notation for chemical elements, with the mass number as a left superscript (e.g. ^{14}N), is undoubtedly the best, the right superscript (N^{14}) is tolerated.

MATHEMATICAL SYMBOLS

To indicate	Use	Do *not* use
a is approximately equal to b	$a \approx b$	$a \sim b$
a is asymptotically equal to b	$a \sim b$	$a \simeq b$
a is of the order of magnitude b	$a = \mathrm{O}(b)$	$a \sim b$
a is proportional to b	$a \propto b$	$a \sim b$
dyadic product of two vectors **a** and **b**	**a b**	
scalar product of **a** and **b**	**a** · **b**	(**ab**), **a**×**b**
vector product of **a** and **b**	**a** ∧ **b**, **a**×**b**	[**ab**]
natural logarithm of x	log x, ln x	lg x
decadic logarithm of x	$\log_{10} x$	log x
sine of x	sin x	Sin x
cosine of x	cos x	Cos x
tangent of x	tg x	tan x
arc tangent of x	arc tg x	$\tan^{-1} x$
hermitian conjugate of matrix A	$A^\dagger$	A^*
complex conjugate of matrix A	A^*	$\bar{A}$
trace of matrix A	tr A, Tr A	Sp A, Spur A

SYMBOLS FOR PREFIXES

deci	10^{-1}	d	kilo	10^{3}	k
centi	10^{-2}	c	mega	10^{6}	M
milli	10^{-3}	m	giga	10^{9}	G
micro	10^{-6}	μ	tera	10^{12}	T
nano	10^{-9}	n			
pico	10^{-12}	p			
femto [a])	10^{-15}	f			
atto [a])	10^{-18}	a			

[a]) Introduced in 1960 by the I.U.P.A.P.

UNITS IN FREQUENT USE

Name	Use	Do *not* use
centimeter	cm	cm.
micrometer	μm	μ
femtometer	fm	*f*, fermi
ångström	Å	A
square centimeter	cm^2	sq. cm.
barn ($\equiv 10^{-24}$ cm^2)	b	
liter	l	
radian	rad	
steradian	sr	sterad.
second	s, sec	
minute	min	m
hour	h	hr
day	d	
year	y	a
gram	g	gm
milligram	mg	
atmosphere	atm	atmos
hertz	Hz	c/sec
kilohertz	kHz	Kc/sec
oersted	Oe	oe
gauss	G	
volt	V	v
ampere	A	amp
coulomb	C	coul
curie	Cur	c, C
microcurie	μCur	μc, μC
electronvolt	eV	ev
kiloelectronvolt	keV	Kev, kev
megaelectronvolt	MeV	Mev
gigaelectronvolt	GeV	Bev

COMPOSITE UNITS

In products of units, a multiplication dot should be used in the middle of the line, like in: $g \cdot cm^{-2}$, $MeV \cdot b$.

Of course, g/cm^2 and mb/sr are just as good as $g \cdot cm^{-2}$ and $mb \cdot sr^{-1}$, but in more complicated expressions the use of negative exponents may be preferable to the use of the solidus. Never write: $counts/cm^2/sec$, but: $counts/cm^2 \cdot sec$.

THE BASLE CONVENTION

In Basle (1960), international agreement has been reached upon the following sign convention for particle polarization:

If $\mathbf{k}_1$ represents the propagation vector of the incident particle and $\mathbf{k}_0$ the propagation vector of the outgoing particle, particles with spin pointing in the direction $\mathbf{k}_1 \times \mathbf{k}_0$ are to be considered as having positive polarization.

NOMENCLATURE

Since the nomenclature in the field of nuclear physics is not yet quite unified and a number of illogical expressions are unfortunately still widely used, it is advisable to give the following indications about the terminology adopted in this journal:

(1) The word 'electron' applies to particles with an elementary charge of either sign. When it is desirable to emphasize the sign of the charge, the words 'positon' (*not:* positron!), and 'negaton' are used. Thus the illogical phrase 'electron-positron pair' is replaced by 'electron pair', or, if required, by 'positon-negaton pair'. However, standard expressions like 'electron capture' are accepted.

(2) Nuclei (or nucleides, *not*: nuclides) are conveniently divided according to the parity of the proton and neutron numbers Z, N, into four families as follows:

even-mass nuclei { even nuclei (Z even, N odd)
odd nuclei (Z odd, N odd)

odd-mass nuclei { odd-proton nuclei (Z odd, N even)
odd-neutron nuclei (Z even, N odd).

Generally, two systems of nomenclature are used concurrently:

System 1		*System* 2	
even nuclei	even-even	even-A nuclei	even-even
	odd-odd		odd-odd
odd nuclei	even-odd	odd-A nuclei	odd-N
	odd-even		odd-Z.

There should be little hesitation in admitting that System 2 is far superior to System 1, and *it is therefore this System 2 which is adopted in this journal*, with modifications of pure form which do not in the least alter its structure: (a) the use of (undefined) symbols A, N, Z is unnecessary clumsiness, since there are plain words fulfilling the same function:

odd-mass nucleus, odd-neutron nucleus convey the same idea as odd-A, odd-N nucleus in a more immediate way; (b) the repetition involved in even-even, odd-odd is obviously superfluous, and to drop it can cause no confusion (within the framework of System 2). One thus arrives at the nomenclature consistently used in this journal. It must be stressed once more that this nomenclature is *not* an innovation, but is *essentially identical* with the widely used System 2. People accustomed to the repetitive names even-even, odd-odd may, if they wish, regard the simple forms even, odd as abbreviations, or read them through a piece of Iceland spar: it will not change their meaning. No ambiguity can arise from the use of the simple form odd, in the meaning of odd-odd, *if there is general agreement to use only System* 2. Since the elimination of System 1 would seem to be desirable also for other reasons (the alternation even-odd, odd-even is utterly confusing), it should not be too difficult (one would hope) to reach such an agreement.

(3) The expressions 'isotopic spin' and 'isotopic quantum number' should be replaced by 'isobaric spin' or 'isospin' and 'isobaric quantum number' or 'isospin quantum number'.

(4) For the elementary particles use must be made of the latest nomenclature adopted by international agreement.

STYLE

Phrases like 'quantum-mechanical' or 'field theoretic' are not idiomatic and cannot be excused on grounds of practical convenience. For the first, the word 'quantal' has been proposed by Prof. C. G. Darwin and ought to be universally adopted. As to the barbarism 'by field theoretic methods', it is not shorter than 'by methods of field theory'.

As a rule, avoid the use of the future tense when the present tense can do just as well. Write 'In section 2 we discuss . . .', 'For simplicity we assume . . .', rather than, '. . . we shall discuss . . .', '. . . we shall assume . . .' If there is some point in using the future, write 'we shall' and *not* 'we will'.

The word 'data' is a plural; write: 'the data are . . .' (*not* 'is'), 'these data' (*not* 'this data').

The correct name of the element Al is 'aluminium' (*not* 'aluminum').

The spelling adopted in *Nuclear Physics* is the English one, *not* the American one. Thus write: centre (*not* center), favourable (*not* favorable), labelled (*not* labeled), etc.

Well-prepared manuscripts are dealt with promptly and smoothly. Badly-prepared manuscripts risk suffering considerable delay.

MODEL TYPESCRIPT (TEXT PAGE)

Nuclear dispersion contribution to high-energy electron scattering

J.K. Smith

Utopia University, Utopia

Abstract: An expression for the contribution of virtual intermediate states of the nucleus (nuclear dispersion) to the elastic and inelastic scattering of high-energy electrons is obtained.

1. Introduction

Calculations of the elastic scattering of high-energy electrons from nuclei have for the most part regarded the nucleus as a rigid structure with no internal degrees of freedom. Such calculations have been done exactly for spherically symmetric charge distributions†, and

(footnote) † See ref. [1], and earlier papers cited there.

approximately for spheroidal charge distributions that can be set into rotation [2,3].

2. Discussion

In the notation of (9), we have

(cap. greek psi lower case greek nu)
$$\Psi_0 \left\{ u_0 e^{i\underline{k}_0\cdot\underline{r}} - \sum_{\gamma} \frac{u_\gamma e^{i\underline{k}_\gamma\cdot\underline{r}}}{E_\gamma - E_0} \sum_{j=1}^{z} e^2 \int \bar{\Psi}_0' \frac{a_{\gamma 0} e^{i(\underline{k}_0 - \underline{k}_\gamma)\cdot\underline{r}'}}{|\underline{r}' - \underline{R}_j'|} \, d\nu' \right\}, \quad (30)$$

where $\underline{u}_0$ and $\underline{u}_\gamma$ are constant spinors and $d\nu'$ is the volume element of the domain considered. Equation (30) is what would be obtained from the Hamiltonian

(script cap H)
$$\mathcal{H} = \mathcal{H}_{nucl} + \mathcal{H}_{el} + V_C$$

to first order by regarding the nucleus as a rigid charge distribution (fig.1), and so is included in the numerically calculated electron wave function [4]. If now eq. (30) is inserted in the first order matrix element (1) in place of $\Psi_0 \underline{u}_0 \exp(i\underline{k}\cdot\underline{r})$, we obtain (1) together with that part of (9) that arises from the $\underline{n} = 0$ term in the summation over intermediate states $\underline{n}$.

The writer is indebted to Dr.W.X. Brown for helpful comments.

MODEL TYPESCRIPT (SEPARATE SHEET WITH REFERENCES)

References

1) Yennie, Ravenhall and Wilson, Phys. Rev. 95 (1954) 500

2) L.I. Schiff, Phys. Rev. 96 (1954) 765

3) Progress in cosmic ray physics, edited by J.G. Wilson (North-Holland Publishing Company, Amsterdam, 1952) p. 797

4) J.M. Blatt and V.F. Weisskopf, Theoretical nuclear physics (Wiley, New York, 1952) p. 293;
J. Jensen , Mat. Fys. Medd. Dan. Vid. Selsk. 12, No. 38 (1963)

CORRECTED PROOF

NUCLEAR DISPERSION CONTRIBUTION TO HIGH-ENERGY ELECTRON SCATTERING

J. K. SMITH
Utopia University, Utopia

Received 29 February 1964

Abstract: An expression for the contribution of virtual intermediate states of the nucleus (nuclear dispersion) to the elastic and inelastic scattering of high-energy electrons is obtained.

1. Introduction

Calculations of the elastic scattering of high-energy electrons from nuclei have for the most part regarded the nucleus as a rigid structure with no internal degrees of freedom. Such distributions have been done exactly for spherically symmetric charge distributions †, and approximately for spheroidal charge distributions that can be set into rotation [2,3]).

2. Discussion

In the notation of (9), we have

$$\psi_0 \left\{ u_0 e^{i\mathbf{k}_0 \cdot \mathbf{r}} - \sum_\nu \frac{u_\nu e^{i\mathbf{k}_\nu \cdot \mathbf{r}}}{E_\nu - E_0} \sum_{j=1}^{z} e^2 \int \bar{\psi}'_0 \frac{a\, e^{i(\mathbf{k}_0 - \mathbf{k}_\nu)\cdot \mathbf{r}'}}{|\mathbf{r}' - \mathbf{R}'_j|} \, \mathrm{d}v' \right\}, \qquad (30)$$

where u_0 and u_ν are constant spinors and dv′ is the volume element of the domain considered. Equation (30) is what would be obtained from the Hamiltonian

$$H = H_{\mathrm{nucl}} + H_{\mathrm{el}} + V$$

to first order by regarding the nucleus as a charge distribution (fig. 1), and so is included in the numerically calculated electron wave function [4]). If now eq. (30) is inserted in the first order matrix element (1) in place of $\psi_0 u_0 \exp(i\mathbf{k} \cdot \mathbf{r})$, we obtain (1) together with that part of (9) that arises from the $n = 0$ term in the summation over intermediate states n.

The writer is indebted to Dr. W. X. Brown for helpful comments.

† See ref. [1]), and earlier papers cited there.

References

1) Yennie, Ravenhall and Wilson, Phys. Rev. **95** (1954) 500
2) L. Schiff, Phys. Rev. **96** (1954) 765
3) Progress in cosmic ray physics, edited by J. G. Wilson (North-Holland Publishing Company, Amsterdam, 1952) p. 797
4) J. M. Blatt and V. F. Weisskopf, Theoretical nuclear physics (Wiley, New York, 1952) p. 293
J. Jensen, Mat. Fys. Medd. Dan. Vid. Selsk. **12**, No. 38 (1963)

FINAL PUBLICATION

NUCLEAR DISPERSION CONTRIBUTION TO HIGH-ENERGY ELECTRON SCATTERING

J. K. SMITH
Utopia University, Utopia

Received 29 February 1964

Abstract: An expression for the contribution of virtual intermediate states of the nucleus (nuclear dispersion) to the elastic and inelastic scattering of high-energy electrons is obtained.

1. Introduction

Calculations of the elastic scattering of high-energy electrons from nuclei have for the most part regarded the nucleus as a rigid structure with no internal degrees of freedom. Such calculations have been done exactly for spherically symmetric charge distributions †, and approximately for spheroidal charge distributions that can be set into rotation [2,3]).

2. Discussion

In the notation of eq. (9), we have

$$\psi_0\left\{u_0 e^{i\mathbf{k}_0\cdot\mathbf{r}} - \sum_\nu \frac{u_\nu e^{i\mathbf{k}_\nu\cdot\mathbf{r}}}{E_\nu - E_0}\sum_{j=1}^{z} e^2 \int \bar{\psi}'_0 \frac{a_{\nu 0}\, e^{i(\mathbf{k}_0-\mathbf{k}_\nu)\cdot\mathbf{r}'}}{|\mathbf{r}'-\mathbf{R}'_j|}\,\mathrm{d}v'\right\}, \qquad (30)$$

where u_0 and u_ν are constant spinors and dv′ is the volume element of the domain considered. Equation (30) is what would be obtained from the Hamiltonian

$$\mathscr{H} = \mathscr{H}_{\mathrm{nucl}} + \mathscr{H}_{\mathrm{el}} + V_{\mathrm{C}}$$

to first order by regarding the nucleus as a rigid charge distribution (fig. 1), and so is included in the numerically calculated electron wave function [4]). If now eq. (30) is inserted in the first order matrix element (1) in place of $\psi_0 u_0 \exp(i\mathbf{k}\cdot\mathbf{r})$, we obtain (1) together with that part of (9) that arises from the $n = 0$ term in the summation over intermediate states n.

The writer is indebted to Dr. W. X. Brown for helpful comments.

† See ref. [1]), and earlier papers cited there.

References

1) Yennie, Ravenhall and Wilson, Phys. Rev. **95** (1954) 500
2) L. I. Schiff, Phys. Rev. **96** (1954) 765
3) Progress in cosmic ray physics, edited by J. G. Wilson (North-Holland Publishing Company, Amsterdam, 1952) p. 797
4) J. M. Blatt and V. F. Weisskopf, Theoretical nuclear physics (Wiley, New York, 1952) p. 293; J. Jensen, Mat. Fys. Medd. Dan. Vid. Selsk. **12**, No. 38 (1963)

PROOF CORRECTION

(1) Indicate your corrections in a clear and distinct manner, bearing in mind that the printer does not understand the meaning of the text or the formulae.

(2) *Correction markings*. The Continental system for indicating corrections is neat, unambiguous and simple, and its use is recommended. The English system, which has the opposite characteristics, is strongly deprecated. However, if you are not familiar with the Continental system, any unconventional marking will do, provided that it is legible and *unambiguous*.

(3) Do not mark the corrections in pencil, but use a conspicuous medium, such as red ink. (A red ball-point is very suitable.)

(4) When longer alterations or additions are necessary, they must be typewritten (with ample space between the lines and wide margins). Do not glue the sheets with these typewritten corrections to the proof, but indicate clearly, by corresponding markings on the proof and on the sheet, where these corrections must be inserted.

(5) For your general guidance, a sample of a corrected page (with unrealistic accumulation of the most common typographical errors) is shown on p. 708; it illustrates the main conventions of the recommended system of proof-marking.

(6) Authors may sometimes find that some lines in the proofs, especially at the top and bottom of the pages, are blurred or broken; as this is only due to the special technique used in printing the first proofs, authors should not bother to correct this.

(7) Together with the proofs, the authors receive their original manuscript. They are invited to use this opportunity of examining how the manuscript has been marked and amended by the editorial staff: with an eye on future publications, their attention may thus be called to some possible failure on their part to observe one or other of the above instructions.

PROCESSING OF MANUSCRIPTS

(1) Manuscripts may be sent with a covering letter either directly to the Editor, or preferably through the intermediary of one of the members of the Editorial Board of the country or region in which the author is working.

(2) The receipt of a manuscript is acknowledged to the person signing the covering letter, or, if such letter should be lacking, to the author first mentioned in the title.

(3) The acceptance of a manuscript is *not* notified to the authors. The accepted manuscript is sent to the printer after preparation by the editorial staff.

(4) Three copies of the first proof are sent to the address indicated on the covering letter, or in default of such indication to the author first mentioned in the title. One copy of the proof may be retained by the author; two identically corrected proofs should be returned to the editor (*not* to the publishers).

(5) Together with the proofs, the author receives an order form for reprints, which should be filled in and sent to the publishers (*not* to the editor).

(6) The corrected proofs are assembled as nearly as possible in the order of their reception to form an issue of the journal, of which the printer prepares a page proof. To speed up the process of publication, page proofs are not sent to the authors, but are checked by the editorial staff. After the last corrections, the issue is printed and distributed.

AUTHOR INDEX

BALACHANDRAN, A. P., *see* RAMAKRISHNAN

BARBER, W. C., *see* VANHUYSE

BATCHELOR, R., *see* GOVE

BAUMANN, K. and R. SEXL, A one-dimensional field theory with degenerate vacuum 117

BENIOFF, P., Nuclear rearrangement and simple nuclear reactions . . . 68

BERG, R. A. and C. N. LINDNER, Electron-proton bremsstrahlung . . . 259

BISHOP, G. R., *see* LACOSTE

BOEHM, F., *see* EDWARDS

BRISBOUT, F. A., C. GAULD, J. LEHANE, C. B. A. MCCUSKER, J. MALOS, K. NISHIKAWA and L. G. VAN LOON, The production and properties of mesons at high energies 634

BRISBOUT, F. A., C. GAULD, C. B. A. MCCUSKER, J. MALOS, K. NISHIKAWA, L. S. PEAK and L. G. VAN LOON, A comparison of pion and nucleon interactions in nuclear emulsions between 10^{11} and 10^{13} eV. 211

BUBB, I. F., *see* LEGGE

CHISHOLM, J. S. R., Changes of variable in quantum field theories . . 469

CHLEBOWSKA, D., *see* SMIRNOV

DAVIDSON, J. P., *see* LIPAS

DELVES, L. M., Elastic and inelastic scattering of neutrons by deuterons near the inelastic threshold 136

DESHPANDE, N. G., *see* RAMAKRISHNAN

DIETZSCH, O., R. A. DOUGLAS and V. GOMES, A search for an isomeric state in Mn^{54} 113

DOUGLAS, R. A., *see* DIETZSCH

DUMOND, J. W. M., *see* EDWARDS

EDWARDS, W. F., J. W. M. DUMOND and F. BOEHM, An intensity calibration of the two metre curved-crystal spectrometer 670

EDWARDS, W. F. and C. J. GALLAGHER, Jr., The decay of Se^{75} 649

FALLIEROS, STAVROS, Centre-of-mass invariance and the energy shift in the nuclear dipole state 594

FERGUSON, J. M. and F. M. TOMNOVEC, Gamma-ray spectrum of Te^{131} 457

FREEMAN, R. M., The magnetic moment of the second excited state of F^{19} 446

FRENCH, J. B., Isobaric-spin relationships between nuclear spectra 161

FRENCH, J. B. and M. H. MACFARLANE, Isobaric-spin splitting of single-particle resonances 168

FRÖHLICH, H., The structure of momentum space, the neutrino and the Pauli principle 324

GALLAGHER, Jr., C. J., *see* EDWARDS
GAULD, C., *see* BRISBOUT
GAULD, C., *see* BRISBOUT
GOLDRING, G. and Z. VAGER, Energy loss of protons in rare earth oxides and reduced transition probabilitites for $2^+ \rightarrow 0^+$ transitions in even rotational nuclei 250
GOMES, V., *see* DIETZSCH
GOVE, H. E., A. E. LITHERLAND and R. BATCHELOR, Proton capture gamma rays in the giant resonance region in light nuclei 480
HUMBLET, J. and L. ROSENFELD, Theory of nuclear reactions I. Resonant states and collision matrix. 529
IOSIFESCU, M., *see* SĂNDULESCU
IWAO, SYUREI, Double fragments and relative parity of Λ and Σ hyperons 1
IYENGAR, K. N., *see* NAIR
JAHN, HELMUT, Die Darstellungen der starken Kopplung und das Resonanzproblem der Meson-Nucleon-Streuung 353
JONES, W. M., D. G. WATERS and V. M. ROUT, The angular distribution of charged particle groups from the deuteron bombardment of nitrogen 203
KATZ, A., On the treatment of a perturbation in a system of paired fermions 129
KRÓLIKOWSKI, W., Some remarks on global symmetry 91
LACOSTE, F. and G. R. BISHOP, Experimental study of the charge distribution of O^{16} and O^{18} by electron scattering 511
LANG, D. W., Analysis of recent measurement of nuclear level density parameters 434
LEADER, E., The optical model in π-nuclear scattering 177
LEGGE, G. J. F., A search for fine structures in the reactions B^{10} (d, α_0) Be^8 and B^{10} (d α_1) Be^{8*} 608
LEGGE, G. J. F. and I. F. BUBB, C^{12} level structure in the excitation region 20.5—26.5 MeV 616
LEHANE, J., *see* BRISBOUT
LINDNER, C. N., *see* BERG
LIPAS, P. O. and J. P. DAVIDSON, Octupole vibrations of deformed even nuclei 80
LIPKIN, H. J., Pairing and quadrupole forces in a two-dimensional soluble model. 147
LITHERLAND, A. E., *see* GOVE
MALOS, J., *see* BRISBOUT
MALOS, J., *see* BRISBOUT
MCCUMBER, D. E., Generalized self-consistent-field and random-phase approximations for multi-phase systems. 286
MCCUSKER, C. B. A., *see* BRISBOUT

McCusker, C. B. A., *see* Brisbout
McCusker, C. B. A., *see* Ueda
Macfarlane, M. H., *see* French
Moscati, G., The $(\gamma, 3n)$ reaction in Pr^{141} 321
Nair, K. G., K. N. Iyengar and R. Ramanna, Energy and angular distributions of protons emitted from Al^{27} due to 14.2 MeV neutron interactions. 193
Nassiff, S. J., *see* Vignau
Ne'eman, Y., Derivation of strong interactions from a gauge invariance 222
Ne'eman, Y., Yukawa terms in the unitary gauge theory 230
Nishikawa, K., *see* Brisbout
Nishikawa, K., *see* Brisbout
Peak, L. S., *see* Brisbout
Ramakrishnan, Alladi, A. P. Balachandran, N. R. Ranganathan and N. G. Deshpande, On an isobaric spin scheme for leptons and the leptonic decays of strange particles 52
Ramanna, R., *see* Nair
Ranganathan, N. R., *see* Ramakrishnan
Rosenfeld, L., Theory of nuclear reactions II. The foundation of the optical model. 579
Rosenfeld, L., *see* Humblet
Rout, V. M., *see* Jones
Šachl, Vladimir, Dispersion relations for photoproduction of π^0-mesons on deuterons 681
Sanderson, E. A., Excitation of the giant dipole resonance by inelastic proton scattering on carbon 420
Săndulescu, A. and M. Iosifescu, On favoured alpha transitions . . 209
Schmid, E. W. and K. Wildermuth, Phase shift calculation on α—α scattering 463
Sexl, R., *see* Baumann
Smirnov, Yu. F. and D. Chlebowska, Reduced widths for nucleon clusters in shell model 306
Solomon, A. I., The new particles and the baryon mass spectrum . . . 452
Sosnowski, R., Z. Wilhelmi and J. Wotjkowska, Relative measurements on the longitudinal polarization of beta rays from Na^{24}, Mn^{56}, Sb^{122}, Ho^{166} and Au^{198} 280
Stein, P. R., *see* Young
Tadić, D., Induced pseudoscalar interaction in $0^- \rightarrow 0^+$ beta transitions 338
Takahashi, Yasushi, The structure of the nucleon core by the Hartree approximation 658
Tomnovec, F. M., *see* Ferguson
Trueman, T. L., Energy level shifts in atomic states of strongly-inter-

acting particles 57
UEDA, A. and C. B. A. MCCUSKER, Characteristics of high-energy nuclear interactions at and above 10^{14} eV 35
VAGER, Z., *see* GOLDRING
VANHUYSE, V. J. and W. C. BARBER, Photoprotons from carbon 233
VAN LOON, L. G., *see* BRISBOUT
VAN WAGENINGEN, R., Elementary derivation of the Minami phase shift ambiguity 126
VERVIER, J., Circular polarization of γ-rays following the capture of polarized neutrons 10
VIGNAU, H. and S. J. NASSIFF, Yield ratios of the isomeric pair $C^{137m/137}$ formed by La^{139} (d, 4n) Ce^{137} reaction 108
WATERS, D. G., *see* JONES
WILDERMUTH, K., *see* SCHMID
WILHELMI, Z., *see* SOSNOWSKI
WOJTKOWSKA, J., *see* SOSNOWSKI
YOUNG, J. E. and P. R. STEIN, A cluster model representation for the 3-body ground state 97

SUBJECT INDEX

1. Nuclear Structure

1.B *Two- and three-body problems*

A cluster model representation for the 3-body ground state, J. E. Young and P. R. Stein 97
Elastic and inelastic scattering of neutrons by deuterons near the inelastic threshold, L. M. Delves 136
Phase shift calculations on α—α scattering, E. W. Schmid and K. Wildermuth 463

1.C *Many-particle systems*

Nuclear rearrangement and simple nuclear reactions, P. Benioff 68
On the treatment of a perturbation in a system of paired fermions, A. Katz 129
Pairing and quadrupole forces in a two-dimensional soluble model, H. J. Lipkin 147
Generalized self-consistent-field and random-phase approximations for multi-phase systems, D. E. McCumber 286
Centre-of-mass invariance and the energy shift in the nuclear dipole state, Stavros Fallieros. 594

1.D *Nuclear models*

1.D.1. *Shell model*

Isobaric-spin relationships between nuclear spectra, J. B. French . . 161
Reduced widths for nucleon clusters in shell model, Yu. F. Smirnov and D. Chlebowska. 306

1.D.2 *Collective model*

Octupole vibrations of deformed even nuclei, P. O. Lipas and J. P. Davidson 80
On favoured alpha transitions, A. Săndulescu and M. Iosifescu . . . 209
Energy loss of protons in rare earth oxides and reduced transition probabilities for $2^+ \rightarrow 0^+$ transitions in even rotational nuclei, G. Goldring and Z. Vager 250

1.E *Properties of nuclei*

1.E.1 *Energy levels*

Circular polarization of γ-rays following the capture of polarized neutrons, J. Vervier. 10
Gamma-ray spectrum of Te^{131}, J. M. Ferguson and F. M. Tomnovec 457

1.E.3 *Electric and magnetic moments*

The magnetic moment of the second excited state of F^{19}, R. M. Freeman 446

1.E.4 *Transition probabilities; Cross sections*

Energy loss of protons in rare earth oxides and reduced transition probabilities for $2^+ \rightarrow 0^+$ transitions in even rotational nuclei, G. Goldring and Z. Vager 250

1.E.5 *Nuclear radii; Matter distributions*

Experimental study of the charge distribution of O^{16} and O^{18} by electron scattering, R. Lacoste and G. R. Bishop 511

1.E.7 *Isobaric spin effects*

Isobaric-spin relationships between nuclear spectra, J. B. French . . 161
Isobaric-spin splitting of single-particle resonances, J. B. French and M. H. Macfarlane 168

2. Nuclear Reactions

2.A *General properties*

2.A.1 *Cross-sections, energy relations*

Nuclear rearrangement and simple nuclear reactions, P. Benioff . . . 68
Yield ratios of the isomeric pair $Ce^{137m/137}$ formed by La^{139} (d, 4n) Ce^{137} reactions, H. Vignau and S. J. Nassiff. 108

2.A.2 *General theory*

Theory of nuclear reactions I. Resonant states and collision matrix, J. Humblet and L. Rosenfeld 529
Theory of nuclear reactions II. The foundation of the optical model, L. Rosenfeld. 579

2.B *Angular distributions, Correlations; Polarization*

Circular polarization of γ-rays following the capture of polarized neutrons, J. Vervier 10
A search for fine structure in the reactions B^{10} (d, α_0) Be^8 and B^{10} (d, α_1) Be^{8*}, G. J. F. Legge 608

2.C *Resonance reactions; R-matrix theory*

Reduced widths for nucleon clusters in shell model, Yu. F. Smirnov and D. Chlebowska 306
Proton capture gamma rays in the giant resonance region in light nuclei, H. E. Gove, A. E. Litherland and R. Batchelor 480
Theory of nuclear reactions I. Resonant states and collision matrix, J. Humblet and L. Rosenfeld 529
C^{12} level structure in the excitation region 20.5—26.5 MeV, G. J. F. Legge and I. F. Bubb 616

2.D *Statistical model*

Energy and angular distributions of protons emitted from Al^{27} due to 14.2 MeV neutron interactions, K. G. Nair, K. N. Iyengar and R. Ramanna 193
The angular distributions of charged particle groups from the deuteron bombardment of nitrogen, W. M. Jones, D. G. Waters and V. M. Rout 203
Analysis of recent measurement of nuclear level density parameters, D. W. Lang 434

2.E *Optical model*

Isobaric-spin splitting of single-particle resonances, J. B. French and M. H. Macfarlane 168
Theory of nuclear reactions II. The foundation of the optical model, L. Rosenfeld 579

2.F *Direct interaction (other than stripping)*

Energy and angular distributions of protons emitted from Al^{27} due to 14.2 MeV neutron interactions, K. G. Nair, K. N. Iyengar and R. Ramanna 193

Excitation of the giant dipole resonance by inelastic proton scattering on carbon, E. A. Sanderson 420

2 I *Photonuclear processes*

Photoprotons from carbon, V. J. Vanhuyse and W. C. Barber 233
The (γ, 3n) reaction in Pr^{141}, G. Moscati 321
Proton capture gamma rays in the giant resonance region in light nuclei, H. E. Gove, A. E. Litherland and R. Batchelor 480
Centre-of-mass invariance and the energy shift in the nuclear dipole state, Stavros Fallieros. 594

2.L *Scattering processes (except two-nucleon system and meson scattering)*

Elementary derivation of the Minami phase shift ambiguity, R. van Wageningen 126
Excitation of the giant dipole resonance by inelastic scattering on carbon, E. A. Sanderson 420
Phase shift calculations on α—α scattering, E. W. Schmid and K. Wildermuth 463

3. Electromagnetic Radiation

3.A *Gamma radiation*

A search for an isomeric state in Mn^{54}, O. Dietzsch, R. A. Douglas and V. Gomes 113
Gamma-ray spectrum of Te^{131}, J. M. Ferguson and F. M. Tomnovec 457
An intensity calibration of the two metre curved-crystal spectrometer, W. F. Edwards, J. W. M. Dumond and F. Boehm 670

3.B *Internal conversion*

The decay of Se^{75}, W. F. Edwards and C. J. Gallagher, Jr. 649

4. Beta decay; Parity

4.C *Evaluation of matrix elements*

Induced pseudoscalar interaction in $0^- \rightarrow 0^+$ beta transitions, D. Tadić . . . 338

4.E *Analysis of data*

The decay of Se^{75}, W. F. Edwards and C. J. Gallagher, Jr. 649

5. Alpha decay

On favoured alpha transitions, A. Săndulescu and M. Iosifescu 209

6. Methods and Instruments

6.A *Experimental*

An intensity calibration of the two metre curved-crystal spectrometer, W. F. Edwards, J. W. M. Dumond and F. Boehm 670

7. Quantum Field Theory

7.A *General*

Changes of variable in quantum field theories, J. S. R. Chisholm 469

7.C *π-meson field (scattering and nuclear forces)*

The optical model in π-nuclear scattering, E. Leader 177
A comparison of pion and nucleon interactions in nuclear emulsions between 10^{11} and 10^{13} eV, F. A. Brisbout, C. Gauld, C. B. A. McCusker, J. Malos, K. Nishikawa, L. S. Peak and L. G. van Loon 217
Electron-proton bremsstrahlung, R. A. Berg and C. N. Lindner 259
The production and properties of mesons at high energies, F. A. Brisbout, C. Gauld, J. Lehane, C. B. A. McCusker, J. Malos, K. Nishikawa and L. G. van Loon 634
The structure of the nucleon core by the Hartree approximation, Yasushi Takahashi. 658
Dispersion relations for photoproduction of π^0-mesons on deuterons, Vladimír Šachl 681

8. Elementary Particles

8.A *Experimental*

Relative measurements on the longitudinal polarization of beta rays from Na^{24}, Mn^{56}, Sb^{122}, Ho^{166} and Au^{198}, R. Sosnowski, Z. Wilhelmi and J. Wojtkowska 280

8.B *Theory: interactions, transformation properties*

Double hyperfragments and relative parity of Λ and Σ hyperons, S. Iwao 1
On an isobaric spin scheme for leptons and the leptonic decays of strange particles, A. Ramakrishnan, A. P. Balachandran, N. R. Ranganathan and N. G. Deshpande 52
Energy level shifts in atomic states of strongly-interacting particles, T. L. Trueman 57
Some remarks on global symmetry, W. Królikowski 91
Derivation of strong interactions from a gauge invariance, Y. Ne'eman . . 222
Yukawa terms in the unitary gauge theory, Y. Ne'eman 230
The structure of momentum space, the neutrino and the Pauli principle, H. Fröhlich 324
The new particles and the baryon mass spectrum, A. I. Solomon 452

8.C *Fundamental theory of matter*

A one-dimensional field theory with degenerate vacuum, K. Baumann and R. Sexl 117
Die Darstellungen der starken Kopplung und das Resonanzproblem der Meson-Nucleon-Streuung, H. Jahn 353

9. Cosmic Radiation

9.A *General*

Characteristics of high-energy nuclear interactions at and above 10^{14} eV, A. Ueda and C. B. A. McCusker 35

A comparison of pion and nucleon interactions in nuclear emulsions between 10^{11} and 10^{13} eV, F. A. Brisbout, C. Gauld, C. B. A. McCusker, J. Malos, K. Nishikawa, L. S. Peak and L. G. van Loon 217
The production and properties of mesons at high energies, F. A. Brisbout, C. Gauld, J. Lehane, C. B. A. McCusker, J. Malos, K. Nishikawa and L. G. van Loon 634

10. News Items

10.D *Book reviews*

A. M. Baldin, V. I. Gol'danskii and I. L. Rozenthal, Kinematics of nuclear reactions (Aage Winther) 693
A. B. McIntosh and T. J. Heal (Editors), Materials for nuclear engineers (Niels Hansen) 693
C. R. Tipton, Jr. (Editor), Reactor handbook, vol. 1: materials (Niels Hansen) 694
J. H. Sanders, The Fundamental Atomic Constants (L. R.) 694
J. E. Drummond, Plasma Physics (L. R.) 694
C. Sanchez del Rio, Fundamentos teóricos de la fisica atómica y nuclear (L.R.) 695
J. B. Marion, 1960 Nuclear Data Tables, part III (L. R.) 695
Summer course in plasma physics (L. R.) 695
J. L. Delcroix, Introduction to the theory of ionized gases (L. R.) 695
J. F. Denisse et J. L. Delcroix, Théorie des ondes dans les plasmas (L. R.) 696
J. Gorter (Editor), Progress in Low Temperature Physics, vol. III (L. R.) 696
Reactors of the world (second series), (L. R.) 696
S. D. Drell and F. Zachariasen, Electromagnetic structure of nucleons (L.R.) 696

10.E *Errata and addenda*

G. Alaga, L. Sips and D. Tadić, Calculations of some relativistic corrections to the allowed and *l*-forbidden beta transitions **6** (1958) 305 351
A. Deloff and J. Wrzencionko, The phenomenological baryon-baryon scattering theory and the relative parity determination **20** (1960) 464 527
J. M. Hansteen, A remark on the Coulomb disintegration of accelerated heavy ions **19** (1960) 309. 527

NORTH-HOLLAND BOOKS

Just out
Second, revised edition

PLASMA Physics

by **J. G. LINHART**
CERN, Geneva

From reviews of the first edition

The author has the three rare qualifications of experience, mathematical facility and inventive imagination. He also possesses didactic ability, but this will be appreciated only by those readers who share with him the advantages of mathematical ability and of an active mind. It is not a book which can be imbibed passively, or uncritically.

The arrangement is so clear, with full description of the experimental methods and with all the relevant theory required to explain the data, that the book can be equally recommended to the student and to the expert research worker.

Nature

The whole book provides an admirable, if laconic, summary to a vast and important field of work of great topical interest.

Journal of the Royal Institute of Chemistry

6 x 9" 290 pp. 125 figs. Gld. 25.00 (50s.)

NORTH-HOLLAND PUBLISHING COMPANY-AMSTERDAM

Sole distributor U.S.A.: Interscience Publishers Inc. New York

NORTH-HOLLAND BOOKS

Proceedings of the VIIth International Conference

on

LOW TEMPERATURE PHYSICS

Toronto
August 29 - September 3, 1960

editors | G. M. GRAHAM and
A. C. HOLLIS HALLETT
University of Toronto

1. Second Fritz London Award
2. The Mössbauer Effect
3. Magnetic Relaxation
4. Liquid and Gaseous H_2
5. Magnetism below 1 K
6. Further Communications on Magnetism
7. Polarization of Protons
8. Nuclear Orientation
9. Fermi Surface
10. Ultrasonic Attenuation
11. Resistance Minima
12. Further Communication on Transport Properties in Solids
13. Theory of Superconductivity
14. Electrical Properties of Superconductors
15. Superconductivity of Hg and Ta
16. Specific Heat of Alloys
17. Intermediate State
18. Further Communications on Superconductivity
19. Flow Properties of Liquid Helium-4
20. Kapitza Boundary Layer
21. Ions in Liquid Helium
22. Helium Film
23. Further Communications on the Properties of He^4
24. Liquid and Solid He^3
25. Thermodynamic Properties of He^3-He^4 Mixtures
26. Further Communications on He^3-He^4 Mixtures
27. Equation of State and Thermodynamic Properties
28. Thermodynamic Properties of Argon
29. Further Communications on Thermodynamic Properties
30. Proposal for a He^3 Temperature Scale

745 pp. Gld. 57.00 (114s.)

Sole distributors outside U.S.A. and Canada:

NORTH-HOLLAND PUBLISHING COMPANY — AMSTERDAM